Approche LPV pour la commande robuste de la dynamique des véhicules : amélioration conjointe du confort et de la sécurité

Anh Lam Do

UNIVERSITÉ DE GRENOBLE

THÈSE

Pour obtenir le grade de

DOCTEUR DE L'UNIVERSITÉ DE GRENOBLE

Spécialité : **Automatique-Productique**

Arrêté ministériel : 7 août 2006

Présentée par

Anh Lam DO

Thèse dirigée par **Olivier SENAME** et **Luc DUGARD**

préparée au sein du **GIPSA-Lab** dans **l'école doctorale EEATS**

Approche LPV pour la commande robuste de la dynamique des véhicules : amélioration conjointe du confort et de la sécurité.

Thèse soutenue publiquement le **14 octobre 2011**,
devant le jury composé de :

M. Michel BASSET
Professeur, Université de Haute-Alsace, Président
M. Germain GARCIA
Professeur, INSA Toulouse, Rapporteur
M. Peter GASPAR
Professeur, Université de Budapest, Rapporteur
M. Sergio SAVARESI
Professeur, Politecnico di Milano, Membre
M. Olivier SENAME
Professeur, Grenoble INP, Directeur de thèse
M. Luc DUGARD
Directeur de recherche, CNRS Grenoble, Directeur de thèse

Table of contents

Acknowlegdement

I would like to thank my advisors, Professors Olivier Sename and Luc Dugard, for their scientific understanding and for their precious support during my PhD studies. I have been so lucky to work with them, who were always available and gave me the best research conditions and professional opportunities. I look forward to further collaboration in the future.

I would like to thank Professor Michel Basset for being the president of my doctoral committee; Professor Germain Garcia and Professor Peter Gaspar for their time to review my PhD thesis.

I would like also to thank Professor Sergio Savaresi (Politecnico di Milano, Milan) for participating in my doctoral committee and, specially, accepting me to join his MOVE team for six months. There, under his supervision, I had the chance to exchange my scientific knowledge with Cristiano Spelta, Diego Delveccio and Mara Tanelli. Besides, thank you very much, Cristiano and Diego, for your kindness in helping me with the lodging in Milan.

My gratitude goes to Professor Joao M. Gomes da Silva Jr. for being available and patient to answer very clearly all my questions on input saturation control. I hope we will continue to work together on this interesting topic.

I will not forget to thank Jorge Lozoya-Santos, my dear Mexican friend, for the collaboration in MR damper modeling and control and Charles Poussot-Vassal for his advice in suspension control and the matlab routines which were really helpful to me.

I have spent happy and unforgettable moments with my dear friends in GIPSA-Lab: Antoine, Irfan, Simona, Joumana, Lizeth, Andra, Amine, Jennifer, Caroline, Valentina, Marouane, Soheib, Sébastien, Gabriel, Felipe, Maria, Haiyang, Emilie, Federico, Boussaad... Without you, my three years of PhD must have been so boring and difficult.

My sincere thanks go to Hieu, Nhung, Thang and Van (in Grenoble); and Thuan, Hung, Cuong, Duc Anh, Hoang...(in other cities) for always being beside me and sharing with me the joy and difficulties as well in France; to my interesting friends Trung, Duong, Thanh, Long, Trinh, Dinh, Ha, Xuan, Hoa, Trang, Thanh, Duy... for letting me to

be among you during my six months in Milan; and to my childhood friends Hai, Hien, Trang, Duong, Tuan, Phung, Hung, Xuyen for always supporting me from Vietnam.

Finally, I am also grateful to Marie-Thérèse, Marielle, Virginie, Houria, Patricia, Olivier Chabert... and all members of the staff of GIPSA-Lab. Without them, my work might have not run smoothly.

Anh-Lam Do
Grenoble, France
November 2011

Abstract

Abstract (in english) This work is concerned by the development of advanced control methods for automotive suspensions to improve passenger comfort and road holding, while meeting technological constraints related to the suspension actuators (passivity constraint, non-linearities, structural limits).
In the first part, we propose two control schemes, polytopic LPV (Linear Parameter-Varying) and Strong Stabilization, with genetic algorithm optimization to solve the conflicts comfort/road holding and comfort/suspension travel (Chapters 3, 4 and 5).
In the second part, to solve the full control problem of semi-active suspensions, we first develop a generic strategy for general LPV systems subject to actuator saturation and state constraints. The problem is studied in terms of linear matrix inequalities (LMIs) that can synthesize an LPV controller with an anti-windup gain guaranteeing the stability and the performance of the closed loop system. Then, this strategy is applied to the case of semi-active suspension control (Chapter 6).
All the proposed methods are validated by simulations on a non-linear quarter-vehicle model.

Keywords: Semi-active suspensions, robust control, LPV modeling and control, input saturation control, anti-windup, genetic algorithms.

Résumé (en français) Ce travail concerne le développement de méthodes de commandes avancées pour les suspensions automobiles afin d'améliorer la tenue de route des véhicules et le confort des passagers, tout en respectant les contraintes technologiques liées aux actionneurs de suspension (passivité, non-linéarités, limites structurelles).
Dans la 1ère partie, nous proposons deux schémas de commande par approche LPV polytopique (Linéaire à Paramètre Variant) et Stabilisation Forte (Strong Stabilization) avec optimisation par algorithme génétique pour résoudre les conflits confort/tenue de route et confort/débattement de suspension (Chapitres 3, 4 et 5).
Dans la 2ème partie, pour résoudre le problème complet de commande de suspensions semi-actives, nous développons d'abord une stratégie générique pour les systèmes LPV généraux soumis à la saturation des actionneurs et à des contraintes d'état. Le problème est étudié sous la forme de résolution d'inégalités linéaires matricielles (LMI) qui permet-

tent de synthétiser un contrôleur LPV et un gain anti wind-up garantissant la stabilité et la performance du système en boucle fermée. Ensuite, cette stratégie est appliquée au cas de la commande des suspensions semi-actives (Chapitre 6).
Les méthodes proposées sont validées par une évaluation basée sur un critère industriel et des simulations effectuées sur un modèle non-linéaire de quart de véhicule

Résumé des contributions (in French)

Cette thèse présente le travail de trois ans (octobre 2008 - septembre 2011), réalisé dans l'équipe SLR (Systèmes Linéaires et Robustesse), département Automatique, GIPSA-Lab, sur "*l'approche LPV pour la commande robuste de la dynamique des véhicules: amélioration conjointe du confort et de la tenue de route*", sous la direction de Mr. Olivier Sename (Professeur, Grenoble INP) et de Mr. Luc Dugard (Directeur de Recherche, CNRS). Ce travail a été financé par une allocation de recherche du Ministère de l'Enseignement Supérieur et de la Recherche (MESR) et il fait aussi partie du projet INOVE (approche INtégrée pour l'Observation et la commande de la dynamique du VEhicule) ANR 2010-2014.

La thèse est la continuité de travaux antérieurs effectués dans l'équipe de recherche SLR

- Ricardo Ramirez-Mendoza (voir [Ramirez-Mendoza, 1997]), "Sur la Modélisation et la Commande de Véhicules automobiles" a été la première étude dans le cadre de l'automobile. Le travail a été axé sur la description et la modélisation des véhicules, ainsi que sur les premières tentatives sur les méthodologies de commande des suspensions actives.

- Damien Sammier (voir [Sammier, 2001]), "Sur la Modélisation et la Commande de la Suspension de Véhicules automobiles" a présenté la modélisation et la conception de régulateur d'une suspension active (utilisant les techniques H_∞ pour les systèmes LTI). La modélisation et la commande de suspension semi-active ont également été étudiées pour un amortisseur semi-actif de PSA Peugeot-Citroën.

- Alessandro Zin (voir [Zin, 2005]), "Sur la Commande Robuste de suspensions automobiles en vue du Contrôle global de châssis", a étendu les travaux antérieurs avec une attention forte sur la commande H_∞/LPV d'une suspension active afin d'améliorer les propriétés de robustesse. Un schéma de commande globale de châssis, grâce à l'utilisation des quatre suspensions, a également été obtenu à l'aide une distribution anti-roulis.

- Charles Poussot-Vassal (voir [Poussot-Vassal, 2008]), "Commande Robuste LPV

Multivariable de Châssis Automobile", a fourni des outils et des méthodologies de conception de contrôleur afin d'améliorer le confort et la sécurité dans les véhicules automobiles. Deux principales contributions sont la commande des suspensions semi-actives (en utilisant l'approche LPV pour améliorer le confort et la tenue de route) et la commande globale de châssis (concernant la commande des actionneurs de freinage et de virage pour l'amélioration de la sécurité des véhicules).

- Sébastien Aubouet (voir [Aubouet, 2010]), "Modélisation et Commande d'une Suspension semi-active SOBEN", a présenté une méthodologie de conception d'observateur permettant au concepteur de suspension de construire et de régler un observateur qui estime des variables non mesurées. Ensuite, les résultats précédents de Charles Poussot-Vassal, pour la commande de la suspension semi-active, ont été étendus au modèle vertical complet de véhicule, et complété avec une méthode de placement de pôles, une stratégie d'ordonnancement basée sur un modèle d'amortissement et une commande d'amortisseur locale.

Pendant ma thèse, la Région Rhônes-Alpes m'a offert une bourse ExploraDoc pour passer six mois dans un institut étranger. Par conséquent, j'ai eu la chance de travailler avec **Sergio Saveresi, Cristiano Spelta, Diego Delvecchio et Mara Tanelli** (au Dipartimento di Elettronica ed Informazione, Politecnico di Milano, Italie) sur la commande de la suspension semi-active. La collaboration a débouché sur deux articles de conférence "*An extension of Mixed Skyhook and ADD to Magneto-Rheological dampers*" [Do, Spelta, Savaresi, Sename, Dugard & Delvecchio, 2010] et "*An LPV control approach for comfort and suspension travel improvements of semiactive suspension systems*" [Do, Sename, Dugard, Savaresi, Spelta & Delvecchio, 2010] et un potentiel article (en préparation) sur la commande de l'amortissement variable et la rigidité variable des systèmes de suspension. J'ai eu aussi la chance de travailler avec **Joao M. Gomes da Silva Jr.** lors de son séjour de recherche de deux mois au GIPSA-Lab. Les discussions sur la commande de saturation d'entrée ont donné lieu à un article de conférence "*Control design for LPV systems with input saturation and state constraints: an application to a semi-active suspension*" [Do, Gomes da Silva Jr., Sename & Dugard, 2011]. Enfin, j'ai collaboré avec **Jorge Santos Lozoya**, doctorant mexicain, dans le cadre du projet MCOS PCP 2007-2010 entre le Tecnologico de Monterrey et le GIPSA-Lab. Nous avons discuté essentiellement sur la commande des amortisseurs magnéto-rhéologiques. L'article sur les "*Modélisation et Commande LPV d'amortisseur Magnéto-Rhéologique*" [Do, Lozoya-Santos, Sename, Dugard, Ramirez-Mendoza & Morales-Menendez, 2010] est l'un des premiers résultats pour la commande des amortisseurs magnéto-rhéologiques nonlinéaires.

Motivation et objectifs

Aujourd'hui, de nouvelles technologies sophistiquées de nombreux domaines tels que la mécanique, l'électronique, la communication, l'automatique peuvent être trouvées dans un véhicule moderne. Par exemple, l'utilisation de moteurs hybrides électriques permet de minimiser le bruit, la consommation de carburant et les émissions de polluants; les technologies à base de caméra pour détecter les alentours dans un véhicule fournissent des informations visuelles et d'avertissement au conducteur; la communication sans fil avec le monde extérieur (avec d'autres véhicules ou des centres de communication) augmente la sécurité et améliore l'expérience de conduite. Bien que ces technologies apportent de plus en plus de plaisir aux utilisateurs, le facteur fondamental qui détermine la performance d'un véhicule est sans doute sa dynamique. En fait, la dynamique du véhicule est un sujet intéressant dans la recherche industrielle et académique. La conception et la commande des principaux actionneurs essentiels à la dynamique du véhicule ont été intensivement étudiés. Dans ce cadre, les systèmes de suspension, ainsi que les systèmes de freinage et de direction, jouent un rôle clé. Il a été prouvé par de nombreuses études, théoriques et pratiques, que les systèmes de suspension améliorent considérablement le confort et la sécurité des véhicules. Récemment, l'invention de nouvelles technologies (amortisseurs électro-rhéologiques, magnéto-rhéologiques...) a ouvert une nouvelle tendance dans l'étude et l'application de tels actionneurs à l'automobile.

Les systèmes de suspension de véhicules utilisant des amortisseurs semi-actifs sont les objets de recherche de cette thèse. Outre la coopération possible avec les systèmes de direction et de freinage pour un meilleur comportement dynamique du véhicule, ils ont une contribution distinctive au confort et à la tenue de route (deux critères principaux pour un véhicule). De nombreuses approches ont été consacrées à optimiser séparément le confort ou la tenue de route. D'autres ont proposé des méthodes générales pour faire face à leur compromis, mais les résultats optimaux (au sens de Pareto optimal) n'ont jamais été discutés pour montrer l'efficacité de ces méthodes. Par ailleurs, il peut être vu, à partir des études existantes sur la commande de la suspension semi-active, que la difficulté commune est la contrainte de passivité. En effet, c'est le principal problème à gérer. Aussi pour une conception plus réaliste, les non-linéarités et les limitations mécaniques d'un système de suspension doivent être prises en compte aussi.

Pour résumer, les problèmes suivants sont intéressants et stimulants pour la commande de la suspension semi-active.

- Problèmes d'optimisation multi-objectif.
- Non-linéarité de systèmes de suspension semi-active.
- Contraintes de commande (contrainte de passivité et de limites mécaniques).

Le rôle important des systèmes de suspension dans des véhicules, en général, et les problèmes théoriques intéressants dans la conception de contrôleur pour ces systèmes, en particulier, ont motivé notre étude. L'objectif de cette thèse est de proposer une méthodologie générique pour obtenir un bon compromis entre confort et tenue de route tout en tenant compte des caractéristiques importantes et des contraintes (non-linéarités, contrainte de passivité et contraintes mécaniques).

Le modèle de quart de véhicule et les critères de performance

Le modèle de quart de véhicule La dynamique verticale, concernant le comfort et la tenue de route, est étudiée dans cette thèse. Par conséquent, le modèle de quart de véhicule (voir Fig. 1) est utilisé. Ce modèle est simple et adapté à une conception préliminaire. Dans ce modèle, le châssis du véhicule est représenté par la masse suspendue (m_s) et la roue par la masse non suspendue (m_{us}). Elles sont reliées par un ressort de coefficient de raideur k_s et par un amortisseur semi-actif. Le pneu est modélisé par un ressort de coefficient de raideur k_t. Comme vu dans la figure 1, z_s (respectivement z_{us}) est le déplacement vertical autour du point d'équilibre de m_s (respectivement m_{us}) et z_r est la variation du profil de la route. Il est supposé que le contact roue-route est assuré.

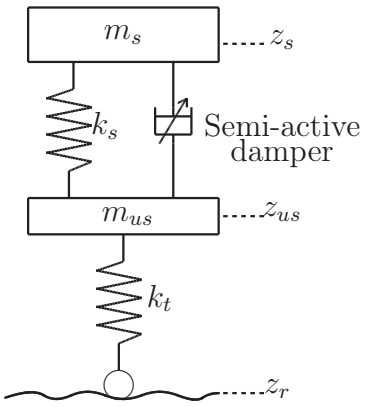

Figure 1: Modèle de quart de véhicule avec suspension semi-active.

En appliquant la deuxième loi de Newton, les équations dynamiques d'un quart de véhicule sont donnés par

$$\begin{cases} m_s \ddot{z}_s &= -F_{spring} - F_{damper} \\ m_{us} \ddot{z}_{us} &= F_{spring} + F_{damper} - F_{tire} \end{cases} \tag{0.0.1}$$

où F_{spring} est la force dynamique du ressort k_s, F_{tire} est la force dynamique du pneu

et F_{damper} est la force de l'amortisseur. Notons $z_{def} = z_s - z_{us}$ le débattement de l'amortisseur et $\dot{z}_{def} = \dot{z}_s - \dot{z}_{us}$ la vitesse de débattement.

Les forces dynamiques du ressort et du pneu sont données par

$$F_{spring} = k_s z_{def} \tag{0.0.2}$$
$$F_{tire} = k_t(z_{us} - z_r) \tag{0.0.3}$$

Les caractéristiques de l'amortisseur sont habituellement représentées par une relation force-débattement-vitesse de débattement:

$$F_{damper} = F_{damper}\left(z_{def}, \dot{z}_{def}\right) \tag{0.0.4}$$

Dans cette thèse, nous utilisons le modèle de quart de véhicule de la Renault Mégane Coupé (1/4 RMC) du modèle de la voiture d'essai disponible au Laboratoire MIPS (Mulhouse, France) (voir [Zin, 2005]).

Critères d'évaluation des performances de suspension Dans la suite, les critères pour évaluer la performance des systèmes de suspension semi-active sont donnés. Prenons le cas du modèle de quart de véhicule (voir Fig. 1). Par abus de langage, dénotons $\ddot{z}_s/z_r$ (respectivement $(z_{us} - z_r)/z_r$)) la réponse "fréquentielle" de la fonction de transfert liant la perturbation de route z_r à l'accélération du corps du véhicule $\ddot{z}_s$ (respectivement la déflexion dynamique du pneu $z_{us} - z_r$), c.à.d le gain de la fonction de transfert pour les systèmes LTI ou le gain calculé en utilisant l'algorithme de "Variance Gain" dans l'annexe B pour les systèmes non-linéaires.

En général, l'accélération de l'habitacle des véhicules entre 0 à 20 Hz doit être filtrée pour garantir un bon confort de conduite, bien qu'il soit intéressant de noter également que le cops humain est le plus sensible à l'accélération verticale autour de 4-8 Hz (ISO 2631). De l'autre côté, pour maintenir le contact route-roues, il est nécessaire que la force dynamique du pneumatique soit plus petite que $g(m_s + m_{us})$ (où g est la gravité). Ainsi, pour l'amélioration de la tenue de route, la force dynamique du pneumatique $k_t(z_{us} - z_r)$, en d'autres termes la déflexion dynamique du pneu $z_{us} - z_r$, devrait être faible dans la gamme de fréquences de 0 à 30 Hz. Notons également que la tenue de route est améliorée en limitant le rebond de roue z_{us} dans les fréquences autour de sa résonance, ie. 10-20 Hz.

En résumé, avec les remarques précédentes, les critères de performance dans le domaine fréquentiel sont décrits explicitement comme suit

- Confort

$$J_{CF} = \min \int_0^{20} \ddot{z}_s/z_r(f)df \tag{0.0.5}$$

- Tenue de route

$$J_{RH} = \min \int_0^{30} (z_{us} - z_r)/z_r(f)df \tag{0.0.6}$$

Les objectifs de la conception du contrôleur sont de minimiser les deux critères. Il est à noter que les deux critères (0.0.5) et (0.0.6 sont compatibles avec ceux donnés dans [Sammier et al., 2003] et [Savaresi et al., 2010].

Le modèle et les critères de performance pour les systèmes de suspension ont été présentés. Dans la prochaine section, nous allons présenter les résultats obtenus. D'abord, on discute des nouvelles méthodes de commande de deux types particuliers de suspensions semi-actives: amortisseur magnéto-rhéologique nonlinéaire et amortisseur hydraulique linéaire. L'objectif est de résoudre les conflits confort/tenue de route ou confort/débattement de suspension. Enfin, une méthode générique pour la commande des système LPV soumis à la saturation d'actionneur et aux contraintes d'état est proposée et appliquée au cas de la commande des suspensions semi-actives, sachant que la contrainte de passivité peut être tranformée en contrainte de saturation tandis que la limite mécanique et la tenue de route peuvent être représentées par des contraintes d'état.

Contribution 1: Commande de l'amortisseur magnéto-rhéologique

Récemment, les amortisseurs magnéto-rhéologiques (MR) sont apparus comme l'un des dispositifs les plus étudiés dans les travaux de recherche industrielles et académiques. Ils utilisent des fluides MR dont les caractéristiques peuvent être modifiées quand ils sont exposés à un champ magnétique. Comparés à d'autres types d'amortisseurs semi-actifs (comme électro-rhéologique, amortisseurs à friction...), ils ont de grands avantages tels que le temps de réponse rapide ainsi que le comportement hystérétique stable sur une large gamme de température et la basse consommation d'énergie. Ils représentent une nouvelle génération d'amortisseurs semi-actifs qui sont utilisés dans de nombreuses applications comme les amortisseurs et les dispositifs d'amortissement, les pauses embrayages, des actionneurs ou des articulations artificielles, des amortisseurs sismiques opérationnels visant à réduire le mouvement dans les bâtiments et bien sûr dans les systèmes automobiles. La Fig. 2 montre un schéma d'amortisseur MR.

Pour la commande des amortisseurs MR, dans notre article en collaboration avec S. Savaresi, C. Spelta, D. Delvecchio (voir [Do, Sename, Dugard, Savaresi, Spelta & Delvecchio, 2010]), les versions étendues du "Skyhook" ([Karnopp et al., 1974]) et du "mixed Skyhook-ADD" [Savaresi & Spelta, 2007] ont été proposées.

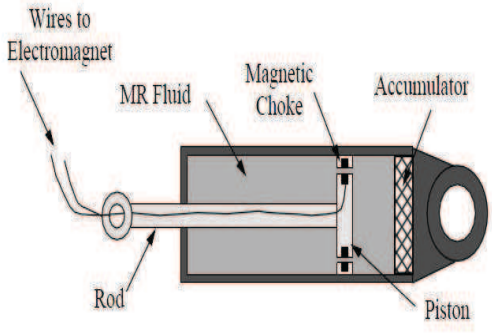

Figure 2: Schéma de principe d'un amortisseur MR.

Ici on présente l'intérêt de cette méthodologie pour la modélisation et la commande LPV de suspension semi-active. Dans cette étude, les développements récents dans nos publications [Do, Sename, Dugard, Aubouet & Ramirez-Mendoza, 2010], [Do, Sename & Dugard, 2010], [Do, Sename, Dugard & Soualmi, 2011] sont présentés pour:

- d'abord, développer un modèle LPV pour un système de suspension automobile à partir d'un modèle non-linéaire d'amortissement semi-actif,
- puis, en utilisant une représentation LPV originale de la dissipativité de l'amortisseur semi-actif, développer un contrôleur H_∞/LPV ad-hoc.
- enfin, proposer une procédure d'optimisation du contrôleur en utilisant des algorithmes génétiques.

L'ensemble du modèle LPV est utilisé pour concevoir un contrôleur polytopique H_∞ pour un système de suspension automobile équipé d'un amortisseur magnéto-rhéologique semi-actif. Ce contrôleur vise à améliorer le confort et/ou la tenue de route, selon les spécifications requises.

Modèle orienté pour la commande Dans [Lozoya-Santos, Ruiz-Cabrera, Morales-Menéndez, Ramírez-Mendoza & Diaz-Salas, 2009], les auteurs ont montré que si chaque coefficient dans le modèle de [Guo et al., 2006] est défini comme une fonction polynomiale du courant électrique, le modèle obtenu approchera mieux les données réelles. Cependant pour l'objectif de commande, un modèle simple orienté pour la commande où un seul paramètre dépendant du signal d'entrée (le courant) a été proposé et étudié la première fois dans [Do, Sename & Dugard, 2010], [Do, Spelta, Savaresi, Sename, Dugard & Delvecchio, 2010]. Selon les auteurs, le modèle suivant est approprié pour la commande:

$$F_{mr} = c_0\dot{x}_{mr} + k_0 x_{mr} + f_I \tanh\left(c_1\dot{x}_{mr} + k_1 x_{mr}\right) \tag{0.0.7}$$

où F_{mr} est la force de l'amortisseur, c_0, c_1, k_0 et k_1 sont des paramètres constants et f_I est le coefficient de force contrôlable et qui varie selon le courant électrique I dans la bobine ($0 \leq f_{Imin} < f_I \leq f_{Imax}$).

En comparaison avec le modèle original dans [Guo et al., 2006] dont les caractéristiques sont statiques et non commandables, le modèle (0.0.7) reflète le comportement réaliste d'un amortisseur MR. Ce modèle permet de satisfaire la contrainte de passivité de l'amortisseur semi-actif et présente une entrée de commande f_I. La limitation du modèle réside dans la supposition que l'hystérésis de l'amortisseur MR est invariante par rapport au courant I. La Fig. 3 présente la dépendance de la force d'amortissement au courant I. La modification du courant dans la bobine d'un amortisseur MR modifie ses caractéristiques. Ici, la bi-viscosité et l'hystérésis peuvent être clairement observées.

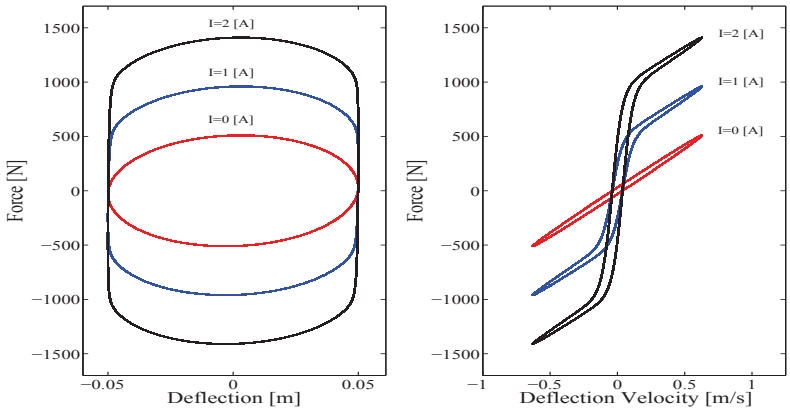

Figure 3: Caractéristiques des amortisseurs MR avec différentes valeurs de courant I: Force vs Débattement (gauche) et Force vs Vitesse (droite)

Les paramètres du modèle utilisé (voir Fig.3) sont les suivants: $c_0 = 810,78[Ns/m]$, $k_0 = 620,79[N/m]$, $c_1 = 13,76[s/m]$, $k_1 = 10,54[1/m]$. Ces paramètres expérimentaux ont été identifiés par Jorge de Jesus Lozoya-Santos (voir [Lozoya-Santos et al., 2010] et [Lozoya-Santos, Morales-Menendez, Ramirez-Mendoza & Nino-Juarez, 2009]) sur le banc d'essai au *Metalsa* [1].

Modèle orienté pour la commande de l'amortisseur semi-actif nonlinéaire En utilisant le modèle de l'amortisseur (0.0.7) et avec quelques manipulations mathéma-

[1] *www.metalsa.com.mx*

tiques, on arrive à formuler le modèle de quart de véhicule sous forme LPV.

$$\begin{cases} \dot{x} = A\left(\rho_1, \rho_2\right) x + Bu + B_1 w \\ z = C_z\left(\rho_1, \rho_2\right) x \\ y = Cx \end{cases} \tag{0.0.8}$$

- x : variables du modèle 1/4 véhicule + variable du filtre
- w: profil de route
- u : commande
- ρ_1 contient la caractéristique de l'amortisseur et la contrainte de passivité.
- ρ_2 apparaît à cause des transformations mathématiques.

Notons aussi que ρ_1 et ρ_2 ne sont pas indépendants. Comme vu dans la Fig. 4, l'ensemble de (ρ_1, ρ_2) représenté par la zone ombrée n'est pas un polytope. Dans la section suivante, une approche polytopique sera appliquée pour le système LPV (0.0.8) en considérant un polytope qui inclut toutes les trajectoires possibles des paramètres variants de (ρ_1, ρ_2) considérés comme indépendants.

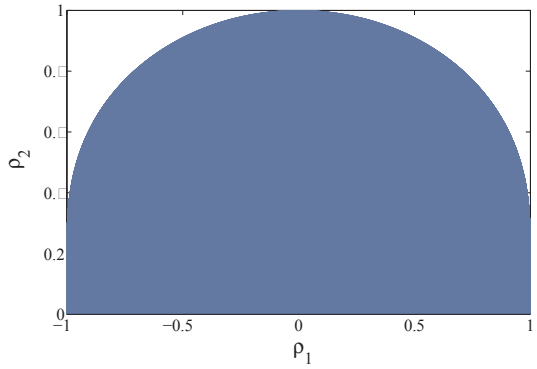

Figure 4: Paramètres variants (ρ_1, ρ_2) (zone ombrée).

En effet, le but est de trouver un contrôleur LPV qui garantit la stabilité et la performance H_∞ pour le système (0.0.8). Il est bien connu que la qualité de ce contrôleur dépend du choix de certaines fonctions de pondération. Par la suite, une procédure générale pour l'optimisation des fonctions de pondération sera proposée puis appliquée à la commande de suspension semi-active.

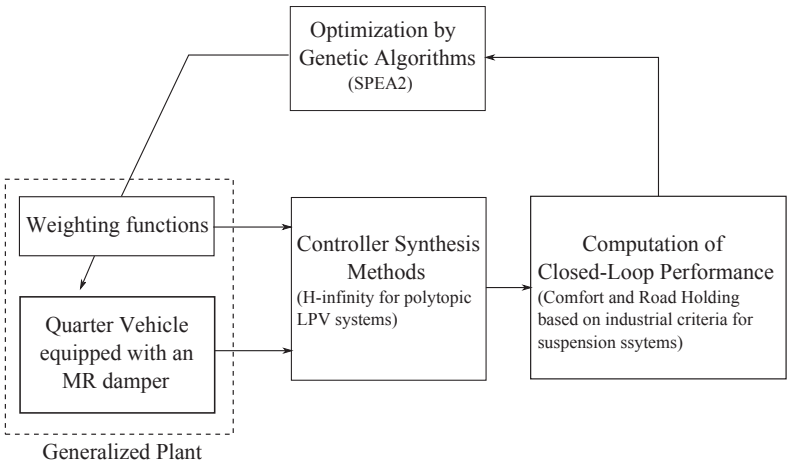

Figure 5: Optimisation du régulateur pour la commande de la suspension semi-active à l'aide d'algorithmes génétiques.

Méthode proposée pour optimiser la commande LPV de suspension semi-active

- Etape 1: Initialiser la première génération avec des valeurs positives aléatoires des paramètres des fonctions de pondération et de la borne supérieure de la norme L_2 du système en boucle fermée.
- Etape 2: Résoudre les LMIs (voir dans [Scherer et al., 1997]) pour obtenir un contrôleur LPV $K_c(\rho)$. Calculer la fonction d'objectif J en utilisant 0.0.9 (notons que $J^D = \infty$ quand les constrôleurs $K_c(\rho)$ sont instables).
- Etape 3: Utiliser l'algorithme SPEA2 [Zitzler et al., 2001] pour sélectionner les meilleurs individus qui peuvent entrer dans la prochaine génération.
- Etape 4: Si le nombre de génération est inférieur à une valeur maximale, revenir à l'étape 2 avec la nouvelle génération obtenue dans l'étape 3. Sinon, arrêter le programme et sauve-garder les individus de la dernière génération. Ces individus seront étudiés a posteriori pour choisir les meilleures solutions (orientés pour le confort ou la tenue de route).

$$J^D = \begin{bmatrix} J^D_{\text{Comfort}} \\ J^D_{\text{RoadHolding}} \end{bmatrix} \tag{0.0.9}$$

$$J^D_{\text{Comfort}} = \sum_{i=1}^{4} \int_0^{12} (\ddot{z}_s / z_r(f)_i) df$$

$$J^D_{\text{RoadHolding}} = \sum_{i=1}^{4} \int_{10}^{20} (z_{us}/z_r(f)_i) df$$

Contribution 2: Commande de l'amortisseur linéaire hydraulique

Bien que la non-linéarité dans le modèle de l'amortisseur doive être prise en compte dans la conception de contrôleur, de nombreuses études ont été basées sur des modèles de système de suspension simple avec amortisseurs hydrauliques linéaires. La raison pour laquelle les amortisseurs linéaires ont été plus intensivement étudiés est que les modèles de véhicules avec ces amortisseurs permettent, a priori, de faire face à des problèmes plus généraux et complexes et de tester l'efficacité des méthodes de conception dans le cas idéal (en omettant la non-linéarité). Dans ce chapitre, nous revisitons le problème de commande de l'amortisseur linéaire. Une nouvelle approche, basée sur la stabilisation forte, est proposée.

Approche par la stabilisation forte pour la commande des amortisseurs semi-actifs linéaires Considérons le modèle de véhicule représenté dans la Fig. 1 équipée d'un amortisseur linéaire caractérisée par l'équation suivante:

$$F_{damper} = c\dot{z}_{def} \tag{0.0.10}$$

Tout d'abord, décomposons la force de l'amortisseur comme $F_{damper} = c_0\dot{z}_{def} + u$ où $c_0 = (c_{min} + c_{max})/2$ et considérons une représentation d'état du modèle quart de véhicule comme suit:

$$\begin{aligned} \dot{x_s} &= A_s x_s + B_{s1} w + B_{s2} u \\ y &= C_s x_s \end{aligned} \tag{0.0.11}$$

où $x_s = (z_s,\ \dot{z}_s,\ z_{us},\ \dot{z}_{us})^T$, $w = z_r$, $y = \dot{z}_s - \dot{z}_{us} = \dot{z}_{def}$.

$$A_s = \begin{bmatrix} 0 & 1 & 0 & 0 \\ \frac{-k_s}{m_s} & \frac{-c_0}{m_s} & \frac{k_s}{m_s} & \frac{c_0}{m_s} \\ 0 & 0 & 0 & 1 \\ \frac{k_s}{m_{us}} & \frac{c_0}{m_{us}} & -\frac{k_s+k_t}{m_{us}} & -\frac{c_0}{m_{us}} \end{bmatrix}, B_{s1} = \begin{bmatrix} 0 & 0 & 0 & \frac{k_t}{m_{us}} \end{bmatrix}^T,$$

$$B_{s2} = \begin{bmatrix} 0 & \frac{-1}{m_s} & 0 & \frac{1}{m_{us}} \end{bmatrix}^T, C_s = \begin{bmatrix} 0 & 1 & 0 & -1 \end{bmatrix}.$$

Remark 0.0.1. En fait, u est la force compensée ajoutée à un amortisseur nominal dont le coefficient d'amortissement est égal à c_0. Pour satisfaire la contrainte de passivité d'un amortisseur semi-actif, l'entrée de commande u doit être limitée par

$$|u(t)| \leq \frac{c_{max} - c_{min}}{2} |\dot{z}_{def}(t)| \quad \forall t \geq 0 \tag{0.0.12}$$

Notons $U(s)$, $\dot{Z}_{def}(s)$ les transformées de Laplace de u et $\dot{z}_{def}$. Considérons la condition suivante

$$|U(j\omega)| \leq \frac{c_{max} - c_{min}}{2} |\dot{Z}_{def}(j\omega)| \quad , \forall \omega \tag{0.0.13}$$

On peut voir que la contrainte (0.0.13) n'implique pas (0.0.12). Cependant, si nous supprimons certains dépassements à court terme dans les réponses de u (ce qui peut violer la contrainte de passivité, à court terme), (0.0.13) est une bonne approximation de (0.0.12) et plus facile à manipuler.

Remark 0.0.2. Comme vu dans (0.0.11), la vitesse de déflection $\dot{z}_{def}$ est une mesure de sortie du système. Ce choix est fait pour la raison suivante. Remarquons que s'il existe un contrôleur stabilisant LTI K pour le système (0.0.11) et que

$$\|K\|_\infty = \frac{\|u\|_2}{\|\dot{z}_{def}\|_2} \leq \frac{c_{max} - c_{min}}{2} \quad \text{pour tout } \dot{z}_{def} \text{ t.q } 0 < \|\dot{z}_{def}\|_2 < \infty \tag{0.0.14}$$

alors K satisfait (0.0.13).

Remark 0.0.3. Si un contrôleur stable est utilisé avec un système stable, nous évitons l'instabilité du système en boucle fermée (précisément l'instabilité du contrôleur, car le système en boucle ouverte est déjà stable) en raison de la non-linéarité entre le système en boucle ouverte et le contrôleur, comme la saturation d'entrée.

Avec les remarques ci-dessus, les contrôleurs stables avec un gain limité semblent être un choix raisonnable pour les systèmes de suspension semi-active, ce qui motive l'utilisation de la stabilisation forte présentée dans le chapitre 4.

Comme la commande H_∞ conventionnelle, dans cette approche, nous utilisons également certaines fonctions de pondération pour atteindre les performances souhaitées (0.0.5) - (0.0.6). Le schéma bloc de commande est représenté dans la Fig. 6 où les fonctions de pondération sont choisies comme

$$W_{z_r} = 3 \times 10^{-2} \tag{0.0.15}$$

$$W_{\ddot{z}_s} = k_{\ddot{z}_s} \frac{s^2 + 2\xi_{11}\Omega_{11}s + {\Omega_{11}}^2}{s^2 + 2\xi_{12}\Omega_{12}s + {\Omega_{12}}^2} \tag{0.0.16}$$

$$W_{z_{us}} = k_{z_{us}} \frac{s^2 + 2\xi_{21}\Omega_{21}s + {\Omega_{21}}^2}{s^2 + 2\xi_{22}\Omega_{22}s + {\Omega_{22}}^2} \tag{0.0.17}$$

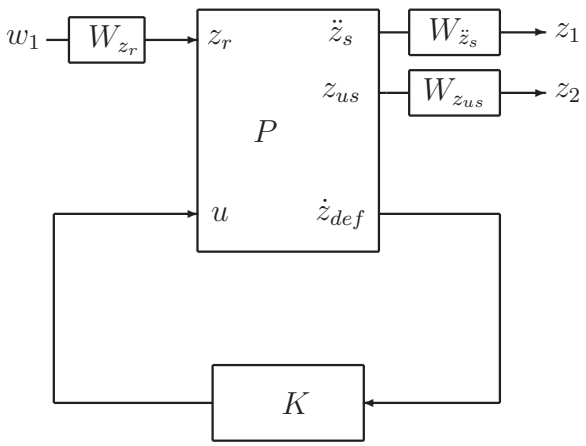

Figure 6: Schéma bloc pour l'approche par stabilisation forte

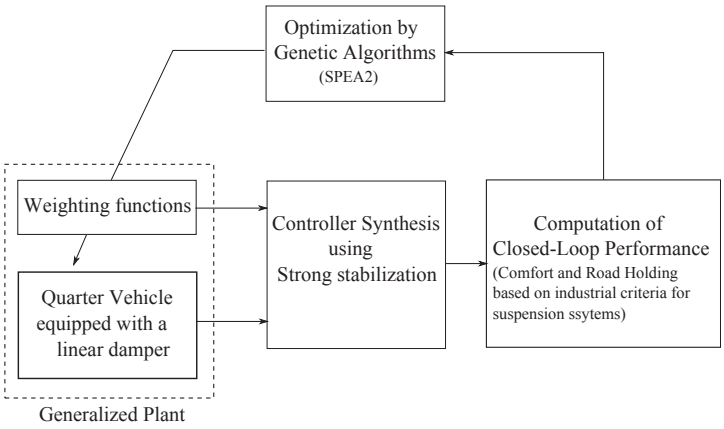

Figure 7: Optimisation du contrôleur de suspension semi-active par algorithmes génétiques.

Encore une fois, la procédure d'optimisation des fonctions de pondération présentée dans la partie de commande d'amortisseur MR est utilisée. L'objectif est de trouver des contrôleurs stables et à gain limité (voir [Gümüssoy & Özbay, 2005] et [Cheng et al., 2007]) tels que la fonction d'objectif suivante soit minimisée:

$$\min_{\{\nu\}\in R_+^{10}} J^D(\nu) = \begin{bmatrix} J^D_{\text{Comfort}}(\nu) \\ J^D_{\text{RoadHolding}}(\nu) \end{bmatrix} \tag{0.0.18}$$

où

$$J^D_{\text{Comfort}} = \alpha_1 \int_0^{1.5} (\ddot{z}_s/z_r - R_1)^2 df + \alpha_2 \int_3^{10} (\ddot{z}_s/z_r - R_2)^2 df + \alpha_3 \frac{\|K\|_\infty}{\gamma} \tag{0.0.19}$$

$$J^D_{\text{RoadHolding}} = \beta_1 \int_{10}^{20} (z_{us}/z_r - R_3)^2 df + \beta_2 \frac{\|K\|_\infty}{\gamma} \tag{0.0.20}$$

où R_1 (respectivement R_2) est la réponse fréquentielle de $\ddot{z}_s/z_r$ de l'amortisseur passif "Hard" (respectivement "Soft") et R_3 est la réponse fréquentielle de z_{us}/z_r de l'amortisseur passif "Hard"; $\alpha_i > 0$ avec $i = 1 : 3$ et $\beta_j > 0$ avec $j = 1 : 2$ sont des coefficients de pondération.

Contribution 3: L'effet de butée sur le confort

Il est bien évident que le compromis confort/tenue de route a été étudié dans de nombreuses approches au cours des dernières décennies. La question sur l'amélioration du débattement de la suspension n'a pas été toujours considéré. Atteindre les limites structurelles, lorsque la perturbation routière est particulièrement importante, dégrade considérablement le confort des passagers (l'effet de butée) et diminue la durée de vie des composants du véhicule.

Dans cette thèse, le compromis entre le confort des passagers et le débattement de suspension est étudié. Les résultats présentés dans ce chapitre ont été obtenus lors de mon séjour de 6 mois au Dipartimento di Elettronica Informazione ed, Politecnico di Milano avec Sergio Savaresi, Cristiano Spelta et Diego Delvecchio.

Le premier résultat a été présenté à la conférence CDC-2010 (voir l'annexe C). Dans ce papier, une méthode hybride basée sur la commutation ADD (Acceleration Driven Damper) et la commande LPV (voir chapitre 3) a été développé pour un modèle de véhicule non-linéaire équipé d'amortisseurs MR non linéaires afin d'améliorer le confort et débattement de suspension.

Dans le chapitre 6, nous présentons un autre résultat obtenu récemment pour les systèmes "dual-stage suspension system" (représentant les sièges du conducteur sur les poids lourds) en utilisant des amortisseurs hydrauliques linéaires. L'objectif de commande est également d'améliorer le confort du conducteur tout en tenant compte du débattement de suspension (la tenue de route n'est plus considérée). Pour y parvenir, nous utilisons l'approche de stabilisation forte pour la commande de suspension semi-active proposée dans le chapitre 4.

Contribution 4: Commande des système LPV soumis à la saturation des entrées et à la contrainte d'états

Motivation La problème complet de commande de suspension semi-active est de réaliser le meilleur compromis entre:

- Le confort en termes d'accélération verticale de la voiture $\ddot{z}_s$.
- La tenue de route en termes de la déflection dynamique du pneu $z_{us} - z_r$.
- La déflection en termes de débattement de l'amortisseur $z_s - z_{us}$.

ainsi que de garantir la contrainte de passivité.

Dans presque toutes les approches trouvées dans la littérature, le problème à résoudre consiste à optimiser un critère multi-objectif:

$$\text{minimiser} \qquad [\|\ddot{z}_s\|, \|z_{uz} - z_r\|, \|z_s - z_{us}\|]^T \tag{0.0.21}$$

$$\text{sous les contraintes de passivité} \tag{0.0.22}$$

Il est important de noter que le débattement de l'amortisseur est une contrainte physique (plutôt qu'un objectif de performance)

$$|z_s - z_{us}| < \Delta_s = const \tag{0.0.23}$$

où Δ_s est la course de la suspension, et que la condition de tenue de route peut être représentée de façon simplifiée par la contrainte suivante

$$z_{us} - z_r < \frac{g(m_s + m_{us})}{k_t} = const \tag{0.0.24}$$

Pour la commande de suspension, les contraintes (0.0.23)-(0.0.24) peuvent être représentées par des contraintes d'états. Le problème d'optimisation multi-objectif 0.0.25-0.0.27 devient un problème d'optimisation avec un seul objectif.

$$\text{minimiser} \qquad \|\ddot{z}_s\| \tag{0.0.25}$$

$$\text{sous la contrainte de passivité} \tag{0.0.26}$$

$$\text{et les contraintes (0.0.23) et (0.0.24)} \tag{0.0.27}$$

Toutes les remarques ci-dessus motivent l'étude du problème général qui est de garantir la stabilité et la performance des systèmes LPV soumis à la saturation d'entrée et à des contraintes sur l'état.

Définition du problème L'objectif est de synthétiser un contrôleur LPV composant un terme anti-windup statique pour le système LPV avec saturation d'entrée de façon à ce que les conditions suivantes soient remplies:
(i) En l'absence de perturbations, ou si les perturbations disparaissent, le contrôleur

garantit la stabilité régionale asymptotique de l'origine pour un paramètre variant arbitraire θ. En présence de perturbations bornées en amplitude, le contrôleur garantit que les trajectoires du système en boucle fermée sont bornées.
(ii) Le contrôleur garantit les contraintes sur les états du système en boucle fermée.
(iii) Lorsque la saturation n'est pas active, le contrôleur garantit une borne supérieure de γ sur la norme L_2 du transfert entre l'entrée des perturbations et la sortie à commander.

Remark 0.0.4. Considérant la même performance L_2 lorsque le système fonctionne de manière linéaire et en mode de saturation peut conduire à des résultats très conservatifs. Nous considérons donc que les performances L_2 devraient être satisfaites uniquement pour le système sans saturation, ce qui correspond à un problème H_∞ classique. D'autre part, si le contrôleur sature, il faut s'assurer que les trajectoires restent bornées et ne violent pas les contraintes d'état.

Considerons le système LPV suivant

$$\begin{aligned} \dot{x} &= A(\theta)x + B_w(\theta)w + B_u u \\ z &= C_z(\theta)x + D_{zw}(\theta)w + D_{zu}u \\ y &= C_y x + D_{yw}w \end{aligned} \tag{0.0.28}$$

et le contrôleur composant un terme anti-windup statique

$$\begin{aligned} \dot{x}_c &= A_c(\theta)x_c + B_c(\theta)u_c + E_c(\theta)(sat(y_c) - y_c) \\ y_c &= C_c(\theta)x_c + D_c(\theta)u_c \end{aligned} \tag{0.0.29}$$

Les hypothèses suivantes sont considérées:

- *Hypothèse 1:* Les matrices B_u, D_{zu}, C_y et D_{yz} sont supposées indépendantes de paramètres variants (pour satisfaire les hypothèses de conception pour les systèmes LPV polytopique).

- *Hypothèse 2:* La perturbation d'entrée est limitée en amplitude, c.à.d $\forall t > 0, w(t) \in \mathcal{W}$ avec
$$\mathcal{W} = \{w \in \mathbb{R}^q : w^T w < \delta\} \tag{0.0.30}$$

- *Hypothèse 3:* Les paramètres variants dépendent des états du système $\theta = \theta(x,t)$ (ie quasi-LPV) et sont bornés dans
$$\Theta = \{\theta : \underline{\theta}_i \leqslant \theta_i \leqslant \overline{\theta}_i, i = 1, ..., k\} \tag{0.0.31}$$

- *Hypothèse 4:* Les entrées de commande sont bornées en amplitude:

$$-\overline{u}_i \leqslant u_i(t) \leqslant \overline{u}_i, \quad i = 1, ..., m \tag{0.0.32}$$

La solution pour la commande des système LPV 0.0.28 soumis à la saturation des entrées et à la contrainte d'états est donné par le théorème suivant.

Theorem 0.0.1. *Si, pour les scalaires donnés $\beta_1 > 0$ et $\gamma > 0$, il existe des matrices symétriques définies positives $X, Y \in \mathbb{R}^{n\times n}$, un scalaire positif β_2, des matrices diagonales défini-positives $S \in \mathbb{R}^{m\times m}$, les matrices $\hat{A}(\theta)\ in R^{n\times n}$, $\hat{B}(\theta)\ in R^{n\times p}$, $\hat{C}(\theta)$, $\hat{Z}_1(\theta)$, $\hat{Z}_2(\theta) \in R^{m\times n}$, $\hat{D}(\theta) \in R^{m\times p}$, $\hat{Q}(\theta) \in R^{n\times m}$ tels que les inégalités matricielles (0.0.34) - (0.0.38) sont vérifiées, alors le contrôleur LPV anti-windup (0.0.29) avec des matrices*

$$\begin{cases} E_c(\theta) = N^{-1}\hat{Q}(\theta) S^{-1} - N^{-1} Y B_u \\ D_c(\theta) = \hat{D}(\theta) \\ C_c(\theta) = [\hat{C}(\theta) - D_c(\theta) C_y X] M^{-T} \\ B_c(\theta) = N^{-1}[\hat{B}(\theta) - Y B_u D_c(\theta)] \\ A_c(\theta) = N^{-1}[\hat{A}(\theta) - N B_c(\theta) C_y X - Y B_u C_c(\theta) M^T \\ \qquad -Y(A(\theta) + B_u D_c(\theta) C_y) X] M^{-T} \end{cases} \tag{0.0.33}$$

où M et N vérifient $MN^T = I - XY$, résoud le problème défini ci-dessus.

$$\begin{bmatrix} \mathcal{L}_{11}(\theta) & \mathcal{L}_{12}(\theta) & \mathcal{L}_{13}(\theta) & \mathcal{L}_{14}(\theta) \\ * & \mathcal{L}_{22}(\theta) & \mathcal{L}_{23}(\theta) & \mathcal{L}_{24}(\theta) \\ * & * & \mathcal{L}_{33}(\theta) & \mathcal{L}_{34}(\theta) \\ * & * & * & \mathcal{L}_{44}(\theta) \end{bmatrix} \prec 0 \tag{0.0.34}$$

$$\begin{bmatrix} \mathcal{O}_{11}(\theta) & \mathcal{O}_{12}(\theta) & \mathcal{O}_{13}(\theta) & \mathcal{O}_{14}(\theta) \\ * & \mathcal{O}_{22}(\theta) & \mathcal{O}_{23}(\theta) & \mathcal{O}_{24}(\theta) \\ * & * & \mathcal{O}_{33}(\theta) & \mathcal{O}_{34}(\theta) \\ * & * & * & \mathcal{O}_{44}(\theta) \end{bmatrix} \prec 0 \tag{0.0.35}$$

$$\begin{bmatrix} X & * & * \\ I & Y & * \\ \hat{C}_i(\theta) - \hat{Z}_{1i}(\theta) & (\hat{D}(\theta) C_y)_i - \hat{Z}_{2i}(\theta) & \bar{u}_i^2 \end{bmatrix} \succeq 0 \quad for\ i = 1:m \tag{0.0.36}$$

$$\begin{bmatrix} X & * & * \\ I & Y & * \\ H_{1i}X & H_{1i} & h_{0i}^2 \end{bmatrix} \succeq 0 \quad for\ i = 1:s \tag{0.0.37}$$

$$\beta_2\delta - \beta_1 \prec 0 \tag{0.0.38}$$

où

$$\begin{aligned}
\mathcal{L}_{11}(\theta) &= A(\theta)X + XA(\theta)^T + B_u\hat{C}(\theta) + \hat{C}(\theta)^T B_u^T + \beta_1 X \\
\mathcal{L}_{12}(\theta) &= A(\theta) + \hat{A}(\theta)^T + B_u\hat{D}(\theta)C_y + \beta_1 I_n \\
\mathcal{L}_{13}(\theta) &= -B_u S + \hat{Z}_1(\theta)^T \\
\mathcal{L}_{14}(\theta) &= B_u\hat{D}(\theta)D_{yw} + B_w(\theta) \\
\mathcal{L}_{22}(\theta) &= YA(\theta) + A(\theta)^T Y + \hat{B}(\theta)C_y + C_y^T\hat{B}(\theta)^T + \beta_1 Y \\
\mathcal{L}_{23}(\theta) &= -\hat{Q}(\theta) + \hat{Z}_2(\theta)^T \\
\mathcal{L}_{24}(\theta) &= \hat{B}(\theta)D_{yw} + YB_w(\theta) \\
\mathcal{L}_{33}(\theta) &= -2S \\
\mathcal{L}_{34}(\theta) &= \hat{D}(\theta)D_{yw} \\
\mathcal{L}_{44}(\theta) &= -\beta_2 I \\
\mathcal{O}_{11}(\theta) &= A(\theta)X + XA(\theta)^T + B_u\hat{C}(\theta) + \hat{C}(\theta)^T B_u^T \\
\mathcal{O}_{12}(\theta) &= \hat{A}(\theta)^T + A(\theta) + B_u\hat{D}(\theta)C_y \\
\mathcal{O}_{13}(\theta) &= B_w(\theta) + B_u\hat{D}(\theta)D_{yw} \\
\mathcal{O}_{14}(\theta) &= XC_z(\theta)^T + \hat{C}(\theta)^T D_{zu}^T \\
\mathcal{O}_{22}(\theta) &= YA(\theta) + A(\theta)^T Y + \hat{B}(\theta)C_y + C_y^T\hat{B}(\theta)^T \\
\mathcal{O}_{23}(\theta) &= YB_w(\theta) + \hat{B}(\theta)D_{yw} \\
\mathcal{O}_{24}(\theta) &= C_z(\theta)^T + C_y^T\hat{D}(\theta)^T D_{zu}^T \\
\mathcal{O}_{33}(\theta) &= -\gamma I_m \\
\mathcal{O}_{34}(\theta) &= D_{zw}(\theta)^T + D_{yw}^T\hat{D}(\theta)^T D_{zu}^T \\
\mathcal{O}_{44}(\theta) &= -\gamma I_p
\end{aligned} \tag{0.0.39}$$

Le théorème ci-dessus est ensuite appliqué au cas de la commande de la suspension semi-active (voir chapitre 6).

Conclusions et perspectives

Conclusions

Cette thèse a été consacrée au problème de l'amélioration de la dynamique du véhicule en termes de confort et de tenue de route. Ceci est principalement réalisé par les systèmes de commande de suspension. En ce qui nous concerne, nous avons plus particulièrement étudié le contrôle de la suspension semi-active qui, en outre, est un problème intéressant pour les aspects à la fois académiques et industriels. Les résultats sur ce sujet ont été

présentés dans les chapitres 3, 4, 5 et 6. En résumé, les principales contributions de la thèse sont les suivantes:

En termes de modélisation:

- Un modèle pour la commande LPV de suspensions semi-actives avec des amortisseurs magnéto-rhéologiques (où les caractéristiques de la bi-viscosité et l'hystérésis sont prises en compte) (chapitre 3).
- Un nouveau modèle pour la commande LPV des amortisseurs linéaires où la vitesse de l'amortisseur est considérée comme un paramètre variant (chapitre 6).

En termes de méthodologie de commande:

- La conception LPV pour la commande des amortisseurs MR non linéaires (chapitre 3).
- Une version étendue du Skyhook-ADD pour la commande des amortisseurs MR non linéaires (annexe A).
- La conception d'une nouvelle loi de commande optimale "clipped" pour les amortisseurs hydrauliques semi-actifs linéaires basée sur l'approche par stabilisation forte (chapitres 4 et 5).
- La conception d'une loi de commande générique LPV avec des contraintes de saturation et d'état. Les résultats obtenus peuvent être éventuellement appliqués à la fois pour les amortisseurs non-linéaires et linéaires (chapitre 6).
- Une procédure d'optimisation multi-objectif à l'aide d'algorithmes génétiques pour le problème de commande de suspensions semi-actives. L'intérêt de la méthodologie se trouve dans le fait qu'il peut fournir un ensemble de contrôleurs qui peuvent approcher les meilleures solutions pour le problème de commande de suspensions semi-actives.

En termes d'application:

- Modèle de quart de véhicule (pour l'amélioration du confort, la tenue de route et le débattement de suspension).
- Modèle de chaise (pour l'amélioration du confort et du débattement de suspension).

Enfin, du point de vue de la mise en oeuvre en pratique, les méthodes proposées sont intéressantes dans les points suivants:

- Simple et facile à mettre en oeuvre: un capteur de déplacement unique sert à mesurer le débattement de suspension (la vitesse de débattement peut être déduite numériquement à partir du débattement de suspension) et les contrôleurs sont stables.
- Robuste face au transfert de charge et à l'incertitude de la masse suspendue (facteurs inévitables qui apparaissent sur un véhicule quand il se déplace).

Perspectives

Bien que certains résultats ont été obtenus, le travail peut être poursuivi avec les quelques orientations suivantes.

Perspectives à court terme

- Pour les amortisseurs MR, l'utilisation de l'approche par stabilisation forte pour des systèmes LPV est un point clé pour réduire le conservatisme. Dans le chapitre 3, les contrôleurs LPV stables n'ont pas été synthétisés. Nous avons juste utilisé une "astuce" (algorithme 1, page 82) pour enlever les contrôleurs instables lors de l'optimisation par algorithmes génétiques. Par ailleurs, l'application des résultats au chapitre 6 (commande des systèmes LPV soumis à des contraintes de saturation et d'état) pour des amortisseurs MR seront testés et comparés avec les méthodes proposées (LPV conventionnelle, le Skyhook-ADD étendu).
- Améliorer les résultats de simulation dans le chapitre 6 est nécessaire. Par ailleurs, les comparaisons avec les autres méthodes de contrôle doivent être faites pour démontrer l'efficacité de la méthode proposée (sous réserve de commande LPV avec les contraintes de saturation et d'état).
- A partir des résultats obtenus dans le chapitre 5, l'étude sur les systèmes "Dual-Stage Suspension" sera étendue à la commande des systèmes de suspension avec l'amortissement et la rigidité variables.
- Un test des méthodes proposées sur une plate-forme réelle sera réalisé.

Perspectives à long terme

- Les recherches sur le commande de commutation d'une loi à une autre sont également à développer. Dans [Geromel & Colaneri, 2006], [Geromel & Colaneri, 2010], les auteurs ont proposé une méthode basée sur les inégalités de Lyapunov-Metzler pour déterminer la loi de commutation de façon à ce que la stabilité et la minimisation d'une fonction de coût soient garanties en même temps. Ce sont des bonnes références initiales pour la poursuite des recherches dans le domaine de la commutation.

- Lorsque l'on travaille avec les systèmes LPV de suspension, il serait préférable de les séparer en des petits sous-systèmes LPV et puis commuter entre eux de façon à ce que la stabilité du système en boucle fermée reste vérifiée et les performances sont optimisées. L'idée est liée à la commande de commutation hybride LPV (voir [Lim & Chan, 2003], [Lu & Wu, 2004] et les références citées.

- Tout au long de la thèse, la procédure commune pour résoudre le problème d'optimisation multi-objectif de commande de suspensions semi-actives a été d'utiliser les algorithmes génétiques. Les fonctions de pondération des paramètres sont le vecteur de décision. Il est également intéressant de considérer la même procédure d'optimisation (algorithme génétique) mais en considérant cette fois ci les paramètres du contrôleur comme un vecteur de décision. Par ailleurs, l'essai avec plusieurs sorties de mesure différentes peuvent être réalisées pour obtenir la meilleure solution.

- Jusqu'à présent, les systèmes de suspension, de direction et de freinage ont été étudiés séparément. La bonne coopération entre ces sous-systèmes n'est pas une tâche triviale. Comme l'a dit Maurice Olley "The engineers had made all parts function excellently, but when put together the whole was seldom satisfactory". Ceci nous motive donc pour étudier et développer une commande globale de châssis.

List of Figures

List of Tables

Thesis framework and contribution

Thesis framework

This thesis presents the three-years work (from October 2008 to September 2011), performed in the SLR (Systèmes Linéaires et Robustesse) team from the Control Systems department of GIPSA-Lab, on the "*LPV Approach for Robust control of vehicle dynamics: Joint improvement of comfort and road holding*", under the supervision of Olivier Sename (Professor, Grenoble INP) and Luc Dugard (Research Director, CNRS). This work has been supported by a Minister of Research (MESR) grant and it is also part of the INOVE (INtegrated approach for Observation and control of VEhicle dynamics) ANR project 2010-2014.

The thesis is the continuity of previous works made in the SLR research team by

- Ricardo Ramirez-Mendoza (see [Ramirez-Mendoza, 1997]), "Sur la modélisation et la commande de véhicules automobiles", which was the first study in the automotive framework. The work was focused on the description and modeling of vehicles, as well as first attempts on control methodologies for active cruise control.

- Damien Sammier (see [Sammier, 2001]), "Sur la modélisation et la commande de suspension de véhicules automobiles" presented the modeling and control design of an active suspension (using H_∞ control for LTI system). The semi-active suspension modeling and control were also studied for a PSA Peugeot-Citroën semi-active damper.

- Alessandro Zin (see [Zin, 2005]), "Sur la commande robuste de suspensions automobiles en vue du contrôle global de châssis", which extended the previous works with a strong attention on H_∞/LPV control of an active suspension in order to improve robustness properties. A sketch of global chassis control through the use of the four suspensions was also derived using an anti-roll distribution.

- Charles Poussot-Vassal (see [Poussot-Vassal, 2008]) "Robust Multivariable Linear Parameter Varying Control of Automotive Chassis" provided tools and control

design methodologies in order to improve comfort and safety in automotive vehicles. Two main contributions are the semi-active suspension control (using an LPV approach to improve the passenger comfort and road holding) and the Global Chassis Control (involving the control of the braking and steering actuators for vehicle active safety improvement).

- Sébastien Aubouet (see [Aubouet, 2010]) presented an observer design methodology allowing the suspension designer to build and adjust an appropriate observer, estimating the non-measured variables. Then, the previous results of Charles Poussot-Vassal, for semi-active suspension control, were extended to the full vertical car, and completed with both a pole placement method, a scheduling strategy based on a damper model and a local damper control.

During three years, the Rhônes-Alpes Region offered me an ExploraDoc scholarship to spend six months in a foreign institute. Therefore, I had chance to work with **Sergio Saveresi, Cristiano Spelta, Diego Delvecchio and Mara Tanelli** (in Dipartimento di Elettronica ed Informazione, Politecnico di Milano, Italia) on semi-active suspension control. The collaboration resulted in two conference papers "*An extension of Mixed Sky-hook and ADD to Magneto-Rheological dampers*" [Do, Spelta, Savaresi, Sename, Dugard & Delvecchio, 2010] and "*An LPV control approach for comfort and suspension travel improvements of semiactive suspension systems*" [Do, Sename, Dugard, Savaresi, Spelta & Delvecchio, 2010] and a potential paper (in preparation) on the control of variable damping and stiffness suspension systems. I had also the chance to work with **Joao M. Gomes da Silva Jr.** when he was at GIPSA-Lab for a two-month research stay. The discussions on the input saturation control gave rise to a conference paper "*Control design for LPV systems with input saturation and state constraints: an application to a semi-active suspension*" [Do, Gomes da Silva Jr., Sename & Dugard, 2011]. And last, I have had a collaboration with **Jorge Lozoya-Santos** (a mexican PhD student involved in the PCP project 2007-2010 MCOS between the Tecnologico de Monterrey and GIPSA-Lab). So far, we have discussed mainly on control of Magneto-Rheological Dampers. The paper on "*Modélisation et commande LPV d'un amortisseur Magnéto-Rhéologique*" [Do, Lozoya-Santos, Sename, Dugard, Ramirez-Mendoza & Morales-Menendez, 2010] is one of the initial results for the control of nonlinear Magneto-Rheological dampers.

Motivation and objectives

Today, almost new and sophisticated technologies of numerous domains such as mechanics, electronics, communication, automatics can be found in a modern vehicle. Let us take for example, the use of hybrid electric engines which are expected to minimize the noise, fuel consumption and pollutants emissions; the camera-based technologies to

sense the surroundings in a vehicle which provide visual information and active warning to driver; wireless communication with the outside world (with other vehicles or communication centers) which increases safety, or enhances the driving experience. Although these technologies provide more and more convenience and pleasure to users, the basic factor that decides the vehicle performance is its dynamics. In fact, the vehicle dynamics have been an attractive subject in both industrial and academic research for a long time. The design and control of main actuators which are essential to vehicle dynamics have been intensively investigated. In this framework, the suspension systems, along with the braking and steering systems, play a key role. It has been proven by many studies, in both automatic control theory and practice, that the suspension systems improve considerably the vehicle comfort, safety and handling. Recently, the invention of new technologies (Electro-Rheological, Magneto-Rheological Dampers...) has opened a new trend in study and application of such actuators to the automobile.

The vehicle suspension systems using semi-active dampers (a particular type of suspension systems in between passive and active ones) are the research objects of this thesis. Besides the possible cooperation with steering and braking elements in an integrated control scheme for a better dynamics improvement, they have a distinguishing contribution to comfort and road holding (two main and basic criteria for a vehicle). Many approaches were devoted to a comfort oriented or road holding oriented enhancement. Others proposed general methods to deal with both of them, but the optimal results (in the sense of Pareto optimal) were never discussed to show their effectiveness. Moreover, it can be seen from the existing studies on semi-active suspension control that the common difficulty is the passivity constraint. Indeed, this is the main problem to handle. Furthermore, for a more realistic design, the nonlinearities and the restrictive travel (due to the mechanical limitation) of a semi-suspension system should be taken into account as well. To summarize, the following problems are interesting and challenging for semi-active suspension control, and part of the dissertation content.

- Multi-objective optimization control problems.
- Nonlinearity of semi-active suspension systems.
- Constrained control (passivity constraint and mechanical limits).

The important role of the suspension systems in vehicles, in general, and the interesting theoretical problems in controller design of semi-active suspension, in particular, motivated our study. The objective of this thesis is to propose a generic method to obtain a good compromise between comfort and road holding while taking into account the important characteristics and constraints (nonlinearities, passivity constraint and mechanical constraint).

Structure of the thesis

- Chapter 1 introduces the general framework of semi-active suspension control. First a brief overview on vehicle dynamic control is made and the suspension system is discussed in terms of performance objectives and mathematical models for control. Finally, the semi-active suspension is emphasized by the classification, characteristics, modeling and existing control methods in the literature.

- Chapter 2 gives some backgrounds on control theory and optimization which are useful for the development of new semi-active suspension controllers in the thesis. For this purpose, some well-known definitions, lemmas and theorems on convex optimization, Linear Matrix Inequaliy (LMI), Linear Parameter Varying (LPV) control, saturation control and multi-objective optimization by genetic algorithms are presented.

- Chapter 3 presents the control of semi-active suspension systems using nonlinear Magneto-Rheological dampers. The extended versions of existing methods for Magneto-Rheological dampers and the new LPV one to improve comfort and road holding are discussed.

- Chapter 4 revisits the classical semi-active suspension control problem based on a linear damper model. A new "clipped method" based on *strong stabilization* approaches is presented. Like in chapter 3, comfort and road holding are design objectives.

- Chapter 5 studies the effect of suspension travel in passenger/driver comfort. In this chapter, we make use of the results obtained in Chapters 3 and 4 to solve the comfort and suspension deflection trade-off of the quarter car model with nonlinear Magneto-Rheological dampers and Dual-Stage Suspension model (chair model) with linear semi-active dampers. These results have been obtained during my 6-months visiting research in Politecnico di Milano.

- Chapter 6 is devoted to a new control method for LPV systems with input saturation and state constraints. Although, the study has not exhaustively investigated yet, the preliminary results seem to be suitable to semi-active suspension control to solve a complete problem in semi-active suspension control (multi-objective optimization, nonlinearity, passivity constraint and mechanical constraint). This is also the first result of our collaboration with Joao M. Gomes da Silva Jr.

Contributions

Book chapter

[1] A. L.Do, O. Sename and L. Dugard, *LPV modelling and control of semi-active dampers in automotive systems*, in **Control of Linear Parameter Varying Systems with Applications** (J. Mohammadpour and C. Scherer, Eds), Springer, 2012.

International conference papers with proceedings

[1] A. L. Do, O. Sename, L. Dugard, S. Aubouet, and R. A. Ramirez-Mendoza, *An lpv approach for semi-active suspension control*, in 11th **Pan-American Congress of Applied Mechanics** - PACAM XI, Foz do Iguau, Paran - BRAZIL, January 04-08, 2010.

[2] A. L. Do, O. Sename, and L. Dugard, *An LPV control approach for semi-active suspension control with actuator constraints*, in Proceedings of the **IEEE American Control Conference** (ACC), Baltimore, Maryland, USA, June 30 - July 2, 2010.

[3] A. L. Do, J. Lozoya-Santos, O. Sename, L. Dugard, R. A. Ramirez-Mendoza, and R. Morales-Menendez, *Modélisation et commande LPV d'un amortisseur Magnéto-Rhéologique*, in Proceedings de la **Conférence Internationale Francophone d'Automatique**, Nancy, France, June 2-4, 2010.

[4] A. L. Do, O. Sename, L. Dugard, S. Savaresi, C. S. C, and D. Delvecchio, *An extension of mixed Skyhook and ADD to Magneto-Rheological dampers*, in Proceedings of the 4th **IFAC Symposium on System, Structure and Control**, Ancona, Italy, September 15-17, 2010.

[5] A. L. Do, C. Spelta, S. Savaresi, O. Sename, L. Dugard, and D. Delvecchio, *An LPV control approach for comfort and suspension travel improvements of semi-active suspension systems*, in Proceedings of the 49th **IEEE Conference on Decision and Control** (CDC), Atlanta, GA, December 15-17, 2010, pp. 5660 - 5665.

[6] A. L. Do, B. Soualmi, J. Lozoya-Santos, O. Sename, L. Dugard, and R. Ramirez-Mendoza, *Optimization of weighting function selection for H_∞/LPV control of semi-active suspensions*, in 12th **Mini Conf on Vehicle Sys. Dyn., Ident. and Anomalies**, Budapest, Hungary, October 08-10, 2010.

[7] A. L. Do, O. Sename, L. Dugard, and B. Soualmi, *Multi-objective optimization by genetic algorithms in H_∞/LPV control of semi-active suspension*, in Proceedings of the 18th **IFAC World Congress** (WC), Milan, Italy, August 02 - September 2, 2011.

[8] A. L. Do, J. M. Gomes da Silva Jr., O. Sename, and L. Dugard, *Control design for LPV systems with input saturation and state constraints: an application to a semi-active suspension* (accepted), Proceedings of the 50th **IEEE Conference on Decision and**

Control (CDC), Orlando, Florida, December 12-15, 2011.

National conference papers with proceedings

[1] A. L. Do, O. Sename, and L. Dugard, *Optimisation par algorithme génétique d'une commande LPV de suspension semi-active*, in **Journées Doctorales MACS**, Marseille, France, June 09-10, 2011.

Chapter 1

Introduction

1.1 Introduction

1.1.1 General introduction to vehicle dynamic control

In the last decades, the vehicle dynamic control has been intensively studied. The problems are numerous but in general they can be classified into two main issues: comfort and safety. For safety oriented problems, efforts are made on stabilizing the vehicle in critical situations through the well-known devices like ABS (Anti-lock Braking System), EPS (Electronic Stability Program)... On the other hand, the use of controllable suspension systems has allowed to improve the passenger comfort. It can be seen from these studies that the knowledge of the forces and moments is essential to understand the vehicle dynamics and to design the controllers. These forces, caused by the engines, gravity, aerodynamics and specially by road disturbances, influence the acceleration, braking, steering and ride performances. Under the view point of system control, to improve the vehicle performance, they must be handled by appropriate control rules.

In a vehicle, besides the engines and the power train system, the other essential actuators can be the braking, steering and suspension subsystems. The problems concerning these three subsystems are very interesting in both vehicle dynamics and automatic control. As in [Gillespie, 1992], braking performance defines the vehicle safety and is determined by the braking coefficient, deriving from adhesive and hysteretic friction. This coefficient depends on the road condition and the wheel-slip (caused by the difference between the tire rotational speed and the forward velocity of the wheel). For a good braking performance, this coefficient must be high. For example, the function of an ABS is based on the principle that the braking coefficient is always kept around the highest value. On the other side, the steering performance is related to the handling (lateral, yaw and roll modes). The important factor for the analysis of steering performance is

the sideslip angle defined by the angle between the actual direction of travel of a rolling wheel and the direction towards which it is pointing. At low-speed, the sideslip angle is negligible, the cornering objective is easy to achieve. However, the high speed steering case, the sideslip angle and the lateral force at each wheel appear. This makes the steering no longer a simple task (in some situations, under-steering or over-steering can happen)...

On the one hand, it can be seen that, in both cases of braking and steering, their performances are related to the tire. Actually, the tire dynamics play a key role in vehicle performance. In many books about vehicle dynamics, the tire is always strongly emphasized [Gillespie, 1992], [Kiencke & Nielsen, 2000], [Pacejka, 2005], [Rajamani, 2006]. On the other hand, the suspension systems turn out to be very important for the vehicle dynamics because they link the tires to the vehicle chassis. Although the suspensions influence only the vertical tire force (or the tire load), it can be seen that the lateral and longitudinal tire forces are indirectly concerned with the suspensions because both forces are related to the vertical one [Gillespie, 1992], [Pacejka, 2005].

When a daily vehicle travels, it is excited by a broad spectrum of vibrations. Without efficient suspension systems, the vehicles can hardly travel safely and provide pleasure to passengers, even on good roads. In fact, not only the vertical dynamics but also the pitch and roll dynamics can be improved by a good suspension system. Moreover, as mentioned previously, because the braking and steering performances are influenced by the tire forces which can be modulated by suspension systems, it can be concluded that these performances can also be improved through the control of the suspension system. For example, in [Hac, 2002], the author proved that in steering mode, the rollover stability would be improved by taking into account the effect of suspension in the design; in [Lu et al., 2011], braking safety and lateral stability can be effectively improved and the occurrence of an unstable situation can be reduced by a global integrated control of suspension, braking and steering systems; in [Alleyne, 1997], for instance, the integration of active suspension components with ABS (Anti-lock Braking System) mechanisms can reduce the stopping distance over just anti-lock brakes; in [Gaspar et al., 2007] and [Poussot-Vassal, Sename, Dugard, Gáspár, Szabó & Bokor, 2010], integrated control structures using active suspensions and an active brake were proposed to improve the safety. So what is exactly a suspension system?

1.1.2 Suspension system

A suspension system is made up of an elastic element and a damping element connected in parallel (see Fig. 1.1). This simple system has about one hundred years of development, from the appearance of passive dampers in Roll Royce (in 1913) to sophisticated controllable Magneto-Rheological (MR) dampers in the most recent cars such as Audi

TT, Audi R8, Ferrari 599 GTB... Today, it plays an important role in the automotive industry because, besides the vibration insulation capacity, they can further improve the safety and the handling of the vehicle. Some more detailed historical facts on suspension systems are presented in [Aubouet, 2010]. In general, suspensions are classified into three types according to their controllability (see e.g. [Isermann, 2003] for a detailed classification):

- *Passive suspensions*, generally found in most of the vehicles, consist of a spring connected in parallel with a passive damper. They can only dissipate the energy and their characteristics are time-invariant.

- *Semi-active suspensions*, available on a certain number of mid-range and expensive passenger vehicles and on some military vehicles, consist of a spring and a semi-active damper. Like passive suspensions, they can only dissipate the energy but their property (the damping coefficient) can be changed by external control signals.

- *Active suspensions*, found in a small number in mid-range and expensive passenger vehicles, use a spring and an active damper. For such types of suspensions, external actuators are required to supply energy to the systems. Hence, they can both dissipate and generate the energy.

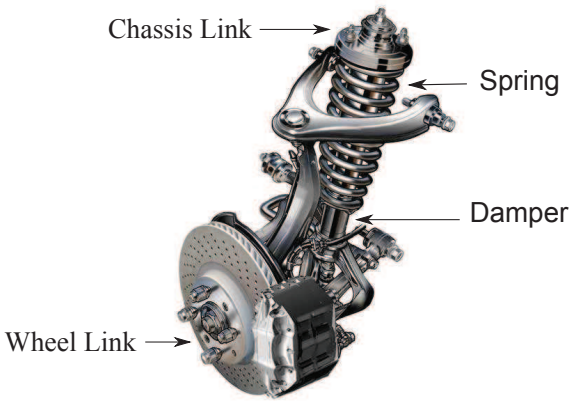

Figure 1.1: An example of suspension system.

In the next section, we discuss about the control oriented quarter vehicle model as well as the performance criteria for suspension control.

1.2 Quarter vehicle model and performance criteria for suspension control

1.2.1 Quarter vehicle model for suspension system control

As mentioned previously, understanding vehicle dynamics is important for the design and development of controllers. This can be achieved by two methods: empirical or analytical. While the empirical understanding, derived from experiments (trial and error to understand which factors influence the vehicle performance in which condition...) often leads to failure, the analytical one, concerned by models built on the laws of physics, is preferred. The main difficulty for studying the performance based on an analytical model is in the computation of a mathematical solution. The complexity in the vehicle dynamics (the large number of components and systems, the nonlinearities...) results in a very complex problem which may be impossible to solve analytically. Today, this task can be much simplified by using powerful computers. Many numerical softwares allow realistic simulations which are useful for the vehicle performance analysis and evaluation before the implementation.

Back to the particular case of suspensions, the following models are of interest:

- A full model of suspension systems with 7 degrees of freedoms is shown in Fig. 1.2. The seven degrees of freedom of the full car model are the heave z, pitch ϕ and roll θ and the road profile inputs at the four wheels that excite the system represented by $z_{r_{fl}}$, $z_{r_{fr}}$, $z_{r_{rl}}$ and $z_{r_{rr}}$. This model allows to study vertical, roll and pitch dynamics [Poussot-Vassal, 2008].

- A half vehicle model (or bicycle model) with four degrees of freedom is shown in Fig. 1.3. The four variables are the pitch ϕ and heave z motions of the vehicle body and the road profile inputs at the front and rear wheels z_{r_f} and z_{r_f}. This model is used for vertical and pitch control [Sammier, 2001], [Poussot-Vassal, 2008] A similar model (with of two front or two rear wheels) can be used for vertical/roll dynamics.

- Quarter vehicle model : a quarter car model with two degrees of freedom is shown on Fig. 1.4. The two variables are the heave and the road profile input at a single wheel. Only the study of vertical dynamics can be performed with this model.

The quarter vehicle model will be investigated in this thesis because comfort and road holding are concerned with the vertical dynamics. The model is simple and suitable for a preliminary design. It represents a single corner of a vehicle. In this model, the quarter vehicle body is represented by the sprung mass (m_s) and the wheel and tire

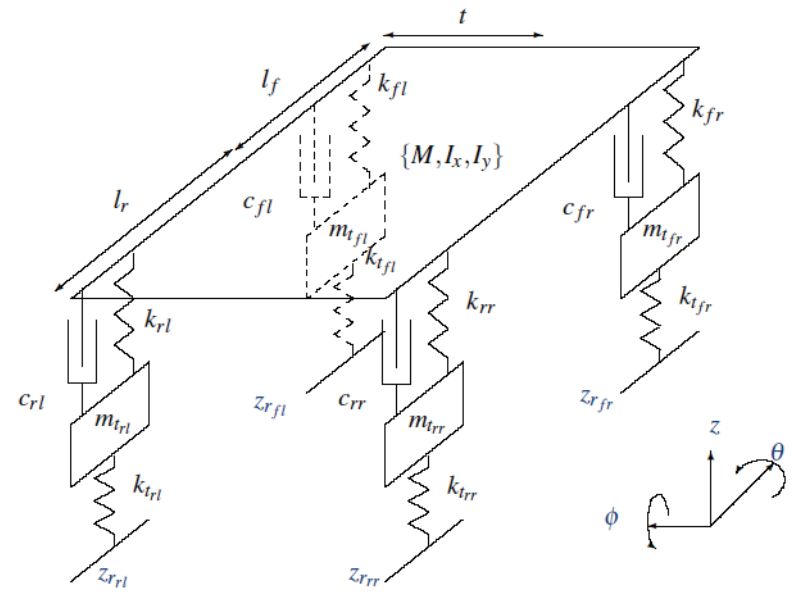

Figure 1.2: Full vehicle model for suspension control.

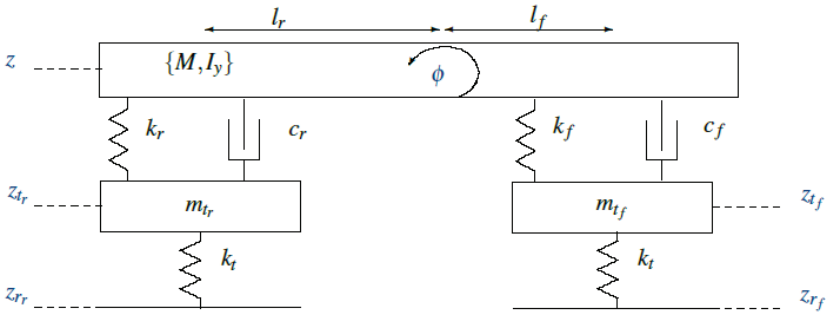

Figure 1.3: Half vehicle model for suspension control.

are represented by the unsprung mass (m_{us}). They are connected by a spring with the stiffness coefficient k_s and a semi-active damper. The tire is modeled by a spring with the stiffness coefficient k_t. As seen in the figure, z_s (respectively z_{us}) is the vertical displacement around the equilibrium point of m_s (respectively m_{us}) and z_r is the variation of the road profile. It is assumed that the wheel-road contact is ensured.

By applying the second law of Newton, the dynamical equations of a quarter vehicle are given by

$$\begin{cases} m_s \ddot{z}_s & = -F_{spring} - F_{damper} \\ m_{us} \ddot{z}_{us} & = F_{spring} + F_{damper} - F_{tire} \end{cases} \tag{1.2.1}$$

where F_{spring} is the dynamical spring force, F_{tire} is the dynamical tire force and

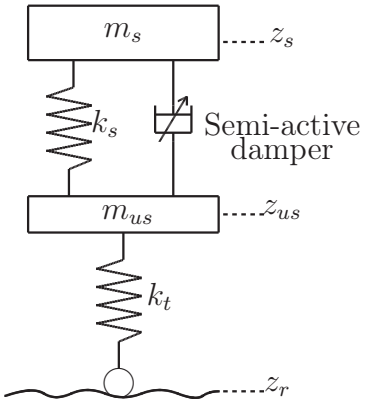

Figure 1.4: Model of quarter vehicle with a semi-active damper.

F_{damper} is the damper force. Let us denote $z_{def} = z_s - z_{us}$ the damper deflection, $\dot{z}_{def} = \dot{z}_s - \dot{z}_{us}$ the damper deflection velocity.

The dynamical spring force and tire force are given by

$$F_{spring} = k_s(z_{def}) \tag{1.2.2}$$
$$F_{tire} = k_t(z_{us} - z_r) \tag{1.2.3}$$

The damper's characteristics are usually represented by a Force-Deflection-Deflection Velocity relation

$$F_{damper} = F_{damper}\left(z_{def}, \dot{z}_{def}\right) \tag{1.2.4}$$

where F_{damper} can be a linear or nonlinear function. For example, with a linear semi-active damper, this force is given by

$$F_{damper} = c\dot{z}_{def}$$

where $c > 0$ is a variable parameter (damping coefficient) (if c is fixed, the damper is passive). For a nonlinear semi-active damper, we will see that the damper force can be of the form:

$$F_{damper} = c_0\dot{z}_{def} + k_0 z_{def} + f_I \tanh\left(c_1\dot{z}_{def} + k_1 z_{def}\right)$$

where c_0, k_0, c_1, k_1 and f_I are positive constant or positive variable parameters.

In this thesis, we will use the 1/4 Renault Mégane Coupé (1/4 RMC) model from the test car available in MIPS Laboratory (Mulhouse, France) (see in [Zin, 2005]. The model parameters are given in Tab. 1.1. It is important to notice that two spring models will be used in this thesis:

- For linear design, the spring force is given by

$$F_{spring} = k_s z_{def} \tag{1.2.5}$$

- For simulation, the spring has a nonlinear characteristic (see Fig. 1.5).

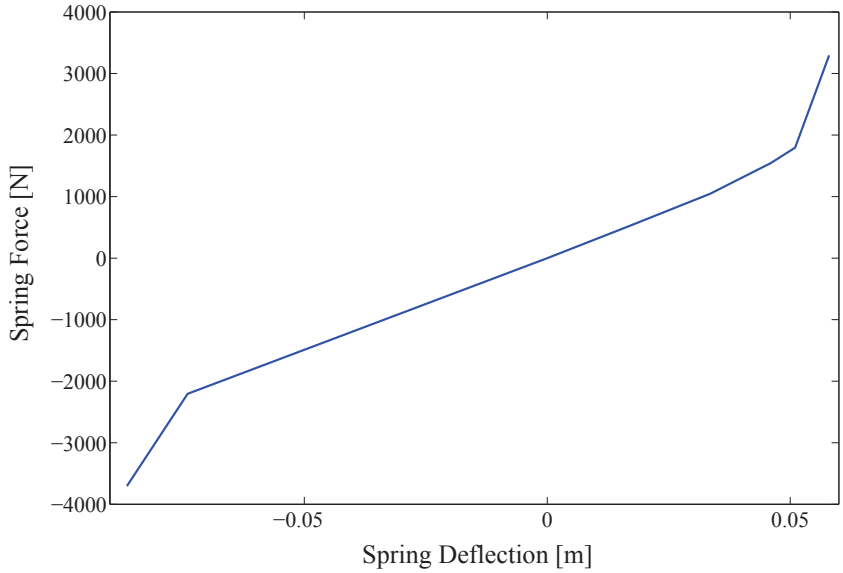

Figure 1.5: Nonlinear RMC Spring.

Table 1.1: Parameter values of the Renault Mégane Coupé quarter car model

Parameter	m_s $[kg]$	m_{us} $[kg]$	k_t $[N/m]$	k_s $[N/m]$
$Value$	315	37.5	29500	210000

1.2.2 Performance criteria

In semi-active suspension control, the two main objectives are ride comfort and road holding. Ride comfort concerns the pleasure of passenger and driver, road holding influences the driving safety. While road holding can be directly related to the dynamic tire force, for ride comfort it is however more difficult to evaluate since it is a subjective matter. The human sensitivity to vibration is frequency-dependent. Furthermore, at the same frequencies, the different parts of the human body feel the vibration in different ways. To answer the question on which is the good measure to evaluate ride comfort, let us recall some criteria existing in the literature (see [Guglielmino et al., 2008]).

Denote X the maximum allowed displacement amplitude, ω the angular frequency, f the frequency and t the time. The Janeway's comfort criterion (1965) relates the comfort to the vertical vehicle body displacement. At low frequencies, the criterion states that

$$X\omega^3 = 12.6 \tag{1.2.6}$$

and at high frequencies, in the range $6-20$ Hz, the vehicle body acceleration peak value should not exceed 0.33 m/s^2, whilst between 20 and 60 Hz the maximum velocity should stay below 2.7 mm/s.

Steffens (1966) proposed to evaluate the comfort using the following criterion

$$X[cm] = 7.62 \times 10^{-3}(1 + \frac{125}{f^2}) \tag{1.2.7}$$

Another criterion is the vibration dose (VD) value proposed by Griffin (1984) which provides an indication based on the integral of the fourth power of the frequency weighted acceleration a

$$VD = \int_0^t a^4 dt \tag{1.2.8}$$

The most general criterion is the standard ISO 2631 (1978) which is applicable not only to vehicles but also to all vibrating environments. It defines the exposure limits for body vibration in the range $1-80\ Hz$, defining limits for reduced comfort, for decreased proficiency and for preservation of health. According to this criterion, the human being is more sensible to the vertical acceleration in the range of $4-8\ Hz$. The ISO 2631 filter applied on the sprung mass acceleration is approximated by the following transfer function (see [Zuo & Nayfeh, 2007]), see Fig. 1.6

$$W_{ISO-2631} = \frac{81.89s^3 + 796.6s^2 + 1937s + 0.1446}{s^4 + 80.00s^3 + 2264s^2 + 7172s + 21196} \tag{1.2.9}$$

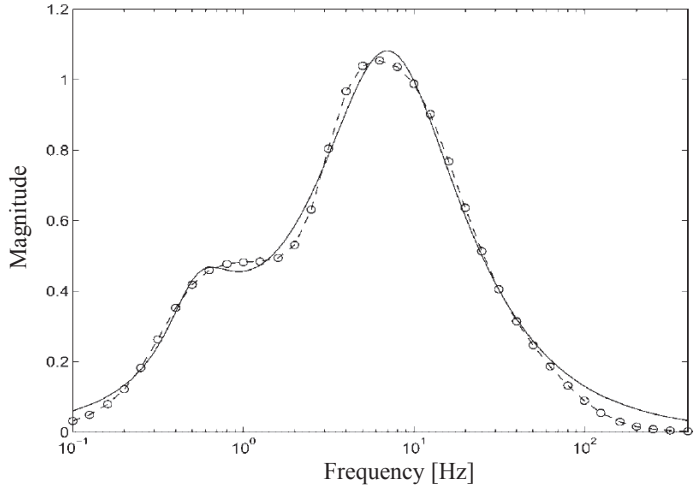

Figure 1.6: ISO 2631 frequency weighting curve (circles) and the fourth-order filter approximation (solid line).

Criteria for suspension performance evaluation In the following, the criteria to evaluate the performance of the semi-active suspension systems are given. Let us consider the case of the quarter vehicle model (see Fig. 1.4). By abuse of language, let denote $\ddot{z}_s/z_r$ (respectively z_{deft}/z_r)) the "frequency response" from the road disturbance z_r to

the vehicle body acceleration $\ddot{z}_s$ (respectively the dynamic tire deflection $z_{us} - z_r$), i.e. the gain of the transfer function for LTI systems or the gain computed using "variance gain" algorithm in Appendix B for nonlinear systems.

In general, the vehicle body acceleration between 0-20 Hz should be filtered to guarantee a good ride comfort, although it is worth noting again that the human is the most sensible to vertical acceleration around 4-8 Hz (ISO 2631). On the other side, to maintain the road-wheel contact, it is necessary that the dynamic tire force is smaller than $g(m_s + m_{us})$ (where g is the gravity). Hence, for the road holding improvement, the dynamic tire force $k_t(z_{us} - z_r)$, in other words the dynamic tire deflection $z_{us} - z_r$, should be small in the frequency range 0-30 Hz. Note also that the road holding is improved by limiting the up and down bouncing of the wheel z_{us} around its resonance 10-20 Hz.

In summary, with the previous remarks, the performance criteria in the frequency domain are described explicitly as follows

- Comfort
$$J_{CF} = \min \int_0^{20} \ddot{z}_s / z_r(f) df \tag{1.2.10}$$
- Road holding
$$J_{RH} = \min \int_0^{30} (z_{us} - z_r)/z_r(f) df \tag{1.2.11}$$

The objectives of the control design is to minimize the two criteria. It is worth noting that the two criteria (1.2.10) and (1.2.11) are consistent with the ones given in [Sammier et al., 2003] and [Savaresi et al., 2010].

It is important to keep in mind that, all the provided analysis in the frequency domain will be based on the criteria (1.2.10) and (1.2.11). However, during the controller design step, if different criteria are used, they will be explicitly explained.

The model and the performance criteria for general suspension systems have been presented. In the next section, we shall discuss about the particular type of suspension systems, which is the object of the thesis: the semi-active one.

1.3 Semi-active suspensions

Among the three types of suspension, the passive suspensions have inherent limitations due to the choice of the spring rate and of the damping characteristics to achieve an acceptable compromise between comfort and road holding for a whole range of working

frequencies. The semi-active and active suspensions can improve the performance objectives with appropriate control methods. This is the reason why the latter suspensions have been studied more intensively in recent years. However, up to now, only the semi-active suspensions are used widely in automotive industry because, compared with fully active suspensions, the semi-active ones provide a better compromise between the cost and the performances. Semi-active suspensions can potentially achieve the majority of the performance objectives (see [Ivers & Miller, 1989], [Patten et al., 1994]) while they are smaller in weight and volume, cheaper in price, more reliable in work (the robustness due to their dissipative property) and less energy consuming (see also [Fialho & Balas, 2002], [Gillespie, 1992], [Hrovat, 1997], [Kiencke & Nielsen, 2000]).

1.3.1 Classification and characteristics

Many semi-active devices utilize forces generated by surface friction or viscous fluids to dissipate vibratory energy in a structural system. These devices are applied in civil engineering [Patten et al., 1994], [Constantinou & Symans, 1994]. Recently, another class of semi-active dampers using Electro-Rheological and Magneto-Rheological technologies has been considered although the controllable ER and MR fluids was invented long time ago (by [W. M. Winslow, 1947] and [Rabinow, 1948], respectively). A distinguishing characteristics of these fluids is that they can be changed rapidly from a free-flowing, linear viscous state to a semi-solid state when being exposed to an electric or magnetic field. There are also many applications of these semi-active dampers in civil engineering [Zhu et al., 2004], [Gavin et al., 1994], automotive [Savaresi et al., 2010] (and references therein).

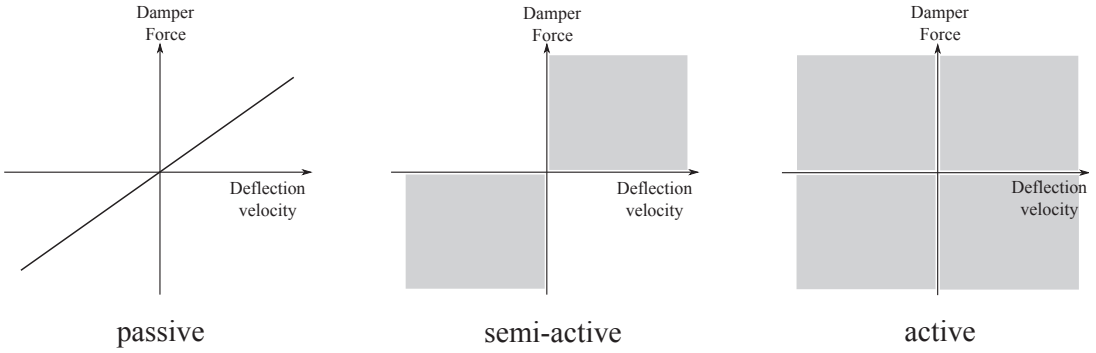

Figure 1.7: Force-velocity characteristic of ideal Passive (continuous line), Semi-Active (dotted region) and Active (shaded region) dampers.

The (ideal) damper characteristics are usually described by the Force-Velocity relation. The characteristics of semi-active dampers, along with passive and active ones, are presented in Section 1.1.2 are shown in Fig. 1.7. In the passive case, this characteristic is invariant due to the uncontrollable property of a passive damper while with an active

damper, this characteristic may span all the space and there is no constraint between the active damper force and its deflection velocity. Unlike these two dampers, the semi-active one has a special property called *passivity constraint*. The passivity constraint of a semi-active damper is characterized by the fact that the damper force and the deflection velocity always have the same sign i.e. as shown in Fig. 1.7, the damper force is limited in the first and third quadrants. The passivity constraint of an ideal semi-active damper is represented mathematically as follows

$$\text{Damper Force} \times \text{Damper Velocity} \geq 0 \tag{1.3.1}$$

1.3.2 Modeling methods

The modeling of semi-active dampers is a challenging problem because of a high non-linear behavior such as the bi-viscosity, the temperature dependency and specially the hysteresis. Many modeling methods have been proposed and generally they can be classified into two kinds: static model and dynamic model (see [Savaresi et al., 2010]). Let us denote F_d the damper force, x the damper deflection and $\dot{x}$ the damper deflection velocity. In the following, we introduce briefly some well-known modeling methods.

- Static model with Coulomb friction:

$$F_d = c(I)\dot{x} - c^{sym}(I)|\dot{x}| + c^{nl}(I)\sqrt{|\dot{x}|}sgn(\dot{x}) \tag{1.3.2}$$

  where c, c^{sym} and c^{nl} are parameters depending on the damping command I. This model describes the presence of the static friction as a constant term, function of the deflection speed sign.

- Dynamic Bouc-Wen model [Bouc, 1967], [Wen, 1976]

$$\begin{cases} F_d = c_0(I)\dot{x} + k_0(I)(x - x^0) + \gamma(I)z \\ \dot{z} = -\beta(I)|\dot{x}|z|z|^{n-1} - \delta(I)\dot{x}|z|^n + A(I)\dot{x} \end{cases} \tag{1.3.3}$$

  where $c_0, k_0, A, \gamma, \beta, \delta, n$ are model parameters (dependent on command input I), x_0 is the critical deflection and z is the internal state that introduces some dynamic in the model and models the hysteresis phenomenon.

- Static Guo model [Guo et al., 2006]

  The behavior of the semi-active damper is represented by the following nonlinear equation:

$$F_d = a_2\left(\dot{x} + \frac{v_0}{x_0}x\right) + a_1 \tanh\left(a_3\left(\dot{x} + \frac{v_0}{x_0}x\right)\right) \tag{1.3.4}$$

  where a_1 is the dynamic yield force of the MR fluid, a_2 and a_3 are related to the post-yield and pre-yield viscous damping coefficients, v_0 and x_0 denote the absolute

value of hysteretic critical velocity $\dot{x}_0$ and hysteretic critical deflection x_0 where $\dot{x}_0$ and x_0 are defined as the velocity and deflection when the MR damper force is zero.

- Non-linear black-box model (static or dynamic) [Savaresi, Bittanti & Montiglio, 2005]:

  This kind of description is not based on physical description of the device, but aims at representing the non-linear input-output dynamical relationship. An example of black box model for an electronic shock absorber is the following:

$$F_d = f(x(t); \dot{x}(t); \ddot{x}(t); ...; x^{(k)}(t); I(t); \dot{I}(t); \ddot{I}(t); ...; I^{(k)}(t)) \tag{1.3.5}$$

  where, in accordance to the notation used so far x is the damper deflection and $x^{(k)}$ is the k^{th} derivative of x, I is the external damping command and $I^{(i)}$ is the i^{th} derivative of I.

1.3.3 Control problem

So far, the control problem for semi-active suspensions has been tackled with many approaches during the last three decades. One of the first comfort-oriented control methods, successfully applied in commercial vehicles, is the Skyhook control proposed by Karnopp *et al.* [Karnopp et al., 1974]. In this control design, the damping coefficient is adjusted continuously or switched between a maximum and a minimum value. Then [Yi & Song, 1999] proposed an improved version of the Skyhook. This new adaptive Skyhook control law, in fact a combination of the sprung mass and unsprung mass velocity feedbacks with time varying gains, showed a performance enhancement in ride comfort and road holding. Recently, [Liu et al., 2005] have studied the vibration isolation characteristics of four established semi-active damping control strategies, which are based on Skyhook control and balance control. By using the principle contrary to the Skyhook, the Groundhook control was proposed by [Valasek et al., 1997] to reduce the dynamic tire force. The reduction of the dynamic tire force is a good way for road holding improvement, this challenging problem was also intensively studied in [Cole & Cebon, 1996].

Then numerous approaches have been also developed for comfort and/or road holding enhancement such as optimal control [Giua et al., 2004], [Savaresi, Silani & Bittanti, 2005], clipped optimal control [Lu & DePoyster, 2002], [Tseng & Hedrick, 1994], [Giorgetti et al., 2006]; H_∞ control [Rossi & Lucente, 2004], [Sammier et al., 2003]; LPV control [Poussot-Vassal et al., 2008] or Model Predictive Control [Canale et al., 2006], [Poussot-Vassal, Savaresi, Spelta, Sename & Dugard, 2010]. Recently, the mixed Skyhook and ADD (SH-ADD) algorithm proposed by [Savaresi & Spelta, 2007] has been known to be one of the most efficient comfort-oriented controllers.

However, the suspension deflection problem is less mentioned in semi-active suspension controller design. Few studies are concerned with this issue, e.g. [Hac & Youn, 1991], [Du et al., 2005]. In the recent paper by [Spelta et al., 2011], the passenger comfort was proved to be dramatically degraded when the suspension deflection exceeds the structural limit.

To summarize, the interesting challenges of the semi-active suspension control problem are:

- A realistic design where the nonlinear behavior (hysteresis and bi-viscosity) of semi-active dampers must be taken into consideration.
- Multi-objectives control (comfort, road holding and suspension deflection) and effective formulation of control objectives for optimization.
- Constrained control due to the passivity constraint of semi-active dampers and structural limits of suspension systems (end-stops).

Besides, concerning the practical point of view, the following requirements, when designing the control strategy, are important as well:

- Flexibility in term of performance to satisfy the customers' need (sport, city cars, heavy vehicles...).
- Adaptiveness to various damper technologies.
- A limited number of available sensors.
- The capability of using low-cost micro-controllers for implementation.

In the following, we present three control methods which will be considered and used as references for the comparison of the proposed methods in the thesis. These methods are well-known in semi-active suspension control because of their simplicity and effectiveness. Another important reason is that they can be implemented directly for different quarter car models; moreover no complex tuning procedure (i.e. the selection of design parameters) is needed.

- The Skyhook by [Karnopp et al., 1974] provides a good insulation at low frequencies $[1-3]\ Hz$. Along with Groundhook, it has been used widely in commercial cars up to now.
- The Groundhook by [Valasek et al., 1997] improves road holding by reducing the wheel acceleration in the range $[10-15]\ Hz$.

- The Mixed Skyhook-ADD by [Savaresi & Spelta, 2007] is almost optimal for passenger comfort.

All these three methods are designed for the quarter vehicle model (6.5.1) equipped with a linear semi-active damper characterized by

$$F_{damper} = c\dot{z}_{def} \quad \text{where} \quad \mathrm{c} > 0 \ \text{ and } \ \mathrm{c} \in [\mathrm{c_{min}}, \mathrm{c_{max}}]$$

Two-states Skyhook The main idea of the Skyhook for a linear suspension system is that the damper exerts a force that reduces the velocity of the body mass $\dot{z}_s$. It is given as follows

$$c = \begin{cases} c_{max} & \text{if} \quad \dot{z}_s \dot{z}_{def} > 0 \\ c_{min} & \text{if} \quad \dot{z}_s \dot{z}_{def} \leq 0 \end{cases} \tag{1.3.6}$$

Groundhook The road-holding oriented control method Groundhook aims at reducing the dynamic tyre force and is given as follows

$$c = \begin{cases} c_{max} & \text{if} \quad \dot{z}_{us} \dot{z}_{def} < 0 \\ c_{min} & \text{if} \quad \dot{z}_{us} \dot{z}_{def} \geq 0 \end{cases} \tag{1.3.7}$$

The Mixed Skyhook-ADD (SH-ADD) It is well-known that the Skyhook provides the best ride comfort at low frequencies while the ADD (Acceleration Driven Damper) by [Savaresi, Silani & Bittanti, 2005] improves considerably ride comfort at high frequencies. The Mixed SH-ADD control developed by [Savaresi & Spelta, 2007] guarantees the best behavior of both Skyhook and ADD and is given as follows

$$c = \begin{cases} c_{max} & \text{if} \quad (\ddot{\mathrm{z}}_\mathrm{s}^2 - \alpha \dot{\mathrm{z}}_\mathrm{s}^2 \leq 0 \wedge \dot{\mathrm{z}}_\mathrm{s} \dot{\mathrm{z}}_\mathrm{def} > 0) \vee \\ & \quad (\ddot{z}_s^2 - \alpha \dot{z}_s^2 > 0 \wedge \ddot{z}_s \dot{z}_{def} > 0) \\ c_{min} & \text{if} \quad (\ddot{\mathrm{z}}_\mathrm{s}^2 - \alpha \dot{\mathrm{z}}_\mathrm{s}^2 \leq 0 \wedge \dot{\mathrm{z}}_\mathrm{s} \dot{\mathrm{z}}_\mathrm{def} \leq 0) \vee \\ & \quad (\ddot{z}_s^2 - \alpha \dot{z}_s^2 > 0 \wedge \ddot{z}_s \dot{z}_{def} \leq 0) \end{cases} \tag{1.3.8}$$

The amount $(\ddot{z}_s^2 - \alpha \dot{z}_s^2)$ is the frequency-range selector where α is the SH-ADD crossover frequency (see [Savaresi & Spelta, 2007]).

1.4 Conclusions

From this brief overview about vehicle dynamics, the role of a suspension systems in a vehicle has been confirmed. This motivated many studies to achieve the optimal

performances for suspension systems. Among three type of suspension systems, the semi-active ones are the most studied. The interests and the challenges in semi-active suspension control has been presented through some historical facts on some existing modeling and control methods.

In the next chapter, we will present some backgrounds on control theory and optimization which are necessary for the synthesis of new controllers for semi-active suspension systems.

Chapter 2

Background on control theory and optimization

This chapter presents some theoretical backgrounds on the control theory and optimization. First, the recall of some basic definitions on convex optimization and LMI (Linear Matrix Inequality) facilitate the reading of the rest of the thesis. The LPV approach is introduced with sufficient information (definition, stabilization and H_∞ performance) because, in this thesis, it is the main strategy to solve semi-active suspension control problem. Input saturation control is always a very interesting problem for all real applications. As seen in Chapter 3 and 6, the passivity constraint of a semi-active suspension can be recast to the input saturation one. The overview on this control problem is hence necessary. Finally, the Genetic Algorithms is introduced. This is a very efficient tool for optimizing the controllers of the proposed semi-active suspension control methods in the next chapters.

2.1 Convex optimization and Linear Matrix Inequality

2.1.1 Convex optimization

Convex optimization is a special class of mathematical optimization problems which has been studied for a century. The relevance of this mathematic branch has been recognized by its applications in many fields such as data analysis, statistics, finance, communications and networks, signal processing. It has been proven, in automatic control, that many control problems can be recast into convex optimization problem for e.g. robust control, LPV control, constrained control... An important reason for the interest of convex optimization problems relies in the practical point of view that they can be solved numerically by efficient methods (interior-point and ellipsoid methods). Before

Figure 2.1: Convex set (left) and non-convex set (right).

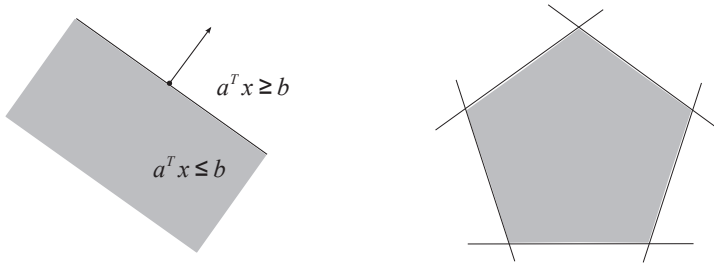

Figure 2.2: An example for the 2-dimensional space: The hyperplane (continuous line) defines 2 half-spaces (left) and a polytope defined by the intersection of 5 half-spaces (right).

introducing the convex optimization problem, let us recall some basic definitions [Boyd et al., 1994], [Scherer & Weiland, 2005].

Definition 2.1.1. ***Affine Set***
The set S in the vector space X is affine if the line through any two points in S lies in S, i.e.

$$\lambda x_1 + (1-\lambda)x_2 \in S, \forall x_1, x_2 \in S \quad \textit{and } \lambda \in R \tag{2.1.1}$$

Definition 2.1.2. ***Convex Set***
The set S in the vector space X is convex if the line segment between any two points in S lies in S (see Fig. 2.1), i.e.

$$\lambda x_1 + (1-\lambda)x_2 \in S, \forall x_1, x_2 \in S \quad \textit{and } 0 \leq \lambda \leq 1 \tag{2.1.2}$$

- The intersection of any family of convex sets is convex.
- The *hyperplane* defined as $\{x \in R^n : a^T x = b\}$ where $a \in R^n, a \neq 0, b \in R$ is affine and the *half-space* defined as $\{x \in R^n : a^T x \leq b\}$ where $a \in R^n, a \neq 0, b \in R\}$ is convex.
- The intersection of finitely many hyperplanes and half-spaces results in a *polyhedron*. A compact polyhedron is said to be a *polytope* (see Fig. 2.2).

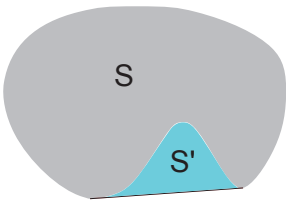

Figure 2.3: The convex hull of set S consists of all convex combinations of all elements of S. As illustrated in this figure $Co\{S\} = S \cup S'$.

Definition 2.1.3. *The convex hull of a set S, denoted $Co\{S\}$, is the set of all convex combinations of points in S (see Fig. 2.3):*

$$Co\{S\} = \{\lambda_1 x_1 + \lambda_2 x_2 + ... + \lambda_n x_n | x_i \in S, \lambda_i \geq 0, i = 1:n, \sum_{i=1}^{n} \lambda_i = 1\} \tag{2.1.3}$$

With the definitions above, the general optimization problem can be described as follows

$$\begin{aligned} &\min \qquad f_0(x) \\ &\text{subject to} \quad f_i(x) < b_i, \quad \text{i=1,2,...,m} \end{aligned} \tag{2.1.4}$$

where $x = (x_1, x_2, ..., x_n)$ is the decision vector, and $f_0 : R^n \mapsto R$ is the objective function, $f_i : R^n \mapsto R$ with $i = 1, 2, ..., m$ are the constraint functions, $b_i \in R$ are the bounds of the constraint functions. A vector x^* is the solution of the problem (2.1.4) if for all z such that $f_i(z) < b_i$, $i = 1, 2, ..., m$ then $f_0(z) \geq f_0(x^*)$.

The problem (2.1.4) is referred to as a *convex optimization problem* if $f_0, f_1..., f_m$ are convex functions, i.e. for all $x, y \in R^n$ and all $\alpha, \beta \in R$, $\alpha + \beta = 1$, $\alpha \geq 0$, $\beta \geq 0$:

$$f_i(\alpha x + \beta y) \leq \alpha f_i(x) + \beta f_i(y) \tag{2.1.5}$$

It can be seen that the set of decision vector satisfying the constraint $f_i(x) < b_i$, $i = 1, 2, ..., m$ is a convex set (knowing that the sub-level $\{x : f_i(x) < b_i\}$ of a convex function f_i is a convex set and the interconnection of infinitely many convex sets is a convex set). Henceforth, in other words, a convex optimization problem is the optimization of a convex function over a convex set.

What is the interest of convex optimization?
The first reason to study the convex optimization is that locally optimal solutions are globally optimal. The second reason is stated in the following proposition:

Proposition 2.1.1. *Let $f : S \mapsto R$ be a convex function where $S = Co\{S_0\}$. Then $f(x) < \gamma$ for all $x \in S$ if and only if $f(x) < \gamma$ for all $x \in S_0$*

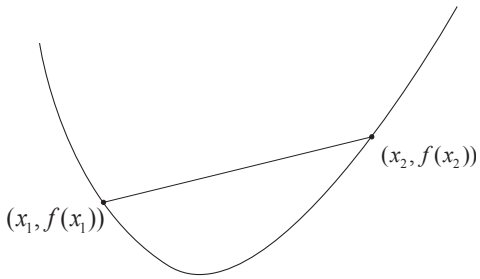

Figure 2.4: An example of a convex function: the line segment between any two points on the graph lies above the graph.

The proposition above is interesting in that if S_0 has a finite number of elements, it is only necessary to check a finite number of inequalities to conclude about $f(x) < \gamma$ or not. This has a great interest in LPV control, since if the set of scheduling parameters belongs to a polytope, then only a finite number of LMI problems needs to be solved to construct a global LPV controller (as seen later).
Finally, as mentioned previously, the interest is also in the practical point of view that convex optimization problems is tractable, i.e. they can be solved numerically by efficient methods (interior-points and ellipsoid methods).

2.1.2 Linear matrix inequality - LMI

It is well known that the linear matrix inequality (LMI) is a very efficient tool for many convex optimization problems in automatic control including the stability and performance analysis of linear systems (LTI, LPV and switching systems). The history of the LMIs began one hundred years ago from the solution of Lyapunov (1890) for the stability problem of the autonomous system

$$\frac{dx(t)}{dt} = Ax(t) \tag{2.1.6}$$

where t is the time instant, $x(t) \in \mathbb{R}^n$, $A \in \mathbb{R}^{n\times n}$ is a real matrix.

In his study, Lyapunov showed that the system (2.1.6) is stable if and only if there exist a positive-definite matrix P such that the following inequality holds

$$A^T P + PA \prec 0 \tag{2.1.7}$$

The condition $\{P \succ 0, A^T P + PA \prec 0\}$ is an example of linear matrix inequality (LMI). Here, $\succ$ (respectively $\prec$) stands for "positive-definite" (respectively "negative-definite") notion, i.e

$$P = P^T \succ 0 \;\; (\text{resp. } \prec 0) \Leftrightarrow \lambda_{min}(P) > 0 \;\; (\text{resp. } \lambda_{max}(P) < 0) \tag{2.1.8}$$

Similarly, $\succeq$ (respectively $\preceq$) stands for "positive semi-definite" (respectively "negative semi-definite") property, i.e

$$P = P^T \succeq 0 \ \ (\text{resp. } \preceq 0) \Leftrightarrow \lambda_{min}(P) \geq 0 \ \ (\text{resp. } \lambda_{max}(P) \leq 0) \tag{2.1.9}$$

Until 1940s, Lur'e was the first to apply Lyapunov's methods to practical control engineering problems. The LMIs were solved analytically (for small order systems). After that, many results on control theory have been interpreted using LMI tool. In the 1960s, the role of LMI is emphasized through the work of Kalman, Yakubovich, Popov and Willems. During the last decades, the LMIs tool has received an intensive attention from practical point of view. With the development of efficient interior-point methods from 1980s, it is allowed to solve numerically the optimal problems instead of finding an analytic solution, which is indeed much more difficult or impossible to be found.

Generally, a linear matrix inequality can be described by the following

$$F(x) = F_0 + x_1F_1 + x_2F_2 + ... + x_nF_n \prec 0 \tag{2.1.10}$$

where $x = (x_1, x_2..., x_n)$ is a vector of n real numbers and called *decision vector*, $F_0, F_1..., F_n$ are real symmetric matrices. Because $F(x)$ is affine, (2.1.10) is a convex constraint on x, i.e. $\{x : F(x) \prec 0\}$ is a convex set.

The LMI problems are numerous but in general they can be classified into two particular cases: the feasibility problem and the optimization one.

Definition 2.1.4. ***Feasibility Problem***
The feasibility problems concern finding elements $x \in X$ such that $F(x) \prec 0$. The LMI $F(x) \prec 0$ is called feasible if such elements x exist, otherwise it is said to be infeasible.

Definition 2.1.5. ***Optimization Problem***
Define an objective function $f : X \mapsto \mathbb{R}$ where $X = \{x : F(x) \prec 0\}$. The following problem

$$\begin{aligned} \textit{min} \quad & f(x) && (2.1.11)\\ \textit{subject to} \quad & F(x) \prec 0 && (2.1.12) \end{aligned}$$

is called an optimization problem with LMI constraint. If f is a convex function, this is a convex optimization problem and the convex programming algorithms can be applied to solve numerically this problem.

The LMI optimization usually concerns the two eigenvalue problems:

- *The eigenvalue problem:* Minimizing a linear objective function under the LMI constraints i.e.

$$\min \quad C^Tx \tag{2.1.13}$$

$$\text{subject to} \quad F(x) \prec 0 \tag{2.1.14}$$

where C is a vector of the same dimension as x.

- *The generalized eigenvalue problem:* This problem is described as follows

$$\min \quad \lambda \tag{2.1.15}$$

$$\text{subject to} \quad P_1(x) \prec \lambda P_2(x) \tag{2.1.16}$$

$$P_2(x) \succ 0 \tag{2.1.17}$$

$$F(x) \prec 0 \tag{2.1.18}$$

where λ is a positive scalar, P_1 and P_2 are matrices with appropriate dimensions.

Some useful tools for the LMI reformulation Usually some following methods are useful to convert a nonlinear optimization problem (for stability or controller design) into a convex linear one.

Lemma 2.1.2. ***Schur's lemma***
The LMI

$$\begin{pmatrix} Q(x) & S(x) \\ S(x)^T & R(x) \end{pmatrix} \prec 0 \tag{2.1.19}$$

is equivalent to

$$\begin{cases} Q(x) \prec 0 \\ R(x) - S(x)^T Q(x)^{-1} S(x) \prec 0 \end{cases} \tag{2.1.20}$$

and equivalent to

$$\begin{cases} R(x) \prec 0 \\ Q(x) - S(x) R(x)^{-1} S(x)^T \prec 0 \end{cases} \tag{2.1.21}$$

It can be seen from the Schur's lemma that the nonlinear inequality (2.1.20)-(2.1.21) can be transformed into a linear inequality (2.1.19).

Lemma 2.1.3. ***Projection lemma*** *[Doyle et al., 1989]*
For given matrices $W = W^T$, M and N, of appropriate size, there exists a real matrix $K = K^T$ such that,

$$W + MKN^T + NK^T M^T \prec 0 \tag{2.1.22}$$

if and only if there exist matrices U and V such that,

$$W + MU + U^T M^T \prec 0 \tag{2.1.23}$$

$$W + NV + V^T N^T \prec 0 \tag{2.1.24}$$

or, equivalently, if and only if there exists a scalar $\epsilon > 0$ *such that,*

$$W \prec \epsilon M M^T \tag{2.1.25}$$
$$W \prec \epsilon N N^T \tag{2.1.26}$$

or, equivalently, if and only if,

$$M_\perp^T W M_\perp \prec 0 \tag{2.1.27}$$
$$N_\perp^T W N_\perp \prec 0 \tag{2.1.28}$$

where $M_\perp$ *and* $N_\perp$ *are the orthogonal complements of* M, N *respectively (i.e.* $M_\perp^T M = 0$*).*

$\mathcal{S}$- Procedure The $\mathcal{S}$-procedure is a method which allows to formulate a problem described by a quadratic constraint verified under other quadratic constraints. It was first introduced by Lur'e and Postnikov [Lur'e & Postnikov, 1944] without any theoretical justification. Then, theoretical foundations of $\mathcal{S}$-procedure were presented by Yakubovich [Yakubovich, 1971]. Although the main drawback of the $\mathcal{S}$-procedure is in the fact that it usually leads to a more conservative formulation than the original problem, it is a useful tool in control theory and robust optimization analysis. We usually find the $\mathcal{S}$-procedure in LMI reformulations and analysis of quadratic programming.

Definition 2.1.6. ***$\mathcal{S}$-Procedure for quadratic function and nonstrict inequalities*** *Let* $F_0, F_1, ...F_p$ *be quadratic functions of the variable* $x \in R^n$*:*

$$F_i(x) = x^T T_i x + 2u_i^T x + v_i, \qquad i = 0, ..., p \tag{2.1.29}$$

where $T_i = T_i^T$, u_i *and* v_i *are known vectors with appropriate dimensions. Now considering the following conditions*
(C_1*)* $F_0 \succeq 0$ *for all* x *such that* $F_i(x) \succeq 0$*, i=1,...,p.*
(C_2*)* $\exists \tau_1, \tau_2 ..., \tau_p \in \mathbb{R}_+$ *such that for all* x $F_0(x) - \sum_{i=1}^p \tau_i F_i(x) \succeq 0$

- *In general cases* $\forall p \neq 1$, $C_2 \Rightarrow C_1$.

- *When* $p = 1$, $C_2 \Leftrightarrow C_1$ *provided that there exists some* x_0 *such that* $F_1(x_0) \succ 0$.

Definition 2.1.7. ***$\mathcal{S}$-Procedure for quadratic function and strict inequalities*** *Let* $T_0, T_1, ..., T_p$ *be symmetric matrices in* $\mathbb{R}^{n \times n}$*. Considering the following conditions*
(C_3*)* $x^T T_0 x > 0$ *for all* $x \neq 0$ *such that* $x^T T_i x \geq 0$*, i=1,...,p.*
(C_4*)* $\exists \tau_1 \geq 0, \tau_2 \geq 0 ..., \tau_p \geq 0$ *such that* $T_0 - \sum_{i=1}^p \tau_i T_i > 0$

- *In general cases* $\forall p \neq 1$, $C_4 \Rightarrow C_3$.

- *When* $p = 1$, $C_3 \Leftrightarrow C_4$ *provided that there exists some* x_0 *such that* $x_0^T T_1 x_0 > 0$.

2.2 LPV control

The linear parameter varying (LPV) approach is a very efficient method in modeling and control of numerous classes of systems: from linear time-varying systems, switching systems to time-delay and nonlinear systems... The study of LPV control has been motivated by the gain-scheduling control [Shamma & Athans, 1990], [Rugh, 1991], [Shamma & Athans, 1992]. Then many studies have been focused on this topic [Gahinet et al., 1996], [Scherer, 2004]. Compared to classical gain-scheduled control, the theory of LPV systems offers great advantages in term of robust stability and performance. Indeed, the gain-scheduling technique is only efficient for systems with slow varying parameters while in LPV design, more information on scheduling parameters (i.e. the parameter bounds and rate bounds if any) [Wu, 2001], [Apkarian & Adams, 1998] can be taken into account. Moreover the resulting LPV controllers are automatically gain-scheduled and do not require any ad hoc methods of gain-scheduling as in the classical methodology.

Let consider a nonlinear system

$$\dot{x} = f(x, u) \tag{2.2.1}$$

and an LPV system

$$\dot{x} = A(\rho)x + B(\rho)u, \rho \in \mathcal{P} \tag{2.2.2}$$

where $f(x, u)$ is a nonlinear function, x is the state, u is the control input, the matrices $A(\rho)$ and $B(\rho)$ depend linearly on the scheduling parameter ρ and have appropriate dimensions and ρ is a scheduling parameter varying in a bounded set $\mathcal{P}$ defined by

$$\mathcal{P} = \{\rho : [\rho_1, \rho_2, ..., \rho_k]^T \in \mathbb{R}^k\} \tag{2.2.3}$$

The main interest of the LPV approach is to formulate an exact LPV description (2.2.2) for the nonlinear system (2.2.1). This formulation offers more advantage in controller design than the original nonlinear one.

As mentioned in [Bruzelius et al., 2004], the LPV description is a bridge between the nonlinear and LDI (Linear Differential Inclusion). To keep the coincidence between the nonlinear system (2.2.1) and the LPV description (2.2.2), both following property is needed:
There exists a relation $\rho = \rho(x)$ such that

$$A(\rho(x))x + B(\rho(x))u = f(x, u) \tag{2.2.4}$$

This property ensures that all the trajectories of the nonlinear system is contained in that of the LPV system.
Moreover, for the purpose of nonlinear controller reconstruction from LPV controller, $\rho(x)$ must be measurable.

Indeed, there are possibly many LPV descriptions (depending on the choice of $\rho(x)$) for a nonlinear system. Although they are all describing exactly the original nonlinear system, there exists one LPV system which is better suited for the controller synthesis than others. The reason is that in LPV controller synthesis, ρ can be considered as a free parameter, only the bounds on ρ and $\dot{\rho}$ are considered. The controller synthesis for LPV descriptions is the same as for LDI cases. This obviously results in some conservatism in terms of closed-loop performance. Despite this difficulty, the LPV approach has been still intensively studied and applied in many fields: aero-dynamics, robotics, automotive control...

2.2.1 Representation of LPV Systems

LPV systems are represented by

$$\begin{aligned} \dot{x} &= A(\rho(t))x + B(\rho(t))u \\ y &= C(\rho(t))x + D(\rho(t))u \end{aligned} \tag{2.2.5}$$

$x \in \mathbb{R}^n$, $u \in \mathbb{R}^m$ and $y \in \mathbb{R}^p$ are the state, the input and the measured output, respectively. $\rho(t) \in \mathbb{R}^k$ is a vector of scheduling parameters and is assumed to be known (measured or estimated) and bounded in $\mathcal{P}$. From now on, $\rho(t)$ is simply denoted as ρ. For simplicity the state-space representation (2.2.5) is sometimes represented by:

$$S(\rho) = \left[\begin{array}{c|c} A(\rho) & B(\rho) \\ \hline C(\rho) & D(\rho) \end{array}\right] \tag{2.2.6}$$

Remark 2.2.1. If $\rho(x)$ depends on the state variables, the system is said to be *quasi-LPV* (q-LPV).

Based on the dependence of the system matrices on the scheduling parameters, the LPV systems are classified into two types: affine and polytopic systems.

Affine systems In this case, all matrices A, B, C, D are affine in the scheduling parameter ρ or $S(\rho)$ is an affine function of ρ, i.e.

$$\begin{aligned} A(\rho) &= A_0 + \textstyle\sum_{i=1}^{N} A_i \rho_i \\ B(\rho) &= B_0 + \textstyle\sum_{i=1}^{N} B_i \rho_i \\ C(\rho) &= C_0 + \textstyle\sum_{i=1}^{N} C_i \rho_i \\ D(\rho) &= D_0 + \textstyle\sum_{i=1}^{N} D_i \rho_i \end{aligned} \tag{2.2.7}$$

ρ_i is the i^{th} element of ρ and A_i are constant matrices.

Polytopic systems The system matrices are represented by

$$\begin{aligned} A(\rho) &= \textstyle\sum_{i=1}^{N} \rho_i A_i \\ B(\rho) &= \textstyle\sum_{i=1}^{N} \rho_i B_i \\ C(\rho) &= \textstyle\sum_{i=1}^{N} \rho_i C_i \\ D(\rho) &= \textstyle\sum_{i=1}^{N} \rho_i D_i \end{aligned} \tag{2.2.8}$$

where $\sum_{i=1}^{N} \rho_i = 1$ and $\rho_i \geq 0$. The polytopic systems offer a great interest in controller design and implementation. As, in this case, the LPV system is a convex hull of a finite number of LTI systems, it allows to solve a finite number of LMI problems (see [Gahinet et al., 1996], [Scherer, 2004]) to find a global LPV controller (which is also a convex hull of a finite number of local LTI controllers).

From LPV system to polytopic system When all scheduling parameters ρ_i of the LPV system are independent and bounded in $[\bar{\rho}_i, \underline{\rho}_i]$, i.e. the set $\mathcal{P}$ is a hypercube of 2^p vertices ω_1, ω_2,...,ω_{2^p}, the LPV system can be represented by an equivalent polytopic one:

$$S(\rho) = \left[\begin{array}{c|c} A(\rho) & B(\rho) \\ \hline C(\rho) & D(\rho) \end{array}\right] = \sum_{i=1}^{N} \alpha_i(\rho) \left[\begin{array}{c|c} A(\omega_i) & B(\omega_i) \\ \hline C(\omega_i) & D(\omega_i) \end{array}\right]$$

where

$$\alpha_i(\rho) = \frac{\prod_{i=1}^{p} |\rho_i - Compl(\omega_i)|}{\prod_{i=1}^{p} (\bar{\rho}_i - \underline{\rho}_i)} \tag{2.2.9}$$

and $Compl(\omega_i)_k$ is the k^{th} component of the vector $Compl(\omega_i)$ defined as

$$Compl(\omega_i)_k := \{\rho_k : \rho_k = \bar{\rho}_k \text{ if } (\omega_i)_k = \underline{\rho}_k \text{ or } \rho_k = \underline{\rho}_k \text{ otherwise}\} \tag{2.2.10}$$

2.2.2 Stability of LPV systems

Definition 2.2.1. ***Quadratic stability***
System (2.2.5) is said to be quadratically stable if there exists a quadratic Lyapunov function $V(x(t)) = x(t)^T P x(t) > 0$ *for every* $x \neq 0$ *and* $V(0) = 0$ *such that*

$$\dot{V}(t) = x(t)^T (A(\rho)^T P + P A(\rho)) x(t) < 0 \tag{2.2.11}$$

for every $x \neq 0$ *and* $V(0) = 0$*, for all* $\rho \in \mathcal{P}$*.*

Definition 2.2.2. ***Robust stability***
System (2.2.5) is said to be robustly stable if there exists a parameter-dependent Lyapunov function $V(x(t)) = x(t)^T P(\rho) x(t) > 0$ *for every* $x \neq 0$ *and* $V(0) = 0$ *such that*

$$\dot{V}(t) = x(t)^T (A(\rho)^T P(\rho) + P(\rho) A(\rho) + \dot{\rho} \frac{\partial P}{\partial \rho}) x(t) < 0 \tag{2.2.12}$$

for every $x \neq 0$ *and* $V(0) = 0$ *for all* $\rho \in \mathcal{P}$*.*

It should be noticed that (2.2.11) and (2.2.12) are infinite dimensional problems since ρ can take any value in $\mathcal{P}$.

2.2.3 LPV synthesis

Consider a general LPV system

$$\begin{aligned} \dot{x} &= A(\rho(t))x + B_1(\rho(t))w + B_2(\rho(t))u \\ z &= C_1(\rho(t))x + D_{11}(\rho(t))w + D_{12}(\rho(t))u \\ y &= C_2(\rho(t))x + D_{21}(\rho(t))w \end{aligned} \tag{2.2.13}$$

where $x \in \mathbb{R}^n$, $u \in \mathbb{R}^m$, $w \in \mathbb{R}^q$, $z \in \mathbb{R}^r$ and $y \in \mathbb{R}^p$ are the state, the input, the disturbance vectors, the controlled output and the measured output, respectively. $\rho(t) \in \mathbb{R}^k$ is a vector of scheduling parameters and is assumed to be known (measured or estimated) and bounded in $\rho(t) \in \mathcal{P}$. From now on, $\rho(t)$ is simply denoted as ρ.

The *LPV* controller associated to the LPV system (2.2.13) is defined as follows

$$K(\rho) : \begin{pmatrix} \dot{x}_c \\ u \end{pmatrix} = \begin{pmatrix} A_c(\rho) & B_c(\rho) \\ C_c(\rho) & D_c(\rho) \end{pmatrix} \begin{pmatrix} x_c \\ y \end{pmatrix} \tag{2.2.14}$$

where x_c, y and u are the state, the input and output of the controller, respectively, of the controller associated to the system (3.5.1). $A_c \in \mathbb{R}^{n \times n}$, $B_c \in \mathbb{R}^{n \times n_y}$, $C_c \in \mathbb{R}^{n_u \times n}$ and

$D_c \in \mathbb{R}^{n_u \times n_y}$.

The LPV synthesis concerns the design of a global LPV controller that guarantees both stability and performance for all scheduling parameters defined in the predefined set $\mathcal{P}$. There are two approaches based on Quadratic and Parameter-Dependent Lyapunov Functions. In the quadratic approach, only the bounds on the scheduling parameter are taken into consideration (i.e. the parameter can vary as fast as possible) while in the parameter-dependent approach, further information on parameter rate is used in the synthesis. Henceforth, the latter approach is less conservative. In the LPV approaches for semi-active suspension control presented in the next chapters, the systems are sometimes q-LPV and unfortunately the rates of scheduling parameters are unknown. As the result, we recall here only the quadratic approach for LPV control.

Stabilization problem

As in [Scherer et al., 1997] et [Apkarian & Gahinet, 1995], if there exist matrices $\hat{A}$, $\hat{B}$, $\hat{C}$ $\hat{D}$, and positive definite matrices X, Y satisfying the following LMIs

$$\begin{bmatrix} \mathcal{M}_{11}(\rho_i) & \mathcal{M}_{12}(\rho_i) \\ \mathcal{M}_{12}^T(\rho_i) & \mathcal{M}_{22}(\rho_i) \end{bmatrix} \prec 0 \qquad \text{for } i = 1 : N \tag{2.2.15}$$

where

$$\begin{aligned} \mathcal{M}_{11}(\rho_i) &= A(\rho_i)X + XA(\rho_i)^T + B_2\hat{C}(\rho_i) + \hat{C}(\rho_i)^T B_2^T \\ \mathcal{M}_{12}(\rho_i) &= \hat{A}(\rho_i) + A(\rho_i)^T + {C_2}^T \hat{D}(\rho_i)^T B_2^T \\ \mathcal{M}_{22}(\rho_i) &= YA(\rho_i) + A(\rho_i)^T Y + \hat{B}(\rho_i)C_2 + {C_2}^T \hat{B}(\rho_i)^T \end{aligned}$$

then the LPV controller (2.2.14) which stabilizes the system (2.2.13) is given by

$$K_c(\rho) = Co\{ \begin{pmatrix} A_c(\rho_i) & B_c(\rho_i) \\ C_c(\rho_i) & D_c(\rho_i) \end{pmatrix} \} \tag{2.2.16}$$

where

$$\begin{aligned} D_c(\rho_i) &= \hat{D}(\rho_i) \\ C_c(\rho_i) &= \left(\hat{C}(\rho_i) - D_c(\rho_i)C_2X\right) M^{-T} \\ B_c(\rho_i) &= N^{-1}\left(\hat{B}(\rho_i) - YB_2D_c(\rho_i)\right) \\ A_c(\rho_i) &= N^{-1}\left(\hat{A}(\rho_i) - YA(\rho_i)X - YB_2D_c(\rho_i)C_2X\right) M^{-T} \\ &\quad -B_c(\rho_i)C_2XM^{-T} - N^{-1}YB_2C_c(\rho_i) \end{aligned} \tag{2.2.17}$$

where M, N are defined such that $MN^T = I_n - XY$ which can be solved through a singular value decomposition and a Cholesky factorization.

H_∞ performance

H_∞ problem for LPV systems - The objective of the synthesis is to find an LPV controller $K(\rho)$ of the form (2.2.14) such that the closed-loop system is quadratically stable and that, for a given positive real γ, the induced-L_2 norm of the operator mapping w into z is bounded by γ i.e

$$\sup_{\rho\in\mathcal{P}} \sup_{w\neq 0, w\in L_2} \frac{\|z\|_2}{\|w\|_2} \leq \gamma \tag{2.2.18}$$

Solution: polytopic approach with quadratic Lyapunov function
It is assumed that the LPV system has a polytopic formulation, i.e. $\rho \in conv\{\rho_1, ...\rho_k\}$ and that the matrices B_2, D_{12}, C_2, D_{21} are parameter independent and $D_{22} = 0$. For a pre-defined real positive scalar γ, the sufficient condition that solves the H_∞/LPV problem is given by Eq. (2.2.19)-(2.2.20) (see the details of the solution in [Scherer et al., 1997]).

$$\begin{bmatrix} \mathcal{M}_{11}(\rho_i) & * & * & * \\ \mathcal{M}_{21}(\rho_i) & \mathcal{M}_{22}(\rho_i) & * & * \\ \mathcal{M}_{31}(\rho_i) & \mathcal{M}_{32}(\rho_i) & -\gamma I_m & * \\ \mathcal{M}_{41}(\rho_i) & \mathcal{M}_{42}(\rho_i) & \mathcal{M}_{43}(\rho_i) & -\gamma I_p \end{bmatrix} \prec 0 \tag{2.2.19}$$

$$\begin{bmatrix} X & I \\ I & Y \end{bmatrix} \succ 0 \tag{2.2.20}$$

$$\text{for i} = 1:4$$

where

$$\begin{aligned}
\mathcal{M}_{11}(\rho_i) &= A(\rho_i)X + XA(\rho_i)^T + B_2\hat{C}(\rho_i) + \hat{C}(\rho_i)^T B_2^T \\
\mathcal{M}_{21}(\rho_i) &= \hat{A}(\rho_i) + A(\rho_i)^T + C_2^T\hat{D}(\rho_i)^T B_2^T \\
\mathcal{M}_{22}(\rho_i) &= YA(\rho_i) + A(\rho_i)^T Y + \hat{B}(\rho_i)C_2 + C_2^T\hat{B}(\rho_i)^T \\
\mathcal{M}_{31}(\rho_i) &= B_1(\rho_i)^T + D_{21}^T\hat{D}(\rho_i)^T B_2^T \\
\mathcal{M}_{32}(\rho_i) &= B_1(\rho_i)^T Y + D_{21}^T\hat{B}(\rho_i)^T \\
\mathcal{M}_{41}(\rho_i) &= C_1(\rho_i)X + D_{12}\hat{C}(\rho_i) \\
\mathcal{M}_{42}(\rho_i) &= C_1(\rho_i) + D_{12}\hat{D}(\rho_i)C_2 \\
\mathcal{M}_{43}(\rho_i) &= D_{11}(\rho_i) + D_{12}\hat{D}(\rho_i)D_{21}
\end{aligned}$$

The controller K_{c_i} at vertex i is then reconstructed as

$$\begin{aligned} D_c(\rho_i) &= \hat{D}(\rho_i) \\ C_c(\rho_i) &= \left(\hat{C}(\rho_i) - D_c(\rho_i)C_2X\right)M^{-T} \\ B_c(\rho_i) &= N^{-1}\left(\hat{B}(\rho_i) - YB_2D_c(\rho_i)\right) \\ A_c(\rho_i) &= N^{-1}\left(\hat{A}(\rho_i) - YA(\rho_i)X - YB_2D_c(\rho_i)C_2X\right)M^{-T} \\ &\quad -B_c(\rho_i)C_2XM^{-T} - N^{-1}YB_2C_c(\rho_i) \end{aligned} \tag{2.2.21}$$

where M, N are defined such that $MN^T = I_n - XY$ which can be solved through a singular value decomposition and a Cholesky factorization. The global H_∞/LPV controller is then the convex combination of these local controllers.

2.3 Multi-objective optimization by genetic algorithms

In this thesis, the semi-active suspension control problem will be linked to different objectives such as passenger comfort, road holding and suspension deflection. Hence the multi-objective framework is an important issue.

2.3.1 Multi-objective optimization

The multi-objective optimization is a very popular problem in practice and can be described as follows

$$\min_{x\in C} F(x) = \begin{bmatrix} f_1(x) \\ f_2(x) \\ \vdots \\ f_{n_{obj}}(x) \end{bmatrix}, \qquad n_{obj} \geqslant 2, \tag{2.3.1}$$

where x is called the decision vector, C the set of possible decision vectors (or the searching space), and $F(x)$ the objective vector.
Finding an ideal solution x^* that can minimize simultaneously all objective functions f_1, f_2... $f_{n_{obj}}$ is in fact rarely feasible. Hence, in this case, the concept of *Pareto-optimal* is usually used to describe the solution of multi-objective optimization problem and it is defined as follows.

Definition 2.3.1. Pareto-Ranking *Consider two decision vectors $a, b \in C$. Vector a dominates b if and only if:*

$$\begin{cases} \forall i \in \{1, 2, ..., n_{obj}\} : f_i(a) \leqslant f_i(b) \\ \exists j \in \{1, 2, ..., n_{obj}\} : f_j(a) < f_j(b) \end{cases} \tag{2.3.2}$$

All decision vectors which are not dominated by any other decision vector are called non-dominated *or* Pareto-optimal. *The family of non-dominated vectors is denoted as* Pareto-front. *In the Pareto-front, one cannot improve any objective without degrading at least one other objective.*

There are many formulations to solve the problem (2.3.1). First, there are the aggregated methods like weighted min-max method, weighted global criterion method, goal programming methods... see [Marler & Arora, 2004] and references therein. One of the most popular and simple approaches is the weighted sum method which converts the multi-objective problem into a single objective problem. A particular case of the weighted sum method, where the multi-objective function F is replaced by the convex combination of different objectives, is described as follows

$$\min J = \sum_{i=1}^{n_{obj}} \alpha_i f_i(x), \qquad s.t \qquad x \in C \tag{2.3.3}$$

where $\sum_{i=1}^{n_{obj}} \alpha_i = 1$.
The vector $\alpha = (\alpha_1, \alpha_2, ...\alpha_{n_{obj}})$ represents the gradient of function J (see Fig. 2.5). By using various sets of α, one can generate several points in the Pareto set. It is worth noting that the solution of (2.3.3) provides a sufficient condition for (2.3.1), i.e., the minimum of (2.3.3) is also Pareto optimal point for (2.3.1), see [Zadeh, 1963] and [Geoffrion, 1968].

Drawback of (2.3.3):

- Need to repeat the single objective optimization procedure many times (with different values of α).
- Although there has been many methods for selecting weights, none guarantees that the final will be acceptable.
- If the Pareto curve is not convex, there does not exist any α to obtain points which lies in the nonconvex part [Das & Dennis, 1997], [Messac et al., 2000] and [Marler & Arora, 2004].
- Even if the Pareto curve is convex, an even spread of weights does not produce an even distribution of points on the Pareto curve.

Other methods based on Pareto-ranking and evolutionary algorithms are indeed more preferable although it is shown in [Purshouse, 2003] that all multi-objective optimization algorithms that use Pareto-ranking as a fundamental selection method will degrade the

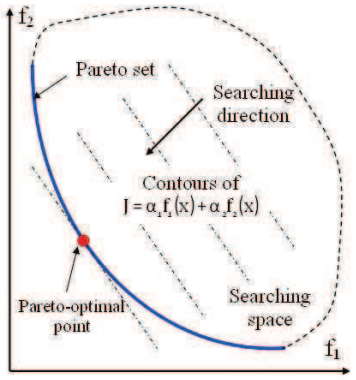

Figure 2.5: Illustration of weighted sum method.

performances with increasing number of objectives (from 4 objectives). Instead of searching one best solution as aggregated methods, the Pareto-ranking based methods allow to obtain many Pareto-optimal points with a single run. Fig. 2.6 presents an example for minimization problem. The best solution (in sense of Pareto) is not unique. Based on Pareto-ranking, the best solutions are $\{1, 2, 3\}$ which are solutions not dominated by others.

In the next section, the multi-optimization using Pareto-ranking and genetic algorithms will be presented.

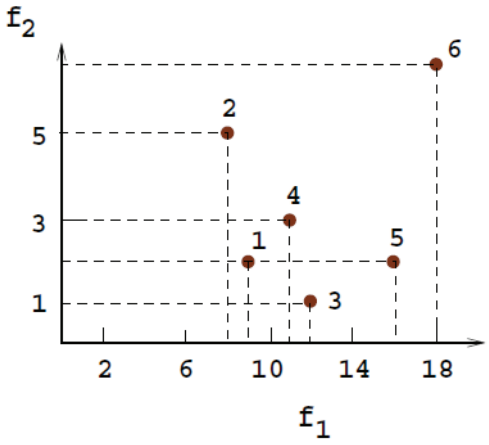

Figure 2.6: Illustration of Pareto-Ranking method. In this example, the minimal solutions are desired and the non-dominated set is $\{1, 2, 3\}$.

2.3.2 Genetic algorithms

The genetic algorithms, the most popular types of evolutionary algorithms, have now grown strongly from the first study of [Holland, 1975], a popular theory-oriented book of [Goldberg, 1989] and an application-oriented book of [Davis, 1991]. The algorithms are based on the mechanism of the natural selection and have been proven to be very effective in optimization with many real applications such as in finance and investment strategies, robotics, engineering design, telecommunications... They are likely global optimization techniques (despite the high computational expense) (see [Marler & Arora, 2004]) using probabilistic, multi-points search, random combination (crossover, mutation) and information of previous iteration to evaluate and improve the population. A great advantage of GAs compared with other searching methods (for example gradient methods) is that they search regardless of the nature of the objective functions and constraints.

The principle of GAs is presented in Fig. 2.7. At the beginning, GAs initializes with a random population. Through the genetic operation: *selection*, *crossover* and *mutation*, new population will be obtained. By using a selection process, the fittest individuals based on their *fitness* values will be chosen; crossover and mutation will be then applied to create the new population. The genetic operation on individuals of population continues until the optimization criterion is satisfied or a certain number of generations is reached.

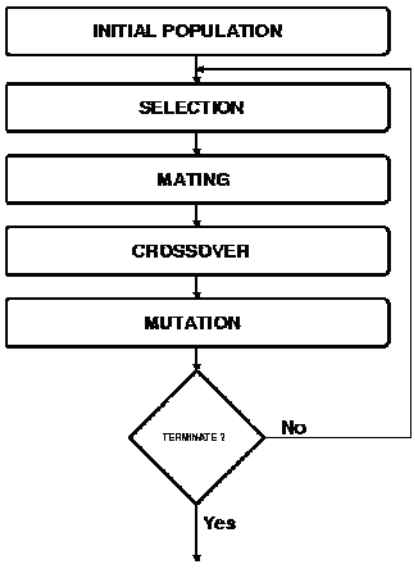

Figure 2.7: Principle of genetic algorithms.

Fitness function - The fitness of an individual is useful for choosing between “good" and “bad" individuals. An individual with a high fitness value will have a great chance to be selected.

Selection - This step is to sort and copy individuals by order of satisfaction of the fitness function. The higher the value of the fitness, associated to an individual, the greater the individual's chances to be selected to participate in the next generation. "Proportionate selection" (see [Holland, 1975]) and "tournament selection" (see [Miller & Goldberg, 1995]) are the two most popular selection methods.

Crossover - This is the main operation acting on the population of parents. It consists of an exchange of parts of chains between two selected individuals (parents) to form two new individuals (children). This exchange may be due either to a single point or to multiple points. The Fig. 2.8 is an example for a binary coding crossover.

Mutation - Mutation operates on a single individual by changing randomly a part of it. In the case of binary coding, this is done by reversing one or more bits in a chromosome (Fig. 2.8). Other methods can be used as determined by subtracting the mutation on a gene or replacing it with a random value chosen from a subset of values.

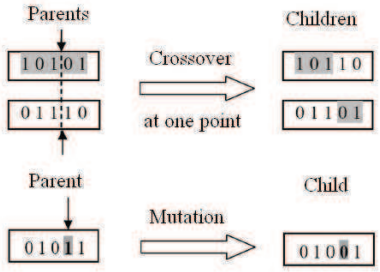

Figure 2.8: Crossover and mutation operation.

As mentioned in [Zitzler et al., 2000], two major problems must be addressed when an evolutionary algorithm in general and a genetic algorithm in particular is applied to multi-objective optimization (see also Fig. 2.9):

- How to accomplish fitness assignment and selection, respectively, in order to guide the search towards the Pareto-optimal set?
- How to maintain a diverse population in order to prevent premature convergence and achieve a well distributed trade-off front?

The question on which algorithms can handle these two important objectives is answered in the next section.

2.3.3 Elitist multi-objective evolutionary algorithms (MOEAs)

In general, genetic algorithms can be classified as elitist and non-elitist strategies. For non elitist strategies like MOGA [Fonseca & Fleming, 1993], NSGA [Srinivas & Deb,

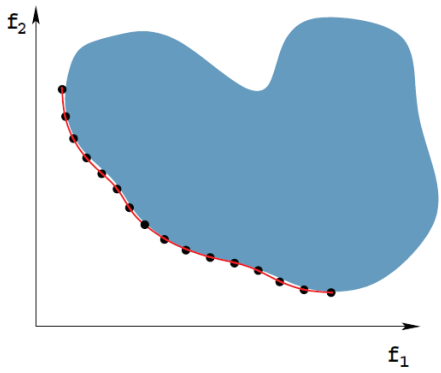

Figure 2.9: Two goals of an evolutionary algorithm: to guide the search towards the Pareto-optimal set and to achieve a well distributed trade-off front.

1995], [Horn et al., 1994]..., the non-dominated individuals are not conserved in the population i.e from old population, a new one will be created randomly (using crossover, mutation and selection). This leads to the loss of good individuals in the old population. Moreover, the diversity on the Pareto front is difficult to maintain and the convergence toward the Pareto front is slow. In contrary, for elitist strategies like PAES [Knowles & Corne, 1999], SPEA2 [Zitzler et al., 2001], NSGA-II [Deb et al., 2002]... they always keep the best individuals by saving them in an external archive (called elitist set) whose size is considerable compared with the population. These elitist individuals are then reinserted in the population. The procedure to update the elitist set and reinsert the elitist individuals in the population are different.

Recent results in [Zitzler et al., 2000] show clearly that elitism can significantly speed up the performance of the GA. The elitist MOEAs like SPEA2, NSGA-II... outperform other non-elitist MOEAs for both the distance to the optimal front and the spread distribution of non-dominated solution.

In the following, the main loop of the elitist MOEAs named SPEA2 will be presented because the two important objectives (good approach to the Pareto-front and good diverse population) are well satisfied for multi-objective optimization problems which have no more than four objective functions. This algorithm will be also applied to the semi-active controller optimization in the next chapters. For further details of the algorithm, it is recommended to read [Zitzler et al., 2001].

Strength Pareto Evolutionary Algorithm 2 (SPEA2) The main loop is as follows

- Step 1: Generate the initial population P and set $\bar{P} = \emptyset$.
- Step 2: Set $P' = P + \bar{P}$ and perform fitness assignment on the extended population

P' of size $N + \bar{N}$.

- Step 3: Update external population by copying all non-dominated members of P to $\bar{P}$ and afterwards by removing double or dominated individuals from $\bar{P}$.
- Step 4: If size of P is larger than N, then calculate reduced non-dominated set P_r of size N by clustering and set $P = P_r$.
- Step 5: Select N individuals out of the N' individuals in P' and perform crossover and mutation to create the next population P''.
- Step 6: Substitute P by P'' and go to Step 2 if the maximum number of generations is not reached.

In SPEA2, the fitness of each solution is defined by strength value (based on Pareto-dominance relation) and density estimation (function of the distance to k-th nearest data point, where $k \in N$ is a predefined number). The information about density estimation is added into the fitness value to improve the diversity of the Pareto-front and prevent the premature convergence.

2.4 Input saturation control

Input saturation control is an interesting problem in terms of practical implementation. In semi-active suspension control, we will see that the passivity constraint can be transformed into that of input saturation and can be handed in different ways. In this section, we present briefly some interesting problems of the input saturation control. The solutions of these problems are not given here but can be accessed through the cited references.

2.4.1 Introduction

In the last years, many studies have focused on the control of saturated (in states, control inputs...) systems which are present in almost all real applications. For a system with input saturation, there is usually an inconsistency between the states of the plant and those of the controller because of the saturated actuator between the system control input and the controller output. This effect, usually called windup, degrades dramatically the closed-loop performances or even worse may cause the system instability. To preserve the consistency, the input to controller needs to be changed by an appropriate signal, which is provided by a compensator called anti-windup. Usually the problems on how to guarantee the (global or local) stabilization of the saturated system in the presence of

disturbance and to ensure some closed-loop performances are the most interesting ones. There are two methods to solve these problems: the two-step and one-step design. The traditional two-step method first designs a linear controller without considering the input saturation effect and then add an anti-windup compensator to minimize the adverse effects of control input saturation on closed-loop performance [Kothare et al., 1994], [Grimm et al., 2003], [Wu & Lu, 2004]. While for the later, the controller and an anti-windup compensator (static in general) are simultaneously computed [Gomes da Silva Jr. et al., 2008], [Mulder et al., 2009]. It can be seen that the control design with input saturation is a nonlinear problem. Many solutions have been proposed to model the saturation effect in such a way that the problem can be treated within a linear framework, for example: the polytopic differential inclusion model [Gomes da Silva Jr. & Tarbouriech, 2001], [Wu et al., 2000], [Hu et al., 2002*a*] and the use of sector conditions [Gomes da Silva Jr. & Tarbouriech, 2005], [Wu & Lu, 2004], [Mulder et al., 2009]. Up to now, numerous results have been obtained for LTI systems. This section will present a brief overview about the control problem with input saturation for the class of LTI systems.

Let consider the following system

$$\dot{x} = Ax + B_1 w + B_2 u \quad \text{and} \quad -u_{min} \leq u \leq u_{max} \tag{2.4.1}$$

where x is the state, w is the disturbance and u is the control input, $u_{min}, u_{max} \in \mathbb{R}_+$. The main interest for the study of such systems concerns the influence of input saturation effect on the stability and performance of the closed-loop system. It has been proven by many studies, only in the case where the open-loop system is already exponentially stable that the global stability can be assured by a controller. In other cases, the stability (and performance) is guaranteed in a local region of stability. If this region is small, the closed-loop system may be unstable depending on the initial states and disturbance input. For example, consider the system below

$$\dot{x} = \begin{bmatrix} 0 & 1 \\ 1 & 0 \end{bmatrix} x + \begin{bmatrix} 0 \\ -1 \end{bmatrix} u, \quad -5 \leq u \leq 5 \tag{2.4.2}$$

Note that the system (2.4.2) is unstable (its poles are ± 1) and it can be stabilized by a state-feedback controller

$$K(x) = \begin{bmatrix} 13 & 7 \end{bmatrix} x \tag{2.4.3}$$

The result presented in Figure 2.10-2.11 shows that the effect of input saturation depends on initial state of the system. In Fig. 2.10, when $x_0 = [-1; 4]$, both the saturated and unsaturated closed-loop systems are stable, but when $x_0 = [-3; 3]$ (Fig. 2.11) the stability of the saturated one is not preserved. We can conclude that the region of stability offered by the controller (2.4.3) is not sufficiently large to assure that under

saturation effect $-5 \leq u \leq 5$, the system still converges to the origin when it starts from the initial point $x_0 = [-3; 3]$.

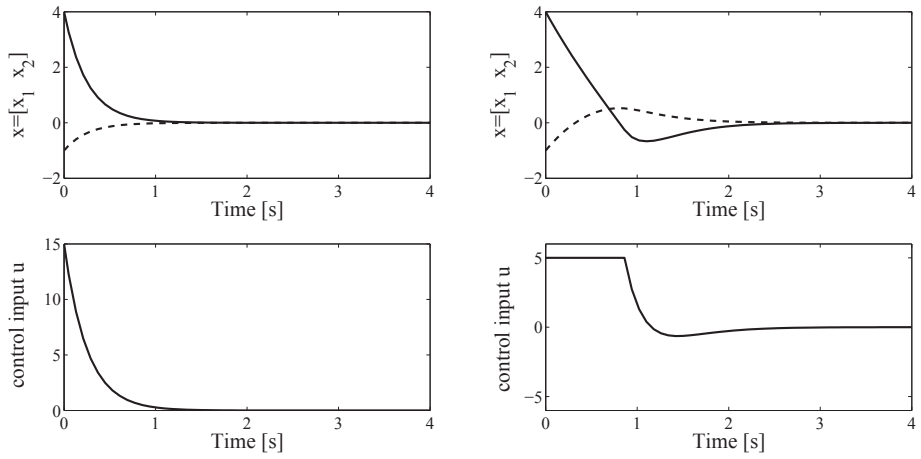

Figure 2.10: Effect of input saturation: $x_0 = [-1; 4]$. Unsaturated system (Left) and Saturated system (Right)

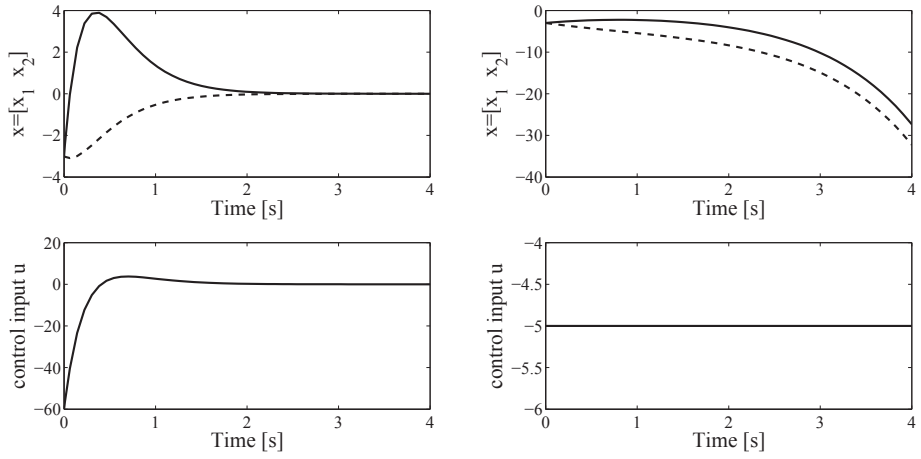

Figure 2.11: Effect of input saturation: $x_0 = [-3; -3]$. Unsaturated system (Left) and Saturated system (Right)

The following definition is useful for the analysis of the input saturation control problem.

Definition 2.4.1. ***Region of stability (attraction)***
The region of stability of the equilibrium x_e is defined as

$$R_A(x_e) = \{x(0) \in \mathbb{R}^n; x(t) \to x_e \quad when \quad t \to \infty\} \tag{2.4.4}$$

The system is globally asymptotically stable if $R_A = \mathbb{R}^n$. However, as mentioned above for the systems subject to input saturation, in general $R_A \neq \mathbb{R}^n$. In these cases, the local (or regional) stability is analyzed. Both following problems are usually encountered:

- *Analysis problem:* Find a set $D_0 \in R_A$, as large as possible, such that: for any $x(0) \in D_0$, $x(t) \to x_e$ when $t \to \infty$. In this case, D_0 is called the estimate of R_A.

- *Synthesis problems:*
  - (1) For a given set D_0, find K such that for all $x(0) \in D_0$, $x(t) \to x_e$ when $t \to \infty$, or,
  - (2) Find a controller K in order to maximize the estimate D_0 of R_A or
  - (3) For a given set D_0, find K such that for all $x(0) \in D_0$, $x(t) \to x_e$ when $t \to \infty$ and minimize some performance criteria...

It can be seen that saturation is a nonlinear effect; to take it into account in the linear analysis and design, the saturation can be modeled by different methods. In the following, three methods are presented. For simplicity and clarity, only the case of state-feedback controller, i.e. $u = Kx$, is considered. Note that X_i stands for the i^{th} element of X.

2.4.2 Saturation modeling

Regions of saturation

Define $\xi \in \mathbb{R}^m$:

- if $u_i = u_{max_i}$ then $\xi_i = 1$
- if $u_i = K_i x$ then $\xi_i = 0$
- if $u_i = -u_{min_i}$ then $\xi_i = -1$

The system (2.4.1) with is now rewritten as

$$\dot{x} = (A + Bdiag(I_m - |\xi_j|)K)x + Bu(\xi_j) \quad j = 1 : m \tag{2.4.5}$$

or equivalent to following linear system with an addictive disturbance

$$\dot{x} = \bar{A}_j x + p_j \tag{2.4.6}$$

See more details in [Gomes da Silva Jr. & Tarbouriech, 1999].

Polytopic

Approach 1: see [Gomes da Silva Jr. et al., 2003]

$$sat(Kx) = \Gamma(\alpha(x))Kx \tag{2.4.7}$$

where $\Gamma(\alpha(x))$ is a diagonal matrix whose diagonal elements are defined for $i = 1 : m$ as

$$\alpha_i(x) = \begin{cases} \frac{u_{max_i}}{K_i x} & \text{if} \quad K_i x > u_{max_i} \\ 1 \quad \text{if} & -u_{min_i} \leq K_i x \leq u_{max_i} \\ \frac{-u_{max_i}}{K_i x} & \text{if} \quad K_i x < -u_{min_i} \end{cases} \tag{2.4.8}$$

$$\dot{x} = (A + B\Gamma(\alpha(x))K)x \tag{2.4.9}$$

Define

$$S(K, u^{\alpha}_{min}, u^{\alpha}_{max}) = \{x \in \mathbb{R}^n; \frac{-u_{min}}{\alpha_{li}} \leq K_i x \leq \frac{u_{max}}{\alpha_{li}}, \forall i = 1 : m\} \tag{2.4.10}$$

where $0 < \alpha_{l_i} < 1$ with $i = 1 : m$. For any $x \in S(K, u^{\alpha}_{min}, u^{\alpha}_{max})$, one gets

$$0 < \alpha_{l_i} \leq \alpha_i(x) \leq 1, \forall i = 1 : m \tag{2.4.11}$$

$$\Gamma(\alpha(x)) \in Co\{\Gamma_1(\alpha_l), \Gamma_2(\alpha_l), \Gamma_{2^m}(\alpha_l)\} \tag{2.4.12}$$

where $\Gamma_j(\alpha_l)$ are diagonal matrices whose elements take the value 1 or α_{l_i}

Lemma 2.4.1. *If $x \in S(K, u^{\alpha}_{min}, u^{\alpha}_{max})$ then*

$$\dot{x} = \sum_{j=1}^{2^m} \lambda_j (A + B\Gamma_j(\alpha_l)K)x \tag{2.4.13}$$

with $\sum_{j=1}^{2^m} \lambda_j = 1$, $\lambda_j \geq 0$.

In this approach, α_l represents the degree of saturation and must be known. As the result, the approach presents some conservatism.

Approach 2: see [Hu et al., 2002b]
Define:

- $$S(H, u_{min}, u_{max}) = \{x \in \mathbb{R}^n; -u_{min_i} \leq H_i x \leq u_{max_i}, i = 1 : m\} \tag{2.4.14}$$

- Γ_j^+ : diagonal matrices whose diagonal elements take the value 1 or 0, $j = 1 : 2^m$
- $\Gamma_j^- = I_m - \Gamma_j^+$

Lemma 2.4.2. *If $x \in S(H, u_{min}, u_{max})$ then*

$$sat(Kx) \in Co\{\Gamma_j^+ Kx + \Gamma_j^- Hx\} \tag{2.4.15}$$

This approach is less conservative than the approach 1 because H is a design matrix. Note that if $H = \Gamma(\alpha_l)K$, this approach is equivalent to approach 1.

Sector nonlinearity

The closed-loop system can be re-written as

$$\dot{x} = Ax + Bsat(Kx) \tag{2.4.16}$$

$$= (A + BK)x - B\psi(Kx) \tag{2.4.17}$$

with $\psi(Kx)$ is the decentralized dead-zone nonlinearity and is defined by

$$\psi(Kx) = Kx - sat(Kx) \tag{2.4.18}$$

The sector condition is one of the most interesting methods to model the saturation effect. Thanks to the two following lemmas, the saturation effect can be taken into consideration in linear design.

Approach 1: Classical sector condition

Lemma 2.4.3. *Let $S(K, u_0^\lambda)$ is a polyhedral set defined as follows:*

$$S(K, u_0^\lambda) = \{x \in \mathbb{R}^n; -\frac{u_{0_i}}{1 - \Lambda_{(i,i)}} \leq K_i x \leq \frac{u_{0_i}}{1 - \Lambda_{(i,i)}}, i = 1 : m\} \tag{2.4.19}$$

then the following holds:

$$\psi(Kx)^T T[\psi(Kx) - \Lambda Kx] \leq 0, \forall x \in S(K, u_0^\lambda), \forall T > 0 \tag{2.4.20}$$

This approach has been used in many studies [Tyan & Bernstein, 1997], [Kiyama & Iwasaki, 2000]. However, it can be seen that the lemma applies for all nonlinearities lying in the sector and not only for deadzone nonlinearities. This is the source of conservatism. The modified version of this lemma is presented as follows.

Approach 2: [Gomes da Silva Jr. & Tarbouriech, 2005]

Lemma 2.4.4. *Let $S(K-G,u_0)$ be a polyhedral set defined as follows:*

$$S(K-G,u_0)=\{x\in\mathbb{R}^n;-u_{0_i}\leq(K_i-G_i)x\leq u_{0_i},i=1:m\} \tag{2.4.21}$$

then the following holds:

$$\psi(Kx)^TT[\psi(Kx)-Gx]\leq 0,\forall x\in S(K-G,u_0),\forall T>0 \tag{2.4.22}$$

- If $G=\Lambda K$, equivalent to Approach 1
- The lemma applies only to the deadzone nonlinearities. Compared to approach 1, this reduces the conservatism.

2.4.3 Stability Analysis

The stability analysis problem is stated as follows: with a given stabilizing controller K, determine the regions of the state space in which the convergence of the trajectories of the closed-loop system towards the origin is guaranteed.
Solution: The basic idea to the problem is to use ellipsoidal or polyhedral contractive set $\mathcal{E}$ associated to the Lyapunov candidate function $V(x)$ and establish an inclusion constraint which ensures the contractive set contained in the validity region of the saturation modeling $\mathcal{S}$ (see Fig. 2.12).

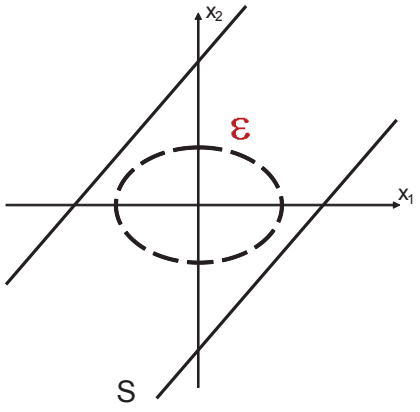

Figure 2.12: Invariant set approach for stability: S validity region of saturation, $\mathcal{E}$ contractive set

It turns out that the stability problem corresponds to the estimation of the region of attraction. In this context, a convex function $f(\mathcal{E})$ associated to the geometry/size of the contractive set $\mathcal{E}$ is usually chosen. The stability analysis concerns the maximization of this set (i.e. maximization of volume, maximization of the minor axis or maximization

in some directions).

In summary, the stability analysis can be done through the following optimization problem

$$\begin{aligned} &\min f(\mathcal{E}) \\ &\text{subject to stability condition} \end{aligned} \tag{2.4.23}$$

2.4.4 Controller design

Consider the following saturated system

$$\begin{aligned} \dot{x} &= Ax + B_1 w + B_2 u \\ z &= C_1 x + D_{11} w + D_{12} u \\ y &= C_2 x \end{aligned} \tag{2.4.24}$$

where $x \in \mathbb{R}^n$, $u \in \mathbb{R}^m$, $w \in \mathbb{R}^q$, $z \in \mathbb{R}^r$ and $y \in \mathbb{R}^p$ are the state, the input, the disturbance vectors, the control output and the measured output, respectively.
Consider also an LTI controller of the form

$$\begin{aligned} \dot{x}_c &= A_c x_c + B_c u_c + v \\ y_c &= C_c x_c + D_c u_c \end{aligned} \tag{2.4.25}$$

where $x_c \in \mathbb{R}^{n_c}$, $u_c \in \mathbb{R}^p$, $y_c \in \mathbb{R}^m$, v is an additional input used for anti-windup compensation.

The unconstrained closed-loop system of the plant (see Fig. 2.13), and the controller, is defined by the following interconnections

$$u = y_c, \quad u_c = y, \quad v = 0 \tag{2.4.26}$$

In case of input saturation control, we consider the following dynamic LTI controller with a static anti-windup action

$$\begin{aligned} \dot{x}_c &= A_c x_c + B_c u_c + E_c(sat(y_c) - y_c) \\ y_c &= C_c x_c + D_c u_c \end{aligned} \tag{2.4.27}$$

where $x_c \in \mathbb{R}^{n_c}$, $u_c \in \mathbb{R}^p$, $y_c \in \mathbb{R}^m$ and E_c is a static anti-windup term. The interconnections between the plant and the controller (see Fig. 2.14) are given by

$$u = sat(y_c), \; u_c = y, \; v = E_c(sat(y_c) - y_c) \tag{2.4.28}$$

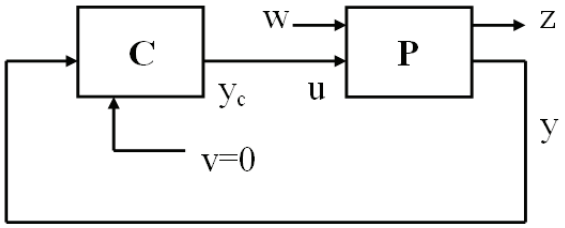

Figure 2.13: Unconstrained closed-loop plant.

where the saturated function $sat(.)$ is defined by

$$sat(y_{c_i}) = \begin{cases} u_{max_i} & \text{if } y_{ci} > u_{max_i} \\ y_{c_i} & \text{if } -u_{min_i} \leq y_{ci} \leq u_{max_i} \\ -u_{min_i} & \text{if } y_{ci} < -u_{min_i} \end{cases} \tag{2.4.29}$$

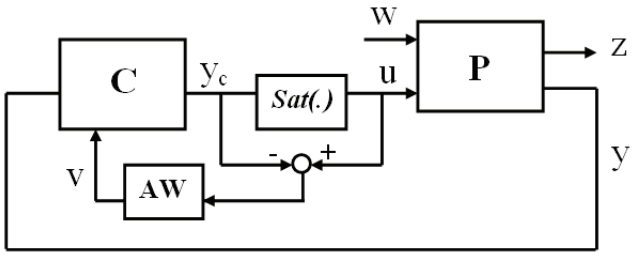

Figure 2.14: Control structure for system with input saturation

Stabilization problem

Asymptotic stabilization In the case of asymptotic stabilization, the saturated system (2.4.24) without disturbance is considered

$$\dot{x} = Ax + B_2 u \tag{2.4.30}$$
$$y = C_2 x \tag{2.4.31}$$

where $-u_{min} \leq u \leq u_{max}$.

The asymptotic stabilization problem can be one of the two following cases:

Definition 2.4.2. ***Problem 1*** *Given a set of admissible initial states D_0. Find a controller K of the form 2.4.27 such that all the trajectories of the closed-loop system initiated in D_0, asymptotically converge towards the origin.*

Definition 2.4.3. ***Problem 2*** *Find a controller K such that the asymptotic closed-loop system is ensured in a region as large as possible. This problem concerns the optimization of a contractive set.*

External stabilization In this case, the stabilization of the closed-loop system in the presence of disturbance is studied. Let consider the following system

$$\dot{x} = Ax + B_1 w + B_2 u \tag{2.4.32}$$
$$y = C_2 x \tag{2.4.33}$$

where $-u_{min} \leq u \leq u_{max}$. In general, the stability of the closed-loop system is not guaranteed for any bounded disturbance input. Usually, one of the following hypotheses are considered in the controller design.

- Amplitude bounds
$$W = \{w \in \mathbb{R}^q, w^T w \leq \delta\} \tag{2.4.34}$$
- Energy bounds
$$W = \{w \in \mathbb{R}^q, \int_0^t w^T w d\tau \leq \delta\} \tag{2.4.35}$$

Concerning the stabilization of a saturated system with the presence of disturbance, two interesting optimization problems are

- Find a controller K that maximizes the admissible disturbance bound δ.
- For a given bound δ on the admissible disturbance, find a controller K ensuring that the trajectories of the closed-loop system are bounded for any $w \in W$, and that the contractive set is maximized.

Local (regional) design for stability and performance

It is showed in [Grimm et al., 2003], [Hu, 2008] that, in the presence of input saturation constraint, for the systems which are not globally exponentially stable, the globally exponential stabilization is never achievable even with a nonlinear controller. The global stabilization can be only achieved with a system which is already globally stable. Otherwise, the local and regional results are always achievable with non-exponentially unstable plants. Due to this fact, a regional analysis is usually performed. Even, for globally stable systems, the region analysis is also useful to reduce the conservatism when the systems operate with a bounded region (bounded disturbance input, bounded states due to physical constraints...).

In the following, three properties and three associated problems for the regional analysis are presented. The solution for these problems are found in [Dai et al., 2006], [Dai et al., 2009] and [Hu, 2008].

Let us define $\mathcal{E}$ the domain of attraction of the plant (2.4.24), $\mathcal{E}_c$ the domain of attraction of the controller (2.4.25).

Property 1: Given a set $\mathcal{E} \subset \mathbb{R}^n$, the plant (2.4.24) is $\mathcal{E}_p$-regional exponentially stabilized by controller (2.4.27) if the origin of the closed-loop system is exponentially stable with the domain of attraction including $\mathcal{E} \times \mathcal{E}_c$ (where $\mathcal{E}_c \subset \mathbb{R}^{n_c}$ is a suitable set including the origin).

Property 2: Given a set $R_p \subset \mathbb{R}^n$ and a number $s > 0$, the controller (2.4.27) guarantees (s, R_p)-reachability for the plant (2.4.24) if the response $(x(t), x_c(t))$, $t \geq 0$ of the closed-loop system starting from the equilibrium point $(x(0), x_c(0)) = (0, 0)$ and with $\|w\|_2 < s$, satisfies $x(t) \in R_p$ for all $t \geq 0$.

Property 3: Given two numbers $s, \gamma > 0$, the controller (2.4.27) guarantees (s, γ)-regional finite $\mathcal{L}_2$ gain for the plant (2.4.24) if the performance output response $z(t)$, $t \geq 0$ of the closed-loop system starting from the equilibrium point $(x(0), x_c(0) = (0, 0))$ and with $\|w\|_2 < s$, satisfies $\|z\|_2 < \gamma \|w\|_2$

Definition 2.4.4. ***Problem 1: Exponential stability***
Consider the linear plant (2.4.24), a bound δ on the input disturbance w (bound on amplitude or energy), a desired reachability region R_p and a bound γ on the desired regional L_2 gain. Design a feedback controller K of the form (2.4.27) guaranteeing (δ, R_p) reachability, (δ, γ)- regional finite L_2 gain and which maximizes the exponential stability region $\mathcal{E}$ of the closed-loop system.

Definition 2.4.5. ***Problem 2: Reachable region***
Consider the linear plant (2.4.24), a bound s on w, a desired stability region $\mathcal{E}$ and a bound γ on the desired regional L_2 gain. Design a feedback controller K of the form (2.4.27) guaranteeing $\mathcal{E}$ regional exponential stability, (s, γ)-regional finite L_2 gain and which minimizes the (s, R_p) reachability region of the closed-loop system.

Definition 2.4.6. ***Problem 3: Global L_2 gain***
Consider the linear plant (2.4.24), a bound s on w, a desired stability region $\mathcal{E}$ and a desired reachability region R_p. Design a feedback controller K of the form (2.4.27) guaranteeing $\mathcal{E}$ regional exponential stability, (s, R_p) reachability and which minimizes the (s, γ)-regional finite L_2 gain of the closed-loop system.

2.5 Conclusions

In this chapter, we have presented some definitions, lemmas and theorems concerning the

- Optimization methods by LMIs, Genetic Algorithms
- LPV control and input saturation control

that will be useful for semi-active suspension control in the next chapters.

Chapter 3

Suspension systems with nonlinear Magneto-Rheological dampers

Recently, the Magneto-Rheological (MR) dampers have appeared to be one of the most investigated devices in both industrial and academic studies on semi-active suspension control. They use MR fluids whose characteristics can be changed through the application of a magnetic field. Compared with other kinds of semi-active dampers (like ER, friction dampers), they have great advantages like fast time response as well as stable hysteretic behavior over a broad range of temperature, low battery voltages consumption. They represent a new generation of semi-active dampers and are applied in many applications like shock absorbers and damping devices, clutches breaks, actuators or artificial joints, operational earthquake dampers to reduce motion in buildings and of course in automotive systems... Fig. 3.1 shows a schematic layout of an MR damper

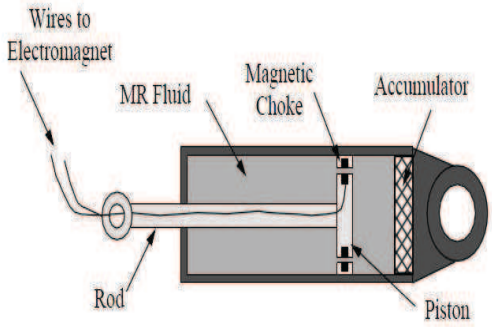

Figure 3.1: Schematic layout of an MR damper.

For the control of MR dampers, in our paper in collaboration with S. Savaresi, C. Spelta, D. Delvecchio (see [Do, Sename, Dugard, Savaresi, Spelta & Delvecchio, 2010]),

the extended versions of well-known Skyhook ([Karnopp et al., 1974]) and Mixed Skyhook-ADD [Savaresi & Spelta, 2007] have been proposed.

The aim of this chapter is to emphasize the interest of the LPV methodology for suspension modelling and control. In this study, recent developments in our publications [Do, Sename, Dugard, Aubouet & Ramirez-Mendoza, 2010], [Do, Sename & Dugard, 2010], [Do, Sename, Dugard & Soualmi, 2011] are presented to:

- first, develop an LPV model for an automotive suspension system starting from a non linear semi-active damper model,
- second, using an original LPV representation of the dissipativity of the semi-active damper, develop an ad-hoc H_∞/LPV controller.
- finally, a controller optimization procedure using genetic algorithms.

The whole LPV model is used to design a polytopic H_∞ controller for an automotive suspension system equipped with a Magneto-Rheological semi-active damper. This controller aims at improving ride comfort and/or road holding, depending on the required specifications.

3.1 Introduction

As mentioned in Chapter 1, the control design problem for semi-active suspensions has been tackled with many approaches during the last three decades such as the Skyhook control [Karnopp et al., 1974], the Groundhook control [Valasek et al., 1997], optimal control [Savaresi, Silani & Bittanti, 2005], [Canale et al., 2006], [Giorgetti et al., 2006], or H_∞ control ([Rossi & Lucente, 2004], [Sammier et al., 2003]), LPV control [Poussot-Vassal et al., 2008]... In these studies, the nonlinear characteristics (the bi-viscous and the hysteretic behaviors of semi-active dampers, see Fig. 3.2) are not taken into account in the controller design. This may result in bad performance when these controllers are implemented and applied to real suspension systems. The main contribution of this chapter is to propose a new control design method for nonlinear semi-active suspensions using the LPV approach. The methodology is based on a nonlinear static model of the semi-active damper where the bi-viscous and hysteretic behaviors of the damper are taken into consideration. The nonlinear system associated with the quarter vehicle model is reformulated in the LPV framework. The dissipativity problem is brought into that of input saturation, using a simple change of variable. To improve ride comfort and road holding, the H_∞ controller for LPV system (see [Apkarian & Gahinet, 1995] and [Scherer et al., 1997]) is used. Finally, an optimization of the weighting function selection for multi-objective H_∞ design using Genetic Algorithms is proposed. The

results in [Do, Sename & Dugard, 2011], [Do, Sename, Dugard & Soualmi, 2011] show that this procedure is quite efficient for the particular problem of semi-active suspension control and it is general enough for other multi-objective optimization designs for LPV systems.

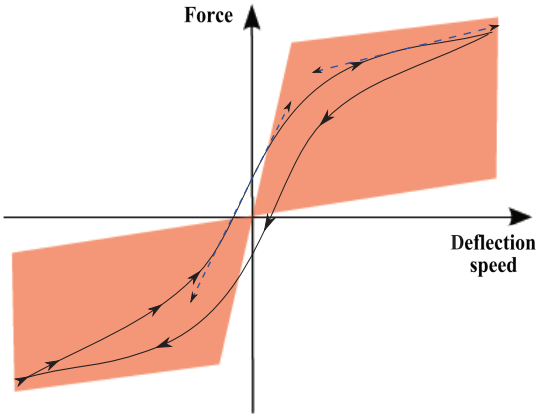

Figure 3.2: Realistic MR damper force with bi-viscosity (pre-yield and post-yield viscous damping) and hysteresis.

3.2 Semi-active suspension modelling for MR dampers

Many models have been proposed for semi-active suspension modelling. For example, the Bingham model is a phenomenological model that describes the behavior of an Electro-Rheological (ER) damper [Stanway et al., 1987]. The model consists of a viscous damper in parallel with a Coulomb friction element. Another well-known method is the semi-phenomenological Bouc-Wen model. It was first introduced by Bouc [Bouc, 1967] and then modified by Wen [Wen, 1976]. This model has been used widely to describe hysteretic systems. For the modelling of MR dampers, in [Spencer Jr et al., 1997] Spencer proposed a modified version the Bouc-Wen model or in [Savaresi, Bittanti & Montiglio, 2005], the authors presented a black box model. [Guo et al., 2006] proposed a semi-phenomenological model. Besides the accuracy, this model has an interesting structure which can be extended for LPV control synthesis.

Shuqi Guo model for MR damper In [Guo et al., 2006], the behavior of the semi-active damper is represented using the following nonlinear equation:

$$F_{\text{shuqi}-\text{guo}} = a_2 \left(\dot{x}_{mr} + \frac{v_0}{x_0} x_{mr} \right) + a_1 \tanh \left(a_3 \left(\dot{x}_{mr} + \frac{v_0}{x_0} x_{mr} \right) \right) \tag{3.2.1}$$

where $F_{shuqi-guo}$ is the damper force, x_{mr} is the suspension deflection, a_1 is the dynamic yield force of the MR fluid, a_2 and a_3 are related to the post-yield and pre-yield viscous

damping coefficients, v_0 and x_0 denote the absolute value of hysteretic critical velocity $\dot{x}_0$ and hysteretic critical deflection x_0 where $\dot{x}_0$ and x_0 are defined as the velocity and deflection when the MR damper force is zero.

The model is of semi-phenomenological type and based on a tangent hyperbolic function to model the hysteresis and bi-viscous characteristic of a damper. This model has a simple and elegant formulation, but the control input signal (current, for MR dampers) is not present. Obviously it cannot be used in that form for the controller synthesis.

Control-oriented MR damper model In [Lozoya-Santos, Ruiz-Cabrera, Morales-Menéndez, Ramírez-Mendoza & Diaz-Salas, 2009], the authors have shown that if each coefficient in (3.2.1) is defined as a polynomial function of electric current, the obtained model will better approach the real data. However for control purpose, a simpler control-oriented model where only one parameter depends on the input signal was proposed and first studied in [Do, Sename & Dugard, 2010], [Do, Spelta, Savaresi, Sename, Dugard & Delvecchio, 2010]. According to the authors, a control-oriented model for semi-active damper can be given by

$$F_{mr} = c_0\dot{x}_{mr} + k_0 x_{mr} + f_I \tanh\left(c_1\dot{x}_{mr} + k_1 x_{mr}\right) \tag{3.2.2}$$

where F_{mr} is the damper force, c_0, c_1, k_0 and k_1 are constant parameters and f_I is the controllable force coefficient which is varying according to the electrical current I in coil $(0 \leq f_{Imin} < f_I \leq f_{Imax})$.

Compared with the model (3.2.1) whose characteristics are static and uncontrollable, the model (3.2.2) reflects the realistic behavior of an MR damper. This model allows fulfilling the passivity constraint of the semi-active damper and introduces a control input f_I. The limitation of the model lies in the assumption that the MR dampers' hysteresis is invariant with respect to the current I. Fig. 3.3 presents the dependency of the damper force to the input current. Changing the current in the coil of an MR damper changes its characteristics. Here, the bi-viscous and the hysteresis can be clearly observed.

The model parameters used in Fig. 3.3 are the following: $c_0 = 810.78[Ns/m]$, $k_0 = 620.79[N/m]$, $c_1 = 13.76[s/m]$, $k_1 = 10.54[1/m]$. These experimental parameters were identified by Jorge de Jesus Lozoya-Santos (see [Lozoya-Santos et al., 2010] and [Lozoya-Santos, Morales-Menendez, Ramirez-Mendoza & Nino-Juarez, 2009]) on the test-rig at *Metalsa* [1] (see Fig. 3.4).

Remark 3.2.1. The experimental test-bench consists of three key blocks: an actuator *FlexTest GT MTS* ^{TM}, an electric current controller and an acquisition system. The man-machine interface interacts with the control system and the acquisition system.

[1] *www.metalsa.com.mx*

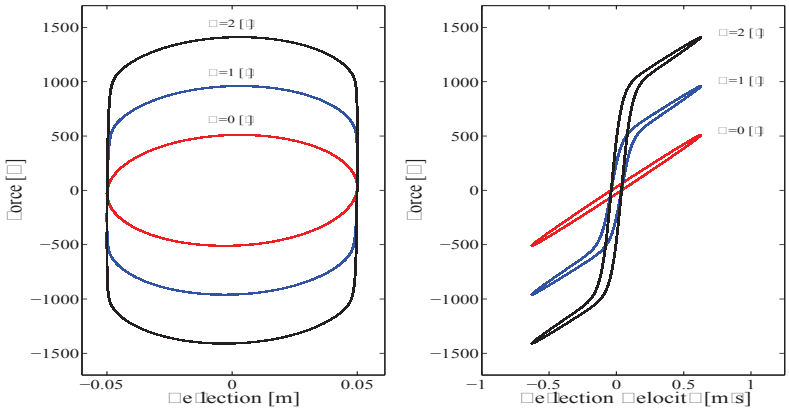

Figure 3.3: MR damper characteristics with different current values I: Force v.s Deflection (Left) and Force v.s Velocity (Right)

The specifications of the actuator are from 25 psi to 3000 psi and a stroke of 150 mm. A sensor is used for measuring the displacement. Electrical current is measured by a resistor connected in series with the coil of the MR damper. An Instron ^{TM} load cell measures the generated forces.

The model identification makes use of a sinusoidal displacement (about 4 Hz) which is randomly modulated in amplitude, and a random signal of electric current. The Fig. 3.5 presents the experimental data in the interval [30-33] [s]. As seen in Fig. 3.6, the model tracks well the real data. The average ESR (Error-to-Signal-Ratio) is around 7%, and the maximum ESR is about 20% (in high frequencies where the MR force changes rapidly). More details on the experimental results may be found in [Lozoya-Santos et al., 2010] and [Lozoya-Santos, Morales-Menendez, Ramirez-Mendoza & Nino-Juarez, 2009].

Let us return to the model (3.2.2), which has an interesting characteristic that can be exploited for LPV design. Note that the function $tanh\,(c_1\dot{x}_{mr} + k_1 x_{mr})$ is bounded in [-1;1] for any value of $\dot{x}_{mr}$ and x_{mr}. Moreover the function value is known because the damper deflection x_{mr} and velocity $\dot{x}_{mr}$ can be measured and computed using a unique displacement sensor. It is hence naturally a scheduling parameter in the LPV design.

3.3 The quarter vehicle model

In this study, the damper force F_{mr} is given as in (3.2.2) and satisfies the passivity constraint, in terms of constraints on f_I

$$0 < f_{Imin} < f_I \leq f_{Imax} \tag{3.3.1}$$

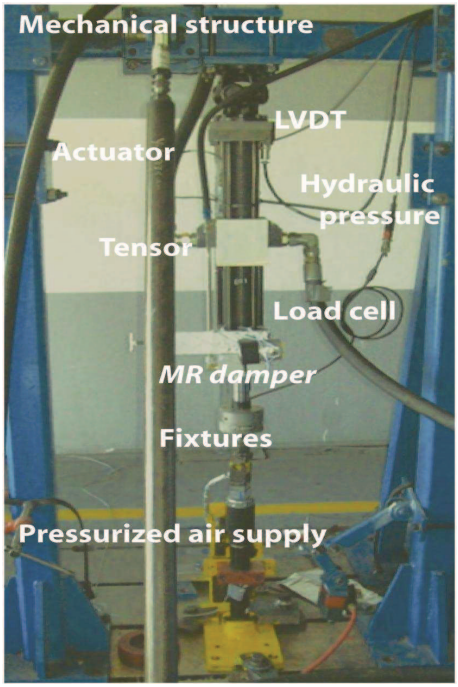

Figure 3.4: Experimental test-rig for MR damper parameter identification

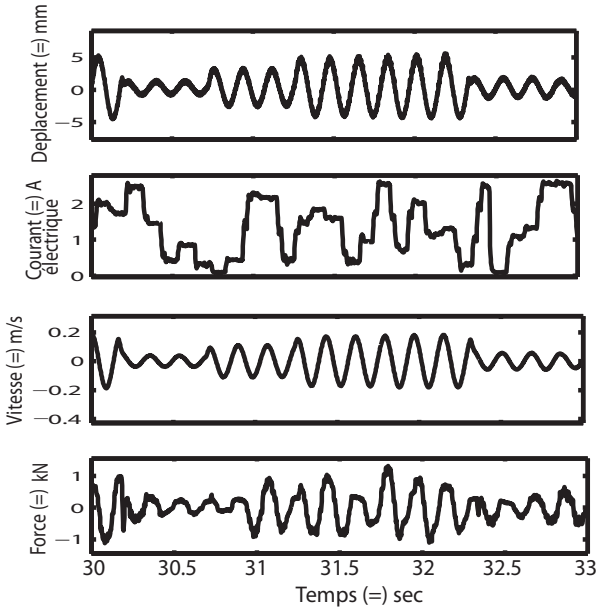

Figure 3.5: Experimental data

The dynamical equations are rewritten as follows

$$\begin{cases} m_s\ddot{z}_s &= -k_s\left(z_s - z_{us}\right) - c_0\left(\dot{z}_s - \dot{z}_{us}\right) - k_0\left(z_s - z_{us}\right) \\ & \quad -f_I \tanh\left(c_1\left(\dot{z}_s - \dot{z}_{us}\right) + k_1\left(z_s - z_{us}\right)\right) \\ m_{us}\ddot{z}_{us} &= k_s\left(z_s - z_{us}\right) + c_0\left(\dot{z}_s - \dot{z}_{us}\right) + k_0\left(z_s - z_{us}\right) \\ & \quad +f_I \tanh\left(c_1\left(\dot{z}_s - \dot{z}_{us}\right) + k_1\left(z_s - z_{us}\right)\right) - k_t\left(z_{us} - z_r\right) \end{cases} \tag{3.3.2}$$

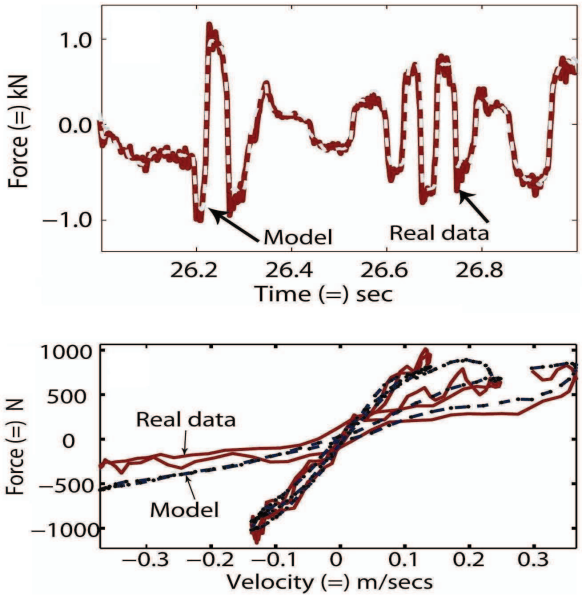

Figure 3.6: Model's force v.s real data

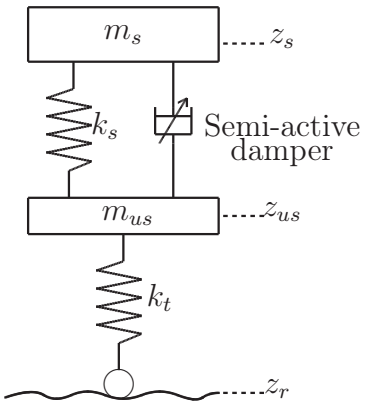

Figure 3.7: Model of quarter vehicle with a semi-active damper.

It is worth noting that (3.3.2) is a nonlinear differential equation system. In this chapter, the 1/4 Renault Mégane Coupé (1/4 RMC) (see Tab. 1.1 in Chapter 1) equipped with an MR damper presented in section 3.2 is studied. The MR damper model parameters are given in Tab. 3.1.

3.4 LPV model for semi-active suspension control

With the defined system and the performance objectives in the previous section, in the following, an LPV model for controller synthesis is formulated for further analysis and control. Denote:

Table 3.1: Parameter values of the quarter car model equipped with an MR damper

Parameter	Value	Unit
c_0	810.78	$[Ns/m]$
k_0	620.79	$[N/m]$
f_{min}	0	$[N]$
f_{max}	800	$[N]$
c_1	13.76	$[s/m]$
k_1	10.54	$[1/m]$

- $c_p = c_0$
- $k_p = k_s + k_0$
- $z_{def} = z_s - z_{us}$
- $\dot{z}_{def} = \dot{z}_s - \dot{z}_{us}$
- $\hat{\rho} = \tanh\left(c_0\left(\dot{z}_s - \dot{z}_{us}\right) + k_0\left(z_s - z_{us}\right)\right)$

From (3.3.2), the state-space representation of the quarter vehicle model can be deduced as follows:

$$\begin{cases} \dot{x}_s = A_s x_s + B_s \hat{\rho} f_I + B_{sw} w \\ z = C_{sz} x_s + D_{sz} \hat{\rho} f_I \\ y = C_s x_s \end{cases} \tag{3.4.1}$$

where x_s=$(z_s,\ \dot{z}_s,\ z_{us},\ \dot{z}_{us})^T$, w=z_r, $y = (z_s - z_{us},\ \dot{z}_s - \dot{z}_{us})^T$, $z = (\ddot{z}_s\ \ z_{us})^T$.

$$A_s = \begin{pmatrix} 0 & 1 & 0 & 0 \\ -\frac{k_p}{m_s} & -\frac{c_p}{m_s} & \frac{k_p}{m_s} & \frac{c_p}{m_s} \\ 0 & 0 & 0 & 1 \\ \frac{k_p}{m_{us}} & \frac{c_p}{m_{us}} & -\frac{k_p+k_t}{m_{us}} & -\frac{c_p}{m_{us}} \end{pmatrix},\ B_s = \begin{pmatrix} 0 \\ -\frac{1}{m_s} \\ 0 \\ \frac{1}{m_{us}} \end{pmatrix},\ B_{sw} = \begin{pmatrix} 0 \\ 0 \\ 0 \\ \frac{k_t}{m_{us}} \end{pmatrix},$$

$$C_s = \begin{pmatrix} 1 & 0 & -1 & 0 \\ 0 & 1 & 0 & -1 \end{pmatrix}^T\ C_{sz} = \begin{pmatrix} \frac{-k_p}{m_s} & \frac{-c_p}{m_s} & \frac{k_p}{m_s} & \frac{c_p}{m_s} \\ 0 & 0 & 1 & 0 \end{pmatrix},\ D_{sz} = \begin{pmatrix} \frac{-1}{m_s} \\ 0 \end{pmatrix}$$

Remark 3.4.1. The considered measurement outputs are the suspension deflection and suspension deflection velocity, which allows to state that $\hat{\rho}$ can be known in real-time.

Remark 3.4.2. As mentioned in the previous section, the performance objectives are ride comfort and road holding. Ride comfort is clearly related to the vehicle body

acceleration $\ddot{z}_s$. Road holding, beside being quantified by the dynamic tire deflection $z_{us} - z_r$, is related to the bouncing of the wheel z_{us}. Consequently, the controlled output vector may be chosen as $z = (\ddot{z}_s \quad z_{us})^T$.

As explained above, to guarantee the dissipativity of an MR damper, the control signal f_I must satisfy the constraint (3.3.1). By defining

$$u_I = f_I - f_0 \tag{3.4.2}$$

where $f_0 = (f_{Imin} + f_{Imax})/2$, the dissipativity constraint on f_I is recast as a saturation constraint on u_I, i.e.

$$-\bar{u} \leq u_I \leq \bar{u} \tag{3.4.3}$$

where $\bar{u} = (f_{Imax} - f_{Imin})/2$.

With this modification, the state-space representation of the quarter vehicle is given as follows:

$$P : \begin{cases} \dot{x}_s = (A_s + B_{s1}\frac{\hat{\rho}}{C_{s1}x_s}C_{s1})x_s + B_s\hat{\rho}u_I + B_{sw}w \\ z = (C_{sz} + D_{s1}\frac{\hat{\rho}}{C_{s1}x_s}C_{s1})x_s + D_{sz}\hat{\rho}u_I \\ y = C_s x_s \end{cases} \tag{3.4.4}$$

where $B_{s1} = \begin{pmatrix} 0 & -\frac{f_0}{m_s} & 0 & \frac{f_0}{m_{us}} \end{pmatrix}^T$, $C_{s1} = \begin{pmatrix} k_1 & c_1 & -k_1 & -c_1 \end{pmatrix}$, $D_{s1} = \begin{pmatrix} \frac{-f_0}{m_s} & 0 \end{pmatrix}$

In this study, the LPV model (3.4.4) can be used to design an LPV controller. However, such a controller may not ensure the closed-loop stability and performances since the saturation constraint (i.e the dissipativity constraint) is not accounted for in the design. Some solutions for this problem have been proposed. For example, in [Poussot-Vassal et al., 2008], a scheduling parameter is indeed defined as the difference between the real controlled damper force and the required one given by the controller. However the dissipativity constraint is not theoretically fulfilled. Another possible method is to add, in the closed-loop system, an AWBT (Anti Wind-up Bumpless Transfer) compensation to minimize the adverse effects of the control input saturation on the closed-loop performance [Gomes da Silva Jr. et al., 2008], [Grimm et al., 2003], [Kothare et al., 1994], [Mulder et al., 2009]. In the next section, a simple method is presented to solve the problem by considering the input saturation as a scheduling parameter. This approach is related to [Wu et al., 2000].

Define the saturation function $sat()$ as follows

$$sat(u_I) = \begin{cases} \bar{u} & \text{if} \quad u_I > \bar{u} \\ u_I & \text{if} \quad -\bar{u} \leq u_I \leq \bar{u} \\ -\bar{u} & \text{if} \quad u_I < -\bar{u} \end{cases} \tag{3.4.5}$$

The state-space representation of the system (3.4.4) subject to the input saturation constraint (3.4.3) is rewritten as

$$P : \begin{cases} \dot{x}_s = (A_s + B_{s1}\frac{\hat{\rho}}{C_{s1}x_s}C_{s1})x_s + B_s\hat{\rho}\frac{sat(u_I)}{u_I}u_I + B_{sw}w \\ z = (C_{sz} + D_{s1}\frac{\hat{\rho}}{C_{s1}x_s}C_{s1})x_s + D_{sz}\hat{\rho}\frac{sat(u_I)}{u_I}u_I \\ y = C_s x_s \end{cases} \tag{3.4.6}$$

Denote $\rho_1 = \hat{\rho}\frac{sat(u_I)}{u_I}$ and $\rho_2 = \frac{\hat{\rho}}{C_{s1}x_s}$. From (3.4.6), the following LPV system is now obtained

$$P : \begin{cases} \dot{x}_s = (A_s + B_{s1}C_{s1}\rho_2)x_s + B_s\rho_1 u_I + B_{sw}w \\ z = (C_{sz} + D_{s1}C_{s1}\rho_2)x_s + D_{sz}\rho_1 u_I \\ y = C_s x_s \end{cases} \tag{3.4.7}$$

In (3.4.7) the control input matrix $B_s\rho_1$ is parameter dependent, which is not consistent with the solution of the H_∞ design problem for polytopic systems [Apkarian & Gahinet, 1995]. This problem can be overcome by adding the following filter into (3.4.7) to make the control input matrix independent from the scheduling parameter:

$$W_f : \begin{pmatrix} \dot{x}_f \\ u_I \end{pmatrix} = \begin{pmatrix} A_f & B_f \\ C_f & 0 \end{pmatrix} \begin{pmatrix} x_f \\ u \end{pmatrix} \tag{3.4.8}$$

with

$$\|W_f\|_\infty \leq 1 \tag{3.4.9}$$

where A_f, B_f, C_f are constant matrices.

Remark 3.4.3. The condition (3.4.9) ensures that the saturation constraint on u_I is kept for the new control input u. It means that the following implies (3.4.3)

$$-\bar{u} \leq u \leq \bar{u} \tag{3.4.10}$$

From Eq. (3.4.7) and Eq. (3.4.8), the control oriented model is now represented by an LPV system with two scheduling parameters ρ_1 and ρ_2:

$$\begin{cases} \dot{x} = A(\rho_1, \rho_2)\, x + Bu + B_1 w \\ z = C_z(\rho_1, \rho_2)\, x \\ y = Cx \end{cases} \tag{3.4.11}$$

where

$$x = \begin{pmatrix} {x_s}^T & {x_f}^T \end{pmatrix}^T$$

$$A(\rho_1,\rho_2)=\begin{pmatrix} A_s+\rho_2 B_{s1}C_{s1} & \rho_1 B_s C_f \\ 0 & A_f \end{pmatrix},\ B=\begin{pmatrix} 0 \\ B_f \end{pmatrix},\ B_1=\begin{pmatrix} B_{s1} \\ 0 \end{pmatrix},$$

$$C=\begin{pmatrix} C_s \\ 0 \end{pmatrix}^T,\ C_z(\rho_1,\rho_2)=\begin{pmatrix} C_{sz}+\rho_2 D_{s1}C_{s1} & \rho_1 D_{sz}C_f \end{pmatrix}$$

$$\rho_1=\tanh(C_{s1}x_s)\frac{sat(c_f x_f)}{c_f x_f},\ \rho_2=\frac{\tanh(C_{s1}x_s)}{C_{s1}x_s}$$

Notice also that ρ_1 and ρ_2 are not independent. As seen in Fig. 3.8, the set of (ρ_1,ρ_2) is represented by the shaded area and this set is not a polytope. In the following section, a polytopic approach will be applied for LPV system (3.4.11) by considering a polytope that includes all possible scheduling parameter trajectories of (ρ_1,ρ_2).

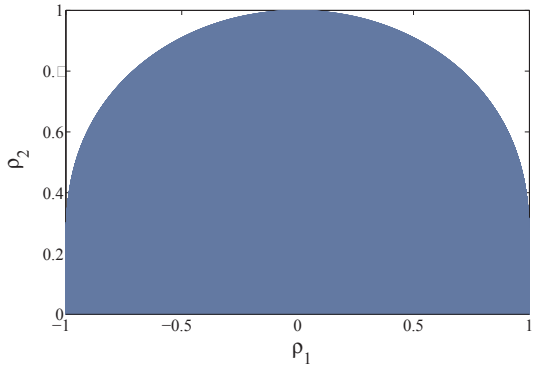

Figure 3.8: Set of scheduling parameters (ρ_1,ρ_2) (shaded area).

Indeed, the aim is to find an LPV controller that guarantees the stability and the H_∞ performance for the system (3.4.11). It is well-known that the quality of this controller depends on the choice of some weighting functions. In the next section, a general procedure for the optimization of the weighting functions selection will be proposed and then applied to the semi-active suspension control.

3.5 Optimizing H_∞/LPV controller for semi-active suspensions

The H_∞ control design approach is an efficient way to improve the performances of a closed-loop system in pre-defined frequency ranges. The key step of the H_∞ control design relies on the selection of the weighting functions which depend on the engineer skill and experience. In many real applications, it is very difficult to choose the weighting functions because the performance specifications are not accurately defined, i.e., it is

simply to achieve the best possible performances (optimal design) or to achieve an optimally joint improvement of more than one objective (multi-objective design). Therefore it appears interesting to optimize the selection of the weighting functions to get the desired closed-loop performances. As studied in [Beaven et al., 1996], [Hu et al., 2000], it has been proposed to consider a system, no matter how complex it is, as a combination of sub-systems of the first and second orders, for which it is easy to find the good weighting functions to be used in the H_∞ control methodology. However, there is no explicit method to find these functions in the general case. The usual way is to proceed by trial-and-error. Recently, as in [Alfaro-Cid et al., 2008], the use of nonlinear optimization tools, such as the Genetic Algorithms, has been proved to be interesting since the parameter design is here related to nonlinear cost functions. Below, the problem formulation of the H_∞/LPV control design for polytopic systems is presented according to the considered application.

In the particular case of semi-active suspension control, ride comfort and road-holding are two essential but conflicting control objectives. It is shown that, for example, it is impossible to improve ride comfort without degrading road holding and vice-versa around the wheel resonance 10-15 Hz. In this section, the aim is to use Genetic Algorithms (GAs) to obtain the best controllers (for ride comfort and/or road holding) through optimizing the selection of the weighting functions for the H_∞/LPV control of semi-active suspensions.

3.5.1 Control scheme

The control configuration for semi-active suspensions is given in Fig. 3.9. The controlled outputs are the vehicle body acceleration $\ddot{z}_s$ (for the ride comfort improvement) and the wheel displacement z_{us} (for the road holding improvement, see the performance criteria in section 1.2.2, in Chapter 1). The measurement outputs are the suspension deflection z_{def} and suspension deflection velocity $\dot{z}_{def}$ (needed for computing the scheduling parameters as well). To obtain the desired closed-loop performances (see the performance criteria 1.2.2 in Chapter 1), the weighting functions on controlled outputs $\{W_{\ddot{z}_s}, W_{z_{us}}\}$ and disturbance input W_{z_r} are used.

Notice that, due to the self-dependence between ρ_1 and ρ_2, the set of all $\bar{\rho} = (\rho_1, \rho_2)$ is not a polytope, as seen in Fig. 3.8. In this study, a polytopic approach is developed for the LPV control design (which leads to some conservatism). As a consequence, ρ_1 and ρ_2 are considered as independent parameters and $\bar{\rho}$ belongs to a polytope Θ whose vertices are $\bar{\rho}_1 = (-1, 0)$, $\bar{\rho}_2 = (1, 0)$, $\bar{\rho}_3 = (1, 1)$, $\bar{\rho}_4 = (-1, 1)$.
Consider the augmented system (corresponding to Fig. 3.9) made of the plant (3.4.11) and the weighting functions, represented by

$$\dot{\xi} \;=\; \mathcal{A}^\nu(\bar{\rho})\xi + \mathcal{B}_1^\nu(\bar{\rho})\bar{w} + \mathcal{B}_2^\nu u$$

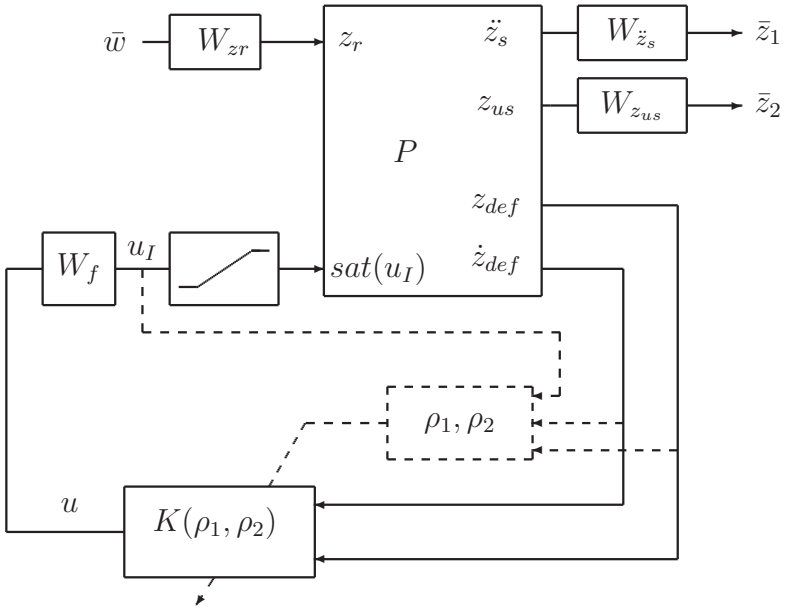

Figure 3.9: Block diagram for semi-active suspension control.

$$\begin{aligned} \bar{z} &= \mathcal{C}_1^\nu(\bar{\rho})\xi + \mathcal{D}_{11}^\nu(\bar{\rho})\bar{w} + \mathcal{D}_{12}^\nu u \\ y &= \mathcal{C}_2\xi + \mathcal{D}_{21}\bar{w} \end{aligned} \tag{3.5.1}$$

where $\xi = \begin{pmatrix} x^T & {x_w}^T \end{pmatrix}^T$, x_w being the state vector of the weighting functions, $\bar{\rho} = (\rho_1, \rho_2)$ the vector of scheduling parameters. Note that ν represents the vector of all weighting function parameters. The LPV controller is defined as follows

$$K(\bar{\rho}) : \begin{pmatrix} \dot{x}_c \\ u \end{pmatrix} = \begin{pmatrix} A_c^\nu(\bar{\rho}) & B_c^\nu(\bar{\rho}) \\ C_c^\nu(\bar{\rho}) & D_c^\nu(\bar{\rho}) \end{pmatrix} \begin{pmatrix} x_c \\ y \end{pmatrix} \tag{3.5.2}$$

where x_c, y and u are respectively the state, the input and output of the controller associated with the system (3.5.1). All matrices have appropriate dimensions.

Remark 3.5.1. Since ν represents the vector of the weighting function parameters, it is used as an exponent in the notation of equations (3.5.1)-(3.5.2) to emphasize the dependence of the generalized plant, and then of the controller, on the parameters of the weighting functions.

H_∞/LPV problem - The objective of the synthesis is to find an LPV controller $K(\rho)$ of the form (3.5.2) such that the closed-loop system is quadratically stable and that, for a given positive real γ, the L_2-induced norm of the operator mapping $\bar{w}$ into $\bar{z}$ is bounded by γ i.e

$$\forall \bar{\rho} \in \Theta, \quad \frac{\|z_w\|_2}{\|w\|_2} \leq \gamma \tag{3.5.3}$$

Here the polytopic approach with a quadratic Lyapunov function is employed. It is stated that for known weighting functions and a suitable pre-defined real positive scalar γ,

the sufficient condition that solves the H_∞/LPV problem is given by Eq. (3.5.4)-(3.5.5) where the decision variables are X, Y, $\hat{A}$, $\hat{B}$, $\hat{C}$ and $\hat{D}$ (see the detail of the solution in [Scherer et al., 1997]). It is worth noting that the weighting function parameter set ν is present in the LMIs problem to cope with optimization purpose of the controller (which is presented in section 3.5.2).

$$\begin{bmatrix} M_{11}^{\nu}(\bar{\rho}_i) & * & * & * \\ M_{21}^{\nu}(\bar{\rho}_i) & M_{22}^{\nu}(\bar{\rho}_i) & * & * \\ M_{31}^{\nu}(\bar{\rho}_i) & M_{32}^{\nu}(\bar{\rho}_i) & -\gamma I_m & * \\ M_{41}^{\nu}(\bar{\rho}_i) & M_{42}^{\nu}(\bar{\rho}_i) & M_{43}^{\nu}(\bar{\rho}_i) & -\gamma I_p \end{bmatrix} \prec 0 \tag{3.5.4}$$

$$\begin{bmatrix} X & I \\ I & Y \end{bmatrix} \succ 0 \quad \text{for} \quad \mathrm{i} = 1:4 \tag{3.5.5}$$

where

$$\begin{aligned}
M_{11}^{\nu}(\bar{\rho}_i) &= \mathcal{A}^{\nu}(\bar{\rho}_i)X + X\mathcal{A}^{\nu}(\bar{\rho}_i)^T + \mathcal{B}_2\hat{C}(\bar{\rho}_i) + \hat{C}(\bar{\rho}_i)^T\mathcal{B}_2^T \\
M_{21}^{\nu}(\bar{\rho}_i) &= \hat{A}(\bar{\rho}_i) + \mathcal{A}^{\nu}(\bar{\rho}_i)^T + \mathcal{C}_2^T\hat{D}(\bar{\rho}_i)^T\mathcal{B}_2^T \\
M_{22}^{\nu}(\bar{\rho}_i) &= Y\mathcal{A}^{\nu}(\bar{\rho}_i) + \mathcal{A}^{\nu}(\bar{\rho}_i)^T Y + \hat{B}(\bar{\rho}_i)\mathcal{C}_2 + \mathcal{C}_2^T\hat{B}(\bar{\rho}_i)^T \\
M_{31}^{\nu}(\bar{\rho}_i) &= \mathcal{B}_1^{\nu}(\bar{\rho}_i)^T + \mathcal{D}_{21}^T\hat{D}(\bar{\rho}_i)^T\mathcal{B}_2^T \\
M_{32}^{\nu}(\bar{\rho}_i) &= \mathcal{B}_1^{\nu}(\bar{\rho}_i)^T Y + \mathcal{D}_{21}^T\hat{B}(\bar{\rho}_i)^T \\
M_{41}^{\nu}(\bar{\rho}_i) &= \mathcal{C}_1^{\nu}(\bar{\rho}_i)X + \mathcal{D}_{12}\hat{C}(\bar{\rho}_i) \\
M_{42}^{\nu}(\bar{\rho}_i) &= \mathcal{C}_1^{\nu}(\bar{\rho}_i) + \mathcal{D}_{12}\hat{D}(\bar{\rho}_i)C_2 \\
M_{43}^{\nu}(\bar{\rho}_i) &= \mathcal{D}_{11}^{\nu}(\bar{\rho}_i) + \mathcal{D}_{12}\hat{D}(\bar{\rho}_i)\mathcal{D}_{21}
\end{aligned}$$

The controller K_{c_i} at vertex i is then reconstructed as

$$\begin{aligned}
D_c^{\nu}(\bar{\rho}_i) &= \hat{D}(\bar{\rho}_i) \\
C_c^{\nu}(\bar{\rho}_i) &= \left(\hat{C}(\bar{\rho}_i) - D_c^{\nu}(\bar{\rho}_i)C_2X\right)M^{-T} \\
B_c^{\nu}(\bar{\rho}_i) &= N^{-1}\left(\hat{B}(\bar{\rho}_i) - YB_2D_c^{\nu}(\bar{\rho}_i)\right) \\
A_c^{\nu}(\bar{\rho}_i) &= N^{-1}\left(\hat{A}(\bar{\rho}_i) - YA(\bar{\rho}_i)X - YB_2D_c^{\nu}(\bar{\rho}_i)C_2X\right)M^{-T} \\
&\quad -B_c^{\nu}(\bar{\rho}_i)C_2XM^{-T} - N^{-1}YB_2C_c^{\nu}(\bar{\rho}_i)
\end{aligned} \tag{3.5.6}$$

where M, N are defined such that $MN^T = I_n - XY$ which can be solved through a singular value decomposition and a Cholesky factorization. The global H_∞/LPV controller is then the convex combination of these local controllers.

$$K_c(\rho) = \alpha_1K_{c1} + \alpha_2K_{c2} + \alpha_3K_{c3} + \alpha_4K_{c4} \tag{3.5.7}$$

where the coefficients α_1, α_2, α_3, α_4 are defined as in (2.2.9) in Chapter 2 for the case where the considered polytope is a hypercube

$$\begin{aligned}
\alpha_1 &= \tfrac{(1-\rho_1)(1-\rho_2)}{2} \quad & \alpha_2 &= \tfrac{(\rho_1+1)(1-\rho_2)}{2} \\
\alpha_3 &= \tfrac{(\rho_1+1)\rho_2}{2} & \alpha_4 &= \tfrac{(1-\rho_1)\rho_2}{2}
\end{aligned} \tag{3.5.8}$$

3.5.2 Controller optimization using Genetic Algorithms

According to the prescribed objectives in section 1.2.2, the following weighting functions are used for the H_∞/LPV synthesis

$$W_{z_r} = 3 \times 10^{-2} \tag{3.5.9}$$

$$W_f = \frac{\Omega_f}{s + \Omega_f} \tag{3.5.10}$$

$$W_{\ddot{z}_s} = k_{\ddot{z}_s} \frac{s^2 + 2\xi_{11}\Omega_{11}s + {\Omega_{11}}^2}{s^2 + 2\xi_{12}\Omega_{12}s + {\Omega_{12}}^2} \tag{3.5.11}$$

$$W_{z_{us}} = k_{z_{us}} \frac{s^2 + 2\xi_{21}\Omega_{21}s + {\Omega_{21}}^2}{s^2 + 2\xi_{22}\Omega_{22}s + {\Omega_{22}}^2} \tag{3.5.12}$$

Define the set of parameters

$$\nu = [\ \Omega_f \quad \Omega_{11} \quad \Omega_{12} \quad \xi_{11} \quad \xi_{12} \quad k_{\ddot{z}_s} \quad \Omega_{21} \quad \Omega_{22} \quad \xi_{21} \quad \xi_{22} \quad k_{z_{us}}\ ]^T \tag{3.5.13}$$

that, in the context of GAs, is a part of the decision vector. By experience, γ was chosen as a decision parameter in order to add more degrees of freedom, and then a sub-optimal H_∞ control problem was solved.

In a usual H_∞/LPV problem, the attenuation level γ is to be minimized to satisfy the H_∞ performance objectives. Thanks to the Genetic Algorithms optimization, the provided methodology will rather allow here to minimize a cost function representing the true performance objectives. Therefore the optimization problem of interest relies on the minimization of this cost function and not on the minimization of γ.

Let us define the optimization problem for semi-active suspension control

$$\min_{\{\nu,\gamma\} \in R_+^{12}} J^D(\nu, \gamma) = \begin{bmatrix} J^D_{\text{Comfort}}(\nu, \gamma) \\ J^D_{\text{RoadHolding}}(\nu, \gamma) \end{bmatrix} \tag{3.5.14}$$

Remark 3.5.2. The dimension of the searching space is 12×1 because there are eleven parameters for the weighting functions ν and one for the attenuation level scalar γ. This space can be made smaller than R_+^{12}. Effectively we can define the bounds of each parameter, basing on the frequency range of interest at which the weighting functions act. This is also an explanation for the question of why we use weighting function parameters optimization instead of controller parameters optimization, specially when the controller order is high.

Based on the remarks on the comfort and road holding performances in section 1.2.2 in Chapter 1, the two objectives are defined so that the vehicle body acceleration at low and middle frequencies and the wheel displacement at high frequencies will be minimized

for each vertex of the considered polytope. Hence, in the optimization problem (3.5.14), the following frequency-based objective functions are considered

$$J^D_{\text{Comfort}} = \sum_{i=1}^{4} \int_0^{12} \ddot{z}_s / z_r(f)_i df \tag{3.5.15}$$

$$J^D_{\text{RoadHolding}} = \sum_{i=1}^{4} \int_{10}^{20} (z_{us} / z_r(f)_i) \tag{3.5.16}$$

Note that, in the equations above, "D" is used to differentiate these design objective functions with the ones in Section 1.2.2 in Chapter 1 and the index "i" stands for the i^{th} vertex of the polytope Θ (see Fig. 3.8). The number of elements in each sum is four, however in this particular case, the polytope is symmetric in ρ_1, only computations at two vertices $\{1, 4\}$ or $\{2, 3\}$ are needed.

Remark 3.5.3. The feasibility of the LMIs (3.5.4)-(3.5.5) may be violated by the "bad" decision vectors generated by GAs. The problem can be overcome by repeating the crossover or mutation until the feasible solution is obtained. However, a simpler way is to assign a large objective value (for instant $J^D = \infty$) to these infeasible solutions and then, they will be eliminated by the selection procedure after some generations.

Remark 3.5.4. In many cases, to preserve the performance of the closed-loop system with input saturation, a stable stabilizing controller is required. Other advantages for the use of stable controllers concern the practical aspects. The stable controllers are easier to be implemented than the unstable ones and the closed-loop system (provided that the open-loop system is already stable, e.g open-loop semi-active suspension systems) remains stable even when the feedback sensors fail. For LTI systems, this problem (usually called *strong stabilization* problem) has been studied by some authors such as [Campos-Delgado & Zhou, 2001], [Cao & Lam, 2000],... Similarly, for the H_∞/LPV control of LPV systems, to obtain a stable LPV controller, it suffices to ensure that all local controllers at each vertex of the polytope are stable. In this study, the theoretical solution for the existence of a stable LPV controller is not given. However, a stable LPV controller can be obtained by eliminating the "unstable solutions" corresponding to at least, one unstable local controller during the synthesis. It can be accomplished with GAs by simply choosing $J^D = \infty$ for "unstable solutions". Due to the "survival of the fittest" property, these "unstable solutions" will disappear after some generations.

The strong stabilization problem will be handled in more details in Chapter 4.

To sum up, the objective function used in GAs is chosen as follows.

Algorithm 1: Objective value assignment
if (3.5.4)-(3.5.5) is feasible **and** all K_{c_i} in (3.5.6) are stable **then**
Calculate J^D using (3.5.15)-(3.5.16)
else
$J^D = \infty$
end.

Proposed weighting function optimization procedure for H_∞/LPV synthesis

- **Step 1:** Initiate with random positive weighting functions $\nu = \nu^0$ and a random positive real $\gamma_{ga} = \gamma_{ga}^0$.
- **Step 2:** Solve the minimization problem of γ subject to the LMIs (3.5.4)-(3.5.5) to compute the minimal real scalar γ_{min}. Solve again the LMIs (3.5.4)-(3.5.5) with the couple (ν, γ) where $\gamma = \gamma_{min} + \gamma_{ga}$. At the end of this step, compute the objective function $J^D(\nu, \gamma)$ using *Algorithm 1.*
- **Step 3:** Select the individuals.
- **Step 4:** Apply crossover and mutation to get a new generation: $\nu = \nu^{new}$ and $\gamma_{ga} = \gamma_{ga}^{new}$.
- **Step 5:** Evaluate the new generation: If the criteria of interest (for example, reaching the limit number of generation) are not satisfied, go to Step 2 with $\nu = \nu^{new}$ and $\gamma_{ga} = \gamma_{ga}^{new}$; Else, stop and save the best individual $\nu^{opt} = \nu^{new}$ and $\gamma^{opt} = \gamma_{ga}^{new}$.

The genetic operations presented in step 3 and 4 can be done using efficient multi-objective optimization algorithms like SPEA2 [Zitzler et al., 2001], NSGA-II [Deb et al., 2002].

Remark 3.5.5. In step 2, to avoid the infeasibility of the LMIs (3.5.4)-(3.5.5) resulting from the bad (i.e too small) value of γ generated by GAs, γ will be decomposed into two positive real elements γ_{min} and γ_{ga} where γ_{min} is the minimal γ satisfying the LMIs (3.5.4)-(3.5.5), and γ_{ga} is tuned by GAs. Due to the convexity of the LMIs problem, the existence of γ_{min} will ensure the feasibility of LMIs (3.5.4)-(3.5.5) with $\gamma = \gamma_{min} + \gamma_{ga}$ for all positive real γ_{ga}. The minimal value γ_{min} can be found by using LMIs toolbox like Yalmip & Sedumi.

The procedure of the proposed method is illustrated in Fig. 3.10.

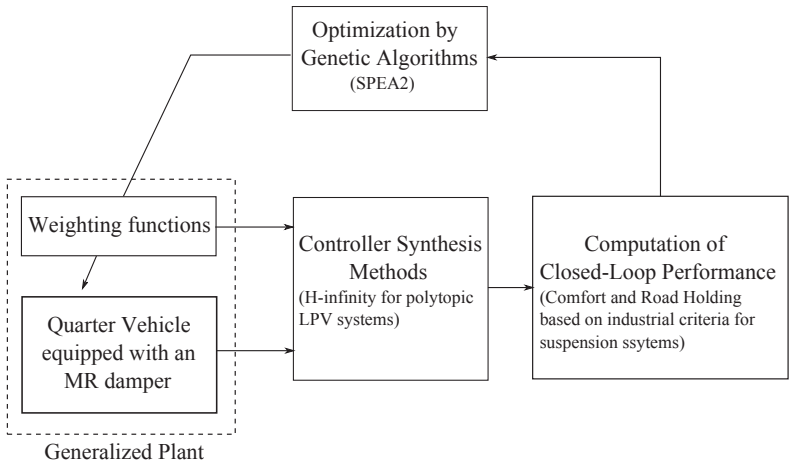

Figure 3.10: Controller optimization for semi-active suspension control using Genetic Optimization.

3.6 Numerical analysis and results

For simulation analysis, we use the nonlinear quarter car Renault Mégane Coupé (RMC) model. It is worth noting that the spring used in this simulation has a nonlinear characteristic i.e. the spring stiffness k_s is not a constant coefficient (see Fig. 1.5 in Chapter 1) and the MR damper force is given by (3.2.2). The implementation scheme is depicted in Fig. 3.11.

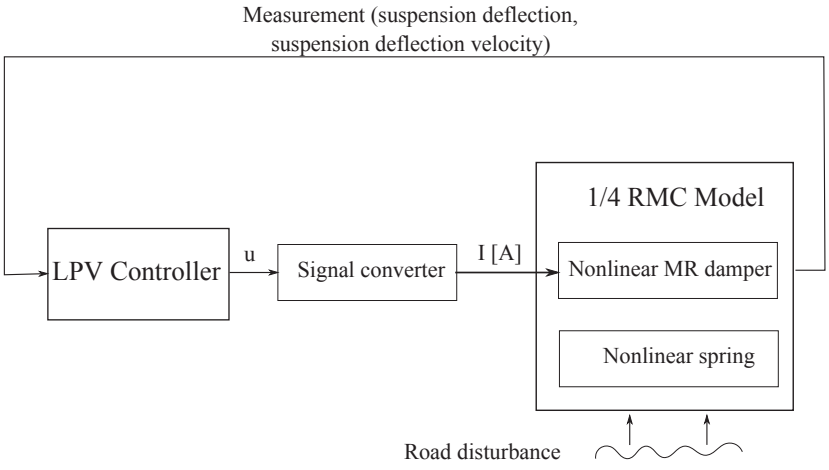

Figure 3.11: Implementation scheme.

With the proposed method, the solution of the multi-objective problem (3.5.14) is given by a Pareto set as in Fig. 3.12. Now the conflicting relation between comfort and road holding criteria can be observed clearly from the figure. Among the solutions in the Pareto set, two LPV controllers are chosen. One is comfort oriented (belonging to Set 1) and the other is road holding oriented (belonging to Set 2, because the solutions

in Set 3 (corresponding to minimal $J^D_{RoadHolding}$ defined in $[10-20]\ Hz$) improve in fact the road holding capability only in high frequencies). The parameters for the synthesis of these two controllers are found in Tab. 3.2 and Tab. 3.3.

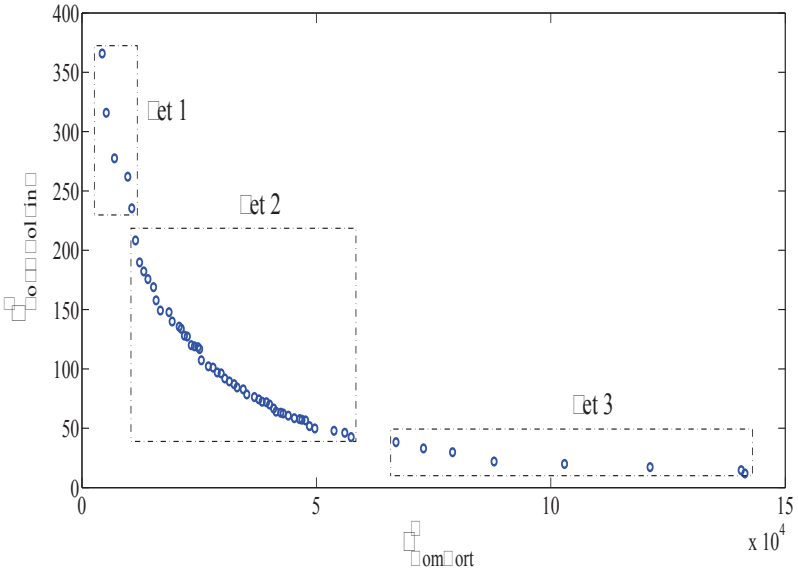

Figure 3.12: Pareto set obtained by proposed method (criteria computed for linear models).

Controllers	**Filter**	$\mathbf{W_{\ddot{z}_s}}$					$\mathbf{W_{z_{us}}}$				
	Ω_f	Ω_{11}	Ω_{12}	ξ_{11}	ξ_{12}	$k_{\ddot{z}_s}$	Ω_{21}	Ω_{22}	ξ_{21}	ξ_{22}	$k_{z_{us}}$
LPV-Comfort	90	48.2	7.1	99	8.48	159	99.9	1.3	5.4	99	90.6
LPV-Road Holding	1.4	60.8	12.9	99.7	29.7	436	83.6	0.29	96	89	145

Table 3.2: Weighting function parameters for H_∞/LPV semi-active suspension design (obtained by Genetic Optimization).

Controllers	**scalar**
	$\gamma_{min} - \gamma_{ga}\ (\times 10^5)$
LPV-Comfort	$0.2 - 1.66$
LPV-Road Holding	$3.7 - 3.16$

Table 3.3: Attenuatation scalars for H_∞/LPV semi-active suspension design (obtained by Genetic Optimization).

Remark 3.6.1. As seen in 3.3, the optimal solutions for H_∞/LPV semi-active suspension design is not associated with a smallest disturbance attenuation γ_{min} but with a greater value $\gamma = \gamma_{min} + \gamma_{ga}$.

In the following, two different closed-loop control strategies as well as passive open-loop ones for MR dampers are presented and considered as referenced methods to evaluate the efficiency of the proposed LPV controllers.

3.6.1 The based-lines

The well-known Skyhook [Karnopp et al., 1974] proposed by Karnopp and the Mixed Skyhook-ADD by [Savaresi & Spelta, 2007] (see Chapter 1) are remarkable control methods. However, these two control strategies have been originally designed for linear dampers where the nonlinear characteristics (i.e the bi-viscous and the hysteretic behaviors) have not been taken into account. In [Do, Sename, Dugard, Savaresi, Spelta & Delvecchio, 2010], the extended versions of the Skyhook and Mixed Skyhook-ADD were proposed for MR dampers. We recall here these control methods.

Extended Skyhook for MR dampers [Do, Sename, Dugard, Savaresi, Spelta & Delvecchio, 2010]
The main idea of the Skyhook for linear suspension system is that the damper exerts a force that reduces the velocity of the body mass $\dot{z}_s$. By using the same principle, the modified Skyhook for MR damper will be as follows (see Appendix A for more explanations)

$$f_I = \begin{cases} f_{max} & \text{if} \quad \dot{z}_s\hat{\rho} > 0 \\ f_{min} & \text{if} \quad \dot{z}_s\hat{\rho} \leq 0 \end{cases} \tag{3.6.1}$$

where $\hat{\rho} = \tanh(c_1\dot{z}_{def} + k_1 z_{def})$.

Extended Mixed Skyhook-ADD (Skyhook-ADD) for MR dampers [Do, Sename, Dugard, Savaresi, Spelta & Delvecchio, 2010]
It is well-known that the Skyhook provides the best ride comfort at low frequencies while the ADD improves considerably ride comfort at high frequencies. The Extended Mixed Skyhook-ADD algorithm guarantees the best behavior of both Skyhook and ADD and is given as follows (see Appendix A)

$$f_I = \begin{cases} f_{max} & \text{if} \quad (\ddot{z}_s^2 - \alpha\dot{z}_s^2 \leq 0 \wedge \dot{z}_s\hat{\rho} > 0) \vee \\ & \quad\;\; (\ddot{z}_s^2 - \alpha\dot{z}_s^2 > 0 \wedge \ddot{z}_s\hat{\rho} > 0) \\ f_{min} & \text{if} \quad (\ddot{z}_s^2 - \alpha\dot{z}_s^2 \leq 0 \wedge \dot{z}_s\hat{\rho} \leq 0) \vee \\ & \quad\;\; (\ddot{z}_s^2 - \alpha\dot{z}_s^2 > 0 \wedge \ddot{z}_s\hat{\rho} \leq 0) \end{cases} \tag{3.6.2}$$

where $\hat{\rho} = \tanh(c_1 \dot{z}_{def} + k_1 z_{def})$. The amount $(\ddot{z}_s^2 - \alpha \dot{z}_s^2)$ is the frequency-range selector and the Skyhook-ADD crossover frequency $\alpha = 2\pi f_{SHADD}\ rad/s$ where $f_{SHADD} = 2\ Hz$ (see [Savaresi & Spelta, 2007]).

Passive MR dampers
Beside the three controlled methods presented above, the three following passive open-loop cases are also useful for the analysis

- Soft MR damper ("Soft MRD") where the controllable input $f_I = f_{min}$
- Hard MR damper ("Hard MRD") where the controllable input$f_I = f_{max}$
- Nominal MR damper ("Nominal MRD") where the controllable input $f_I = (f_{min} + f_{max})/2$ (i.e. when control input $u = 0$)

3.6.2 Frequency domain analysis

In this section, the evaluation in the frequency domain of referenced and proposed methods is performed via the nonlinear frequency responses which are computed by the "Variance Gain" algorithm [Savaresi, Bittanti & Montiglio, 2005]. This algorithm is simple and provides a good approximation to frequency response.

Some general remarks can be done from the Fig. 3.13 and 3.14:

- Between 0-2 Hz, the Hard MRD is the best strategy for both ride comfort and road holding.
- Between 2-12 Hz, the Soft MRD is the best strategy for both ride comfort and road holding.
- Between 12-30 Hz, the trade-off between ride comfort and road holding is unavoidable. The best for ride comfort is the Soft MRD, the best for road holding is the Hard MRD.

With the remarks above, the optimal solutions for ride comfort and road holding can be roughly defined and once again, the conflict between two objectives, at high frequency (12-30 Hz) can be seen from Tab. 3.4.

Some remarks can be made for the five strategies, in the frequency range of interest 0-30 Hz.
The **Nominal MRD** and the **Extended Skyhook** provide medium performances for both ride comfort and road holding.

Controllers	0-2 Hz	2-12 Hz	12-30 Hz
Comfort-Oriented	$f_I = f_{Imax}$	$f_I = f_{Imin}$	$f_I = f_{Imin}$
Road Holding-Oriented	$f_I = f_{Imax}$	$f_I = f_{Imin}$	$f_I = f_{Imax}$

Table 3.4: Optimal controllers.

The **Extended Mixed Skyhook-ADD** is the best one for ride comfort. It approaches the optimal solution of the comfort-oriented controller. As a consequence, this controller does not guarantee a good road holding around the wheel resonance which is more important than in other frequency ranges.
The **LPV - Road Holding** is the best one for road holding.
The **LPV - Comfort** approaches very well the Extended Mixed Skyhook-ADD from 3-30 Hz. At low frequencies 1-4 Hz, it is not so good but this is not really important because, as mentioned before in section 1.2.2 in Chapter 1, the human being is more sensible to vehicle acceleration in the frequencies around 4-8 Hz.

The remarks above are summarized by Fig. 3.15. The performance criteria (1.2.10) and (1.2.11) in section 1.2.2 in Chapter 1 are calculated for each strategy; then they are normalized by the performance values of the nominal MR damper and compared with the soft and hard MR dampers.

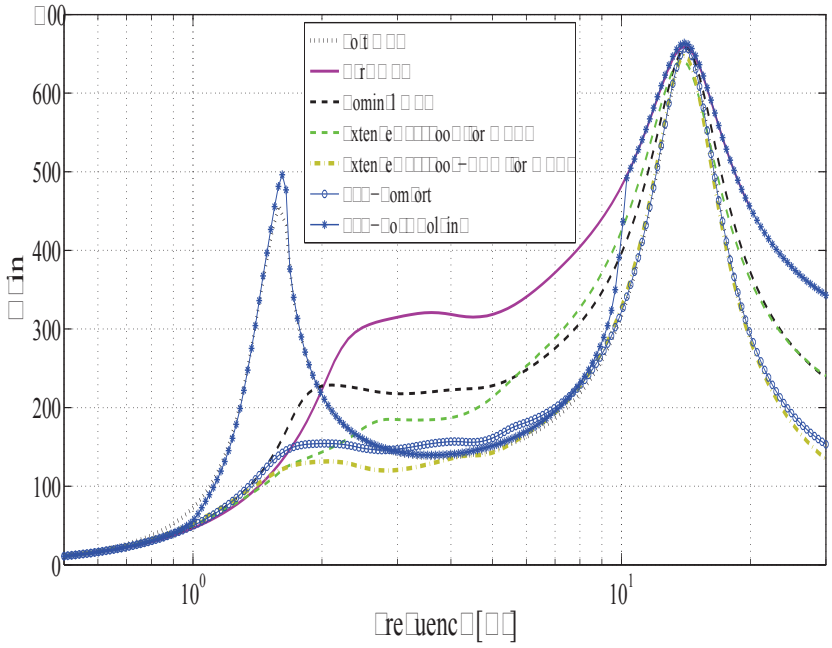

Figure 3.13: Frequency Responses $\ddot{z}_s/z_r$.

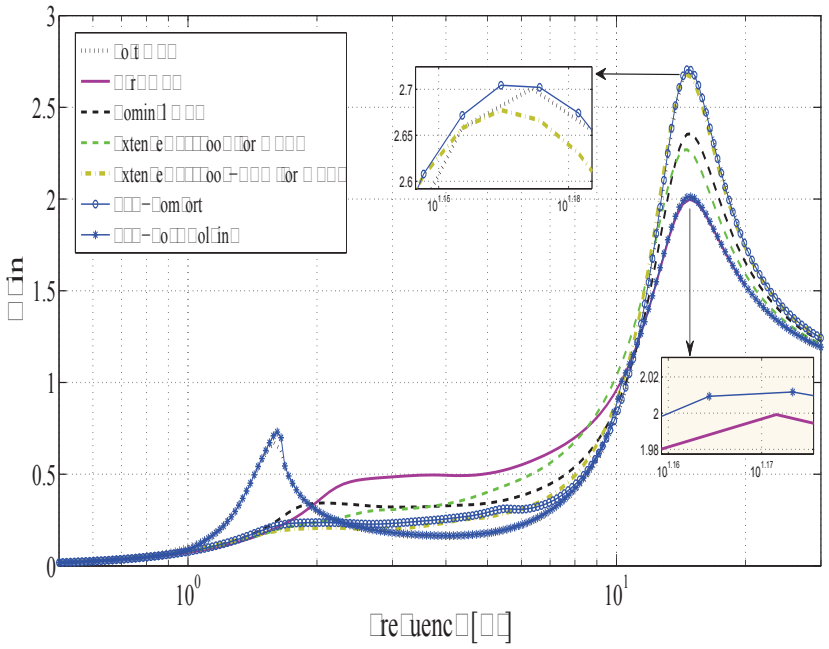

Figure 3.14: Frequency Responses $(z_{us} - z_r)/z_r$.

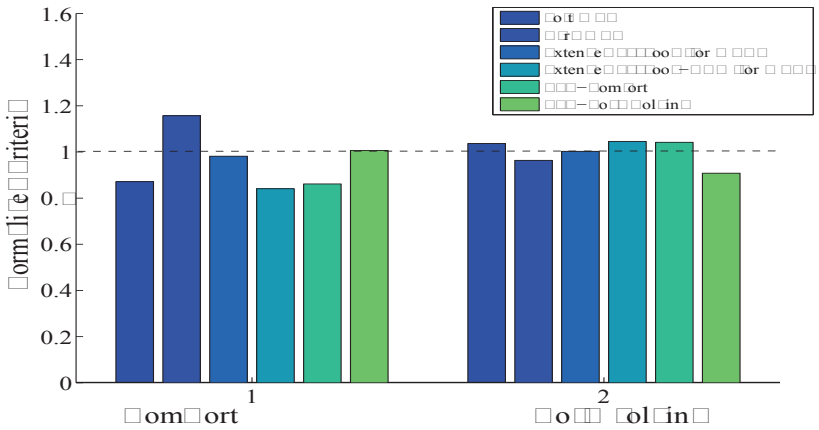

Figure 3.15: Performances comparison (in frequency domain).

3.6.3 Time domain analysis

The road profile could be viewed as a random signal, because it is not predicted by the vehicle. However, in practice, its band-width is limited. In this test, a road profile is represented by an integrated white noise, band-limited within the frequency range [0-30] Hz (see Fig. 3.16). To evaluate the performances of the strategies, the spectrum of vehicle acceleration and dynamic tire deflection are depicted in Fig. 3.18-3.19. The results obtained are coherent with the frequency domain analysis: the Extended Mixed

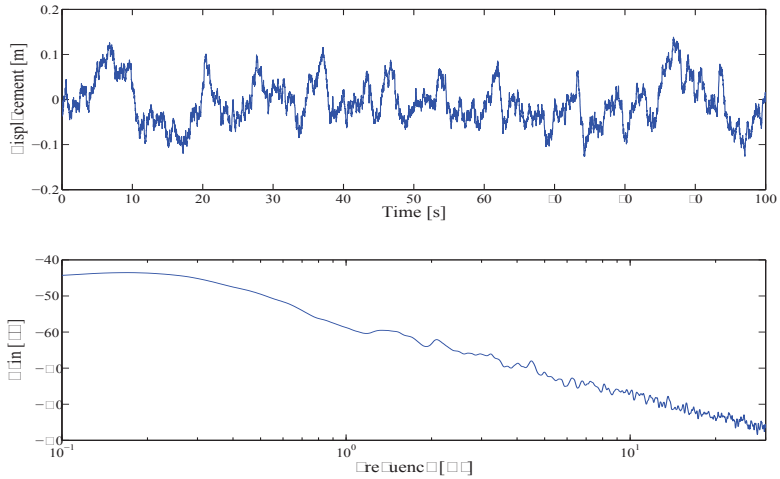

Figure 3.16: Road profile z_r.

Skyhook-ADD and LPV-Comfort are the best strategies for ride comfort, the LPV-Road Holding and Hard MRD are the most suitable for the road holding improvement. Furthermore, the comfort in time domain can be evaluated, using the following criterion

$$RMS_{\text{Comfort}} = \sqrt{\frac{\int_0^T \ddot{\overline{z}}_s^2(t)dt}{T}} \tag{3.6.3}$$

where $\ddot{\overline{z}}_s(t)$ is the filtered vehicle body acceleration (by the approximated ISO 2631 filter (1.2.9)) $[m/s^2]$ and T is the simulation time $[s]$. In Fig. 3.17, the RMS_{Comfort} values of different strategies, normalized by that value for the nominal damper, are depicted. The results mentioned previously have been proved again. The LPV-Comfort approaches the Extended Mixed Skyhook-ADD.

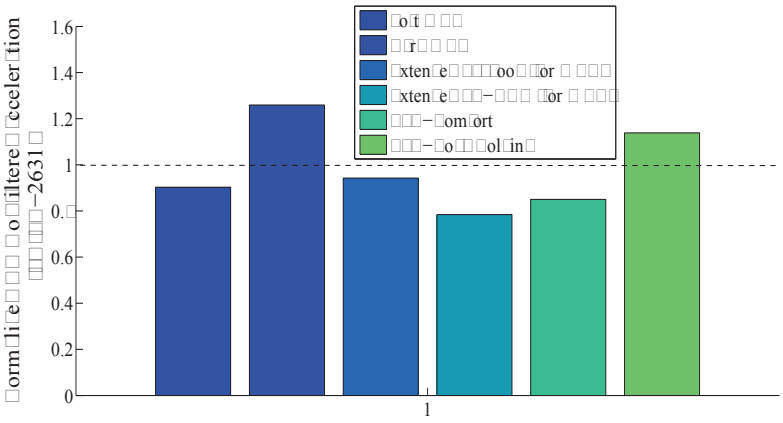

Figure 3.17: Normalized RMS value of filtered $\ddot{z}_s$ (by ISO-2631).

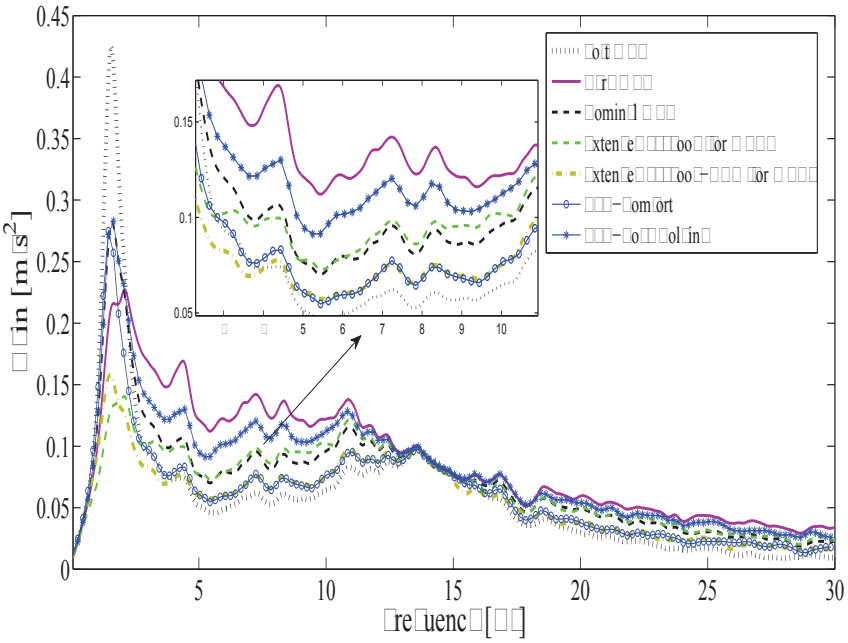

Figure 3.18: Spectrum of $\ddot{z}_s$.

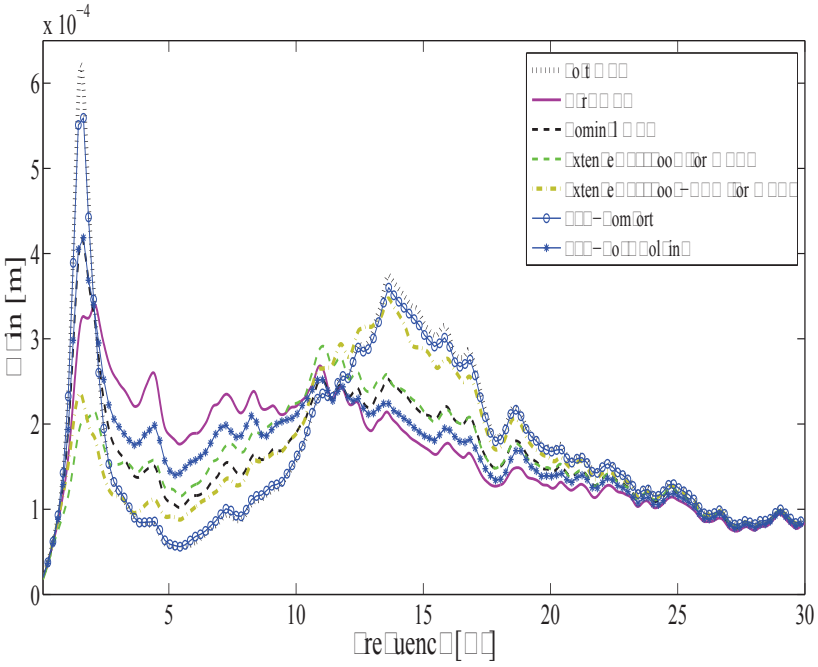

Figure 3.19: Spectrum of $z_{us} - z_r$.

3.6.4 Robustness evaluation

Vehicles in general and specially public vehicles (like bus) can be considered as systems with large uncertainties. It can be seen immediately, that their mass changes dramatically, depending on working conditions (free or overcharged) and the load transfer (when a vehicle goes around a corner, it transfers load from the inside tires to the outside tires). In this section, we will test the proposed controllers considering a change in the sprung mass (see Fig. 3.20).

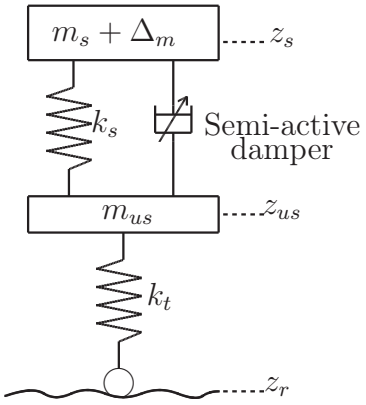

Figure 3.20: Model of a quarter vehicle with sprung mass uncertainty.

Overcharged working condition

For testing the robustness of the proposed controllers in overcharged state, we consider a constant (time-invariant) uncertainty. We take $\Delta_m = 0.75 m_s$ (i.e the sprung mass changes 75 % w.r.t the design value).

Load transfer

For load transfer analysis, we consider a time-varying uncertainty $\Delta_m(t)$. we take for example $\Delta(t)$ varying from -25% to $+25\%$ of the sprung mass (see Fig. 3.23).

As seen in Fig. 3.21-3.22 (for the overcharged case) and 3.24-3.25 (for the load transfer case), the effectiveness of the proposed controllers is still preserved.

We now consider the RMS value of the sprung mass acceleration (filtered by ISO-2631) for each strategy in three working conditions: nominal design, overcharged and load transfer. The results are given in Fig. 3.26. In this figure, the values in percent represent either the improvement (with "+") or the degradation (with "-") of the corresponding strategies in load transfer and overcharged mode w.r.t that when working in nominal working condition design.

In terms of comfort analysis, we have the following remarks. The two comfort oriented controllers LPV-comfort and Extended Skyhook-ADD seem to be more sensible to load

transfer mode than other strategies. However, these two controllers are always the best ones for comfort (in all working conditions).

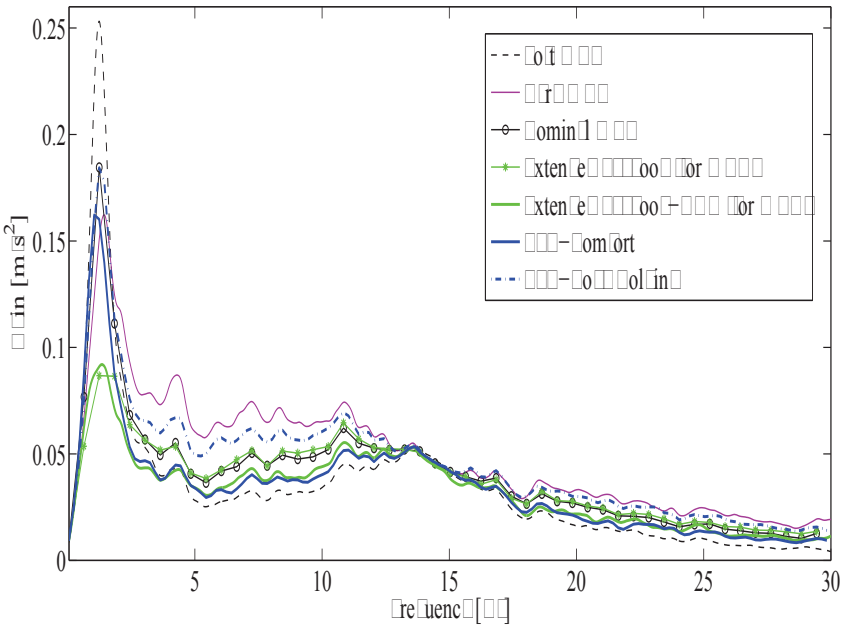

Figure 3.21: Spectrum of $\ddot{z}_s$ (test with an increase of 75% in sprung mass).

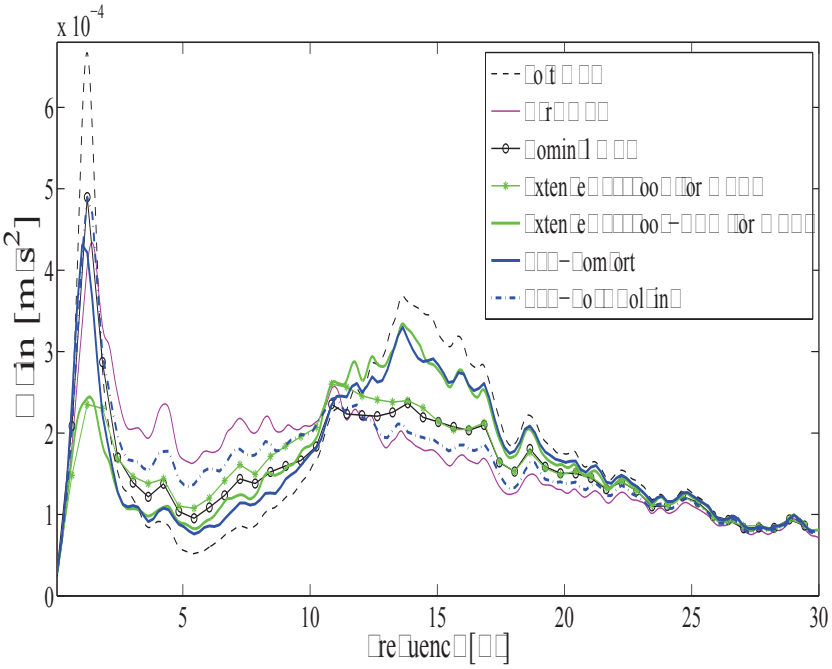

Figure 3.22: Spectrum of $z_{us} - z_r$ (test with an increase of 75% in sprung mass).

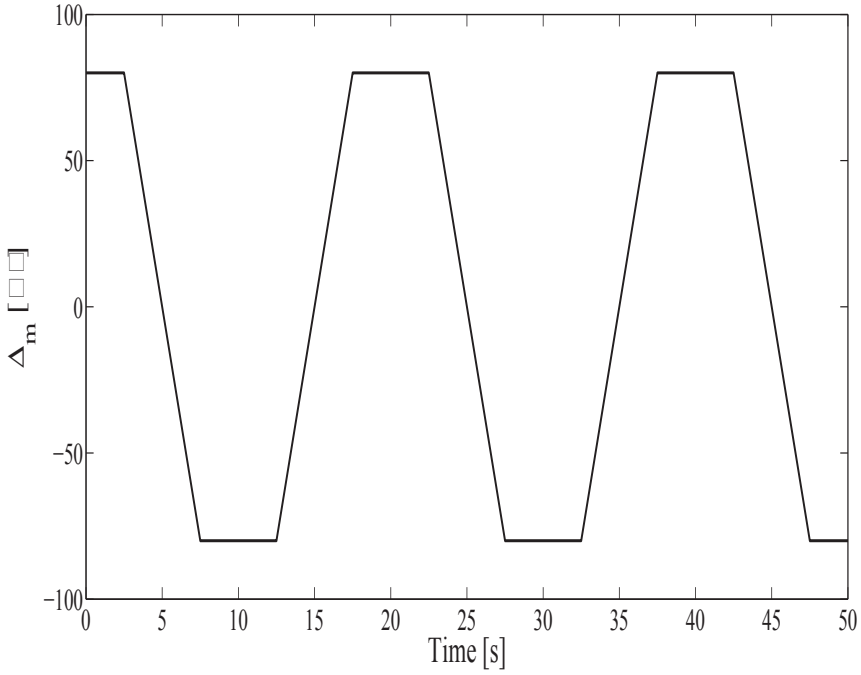

Figure 3.23: Load transfer.

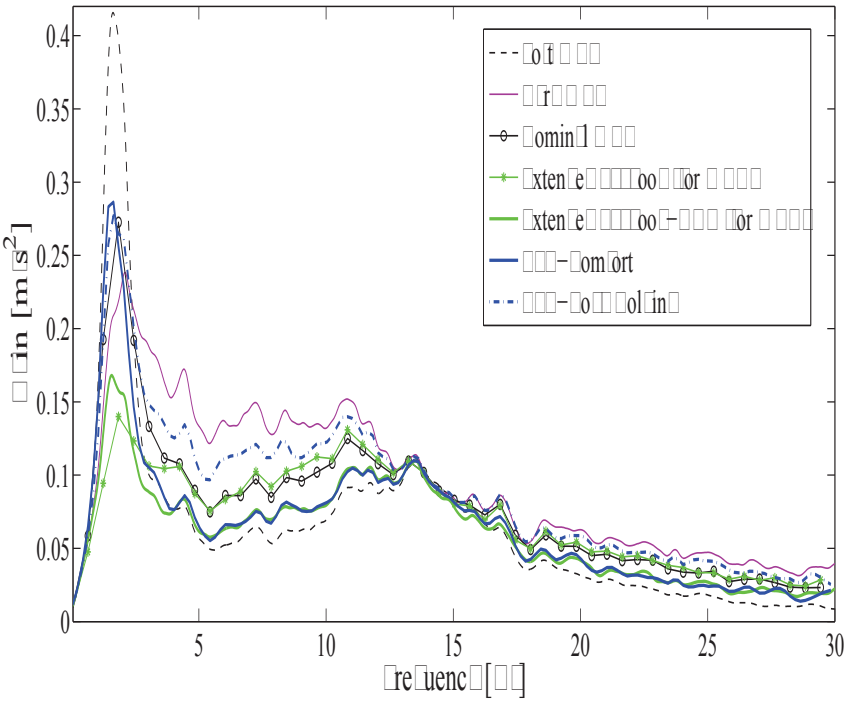

Figure 3.24: Spectrum of $\ddot{z}_s$ (test with a load transfer condition).

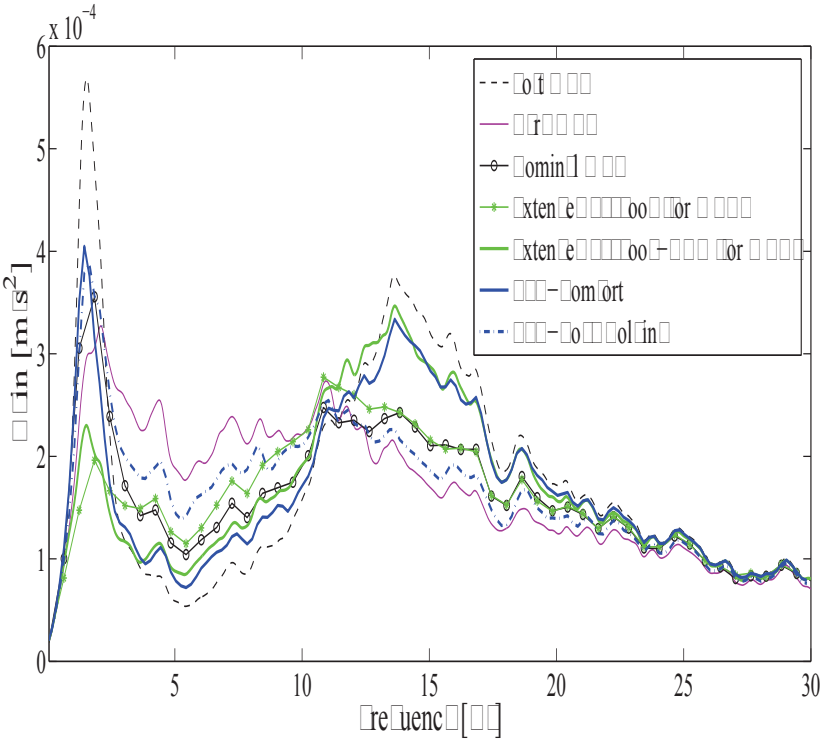

Figure 3.25: Spectrum of $z_{us} - z_r$ (test with a load transfer condition).

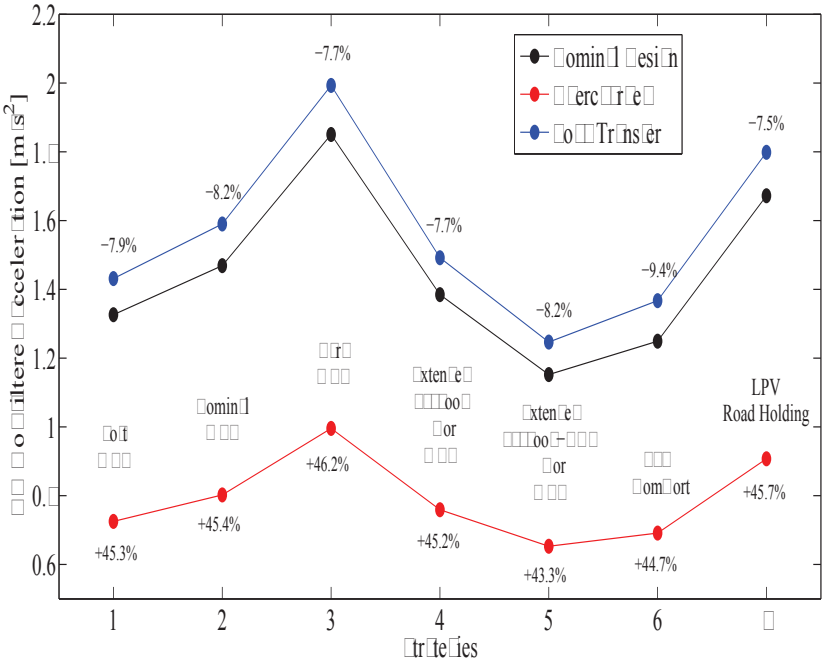

Figure 3.26: Absolute RMS value of filtered $\ddot{z}_s$ in different working conditions.

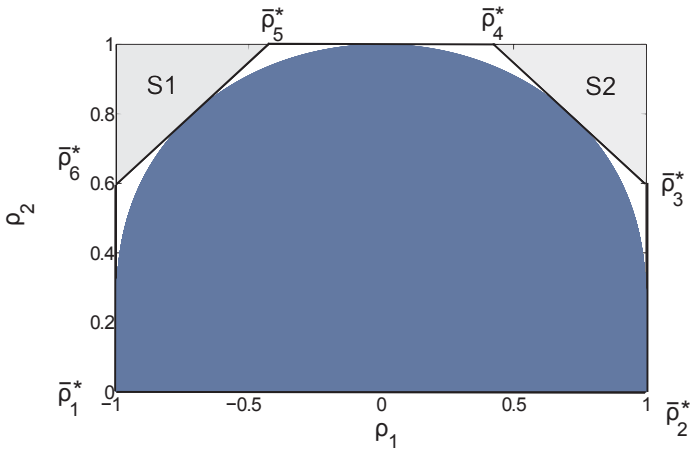

Figure 3.27: Reduced-polytope with 6 vertices

3.7 Reducing the conservatism in the synthesis

As mentioned in the preliminary study in Sec. 3.5.1, the polytope with 4 vertices $\bar{\rho}_1 = (-1, 0)$, $\bar{\rho}_2 = (1, 0)$, $\bar{\rho}_3 = (1, 1)$, $\bar{\rho}_4 = (-1, 1)$ is used for the synthesis of an LPV controller. In this section, a smaller polytope with 6 vertices containing the trajectories of the scheduling parameter $\{\rho_1, \rho_2\}$ will be considered.

As seen in Fig. 3.27, the two lower vertices of the old polytope (in Sec 3.5.1) remain, i.e. $\bar{\rho}_1^* \equiv \bar{\rho}_1$, $\bar{\rho}_2^* \equiv \bar{\rho}_2$. The four new ones $\bar{\rho}_3^*$, $\bar{\rho}_4^*$, $\bar{\rho}_5^*$ and $\bar{\rho}_6^*$ of the new polytope are determined in such a way that the new polytope contains the set defined by all possible trajectories of $\{\rho_1, \rho_2\}$ and that its area is minimized.

The area minimization problem of the new polytope is equivalent to the area maximization of the triangles S_1 and S_2. By solving this optimization problem the four new vertices are found

$$\begin{aligned} \bar{\rho}_3^* &= (1, 0.6) \qquad \bar{\rho}_4^* = (0.45, 1) \\ \bar{\rho}_5^* &= (-0.45, 1) \quad \bar{\rho}_6^* = (-1, 0.6) \end{aligned} \tag{3.7.1}$$

The new LPV controller is defined as

$$K_c^*(\rho) = \sum_{i=1}^{6} \alpha_i K_{ci} \tag{3.7.2}$$

where $\sum_{i=1}^{6} \alpha_i = 1$ and $\alpha_i \geq 0$, $i = 1 : 6$.

It is worth noting that in this case the considered polytope is not a hypercube, henceforth the coefficients α_i are not explicitly given as in (2.2.9) in Chapter 2. One way to overcome this problem is to use the following optimization procedure which is given in [Scherer & Weiland, 2005]

$$\text{minimize} \quad \sum \alpha_i^2 \tag{3.7.3}$$

$$\text{subject to} \quad \sum_{i=1}^{6} \alpha_i = 1, \quad \alpha_i \geq 0 \quad i = 1:6 \tag{3.7.4}$$

$$\sum_{i=1}^{6} \alpha_i \bar{\rho}_1^* = (\rho_1, \rho_2) \tag{3.7.5}$$

The sum of squares (3.7.3) is used to ensure a unique solution of α_i because this is a convex optimization problem (both the objective function and the constraints are convex). The constraints (3.7.4) and (3.7.5) guarantee the equivalence between the original LPV system and its polytopic representation. Notice that ρ_1 and ρ_2 are time-varying parameters, the optimization (3.7.3) must be solved numerically online. At the instant t_k, the coefficients $\alpha_i(t_k)$ with $i = 1:6$ are exactly updated as follows

$$\begin{aligned}
&\text{minimize} \quad \textstyle\sum \alpha_i^2(t_k) \\
&\text{subject to} \quad \textstyle\sum \alpha_i(t_k) = 1, \quad \alpha_i(t_k) \geq 0 \quad i = 1:6 \\
&-\alpha_1(t_k) + \alpha_2(t_k) + \alpha_3(t_k) + 0.45\alpha_4(t_k) - 0.45\alpha_5(t_k) - \alpha_6(t_k) = \rho_1(t_k) \\
&\qquad\qquad 0.6\alpha_3(t_k) + \alpha_4(t_k) + \alpha_5(t_k) + 0.6\alpha_6(t_k) = \rho_2(t_k)
\end{aligned} \tag{3.7.6}$$

With the new reduced polytope, we use the same procedure for the synthesis and controller optimization by GAs proposed in previous section. Two new controllers are obtained: **LPV-Comfort Improved** and **LPV-Road Holding Improved**. As seen in Fig. 3.29-3.28, slight improvements are obtained when using the reduced polytope for the controller synthesis. However, the price paid for these performance improvements relies in the time-consumption in simulation. Due to the online optimization computation (3.7.6), the closed-loop system with the new controllers has slow dynamics.

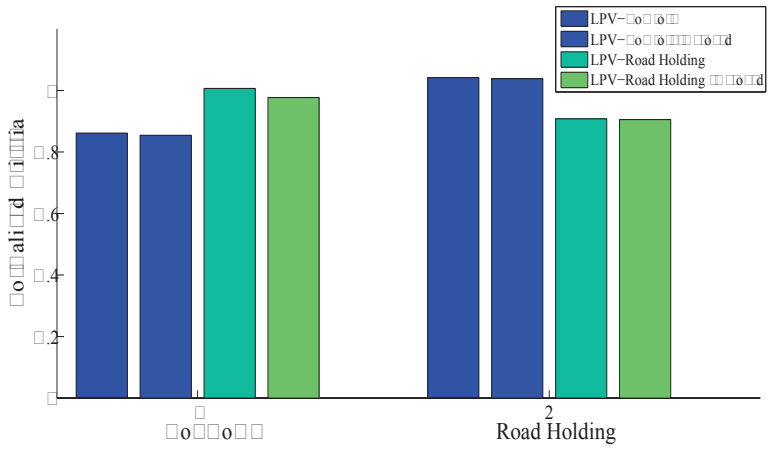

Figure 3.28: Frequency Responses $(z_{us} - z_r)/z_r$.

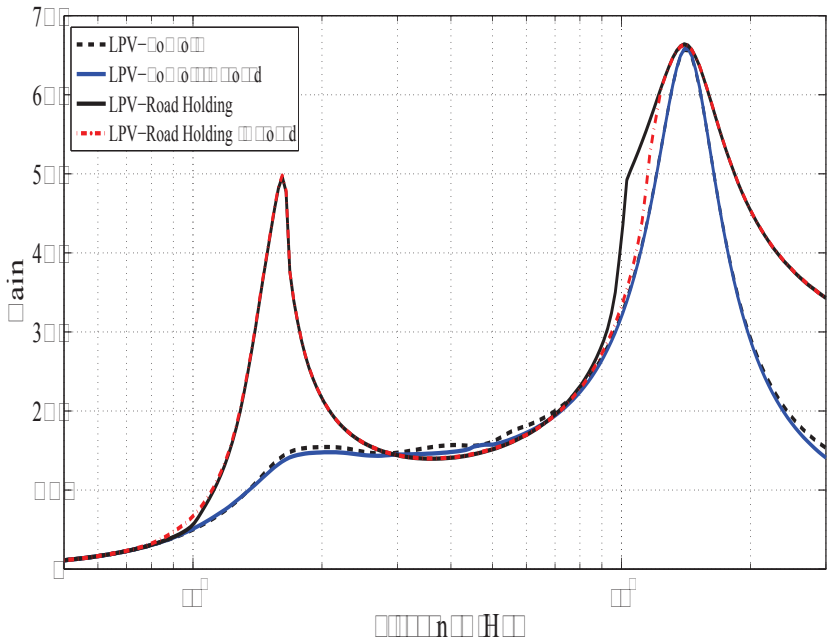

Figure 3.29: Frequency Responses $\ddot{z}_s/z_r$ (synthesis using polytope of 6 vertices v.s 4 vertices).

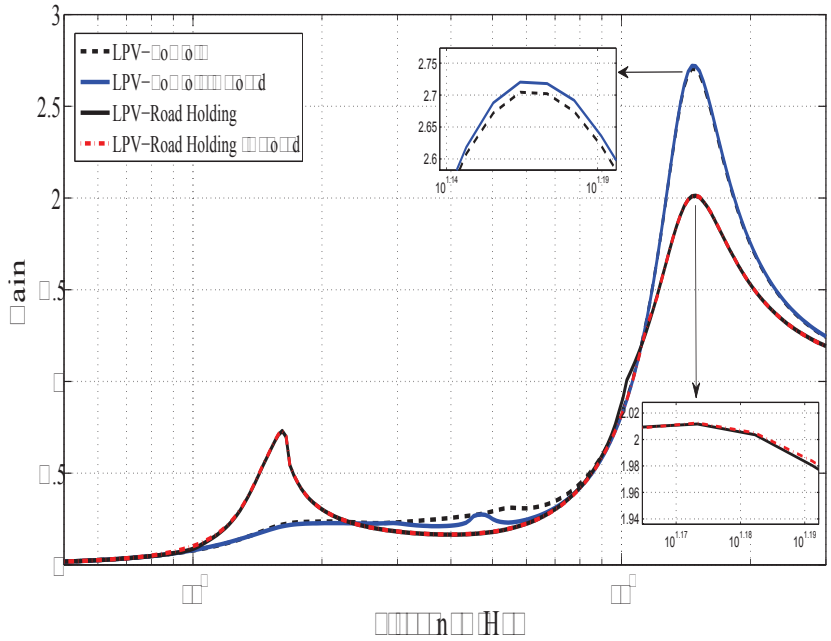

Figure 3.30: Frequency Responses $(z_{us} - z_r)/z_r$ (synthesis using polytope of 6 vertices v.s 4 vertices).

3.8 Conclusion

In this chapter, the control of semi-active suspensions using Magneto-Rheological dampers has been presented. The contributions of the chapter are two folds: the extended version of Mixed Skyhook-ADD (see Appendix A) and the LPV control method.

For the LPV approach, the obtained results can be summarized as follows:

- An LPV control-oriented model of MR dampers is proposed where the bi-viscous and hysteresis characteristics are taken into account. This model was validated by experimental tests. It can be seen that the model provides a good approximation of a real MR damper.
- The quarter vehicle model equipped with the proposed MR damper model is written in an LPV framework which can be used for LPV design (H_∞, H_2 or mixed H_∞/H_2...).
- A multi-objective optimization procedure using genetic algorithms that achieves the desired suspension performances is also introduced. It leads to a generic methodology to find a controller satisfying the required performance whatever the criteria are.
- From the practical point of view, as seen in Fig. 3.9, the proposed control method is simple and easy to implement: a single relative displacement sensor to measure the suspension deflection (the deflection velocity can be deduced numerically from the deflection) is needed and the LPV controller is stable.
- An improvement of the controllers based on polytopic reduction is also obtained.

The simulations on the nonlinear quarter vehicle model equipped with a validated MR damper (in the frequency and time domains) have been analyzed. The results have shown the interest of the proposed method: the obtained comfort-oriented and road holding-oriented LPV controller can then be used with a switching rule which can be adapted to different road conditions (in cities and suburbs).

Chapter 4

Suspension systems with linear hydraulic dampers

Though the nonlinearity in the damper model needs to be taken into account in the controller design, many studies have been based on suspension system models with linear hydraulic dampers. The schematic layout of a hydraulic damper is depicted in Fig. 4.1. Hydraulic dampers consist of a pressure tube (body), a piston rod with a special piston system, and the damping medium oil. In principle, the damping coefficient of the damper can be changed using an external actor (e.g. solenoid valve) (see [Aubouet, 2010]).

The reason for which the linear dampers have been more intensively studied is that the vehicle models with these dampers allow, a priori, to deal with more general and complex problems and to test the effectiveness of the design methods in the ideal case (by omitting the nonlinearities). In this chapter we revisit the linear suspension control problem. A new approach, based on *Strong Stabilization*, is proposed.

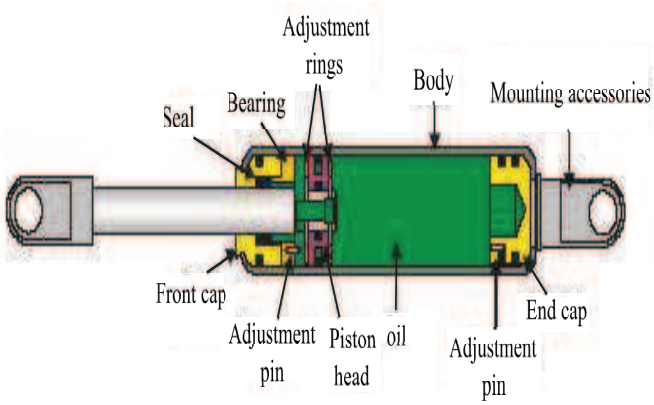

Figure 4.1: Schematic layout of a hydraulic damper.

4.1 Introduction

4.1.1 Quarter car model equipped with a linear semi-active damper

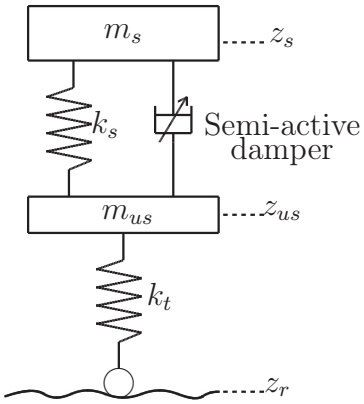

Figure 4.2: Model of a quarter vehicle with a linear damper.

Consider the quarter vehicle model depicted in Fig. 4.2 equipped with a linear damper characterized by the following equation:

$$F_{damper} = c\dot{z}_{def} \tag{4.1.1}$$

As previously stated in Chapter 1, the dynamical equations of a quarter vehicle will be given by

$$\begin{cases} m_s\ddot{z}_s &= -k_s z_{def} - c\dot{z}_{def} \\ m_{us}\ddot{z}_{us} &= k_s z_{def} + c\dot{z}_{def} - k_t\left(z_{us} - z_r\right) \end{cases} \tag{4.1.2}$$

where $z_{def} = z_s - z_{us}$ is the damper deflection $[m]$, $\dot{z}_{def} = \dot{z}_s - \dot{z}_{us}$ is the deflection velocity $[m/s]$

The passivity constraint of a semi-active damper is characterized by:

$$0 \leqslant c_{min} \leqslant c \leqslant c_{max} \tag{4.1.3}$$

or equivalently

$$\begin{aligned} c_{min}\dot{z}_{def} \leq F_{damper} \leq c_{max}\dot{z}_{def} \quad &\text{if} \quad \dot{z}_{def} > 0 \\ c_{max}\dot{z}_{def} \leq F_{damper} \leq c_{min}\dot{z}_{def} \quad &\text{if} \quad \dot{z}_{def} \leq 0 \end{aligned} \tag{4.1.4}$$

In this chapter, we use $c_{min} = 700$ $[Ns/m]$ and $c_{max} = 5000$ $[Ns/m]$.

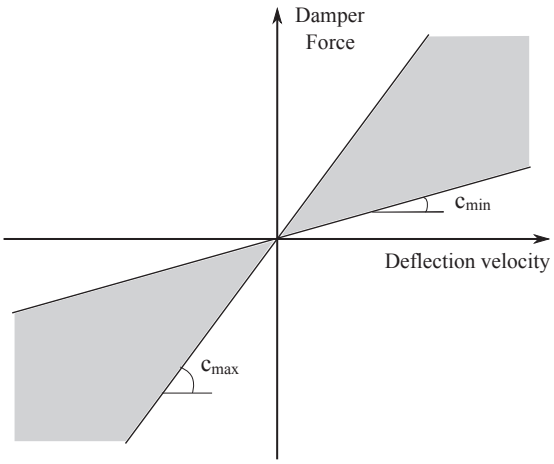

Figure 4.3: Semi-active damper: Force vs Velocity.

4.1.2 Performance objectives

As mentioned in section 1.2.2 in Chapter 1, we recall here the frequency-based performance criteria domain calculated for the quarter vehicle model 4.1.2:

- Comfort

$$J_{CF} = \int_0^{20} \ddot{z}_s / z_r(f) df \tag{4.1.5}$$

- Road holding

$$J_{RH} = \int_0^{30} (z_{us} - z_r) / z_r(f) df \tag{4.1.6}$$

The objective of the control design is to minimize these two performance criteria.

4.2 Strong stabilization approach

In this section, we present a new approach for the control of the linear semi-active suspension system (4.1.2). As in Chapter 4, the aim is to obtain a good Pareto front of two conflicting performances: comfort and road holding. Let us motivate the use of the strong stabilization approach for semi-active suspension control.

4.2.1 Motivation

First, decompose the total semi-active damper force as $F_{damper} = c_0 \dot{z}_{def} + u$ where $c_0 = (c_{min} + c_{max})/2$ and consider a state-space representation of the quarter car model

given as follows

$$\begin{aligned} \dot{x_s} &= A_s x_s + B_{s1} w + B_{s2} u \\ y &= C_s x_s \end{aligned} \tag{4.2.1}$$

where $x_s = (z_s,\ \dot{z}_s,\ z_{us},\ \dot{z}_{us})^T$, $w = z_r$, $y = \dot{z}_s - \dot{z}_{us} = \dot{z}_{def}$.

$$A_s = \begin{bmatrix} 0 & 1 & 0 & 0 \\ \frac{-k_s}{m_s} & \frac{-c_0}{m_s} & \frac{k_s}{m_s} & \frac{c_0}{m_s} \\ 0 & 0 & 0 & 1 \\ \frac{k_s}{m_{us}} & \frac{c_0}{m_{us}} & -\frac{k_s+k_t}{m_{us}} & -\frac{c_0}{m_{us}} \end{bmatrix}, B_{s1} = \begin{bmatrix} 0 & 0 & 0 & \frac{k_t}{m_{us}} \end{bmatrix}^T,$$

$$B_{s2} = \begin{bmatrix} 0 & \frac{-1}{m_s} & 0 & \frac{1}{m_{us}} \end{bmatrix}^T, C_s = \begin{bmatrix} 0 & 1 & 0 & -1 \end{bmatrix}.$$

The model (4.2.1) is usually used in many control strategies for both semi-active and active suspension systems, e.g. optimal control, H_∞ and H_2 control, MPC control... In this section, we present a new approach for semi-active suspension control based on this model. Let us consider the following remarks.

Remark 4.2.1. In fact, u is the compensated force added to a nominal damper whose damping coefficient equals c_0. To satisfy the passivity constraint (4.1.4) of a semi-active damper (see also Fig. 4.4), the control input u must be constrained by

$$|u(t)| \leq \frac{c_{max} - c_{min}}{2} |\dot{z}_{def}(t)| \quad \forall t \geq 0 \tag{4.2.2}$$

Denote $U(s)$, $\dot{Z}_{def}(s)$ the Laplace transforms of u and $\dot{z}_{def}$. Let us consider the following condition

$$|U(j\omega)| \leq \frac{c_{max} - c_{min}}{2} |\dot{Z}_{def}(j\omega)| \quad , \forall \omega \tag{4.2.3}$$

It can be seen that the constraint (4.2.3) does not imply (4.2.2). However, if we discard some short term over-shots in the time responses of u (which can violate the passivity constraint, in short term), (4.2.3) is a good approximation of (4.2.2) and easier to handle.

Remark 4.2.2. As seen in (4.2.1), the deflection velocity $\dot{z}_{def}$ is a measurement output of the system. This is an intentional choice because of the following reason. Remark that if there exists a stabilizing LTI controller K for the plant (4.2.1) and that

$$\|K\|_\infty = \frac{\|u\|_2}{\|\dot{z}_{def}\|_2} \leq \frac{c_{max} - c_{min}}{2} \quad \text{for all } 0 < \|\dot{z}_{def}\|_2 < \infty \tag{4.2.4}$$

then K is a controller satisfying (4.2.3).

Remark 4.2.3. If a stable controller is used with a stable plant we can avoid the instability of the closed-loop system (precisely the instability of the controller because the plant is already stable) due to the nonlinearities between the plant and the controller, such as the input saturation.

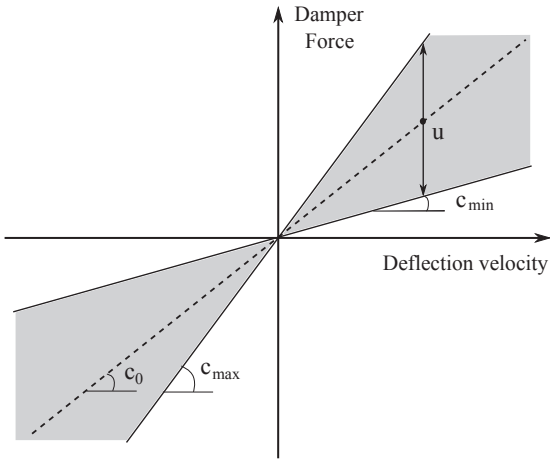

Figure 4.4: Illustration of semi-active control: The control input u must be bounded by $\pm|\dot{z}_{def}|(c_{max} - c_{min})/2$.

With the remarks above, the stable controllers with bounded gain seem to be a reasonable choice for semi-active suspension systems. This motivates the investigation of the *strong stabilization approach* presented in the next section.

4.2.2 Strong stabilization

The strong stabilization consists in finding a stable feedback controller which stabilizes a given plant. The advantages for the use of stable controllers concern the practical aspect. If a stable controller is used for a stable plant, the closed-loop system is always stable under sensors failure or input saturation effect. Moreover, the stable controllers are easier to implement than the unstable ones [Cao & Lam, 2000], [Campos-Delgado & Zhou, 2001]. On the other hand, stabilization using an unstable compensator always introduces additional right half plane zeros into the closed-loop transfer function matrix beyond those of the original plant. As it is known that the right half plane zeros of a system affect its ability to track reference signals and/or to reject disturbances, it is preferable to use a stable stabilizing compensator. In addition, several other problems in reliable stabilization are related to strong stabilizability, such as the simultaneous stabilization problem. It is proven that the simultaneous stabilization of $n \geq 2$ plants with a common compensator is equivalent to the stabilization of $n - 1$ plants with a common stable compensator [Vidyasagar, 1985].

In fact, this problem was first addressed and solved for SISO systems by [Youla et al., 1974]. In this study, a tractable condition, known as the parity interlacing property (PIP) was proposed to check whether a given plant is strongly stabilizable or not. It was stated that a necessary and sufficient condition for the existence of stable stabilizing controllers is that the number of unstable real poles (counted according to their McMillan degree) of a real-rational plant between every pair of its right-half-plane real blocking zeros, is even. The PIP was then generalized to MIMO systems by [Vidyasagar, 1985]. Although the PIP is an elegant result, it does not indicate how to find such a stable controller if it exists. In [Zeren & Özbay, 2000], [Choi & Chung, 2001], based on the ARE (Algebraic Riccati Equation) methods, a sufficient condition to determine a stable H_∞ controller is given. Recently, some new results for this problem were obtained with LMI solutions [Yang et al., 2002], [Chou et al., 2007].

For the application of the strong stabilization approach in semi-active suspension control, two interesting problems are the *strong* $\gamma_{cl}-H_\infty$ and *strong* $\gamma_k-\gamma_{cl}$ H_∞ problems (see [Cheng et al., 2007]), defined as follows.

Definition 4.2.1. *Strong* $\gamma_{cl} - H_\infty$ *problem*
Given a system $G(s)$ *and* H_∞ *performance levels* γ_{cl} *and* $G(s)$ *is said to be strongly stabilizable with an* H_∞*-norm bound* γ_{cl} *or strongly* $\gamma_{cl} - H_\infty$ *stabilizable if there exists a stable controller* $K(s) \in RH_\infty$ *satisfying* $\|K\|_\infty < \gamma_{cl}$ *such that the closed-loop system* T_{zw} *is internally stable with* $\|T_{zw}\|_\infty < \gamma_{cl}$.

Definition 4.2.2. *Strong* $\gamma_k - \gamma_{cl}$ H_∞ *problem*
Given a system $G(s)$ *and an* H_∞ *performance level* γ_k, γ_{cl}, $G(s)$ *is said to be strongly* $\gamma_k-\gamma_{cl}$ H_∞ *stabilizable if there exists a stable controller* $K(s) \in RH_\infty$ *satisfying* $\|K\|_\infty < \gamma_k$ *such that the closed-loop system* T_{zw} *is internally stable with* $\|T_{zw}\|_\infty < \gamma_{cl}$.

Remark 4.2.4. If $\gamma_k = \gamma_{cl}$, Definition 2 reduces to Definition 1.

In this chapter, two solutions proposed by [Cheng et al., 2007] and [Gümüssoy & Özbay, 2005] for the above strong H_∞ problems will be introduced.

4.2.3 Strong stabilization - Approach 1

Before presenting the results, let us define some notations.

- A state-space representation of a transfer function, $N(s) = C(sI - A)^{-1}B + D$, is given by

$$N(s) = \left[\begin{array}{c|c} A & B \\ \hline C & D \end{array}\right]$$

- The lower Linear Fractional Representation $\|\mathcal{F}_l(N;K)\|$ is given as $N_{11}+N_{12}K(I-N_{22}K)^{-1}N_{21}$ where N is partitioned as

$$N = \begin{bmatrix} N_{11} & N_{12} \\ N_{21} & N_{22} \end{bmatrix}$$

- We define $\Gamma(M,N) := MN + N^T M^T$ where M, N are matrices with compatible dimensions.

The standard H_∞ problem for a certain plant P is to find a stabilizing controller M such that the lower Linear Fractional Representation $\|\mathcal{F}_l(P;M)\|_\infty < \gamma_{cl}$ where $\gamma_{cl} > 0$ is the closed-loop performance level. As stated in [Doyle et al., 1989] and [Zhou et al., 1995], if two AREs have unique positive semi-definite solutions and the spectral radius condition is satisfied, then the standard H_∞ problem is solvable. All suboptimal H_∞ controllers can be parameterized as $M = \mathcal{F}_l(M_C; M_Q)$ where M_C is the central controller given in the form

$$M_C(s) = \left[\begin{array}{c|cc} A_c & B_{c1} & B_c \\ \hline C_{c1} & D_{c11} & D_{c12} \\ C_c & D_{c21} & 0 \end{array}\right] \tag{4.2.5}$$

and M_Q is a free parameter satisfying $M_Q \in RH^\infty$ and $\|M_Q\|_\infty < \gamma_{cl}$. The calculation of M_C is given in [Doyle et al., 1989] and [Zhou et al., 1995]. For the determination of M_Q, let us consider first the following lemma.

Lemma 4.2.1. *[Gümüssoy & Özbay, 2005].*
Given a generalized plant

$$G(s) = \left[\begin{array}{c|cc} A & B_1 & B_2 \\ \hline C_1 & D_{11} & D_{12} \\ C_2 & D_{21} & 0 \end{array}\right] \tag{4.2.6}$$

where the matrices A, B_1, B_2, C_1, C_2, D_{11}, D_{12} and D_{21} have compatible dimensions and satisfy the standard assumptions (see [Gümüssoy & Özbay, 2005]), there exists a stable stabilizing control, $K \in \mathcal{RH}^\infty$ if there exist $X_k = X_k^T > 0$ and Z for some $\gamma > 0$ satisfying the LMIs

$$\begin{gathered} \Gamma(X_k, A) + \Gamma(Z, C_2) \prec 0 \\ \begin{bmatrix} \Gamma(X_k, A_X) + \Gamma(Z, C_2) & -Z & -XB_2 \\ * & -\gamma I & 0 \\ * & * & -\gamma I \end{bmatrix} \prec 0 \end{gathered} \tag{4.2.7}$$

where $A_X = A - B_2 B_2^T X$ and $X > 0$ is the solution of the ARE (note that $X \neq X_k$)

$$A^T X + XA - XB_2 B_2^T X = 0 \tag{4.2.8}$$

Then the controller K is represented by

$$K(s) = \left[\begin{array}{c|c} A_k & B_k \\ \hline C_k & D_k \end{array}\right] = \left[\begin{array}{c|c} A_X + X_k^{-1} Z C_2 & -X_k^{-1} Z \\ \hline -B_2^T X & 0 \end{array}\right] \tag{4.2.9}$$

and

$$\|K(s)\|_\infty < \gamma \tag{4.2.10}$$

Back to the standard H_∞ problem, if we consider the $G = M_C$ and $\gamma = \gamma_{cl}$, then the Lemma 4.2.1 allows to find the free parameter $M_Q = K$.

4.2.4 Strong stabilization - Approach 2

Theorem 4.2.2. *[Cheng et al., 2007]*
Given a standard system $G(s)$ as in 4.2.6, it is strongly $\gamma_k - \gamma_{cl}$ H_∞ stabilizable if there exist $X \succ 0$, $Y \succ 0$ satisfying the following conditions:

$$A^T X + XA + X(\gamma_{cl}^{-2} B_1 B_1^T - B_2 B_2^T) X + C_1 C_1^T = 0 \tag{4.2.11}$$

$$AY + YA^T + Y(\gamma_{cl}^{-2} C_1^T C_1 - C_2 C_2^T) Y + B_1 B_1^T \preceq 0 \tag{4.2.12}$$

$$A_{\gamma_{cl},X} Y Z^T + Z Y A_{\gamma_{cl},X}^T + \gamma_k^{-2} Z Y X B_2 B_2^T X Y Z - Z Y C_2^T C_2 Y Z^T \preceq 0 \tag{4.2.13}$$

$$\rho(XY) < \gamma_{cl}^2 \tag{4.2.14}$$

where

$$A_{\gamma_{cl},X} = A + \gamma_{cl}^{-2} B_1 B_1^T X - B_2 B_2^T X \tag{4.2.15}$$

$$Z = (I - \gamma_{cl}^{-2} Y X)^{-1} \tag{4.2.16}$$

Then a strong $\gamma_k - \gamma_{cl}$ H_∞ controller can be constructed as

$$K(s) = \left[\begin{array}{c|c} A_k & B_k \\ \hline C_k & D_k \end{array}\right] = \left[\begin{array}{c|c} A_{\gamma_{cl},X} - Z Y C_2^T C_2 & Z Y C_2^T \\ \hline -B_2^T X & 0 \end{array}\right] \tag{4.2.17}$$

By defining $S = \gamma_{cl} Y^{-1}$, $\alpha_k = \gamma_k^2$, $\Gamma_S = \gamma_{cl}^{-1} S - \gamma_{cl}^{-2} X$ and using Schur's lemma, the inequalities (4.2.12), (4.2.13) and (4.2.14) can be respectively replaced by the following LMIs

$$\left[\begin{array}{ccc} A^T S + SA - \gamma_{cl} C_2^T C_2 & SB_1 & C_1^T \\ B_1^T S & -\gamma_{cl} I & 0 \\ C_1 & 0 & -\gamma_{cl} I \end{array}\right] \preceq 0 \tag{4.2.18}$$

$$\begin{bmatrix} A_{\gamma_{cl},X}^T \Gamma_S + \Gamma_S A_{\gamma_{cl},X} - C_2^T C_2 & -XB_2 \\ -B_2^T X & -\alpha_k \end{bmatrix} \preceq 0 \tag{4.2.19}$$

$$\begin{bmatrix} \gamma_{cl} X^{-1} & I \\ I & S \end{bmatrix} \succeq 0 \tag{4.2.20}$$

For a given γ_k, the following Bisection Algorithm can be used to minimize the closed-loop H_∞-norm bound γ_{cl}.

- Step 1: Select $\gamma_l = 0, \gamma_{cl} = \gamma_u = \gamma_0$ which sures that the equation (4.2.11) is solvable, i.e. there exists $X = X_0 \succ 0$, and the LMIs (4.2.18)-(4.2.20) are feasible.
- Step 2: If $|\gamma_u - \gamma_l| \leq \delta$ which is a specified level, stop and the optimal $\gamma_{cl} = \gamma_u$. Otherwise go to Step 3.
- Step 3: Set $\gamma_{cl} = (\gamma_u + \gamma_l)/2$.
- Step 4: If (4.2.11) has a solution $X = X_0 \succ 0$, go to Step 5, else go to Step 6.
- Step 5: If the LMIs (4.2.18)-(4.2.18) are feasible, set $\gamma_u = \gamma_{cl}$ and go to Step 2, otherwise go to Step 6.
- Step 6: Set $\gamma_l = \gamma_{cl}$ and go to Step 2.

4.2.5 Strong stabilization approach in semi-active suspension control

The Lemma 4.2.1 and the Theorem 4.2.2 are used for the synthesis of stable controllers with a bounded H_∞-norm. With the remark that $\dot{z}_{def}$ is used as an input, we make use of these results to find a stable controller which satisfies $\|K\|_\infty \leq \frac{c_{max}-c_{min}}{2}$ (see remark 4.2.2).

Like conventional H_∞ control, in this approach, we make use of some weighting functions to achieve the desired performances (4.1.5)-(4.1.6). The control block diagram is depicted in Fig. 4.5 where the weighting functions are chosen as

$$W_{z_r} = 3 \times 10^{-2} \tag{4.2.21}$$

$$W_{\dot{z}_s} = k_{\dot{z}_s} \frac{s^2 + 2\xi_{11}\Omega_{11}s + {\Omega_{11}}^2}{s^2 + 2\xi_{12}\Omega_{12}s + {\Omega_{12}}^2} \tag{4.2.22}$$

$$W_{z_{us}} = k_{z_{us}} \frac{s^2 + 2\xi_{21}\Omega_{21}s + {\Omega_{21}}^2}{s^2 + 2\xi_{22}\Omega_{22}s + {\Omega_{22}}^2} \tag{4.2.23}$$

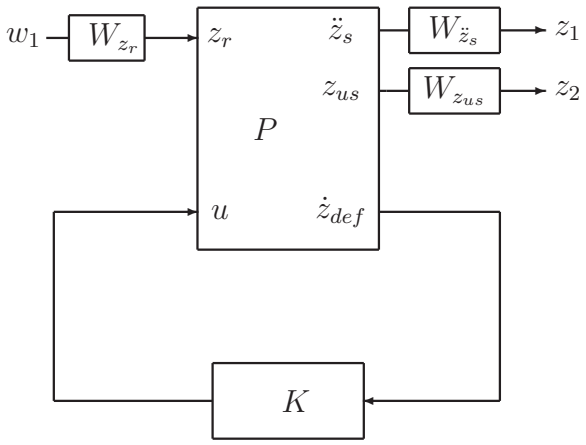

Figure 4.5: Control Block Diagram for Strong Stabilization Approach

In the following, the optimization of the stable controllers obtained by the two strong stabilization approaches presented previously will be discussed. The optimization procedure is similar to the one for H_∞/LPV controller optimization proposed in Chapter 3. It is worth noting that the Lemma 4.2.1 and the Theorem 4.2.2 must be used for the generalized plant composed of the plant and the (stable) weighting functions.

For the purpose of GA optimization, let us define the set of parameters

$$\nu = [\ \Omega_{11} \quad \Omega_{11} \quad \xi_{11} \quad \xi_{12} \quad k_{\ddot{z}_s} \quad \Omega_{21} \quad \Omega_{22} \quad \xi_{21} \quad \xi_{22} \quad k_{z_{us}}\ ]^T \tag{4.2.24}$$

that, in the context of GAs, is a part of the decision vector.

Controller optimization procedure for Approach 1

Remark 4.2.5. The original problem in [Gümüssoy & Özbay, 2005] concerns the synthesis of a stable H_∞ controller (the *strong* $\gamma_{cl} - H_\infty$ *problem*) where the system $G(s)$ in (4.2.6) represents the central controller (not the open-loop system). Here we aim at using this lemma for the synthesis of a stable controller, whose H_∞-norm is bounded, for semi-active suspension system. In our case, it is important to notice that *the system* $G(s)$ *represents the generalized plant* (the plant (4.2.1) + the weighting functions). This generalized plant is stable because both the plant and the weighting function are stable. As the result, by solving the ARE (4.2.8), a trivial solution $X = 0$ (i.e. a zero controller) is obtained.

In fact, the ARE in (4.2.8) is a carefully chosen Riccati equation. The reason to choose such an equation is as follows (see more details in [Gümüssoy, 2004]). The dynamic

matrix of the closed-loop system (4.2.6)+(4.2.9) is

$$A_{CL} = \begin{bmatrix} A & B_2C_k \\ B_kC_2 & A_k \end{bmatrix} \tag{4.2.25}$$

If we multiply this matrix from left by $\begin{bmatrix} I & -I \\ 0 & I \end{bmatrix}$ and from right by $\begin{bmatrix} I & I \\ 0 & I \end{bmatrix}$, we obtain the following matrix

$$\begin{bmatrix} A - B_kC_2 & A + B_2C_k - B_kC_2 - A_k \\ B_kC_2 & A_k + B_kC_2 \end{bmatrix} \tag{4.2.26}$$

Set $A_k = A + B_2C_k - B_kC_2$, then by using similarity transformation, we can show that A_{CL} is stable if $A_k + B_kC_2$ and $A - B_kC_2$ are stable; and the controller is stable if A_k is stable, i.e. $A + B_2C_k - B_kC_2$ is stable.

If we choose $C_k = -B_2^T X$, where X is the solution of the Riccati equation (4.2.8) then $A+B_2C_k$ is stable. Henceforth, we need to stabilize only the following matrices $A-B_kC_2$ and $A_X - B_kC_2$ (where $A_X = A - B_2B_2^T X$) which can be achieved by the LMIs (4.2.7).

To conclude, the Riccati equation (4.2.8) is given as one of the conditions to find the solution for the strong stabilization problem. Since the Riccati equation is chosen to satisfy certain conditions (the special structure of the controller) of the considered problem, the full ARE equation ($A^TX + XA - XB_2R^{-1}B_2^TX + Q = 0$) is not applicable. The structure of $R = I$ is required, however the case of $Q \succ 0$ can be used. Note that (4.2.8) gives the critical solution X and contains any solution with $Q \succ 0$. As a result, we propose to modify (4.2.8) by the following ARE

$$A^TX + XA - XB_2B_2^TX + Q = 0 \tag{4.2.27}$$

where $Q \succ 0$, to apply this lemma to stable plants.

Remark 4.2.6. The influence of Q in the final results is not analyzed in this study. In section 4.3, we simply choose $Q = I$.

Define the following objective function which contains two criteria concerning the passenger comfort and road holding capability (like the ones used in Chapter 4):

$$\min_{\nu \in \mathbb{R}_+^{10}} J^D(\nu) = \begin{bmatrix} J^D_{\text{Comfort}}(\nu) \\ J^D_{\text{RoadHolding}}(\nu) \end{bmatrix} \tag{4.2.28}$$

where

$$J^D_{\text{Comfort}} = \int_0^{12} (\ddot{z}_s / z_r(f))df \tag{4.2.29}$$

$$J^D_{\text{RoadHolding}} = \int_{10}^{20} (z_{us}/z_r(f))df \tag{4.2.30}$$

where ν is the decision vector and given in (4.2.24).

The optimization procedure using the strong stabilization Approach 1 for semi-active suspension control is defined as follows.

- **Step 0:** In the LMI (4.2.7), choose $\gamma = (c_{max} - c_{min})/2$ to constrain $\|K\|_\infty \leq (c_{max} - c_{min})/2$.
- **Step 1:** Initiate with random positive weighting functions parameters $\nu = \nu^0$.
- **Step 2:** Solve the ARE (4.2.27) and the LMI problem (4.2.7) to obtain a stable controller $K(s)$ (4.2.9). Then compute the objective function (closed-loop performance) $J^D(\nu)$ defined in (4.2.28)-(4.2.30).
- **Step 3:** Calculate the fitness value and select the best ν (associated with the smallest objective function).
- **Step 4:** Apply the genetic operation (crossover and mutation) to get a new generation: $\nu = \nu^{new}$.
- **Step 5:** Evaluate the new generation: If the criteria of interest (for example, reaching the limit number of generation) are not satisfied, go to Step 2 with $\nu = \nu^{new}$; Else, stop and save the best individual $\nu^{opt} = \nu^{new}$ and the associated controller.

Controller optimization procedure in Approach 2 Define the following objective function which is the same as the one used for approach 1:

$$\min_{\{\nu,\gamma_{cl}\}\in R^{11}_+} J^D(\nu) = \begin{bmatrix} J^D_{\text{Comfort}}(\nu) \\ J^D_{\text{RoadHolding}}(\nu) \end{bmatrix} \tag{4.2.31}$$

where $J^D_{\text{Comfort}}(\nu)$ and $J^D_{\text{RoadHolding}}(\nu)$ are defined exactly the same as for Approach 1.

In this case, γ_k is fixed and γ_{cl}, along with ν, is a part of the decision vector for Genetic optimization (see also section 3.5.2 in Chapter 3 for the explanation of this choice of decision vector). The optimization procedure using the strong stabilization approach 2 for semi-active suspension control is defined as follows.

- **Step 0:** Choose $\gamma_k = (c_{max} - c_{min})/2$ to constrain $\|K\|_\infty \leq (c_{max} - c_{min})/2$
- **Step 1:** Initiate with random positive weighting functions $\nu = \nu^0$ and random positive real $\gamma_{ga} = \gamma^0_{ga}$.

- **Step 2:** Solve the minimization problem of γ_{cl} using the Bisection Algorithm presented in Section 4.2.4 to compute the minimal real scalar γ_{min}. Solve again the ARE (4.2.11) and the LMIs (4.2.18)-(4.2.20) with the couple (ν, γ_{cl}) where $\gamma_{cl} = \gamma_{min} + \gamma_{ga}$ to construct a stable controller $K(s)$ (4.2.17). With the obtained controller, compute the objective function $J^D(\nu, \gamma_{cl})$ defined in (4.2.31).
- **Step 3:** Calculate the fitness value and select the best ν (associated with the smallest objective function).
- **Step 4:** Apply crossover and mutation to get a new generation: $\nu = \nu^{new}$ and $\gamma_{ga} = \gamma_{ga}^{new}$.
- **Step 5:** Evaluate the new generation: If the criteria of interest (for example, reaching the limit number of generation) are not satisfied, go to Step 2 with $\nu = \nu^{new}$ and $\gamma_{ga} = \gamma_{ga}^{new}$; Else, stop and save the best individual $\nu^{opt} = \nu^{new}$ and $\gamma^{opt} = \gamma_{ga}^{new}$.

4.3 Numerical analysis and results

Some discussions on numerical analysis will be provided here following the same strategy in Chapter 3. It is important to keep in mind the following points:

- All the nonlinear simulations are performed with the nonlinear quarter car Renault Mégane Coupé (RMC) (se Fig. 4.6).
- For the time domain analysis, the road profile with banwidth limited in $[0 - 30]$ Hz as depicted in Fig. 3.16 in Chapter 3) is used.
- To compute the (nonlinear) frequency responses of nonlinear systems, we use the "Variance Gain" algorithm (see Appendix B).
- It is important to note that the controllers obtained by the proposed Approach 1 and 2 are not semi-active. As a result, in simulation, a "clipped" behavior needs to be performed on the controller output to guarantee the passivity constraint (4.2.2). The controllers obtained after the design procedures (by Approach 1 and 2) are called "**Active**" and when they are used in nonlinear simulation, they are called "**Clipped**" ones.

4.3.1 Based-Lines

To evaluate the efficiency of the proposed method, the following referenced methods are used.

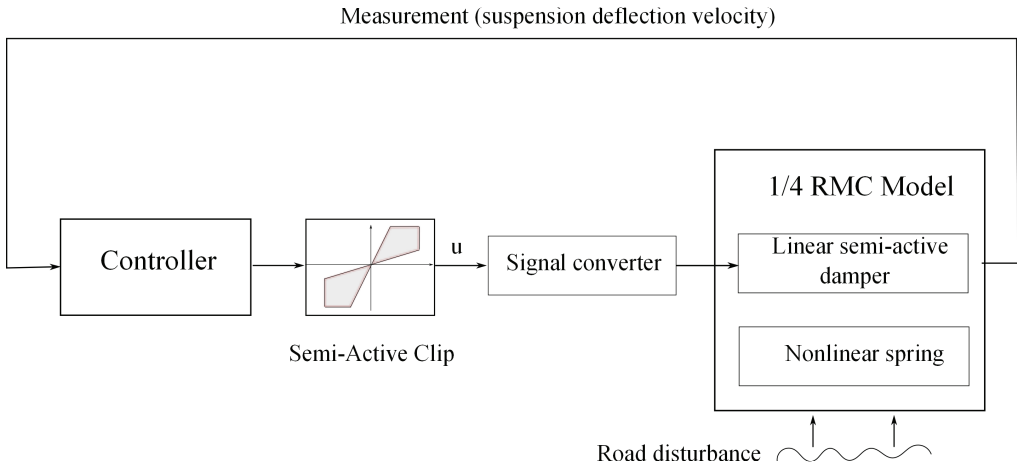

Figure 4.6: Implementation scheme.

- Soft Damper ("Soft") where $c = c_{min}$.
- Hard Damper ("Hard") where $c = c_{max}$.
- Nominal Damper ("Nominal") where $c = (c_{max} + c_{min})/2$.
- Skyhook, Groundhook and Skyhook-ADD (where the design parameter $\alpha = 2\pi 2$ rad/s) are presented in 1.3.3 in Chapter 1.

4.3.2 Preliminary design and analysis

Figure 4.7 shows the trade-off between comfort and road holding performances. In the figure, J^*_{CF} (respectively J^*_{RH}) is J_{CF} in (4.1.5) (respectively J_{RH} in 4.1.6) computed for different strategies applied for a nonlinear RMC model and then normalized by the one obtained with the Nominal Damper. The smaller these criteria are, the better the performances of the corresponding strategies are.

It is worth noting that the "Passive" curve is obtained by computing the normalized criteria J^*_{CF} and J^*_{RH} for the passive dampers with a constant damping coefficient in the range $[c_{min}, c_{max}]$ (i.e. for each value of damping coefficient in the range, we obtain one point in the "Passive" curve). Besides, the proposed methods using Approach 1 and Approach 2 are obtained under the same synthesis condition for Genetic Algorithms optimization.

From the figure, we can see that the Skyhook-ADD is the best strategy for comfort and the Groundhook is the best one for road holding. The Skyhook is known to improve very well the comfort in low frequencies and as a result is not a good one when a wide range of frequencies is considered. The proposed Approach 1 and Approach 2 seem to slightly improve the road holding and the middle trade-off (the trade-off near the middle part

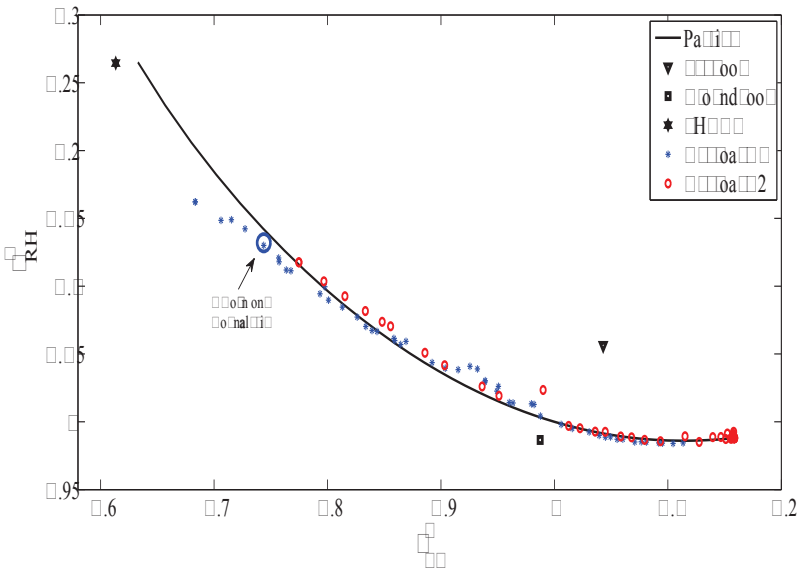

Figure 4.7: Comfort and road holding trade-off of different strategies.

of the passive curve) only. Why did the proposed methods not approach the optimal bounds of comfort and road holding? We may have the answer to the raised question by considering the following remark.

Remark 4.3.1. *"The optimal control law of a semiactive suspension with comfort objective without preview (road profile prediction) is a genuine on - off strategy"* [Savaresi, Silani & Bittanti, 2005].

The Skyhook-ADD, known to be optimal for comfort, is a good example to support the remark. In this control law, the damping coefficient switches between c_{min} and c_{max} by an external control signal. Although the remark is done only for comfort oriented controllers, it is true for road holding oriented controllers as well. The proof is not given here but the idea is to mimic the proof of the comfort oriented controller by replacing the comfort objective $\int \ddot{z}_s$ by the road holding one $\int (z_{us} - z_r)$.

How can we conclude from the remark for our case?

The remark means that, to obtain an optimal controller, the condition (4.2.2) should be replaced by

$$|u| = \frac{c_{max} - c_{min}}{2} |\dot{z}_{def}| \tag{4.3.1}$$

As a result, in the ideal case, it is necessary that the controller gain must equal to $(c_{max} - c_{min})/2$ for all frequency ranges. Let us return to the case of our proposed controllers. Because the obtained controllers by Approach 1 and Approach 2 have the same characteristics: they are stable and gain-limited by $(c_{max} - c_{min})/2$, we can choose

to consider the following one (corresponding to the encircled point in Fig. 4.7))

$$K(s) = \frac{-3858204(s+67851)(s+245.8)(s+96.54)(s+1.779)(s+0.2384)(s^2+6.338s+39.58)}{(s+67850)(s+1578)(s+499.1)(s+43.81)(s+12.47)(s+4.079)(s+1.779)(s+0.2405)} \tag{4.3.2}$$

The gain of the controller is depicted in Fig. (4.8) and the performances of the linear closed-loop system are depicted in Fig. 4.9-4.10.

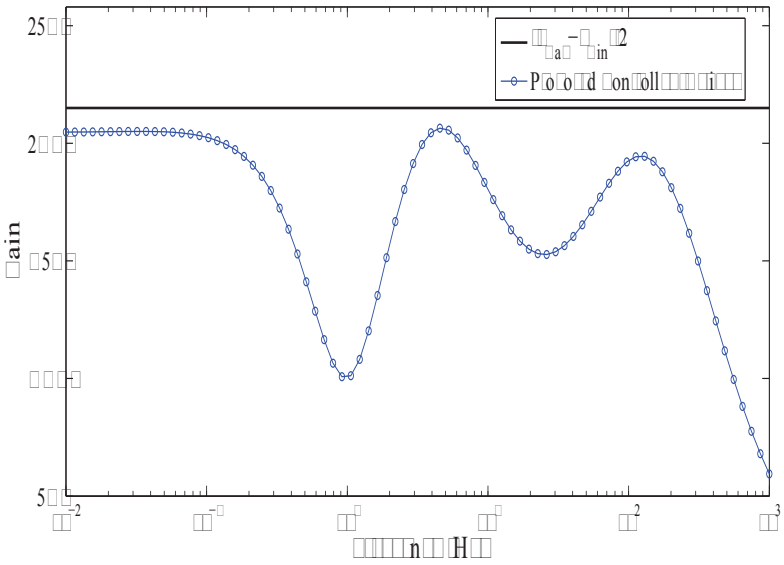

Figure 4.8: Controller gain $u/\dot{z}_{def}$.

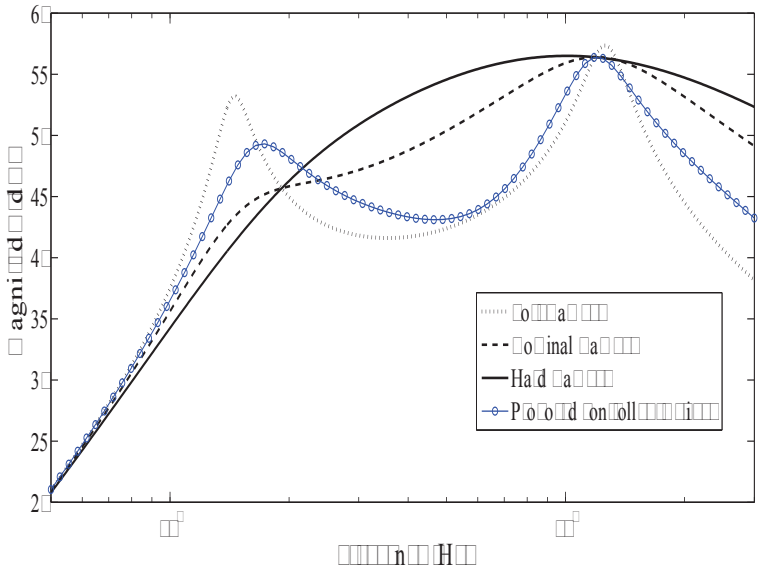

Figure 4.9: Bode diagram $\ddot{z}_s/z_r$.

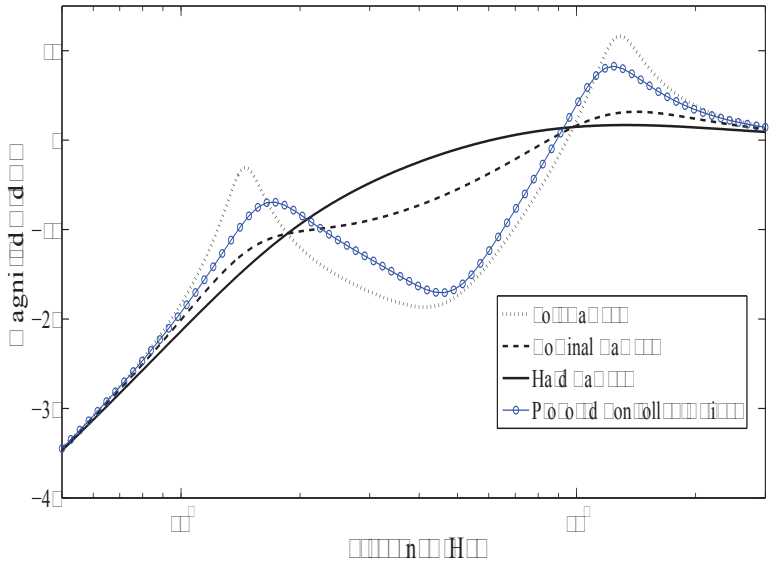

Figure 4.10: Bode diagram $(z_{us} - z_r)/z_r$.

It is worth noting that the condition $\|K\|_\infty < (c_{max} - c_{min})/2$ presented in (4.3.2) is satisfied in this case. To show that this condition is a good approximation to the passivity constraint (4.2.2), we present here the time domain result. The damper force obtained with the nonlinear closed-loop system using the clipped controller will be compared with the active controller. Figures (4.11)-(4.12) show that there are differences between the design force (given by active controller) and the real force (given by clipped force), but in fact these differences appeared during short time and are considerably large at very small damper velocities where the performances of the closed-loop system (in terms of comfort and road holding) are almost invariant w.r.t control methods.

In fact this condition (4.3.2) is very conservative because, as mentioned in (4.3.1), the necessary condition to obtain an optimal solution is that the controller gain equals $(c_{max} - c_{min})/2$ for all frequencies. This is the reason why the optimal performance was not achieved with the controller (4.3.2). A possible solution to this problem is to relax the bound on the controller gain, for example, by modifying γ (or γ_k) in Approach 1 (or in Approach 2, respectively) to

$$\gamma(\text{or } \gamma_k) = \tau \frac{c_{max} - c_{min}}{2} \quad \text{where} \quad \tau \in \mathcal{R}^+ \quad \text{and} \quad \tau > 1 \tag{4.3.3}$$

and then adding the following function in each criterion (comfort and road holding) of the objective vector (4.2.28) and (4.2.31)

$$\int_0^\infty (|K(j2\pi f)| - \frac{c_{max} - c_{min}}{2})^2 df \tag{4.3.4}$$

In the following, we present only the result obtained using Approach 1 (Approach 2

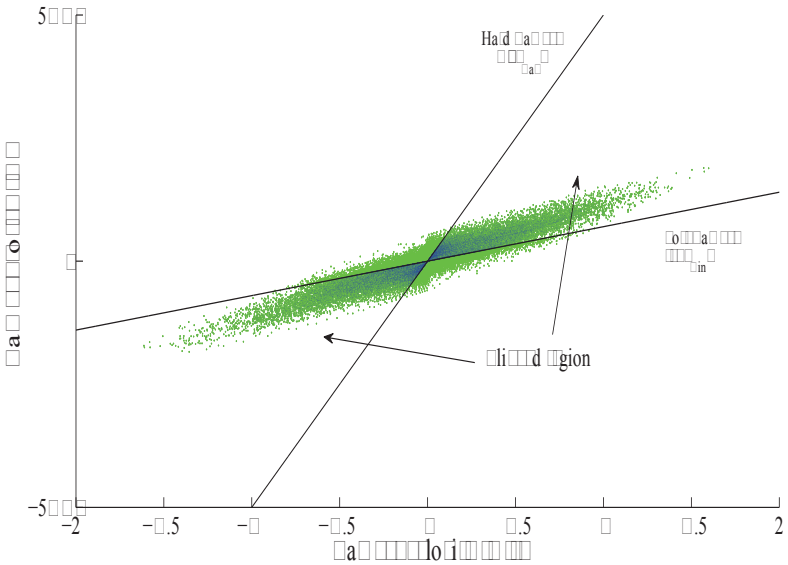

Figure 4.11: Damper Force v.s Damper Velocity. The active forces are present in all the plane while the semi-active forces are limited in the clipped region.

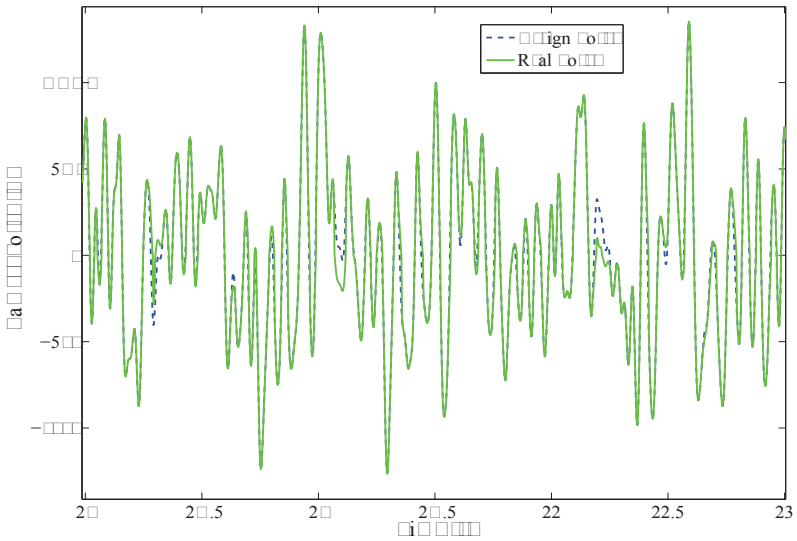

Figure 4.12: Comparison between design (with proposed controller) and real (clipped by Semi-active constraint) damper forces

seems to be less effective in both final results (as seen in Fig. 4.7) and time-consumption due to the BMI + one ARE formulation of the solution, compared with the LMI + one ARE of the Approach 1). The more complete analysis and comparison between both approaches will be an interesting future work.

As we know that the optimal method for comfort in low frequencies is using the hard damper ($c = c_{max}$) and in high frequencies is using the soft damper ($c = c_{min}$), we will use the following objective functions for the optimization procedure:

$$\min_{\{\nu\}\in R_+^{10}} J^D(\nu) = \begin{bmatrix} J^D_{\text{Comfort}}(\nu) \\ J^D_{\text{RoadHolding}}(\nu) \end{bmatrix} \tag{4.3.5}$$

where

$$J^D_{\text{Comfort}} = \alpha_1 \int_0^{1.5} (\ddot{z}_s/z_r - R_1)^2 df + \alpha_2 \int_3^{10} (\ddot{z}_s/z_r - R_2)^2 df + \alpha_3 \frac{\|K\|_\infty}{\gamma} \tag{4.3.6}$$

$$J^D_{\text{RoadHolding}} = \beta_1 \int_{10}^{20} (z_{us}/z_r - R_3)^2 df + \beta_2 \frac{\|K\|_\infty}{\gamma} \tag{4.3.7}$$

where R_1 (respectively R_2) is the frequency response $\ddot{z}_s/z_r$ of the hard damper (respectively the soft damper) and R_3 is the frequency response z_{us}/z_r of the hard damper; α_i with $i = 1:3$ and β_j with $j = 1:2$ are weighting parameters.

In the optimization procedure for Approach 1, $\gamma = 150\frac{c_{max}-c_{min}}{2}$.

Figure 4.13 presents the trade-off in performance objectives of the nonlinear closed-loop system. Compared with the results presented previously in Fig. 4.7, the new ones are much better.

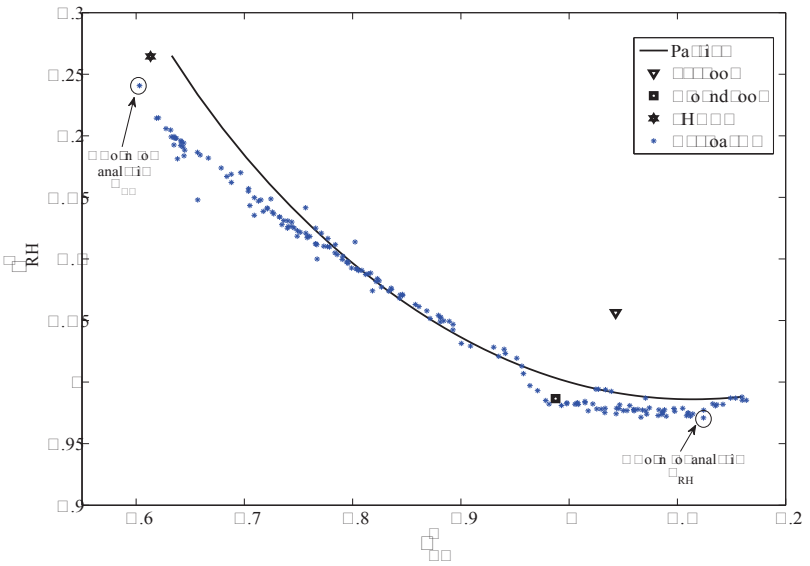

Figure 4.13: Comfort and road holding trade-off of different strategies.

In Fig. 4.13, we choose in the set of proposed controllers the two following ones: one is oriented for comfort (marked by a circle) and the other is oriented for road holding (marked by a square).

- The *"Approach 1 - Comfort oriented controller"* is denoted as K_{CF} and given as follows

$$K_{CF}(s) = \frac{-4015191.4923(s+5222)(s+821.6)(s+126.3)(s+5.406)(s+1.06)(s^2+7.565s+81.02)}{(s+3484)(s+5222.1)(s+414.1)(s+118.7)(s+1.06)(s+0.09755)(s^2+10.11s+41.39)} \tag{4.3.8}$$

- The *"Approach 1 - Road holding oriented controller"* is denoted as K_{RH} and given as follows

$$K_{RH}(s) = \frac{257399.483(s+5805)(s+22.28)(s+5.982)(s+1.375)(s+0.09611)(s^2+54.73s+4426)}{(s+6456)(s+141.8)(s+1.375)(s+0.0961)(s^2+9.045s+74.52)(s^2+52.59s+6026)} \tag{4.3.9}$$

Notice also that the two controllers are stable.

4.3.3 Frequency domain analysis

Linear design analysis
The *"Approach 1 - Comfort oriented controller"*
Figure 4.14 shows that the gain of $K_{CF}(s)$ is almost equal to $(c_{max} - c_{min})/2$ in the range $[1-30]$ Hz. The gain is very high in low frequencies for which we can predict a loss of performance in the same frequencies. Figures 4.15-4.16 depict the frequency responses of the linear closed-loop systems (Bode diagrams). It can be seen that $K_{CF}(s)$ improves considerably the passenger comfort while the road holding capacity is not preserved.

The *"Approach 1 - Road holding oriented controller"*
For this controller, although the H_∞-norm of the controller is not high, its gain is not close to $(c_{max} - c_{min})/2$ either. We cannot expect an optimal performance from this controller. However as shown in the later analysis, it is a good controller for road holding (see also Fig. 4.18-4.19).

Nonlinear design analysis The nonlinear frequency responses (Pseudo-Bode) using "Variance Gain" Algorithm (see Appendix B) are obtained on a nonlinear RMC model with the above K_{CF} and K_{RH} clipped controllers and other strategies (passive, Skyhook, Groundhook, Skyhook-ADD).

In Fig. 4.20, the comfort oriented controller K_{CF} offers a very good result and is comparable with the Skyhook-ADD (optimal for comfort). There is a small loss of performance in $[1-2]$ Hz which was predicted because of the large gain of K_{CF} in low frequencies.

In Fig. 4.21, the road holding oriented controller K_{RH} improves considerably the road holding around $[10-20]$ Hz. This controller is comparable with the Groundhook in terms of road holding improvement.

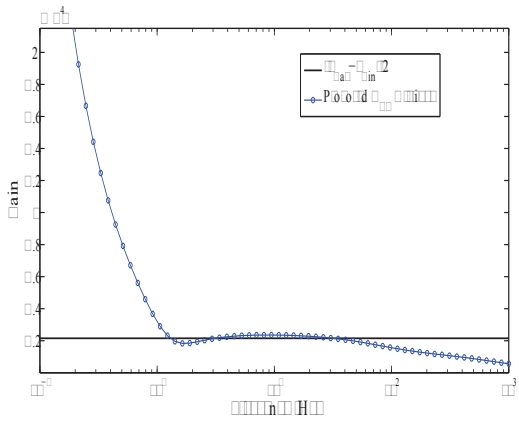

Figure 4.14: Bode diagram: controller gain $u/\dot{z}_{def}$ (Comfort controller K_{CF}).

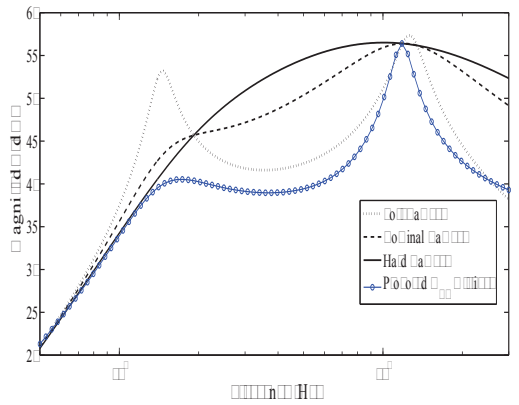

Figure 4.15: Bode diagram: vehicle body acceleration $\ddot{z}_s/z_r$ (Comfort controller K_{CF}).

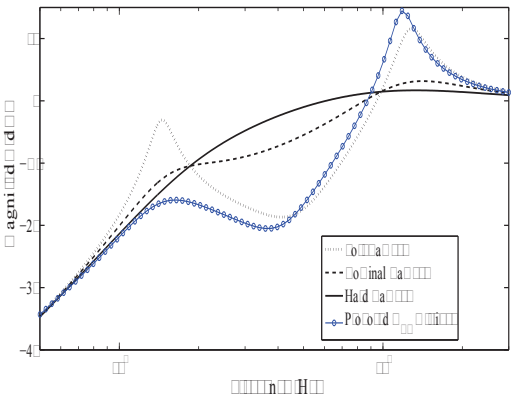

Figure 4.16: Bode diagram: dynamic tire deflection $(z_{us} - z_r)/z_r$ (Comfort controller K_{CF}).

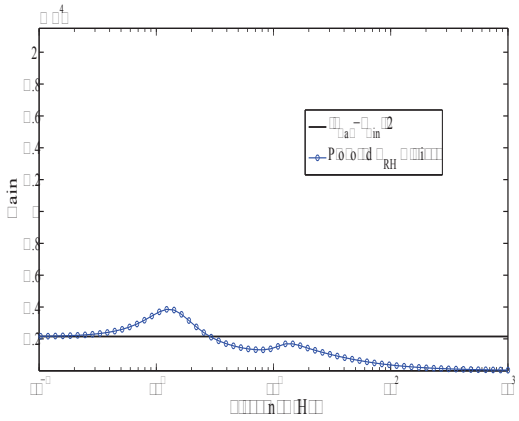

Figure 4.17: Bode diagram: Controller gain $u/\dot{z}_{def}$ (Road Holding Controller K_{RH}).

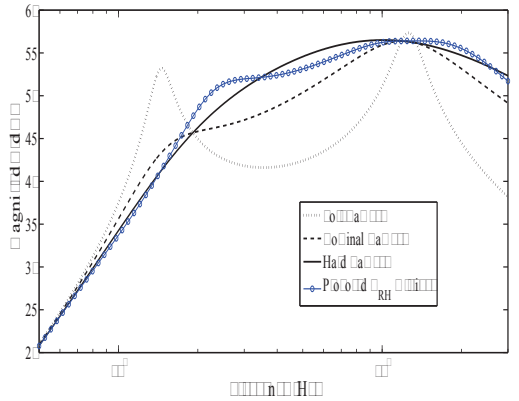

Figure 4.18: Bode diagram: vehicle body acceleration $\ddot{z}_s/z_r$ (Road Holding Controller K_{RH}).

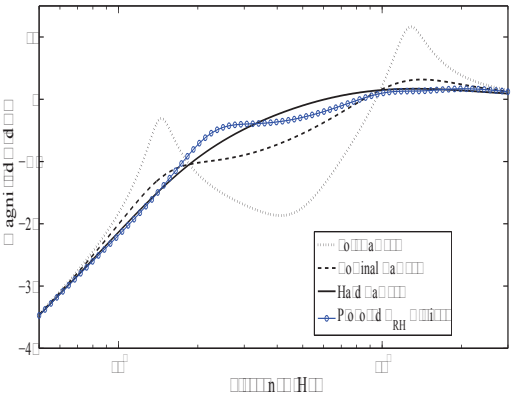

Figure 4.19: Bode diagram: dynamic tire deflection $(z_{us} - z_r)/z_r$ (Road Holding Controller K_{RH}).

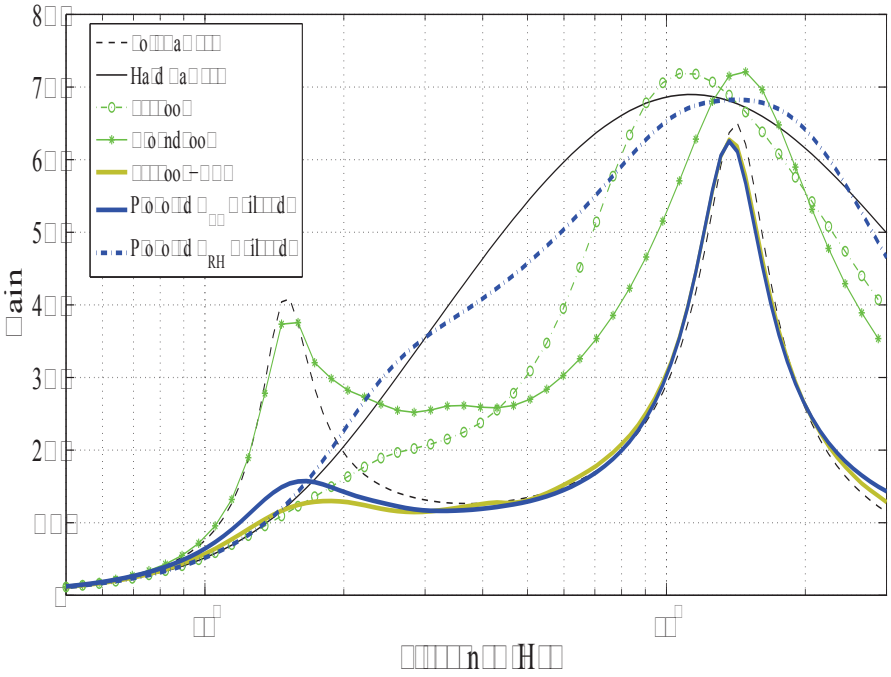

Figure 4.20: Nonlinear frequency responses $\ddot{z}_s/z_r$ (nonlinear simulation).

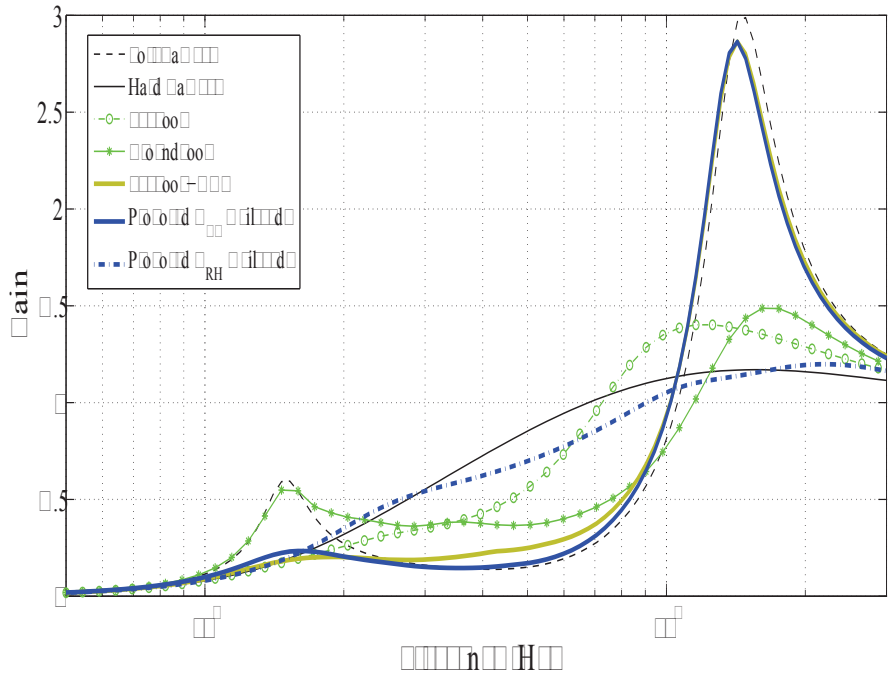

Figure 4.21: Nonlinear frequency responses $z_{us} - z_r/z_r$ (nonlinear simulation).

4.3.4 Time domain analysis

For the time domain analysis, we use the same random road profile as that presented in Fig. 3.16 in Chapter 3. The road profile is represented by an integrated white noise, band-limited within the frequency range [0-30] Hz.

The spectrum of the vehicle acceleration and the dynamic tire deflection are depicted in Fig. 4.23-4.24. The results are coherent with the frequency analysis. The Skyhook-ADD and the "Approach 1 - Comfort" are the best for comfort. The Groundhook and "Approach 1 - Road Holding" are the most suitable for road holding.

Furthermore, as in Chapter 3, the comfort in time domain can be evaluated, using the following criterion

$$RMS_{\text{Comfort}} = \sqrt{\frac{\int_0^T \ddot{\bar{z}}_s^2(t)dt}{T}}$$

where $\ddot{\bar{z}}_s(t)$ is the filtered vehicle body acceleration (by the approximated ISO 2631 filter (1.2.9)) $[m/s^2]$ and $T = 50$ is the simulation time $[s]$. In Fig. 4.22, the RMS_{Comfort} values of different strategies, normalized by that value for the nominal damper, are depicted. The "Approach 1 - Comfort" is slightly better than the Extended Mixed SH-ADD for the considered road profile.

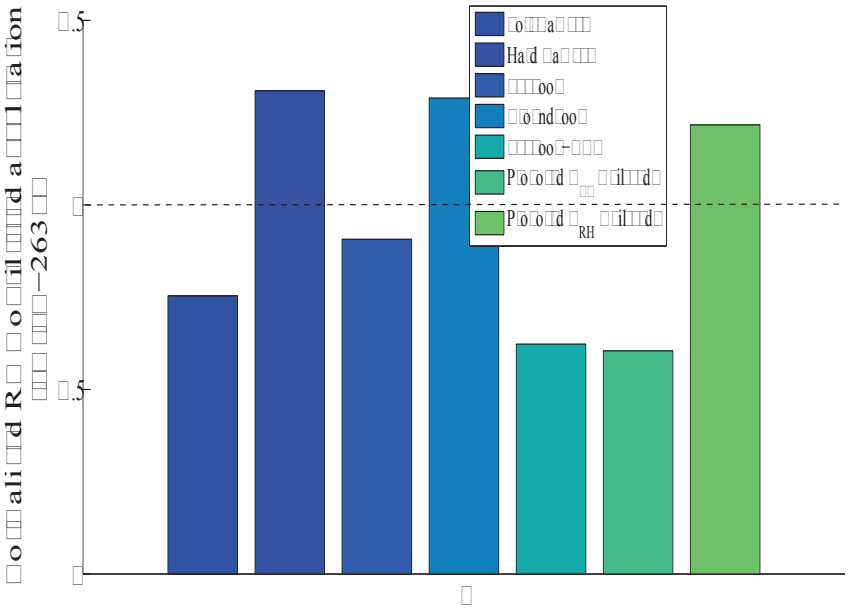

Figure 4.22: Normalized RMS value of filtered $\ddot{z}_s$ (by ISO-2631).

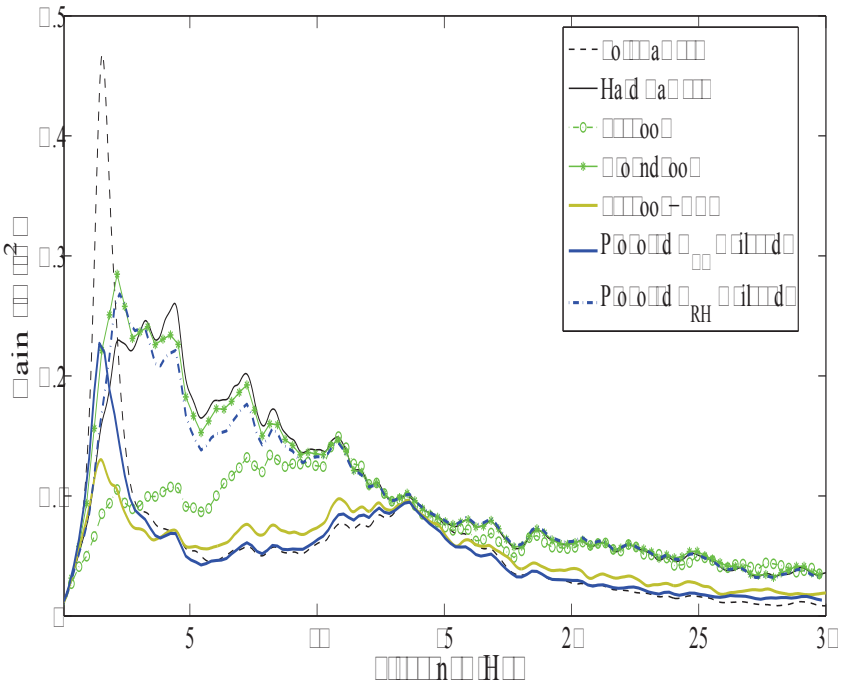

Figure 4.23: Spectrum of $\ddot{z}_s$ (nonlinear simulation).

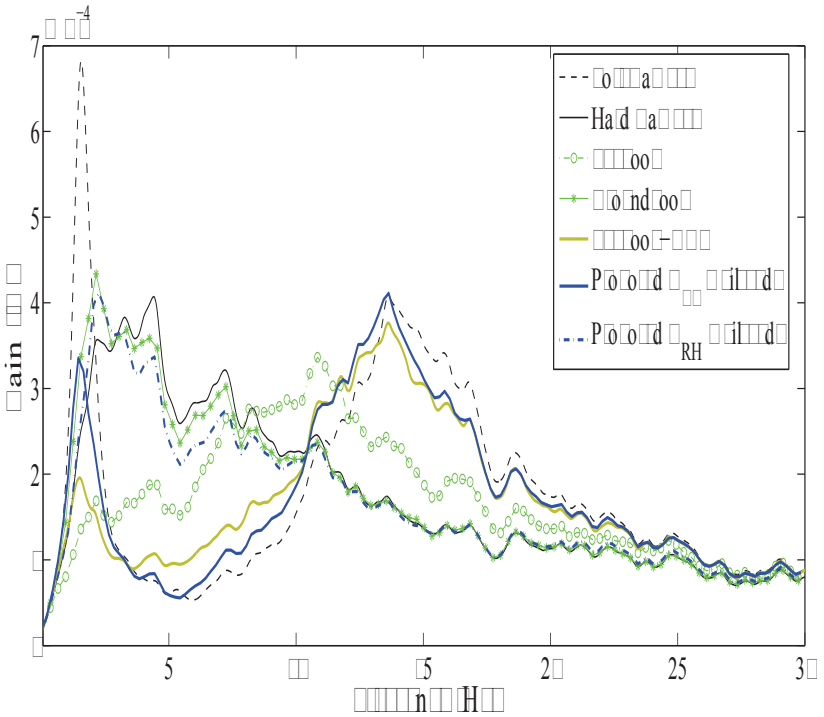

Figure 4.24: Spectrum of $z_{us} - z_r$ (nonlinear simulation).

In the following, we comment a little further on the behavior of the controlled suspension systems with comfort and road holding controllers. As seen in Fig. 4.25, the Skyhook-ADD and the "Approach 1 - Comfort" K_{CF} controller have similar behaviors, the total damper forces are distributed more in the lower bound (c_{min}) in high velocities (or high frequencies) to improve comfort. In the contrary, for the Groundhook and "Approach 1 - Road Holding" K_{RH}, these forces lie mostly in the upper bound (c_{max}) in high frequencies to enhance road holding.

Another remark concerning the controller gain based on the results presented in Fig. 4.11 and 4.25. Among the three corresponding controllers, the "Approach 1 - Comfort" K_{CF} resulted in a large difference between design forces (all forces, in blue and green) and real force (clipped one, in blue), while controller (4.3.2) resulted in a smallest difference. This can be explained, when looking at the gain of these controllers in Fig. 4.8, 4.14 and 4.17. We can conclude from the remark that the higher the gain of the controller is, the more the passivity constraint is violated.

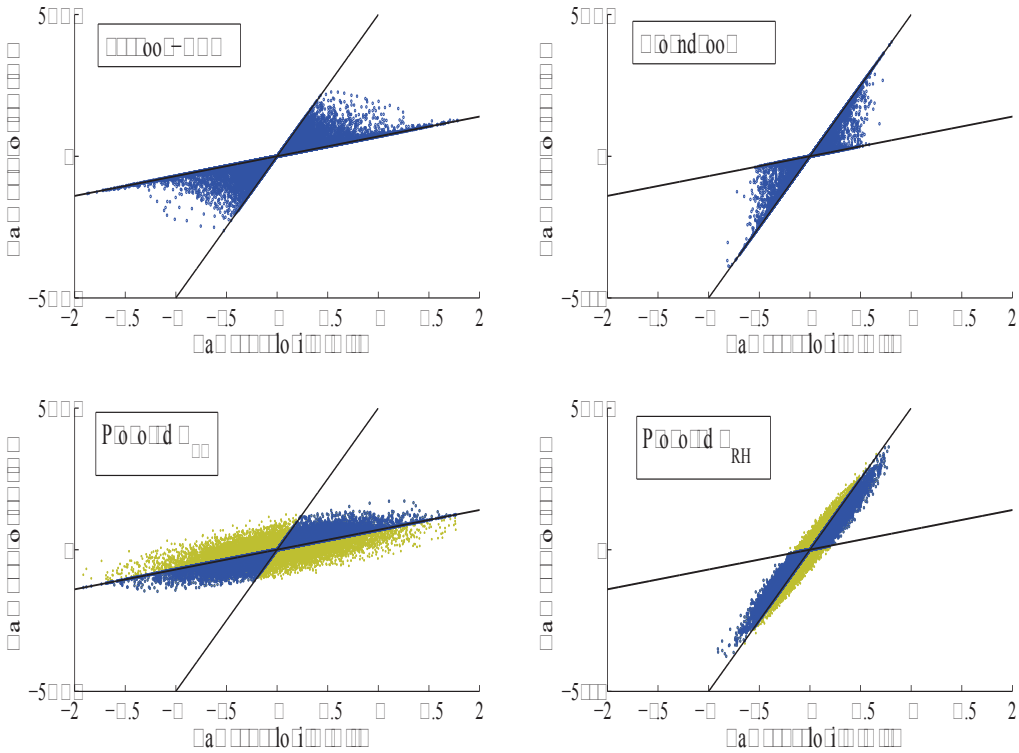

Figure 4.25: Comparison of the Force-Velocity characteristics.

4.3.5 Robustness evaluation

As in Chapter 3, we will evaluate the robustness of the proposed controllers by the two following tests.

- Overcharged working condition: We consider a constant (time-invariant) uncertainty in sprung mass, $\Delta_m = 0.75m_s$ (i.e the sprung mass changes 75 % w.r.t the design value).

  As seen in Fig. 4.26-4.27, the effectiveness of the proposed controllers is still preserved. However, compared to the road holding controller K_{RH}, the comfort oriented one K_{CF} seems to have a better improvement (in terms of relative comparison with other strategies). Precisely, the nonlinear frequency response of closed-loop system using K_{RH} is very close to those of the Hard Damper and the Groundhook controller. The improvement of the K_{CF} over the Skyhook-ADD in this case is even better than in the nominal case ($\Delta_m = 0$) (see also Fig. 4.30). The reason can be given as follows.

  With a fixed spring k_s, the change in sprung mass will change the sprung mass natural frequency $\sqrt{m_s/k_s}$ (around $[1.5 - 2.5]$ Hz for performance (race) cars and $[1 - 1.5]$ Hz for other cars) at which there is usually a peak in the sprung mass acceleration. In our case, there is an increase in the sprung mass, the natural frequency decreases. As seen in Fig. 4.20, the comfort oriented controller K_{CF} is better than Skyhook-ADD in high frequencies but worse in low frequencies, the decrease of the natural frequency will also decrease the contribution of responses in low frequencies in the total performance (here the RMS value). As a result, in this case (increase of 75 % in sprung mass), the comfort oriented controller K_{CF} improves the RMS value of sprung mass acceleration better than the Skyhook-ADD (see also Fig. 4.30).

- Load transfer: We consider a time-varying uncertainty $\Delta_m(t)$. we take for example $\Delta(t)$ varying from -25% to $+25\%$ of the sprung mass (see Fig. 3.23 in Chapter 3).

  As seen in Fig. 4.28-4.29, the performances of the proposed controllers (i.e. the comfort improvement offered by K_{CF} and the road holding improvement offered by K_{RH}) are quite robust w.r.t load transfer.

In terms of comfort analysis, when looking at the Fig. 4.30, the two comfort oriented controllers K_{CF} and the Skyhook-ADD seem to be more sensible to load transfer than other strategies (degradation of 8.2 % and -9.4 % w.r.t the nominal design condition ($\Delta_m = 0$)). However, these two controllers are always the best ones for comfort (for all working conditions).

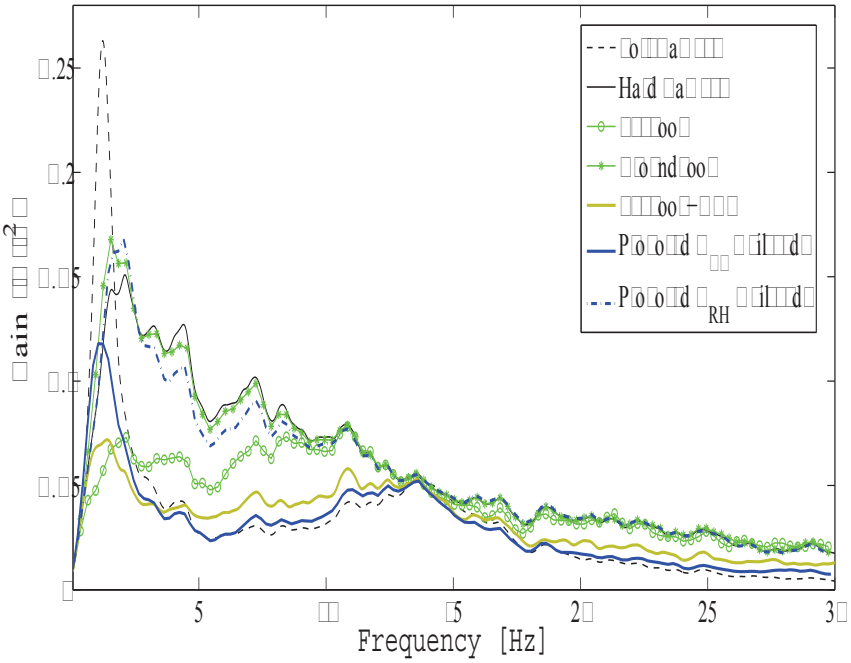

Figure 4.26: Spectrum of $\ddot{z}_s$ (test with an increase of 75% in sprung mass).

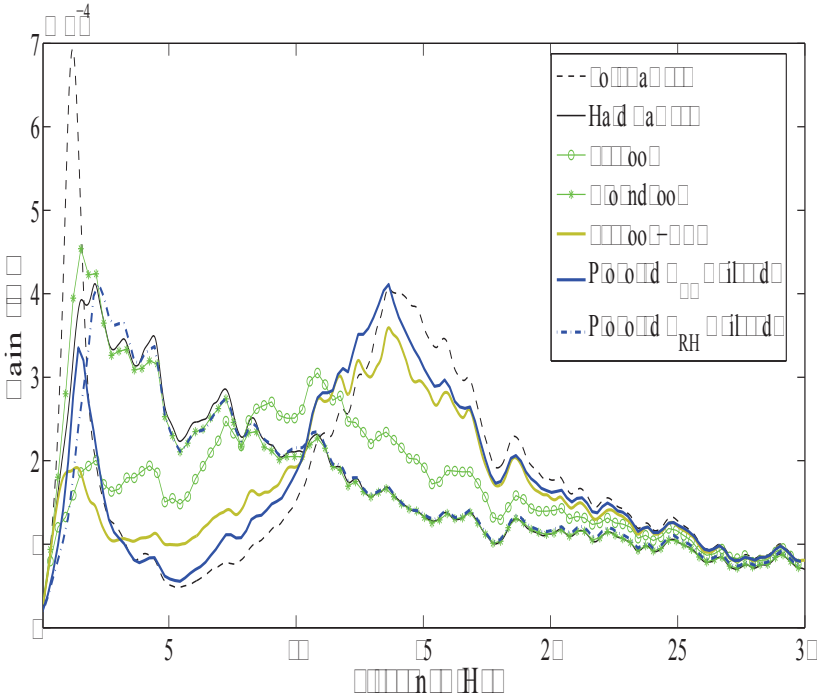

Figure 4.27: Spectrum of $z_{us} - z_r$ (test with an increase of 75% in sprung mass).

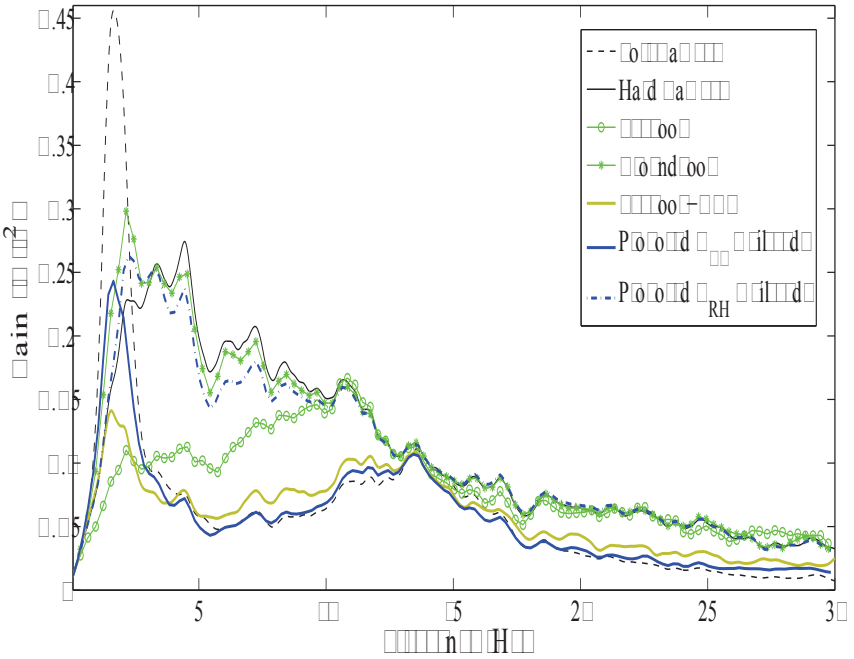

Figure 4.28: Spectrum of $\ddot{z}_s$ (test with a load transfer condition).

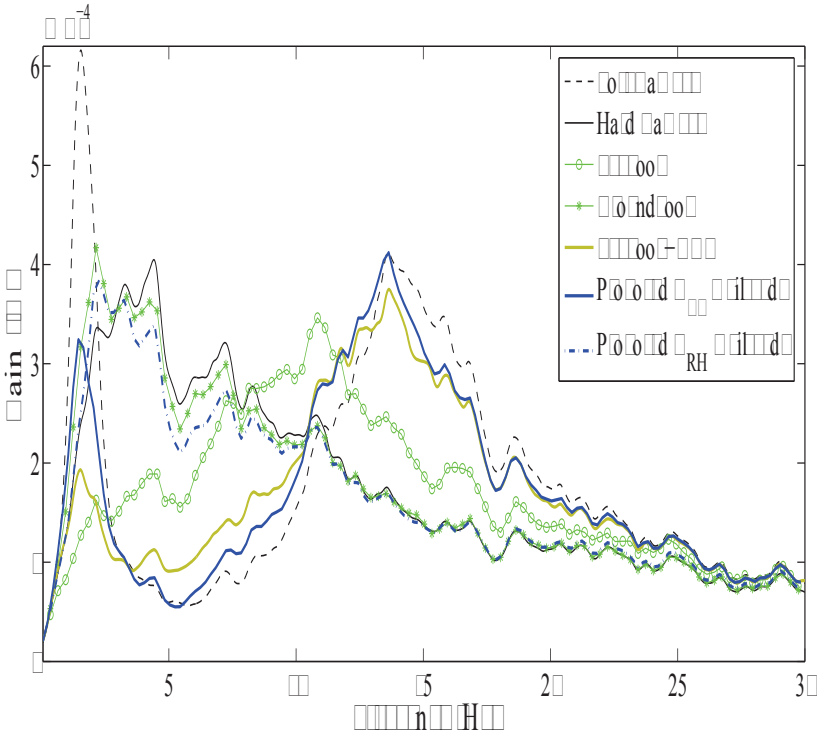

Figure 4.29: Spectrum of $z_{us} - z_r$ (test with a load transfer condition).

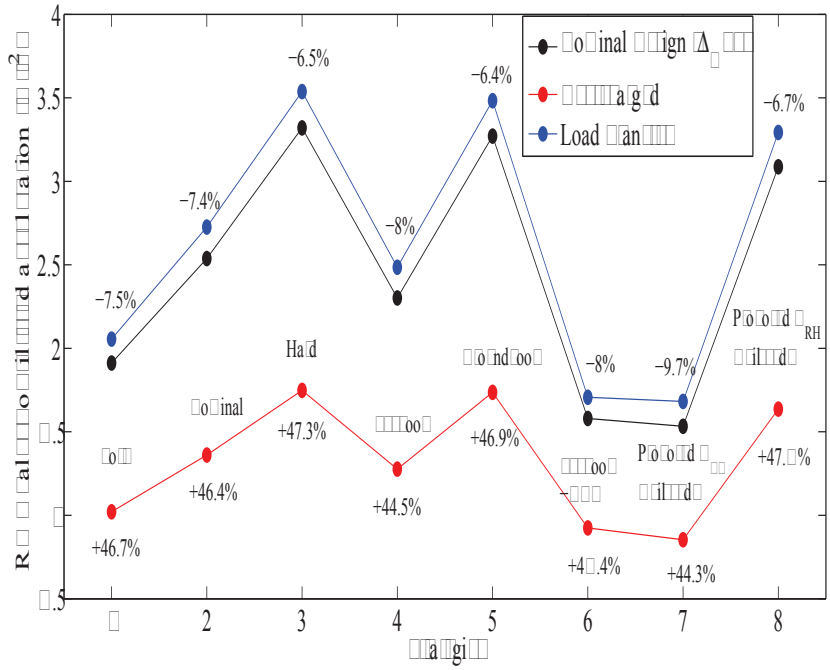

Figure 4.30: Absolute RMS value of filtered $\ddot{z}_s$ in different working conditions.

4.4 Conclusions

In conclusion, let us recall the interesting question raised in the optimal control of semi-active suspensions: *"Is the clipped-optimal still optimal?"*.

Concerning the question, it has been proved in many approaches that using clipped active controller for semi-active suspensions resulted in the loss of the closed-loop performance and, even worse, of the stability (see [Sammier et al., 2003], [Giorgetti et al., 2006], [Canale et al., 2006]). The idea for the investigation of the strong stabilization approach in this chapter is based on the particular properties of semi-active suspension: the open-loop is stable and the optimal solution (for comfort and road holding oriented objectives) can be achieved with a switching law. Precisely, because the designed controller is stable, the stability of the closed-loop semi-active suspension system is always stable under the clipped behaviors. Moreover, if the designed controller is optimal and its gain is small enough, the loss of performance (compared with optimal solution for semi-active suspensions) may be reduced.

The results, both in frequency and time domains have shown that the clipped optimal stable small-gained controllers can be a very promising solution to the above question: The obtained comfort and road holding oriented controllers can be comparable to the optimal comfort and the road holding controller Skyhook-ADD and Groundhook, respectively. Moreover, these controllers are very robust in terms of stability and performance.

Certainly, a more complete analysis (both in theoretical and practical aspects) needs to be performed to prove completely the effectiveness of the proposed method.

In the next chapter, we will present the application of the proposed approach to improve comfort and suspension deflection of a driver's seat.

Chapter 5

Comfort and suspension deflection improvement

It is quite obvious, while the comfort/handling trade-off has been studied in many approaches during the past decades, that the suspension travel issue has not been always considered. Hitting the structural limits when road disturbance is particularly tough, degrades dramatically the passenger comfort (the so-called end-stop effect) and decreases the lifetime of vehicle components.

In this chapter, the trade-off between passenger comfort and suspension deflection is investigated. The results presented in this chapter were obtained during my 6 month stay in Dipartimento di Elettronica ed Informazione, Politecnico di Milano with Sergio Savaresi, Cristiano Spelta and Diego Delvecchio.

The first result was presented in the CDC-2010 paper (see Appendix C). In this paper, a hybrid method based on switching ADD (Acceleration Driven Damper) and LPV control (see Chapter 3) was developed for a nonlinear quarter vehicle model equipped with nonlinear MR dampers to improve both comfort and suspension deflection.

In this chapter, we present another result recently obtained for Dual Stage Suspension systems (representing driver's seats on heavy vehicles) using linear hydraulic dampers. The control objective is also to improve the driver comfort while taking into account the suspension deflection (since the system represents a driver sear, road holding is no longer considered) To achieve this, we make use of the strong stabilization approach for semi-active suspension control proposed in Chapter 4.

5.1 Problem introduction

5.1.1 Dual-Stage Suspension System (DSS) and Equivalent One-Stage Suspension (OSS) System

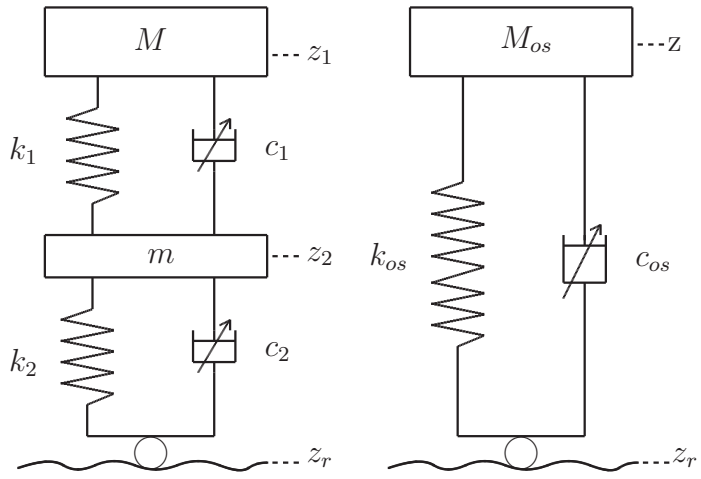

Figure 5.1: DSS model and equivalent OSS model

The left hand-side of Fig. 5.1 represents the Dual-Stage Suspension DSS model. In this model, M is the seat mass connected with the vehicle chassis by two spring-damper subsystems (k_1, c_1) and (k_2, c_2); m represents the mass of the link between these two suspension subsystems ($m \ll M$). As seen in the figure, z_1 (respectively z_2) is the vertical displacement around the equilibrium point of M (respectively m) and z_r is the variation of the vehicle chassis. It is worth noticing that the two dampers are semi-active ones where:

$$c_1 \in [c_{1min}, c_{1max}] \tag{5.1.1}$$

$$c_2 \in [c_{2min}, c_{2max}] \tag{5.1.2}$$

Let us denote $\Delta_{1,2}$ the strokes of these two dampers. When the suspension deflections exceed these values, the End-stop phenomenon occurs (see in the next section 5.1.3) leading to the deterioration of the passenger comfort.

By applying the second law of Newton, the dynamical equations of the DSS model are given by

$$\begin{aligned} M\ddot{z}_1 &= -k_1(z_1 - z_2) - c_1(\dot{z}_1 - \dot{z}_2) \\ m\ddot{z}_2 &= k_1(z_1 - z_2) + c_1(\dot{z}_1 - \dot{z}_2) - k_2(z_2 - z_r) - c_2(\dot{z}_2 - \dot{z}_r) \end{aligned} \tag{5.1.3}$$

It can be seen in the literature that almost all suspension control methods are designed for single spring-damper systems. In this study, we will find such a system model (see the right model in Fig. 5.1) which has similar dynamics to that of the DSS one. The model is called *equivalent OSS* system. The equivalent OSS system controlled by conventional strategies (like Skyhook, Skyhook-ADD...) can be used as references to evaluate the efficiency of the proposed method presented in Section 5.2.

In the OSS model, M_{os} is the sprung mass and connected to the vehicle chassis by a spring with stiffness k_{os} and a semi-active damper with damping coefficient c_{os} where

$$c_{os} \in [c_{os_{min}}, c_{os_{max}}] \tag{5.1.4}$$

Let us denote also z the vertical displacement around the equilibrium point of M_{os} and Δ_{os} the stroke of the OSS model.

The dynamical equation of the One-Stage Suspension (OSS) model is given by

$$M_{os}\ddot{z} = -k_{os}(z - z_r) - c_{os}(\dot{z} - \dot{z}_r) \tag{5.1.5}$$

5.1.2 Parameters identification for OSS model

It is worth noting that the OSS sprung mass is equal to the DSS seat mass and the OSS spring is the series of the two springs of the DSS model (so that the static behavior of both models are the same), i.e.

$$M_{os} = M \tag{5.1.6}$$

$$k_{os} = \frac{k_1 k_2}{k_1 + k_2} \tag{5.1.7}$$

The bounds on the damping coefficient of the OSS model $c_{os_{min}}$ and $c_{os_{max}}$ are identified by matching the frequency responses (of the accelerations and suspension deflections) in extreme modes (lowest and highest damping rates) with those of the DSS model.

$$\frac{\ddot{z}_1}{z_r} \approx \frac{\ddot{z}}{z_r} \tag{5.1.8}$$

$$\frac{z_1 - z_r}{z_r} \approx \frac{z - z_r}{z_r} \tag{5.1.9}$$

Here in this chapter, we make use of Genetic Algorithms for the identification. The frequency responses of the extreme modes (i.e. $c_1 = c_{1min}, c_2 = c_{2min}$ (lowest damping rate) and $c_1 = c_{1max}, c_2 = c_{2max}$ (highest damping rate) for DSS model; and $c_{os} = c_{os_{min}}$,

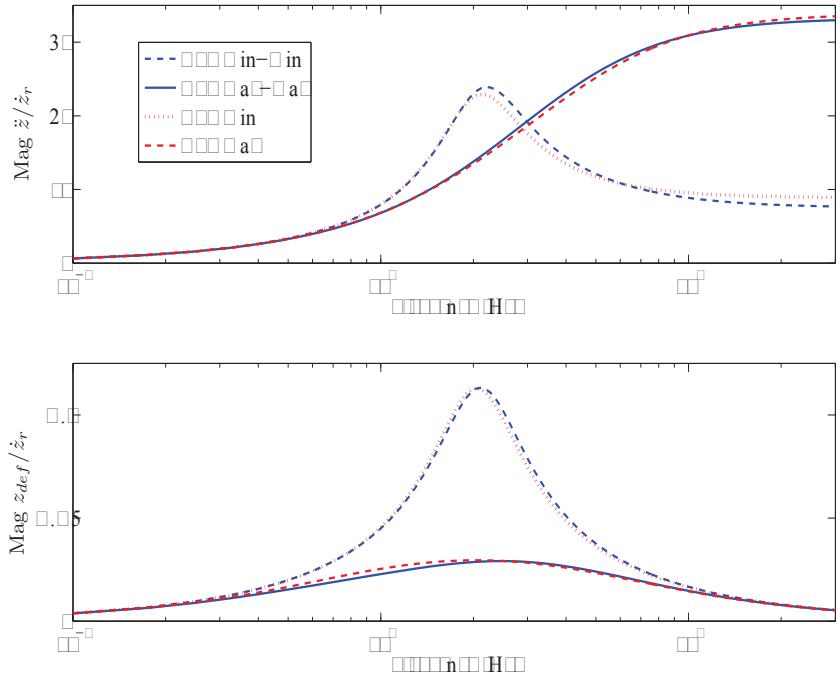

Figure 5.2: Frequency responses of DSS (in blue) and equivalent OSS (in red).

$c_{os} = c_{os_{max}}$ for OSS model) are depicted in Fig. 5.2. It can be seen that these two models are (almost) equivalent in terms of sprung mass acceleration and total suspension deflection performances (in extreme cases).

Moreover, to guarantee a fair comparison, we suppose that both systems have the same total strokes:

$$\Delta_1 + \Delta_2 = \Delta_{os} \tag{5.1.10}$$

Finally, the parameters of these two models are given as in Tab. 5.1. With the model parameters, we depict all the frequency responses obtained by varying the damping coefficients of the dampers in their ranges (for both DSS and OSS systems) in Fig. 5.3. As seen in this figure, the equivalent passive OSS system can achieve almost the same performance as the passive DSS system, except for a small different in the sprung mass acceleration response; however this difference is not important because it does not contain the lower bound of the DSS system (the best achievable performance).

With the comparison performed in Fig. 5.2 and Fig. 5.3, we may conclude that the two considered linear models are "equivalent".

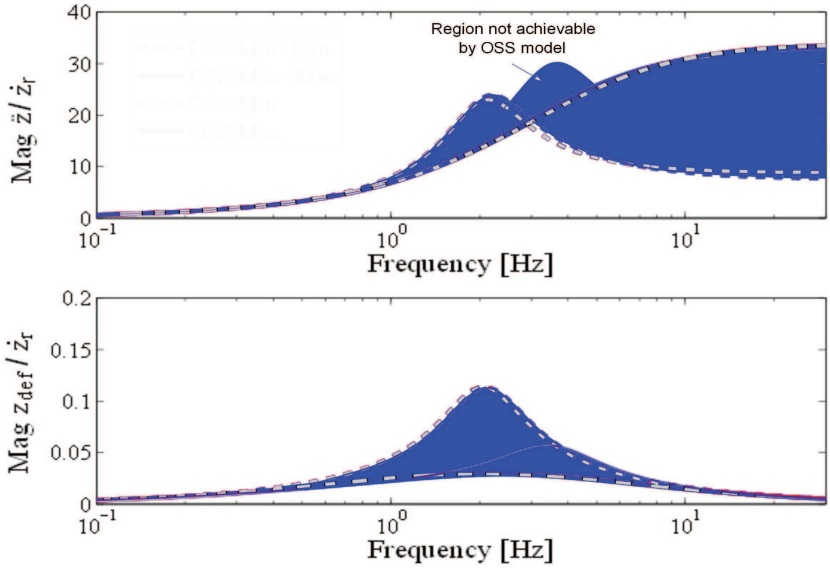

Figure 5.3: All frequency responses of DSS system for all $c_1 \in [c_{1min}, c_{1max}]$, $c_2 \in [c_{2min}, c_{2max}]$ (in blue region) and all frequency responses of equivalent OSS system for all $c_{os} \in [c_{os_{min}}, c_{os_{max}}]$(region limited by two dash lines).

DSS Model	Value	OSS Model	Value	Unit
M	60	M_{os}	60	$[kg]$
m	0.5			$[kg]$
k_1	37670	k_{os}	9959	$[N/m]$
k_2	13538			$[N/m]$
$k_{endstop}$	750000	$k_{endstop}$	750000	$[N/m]$
c_1	$\{900, 4000\}$	c_{os}	$\{527, 2033\}$	$[Ns/m]$
c_2	$\{900, 4000\}$			$[Ns/m]$
Δ_1	0.02	Δ_{os}	0.04	$[m]$
Δ_2	0.02	–	–	$[m]$

Table 5.1: Model Parameters.

5.1.3 The End-stop Phenomenon

The End-stop effect happens when the piston hits the rubber bushings because of the tough road disturbance. This effect generates a shock that makes passengers feel uncomfortable. In this chapter, the end-stop effect is simply modeled as follows:

$$F_{spring} = \begin{cases} k_s z_{def} & \text{if} \quad |z_{def}| < \Delta \\ k_{es} z_{def} & \text{if} \quad |z_{def}| \geq \Delta \end{cases} \tag{5.1.11}$$

where Δ is the suspension stroke and $k_{es} \gg k_s$ (typically represents the stiffness of rubber bushings).

An illustration of the end-stop effect is shown in Fig. 5.4. It is obvious that hitting the structural limits deteriorates dramatically the car body acceleration (i.e the passenger comfort).

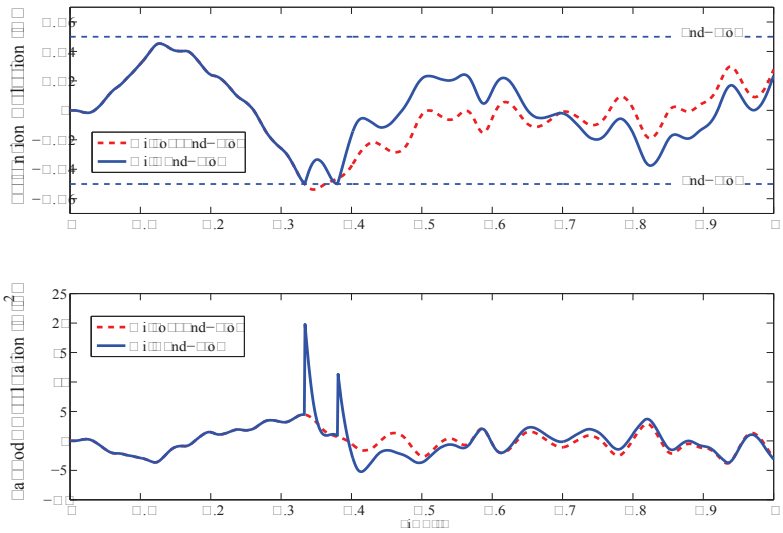

Figure 5.4: Time history of the suspension deflection (top) and the body acceleration (bottom), with and without the end-stops.

The End-stop model is taken into account during simulation to evaluate the efficiency of different strategies.

5.1.4 Problem definition

The aim is to design a controller for the DSS system that handles the trade-off between the comfort (represented by the seat acceleration) and the suspension deflections.

As mentioned previously, in this chapter, the equivalent OSS system controlled by the Skyhook-ADD will be used as a references to evaluate the efficiency of the proposed method for DSS systems.

5.2 Controller design for DSS system

In this chapter, we will apply the strong stabilization Approach 1 (presented in Chapter 4) for the DSS control. Let us begin the controller synthesis with a state-space representation of the DSS system.

5.2.1 State-space representation

From equation (5.1.3), the control system for DSS model can be described as follows

$$\begin{cases} M\ddot{z}_1 = -k_1(z_1 - z_2) - c_{10}(\dot{z}_1 - \dot{z}_2) - u_1 \\ m\ddot{z}_2 = k_1(z_1 - z_2) + c_{10}(\dot{z}_1 - \dot{z}_2) + u_1 \\ \qquad -k_2(z_2 - z_r) - c_{20}(\dot{z}_2 - \dot{z}_r) - u_2 \end{cases} \tag{5.2.1}$$

where $c_{10} = (c_{1min} + c_{1max})/2$, $c_{20} = (c_{2min} + c_{2max})/2$, u_1 and u_2 are control inputs.

From (5.2.1), a state-space representation for DSS model (5.1.3) is obtained

$$\begin{cases} \dot{x}_s = A_s x_s + B_{sw} w + B_{su} u \\ y = C_s x_s \end{cases} \tag{5.2.2}$$

where $x_s = \begin{bmatrix} z_1 - z_2 \\ \dot{z}_1 \\ z_2 - z_r \\ \dot{z}_2 \end{bmatrix}$, $\mathrm{A}_s = \begin{bmatrix} 0 & 1 & 0 & -1 \\ \frac{-k_1}{M} & \frac{-c_{10}}{M} & 0 & \frac{c_{10}}{M} \\ 0 & 0 & 0 & 1 \\ \frac{k_1}{m} & \frac{c_{10}}{m} & \frac{-k_2}{m} & \frac{-c_{10}-c_{20}}{m} \end{bmatrix}$,

$B_{sw} = \begin{bmatrix} 0 \\ 0 \\ -1 \\ \frac{c_{20}}{m} \end{bmatrix}$, $B_{su} = \begin{bmatrix} 0 & 0 \\ \frac{-1}{M} & 0 \\ 0 & 0 \\ \frac{1}{m} & \frac{-1}{m} \end{bmatrix}$, $u = \begin{bmatrix} u_1 \\ u_2 \end{bmatrix}$, $w = \dot{z}_r$

C_s (or the measurement output y) will be defined and discussed later in section 5.4.

5.2.2 Controller optimization

The control block diagram for DSS systems is presented in Fig. 5.5. With the defined control problem (see 5.1.4), the controlled outputs will be the seat acceleration $\ddot{z}_1$ and the suspension deflections of two dampers z_{def_1} and z_{def_2}.

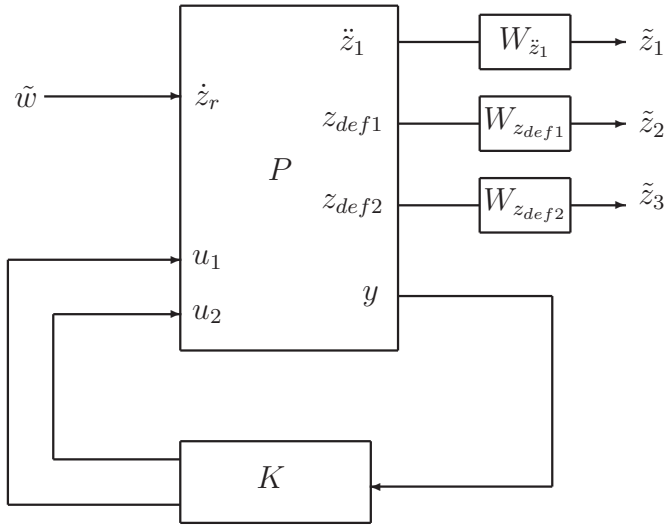

Figure 5.5: Control block diagram for DSS systems

The weighting functions for the synthesis are 2^{nd} order transfer functions:

$$W_{\ddot{z}_s} = k_{\ddot{z}_s} \frac{s^2 + 2\xi_{11}\Omega_{11}s + {\Omega_{11}}^2}{s^2 + 2\xi_{12}\Omega_{12}s + {\Omega_{12}}^2} \tag{5.2.3}$$

$$W_{z_{def1}} = k_{z_{def1}} \frac{s^2 + 2\xi_{21}\Omega_{21}s + {\Omega_{21}}^2}{s^2 + 2\xi_{22}\Omega_{22}s + {\Omega_{22}}^2} \tag{5.2.4}$$

$$W_{z_{def1}} = k_{z_{def2}} \frac{s^2 + 2\xi_{31}\Omega_{31}s + {\Omega_{31}}^2}{s^2 + 2\xi_{22}\Omega_{32}s + {\Omega_{32}}^2} \tag{5.2.5}$$

The optimization procedure is similar to the one using the *Strong Stabilization Approach 1* presented in 4.2.5 in Chapter 4. The objective function is the following:

$$\min_{\{\nu,\gamma_{cl}\}\in\mathbb{R}_+^{10}} J^D(\nu) = \begin{bmatrix} J^D_{\text{Comfort}}(\nu) \\ J^D_{\text{Stroke}}(\nu) \end{bmatrix} \tag{5.2.6}$$

where

$$J^D_{\text{Comfort}} = \alpha_1 \int_0^2 (\ddot{z}_1/\dot{z}_r - R_1)^2 df + \alpha_2 \int_{3.5}^{20} (\ddot{z}_1/\dot{z}_r - R_2)^2 df + \alpha_3 \frac{\|K\|_\infty}{\gamma_k} \tag{5.2.7}$$

$$J^D_{\text{Stroke}} = \alpha_4 \int_1^5 (z_{def1}/\dot{z}_r - R_3)^2 df + \alpha_5 \int_1^5 (z_{def1}/\dot{z}_r - R_4)^2 df + \alpha_6 \frac{\|K\|_\infty}{\gamma_k} \tag{5.2.8}$$

where R_1 (respectively R_2) is the linear frequency response $\ddot{z}_1/\dot{z}_r$ of the hard dampers (respectively the soft dampers) and R_3 (respectively R_4) is the linear frequency response $z_{def1}/\dot{z}_r$ ($z_{def2}/\dot{z}_r$) of the hard dampers; α_i with $i = 1:6$ are weighting parameters.

Remark 5.2.1. The similar procedure is applied for the OSS system.

5.3 Test scenario and performance criterion for evaluation

In the following, we present the test scenario and the performance index which is useful for the evaluation of the proposed methods.

5.3.1 Road Profile

The road profiles used for the simulation is in fact a road profile standard $\bar{z}_r$ scaled by a factor β. The higher the value of β, the rougher the road. For this class of road profile it is supposed that the vehicle velocity is the same for all road profiles z_r.

$$z_r \in \{\beta \bar{z}_r, \beta \in [0.5, 1.5]\} \tag{5.3.1}$$

The standard road profile $\bar{z}_r$ is represented by an integrated white noise, band-limited within the frequency range [0-30] Hz (see Fig. 5.6).

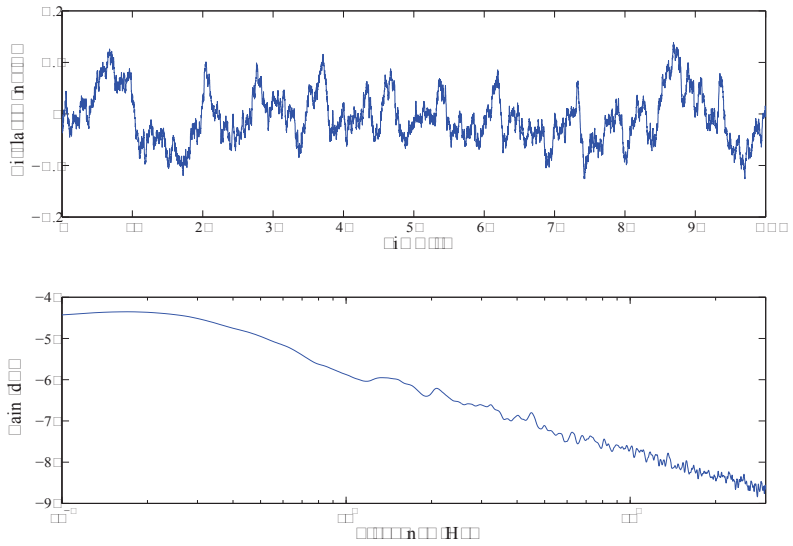

Figure 5.6: Standard road profile.

5.3.2 Performance Index

For each kind of road profile or each value of β, the following performance index will be calculated.

$$PI = \sqrt{\frac{\int_0^T \ddot{\bar{z}}_s^2(t)dt}{\int_0^T \beta^2 \bar{z}_r^2(t)dt}} \tag{5.3.2}$$

where $\ddot{\bar{z}}_s(t)$ is the filtered car body acceleration (by ISO 2631 filter, see 1.2.9 in Chapter 1) $[m/s^2]$ (for DSS system $z_s \equiv z_1$, for OSS system $z_s \equiv z$), $\bar{z}_r$ is the standard road profile and T is the simulation running time $[s]$.

5.4 Numerical Results

From the set of controllers obtained by Genetic optimization for OSS and DSS systems, we choose the following controllers.

- For the OSS system, we obtain a comfort oriented controller (using the suspension deflection $z - z_r$ as measurement output), denoted as $K^{OSS}_{Comfort}$.

For the DSS system, we obtain two controllers: a comfort oriented controller and a stroke oriented controller.

- The comfort oriented controller (using the suspension deflection $[z_1 - z_2; z_2 - z_r]$ as measurement output) is denoted as $K^{DSS}_{Comfort}$.
- The stroke oriented controller (using the suspension deflection velocity $[\dot{z}_1 - \dot{z}_2; \dot{z}_2 - \dot{z}_r]$ as measurement output) is denoted as K^{OSS}_{Stroke}.

The purpose is to design controllers for the DSS system. For OSS system, we choose only one controller, the comfort oriented controller, for the comparisons with the comfort oriented one for the DSS system to evaluate the effectiveness of proposed method and to see if there is any difference between the two models when using with the controllers having the same behaviors. For more details of these controllers, see Appendix D.

Remark 5.4.1. Many tests were made and we found that the use of the suspension deflections as measurement output results in better comfort oriented controllers. In the contrary, the use of the suspension deflection velocity as measurement output gives better stroke oriented controllers. It may be interesting to consider the influence of different types of measurement outputs on the quality of controller (in future work).

It is worth noticing also that all the frequency analysis are made for nonlinear models (OSS & DSS) without the Endstop behaviors. Only in time domain analysis, the nonlinear model with Endstop effect are used. Besides, all the proposed controllers (using strong stabilization) are clipped.

5.4.1 Baselines

To evaluate the efficiency of the proposed method, the following referenced methods are used.

- Passive OSS Min (i.e $c_{os} = c_{min}$), OSS Mean ($c_{os} = (c_{max} + c_{min})/2$) and OSS Max ($c_{os} = c_{max}$).

- Controlled OSS: Skyhook-ADD (where the design parameter $\alpha = 2\pi 3\ rad/s$), Clipped Comfort-Oriented Controller (Proposed Method) - 1 Example .

- Passive DSS Min-Min (i.e $c_1 = c_2 = c_{min}$), DSS Min-Max (i.e $c_1 = c_{1min}$, $c_2 = c_{2max}$), DSS Max-Min (i.e $c_1 = c_{1max}$, $c_2 = c_{2min}$), DSS Mean-Mean ($c_1 = c_2 = (c_{max} + c_{min})/2$) and DSS Max-Max ($c_1 = c_2 = c_{max}$).

5.4.2 Frequency domain analysis

OSS system Figures 5.7-5.8 shows the nonlinear frequency responses of the OSS with two comfort oriented controllers $K^{OSS}_{Comfort}$ and the Skyhook-ADD (along with passive cases). The results show that $K^{OSS}_{Comfort}$ is a little better than Skyhook-ADD in high frequencies (significant for comfort) but worse in low frequencies. The Skyhook-ADD, besides providing a good comfort, improves the suspension deflection as well.

DSS system Figure 5.9-5.10 show the nonlinear frequency responses of the DSS with two controllers: the comfort oriented controller $K^{DSS}_{Comfort}$ and the stroke oriented controller K^{DSS}_{Stroke}. The comfort controller improves fairly well the comfort in high frequencies, it is less effective in low frequencies. The stroke oriented controller improves very well the suspension deflection of the higher damper ($z_1 - z_2$). In this point, it is similar to the "$DSS\ Max - Min$" but more efficient in comfort and lower damper's deflection improvements. It is worth noticing also that, among 4 passive cases of DSS system, the $DSS\ Max - Min$ provide the best compromise.

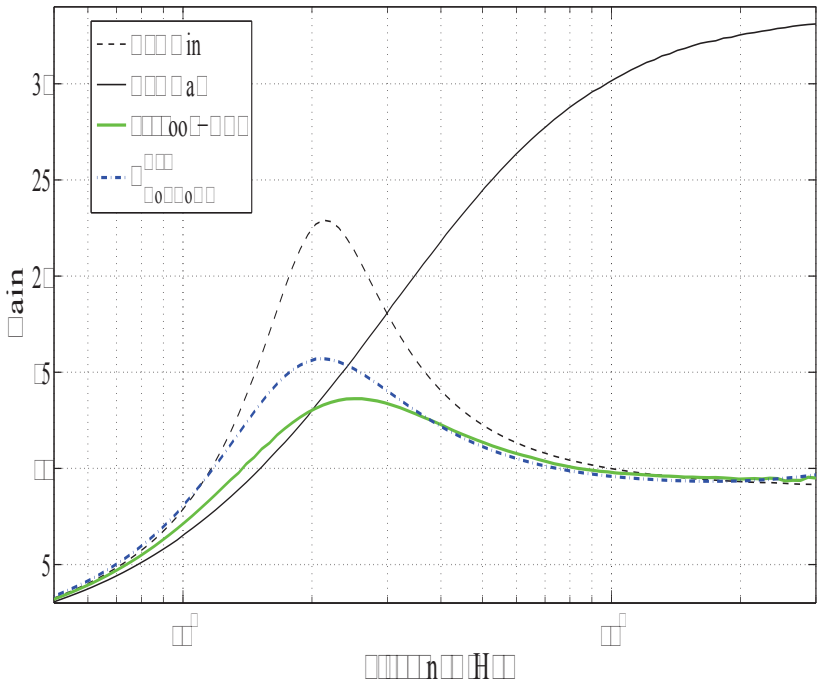

Figure 5.7: OSS system - Nonlinear frequency responses $\ddot{z}/\dot{z}_r$.

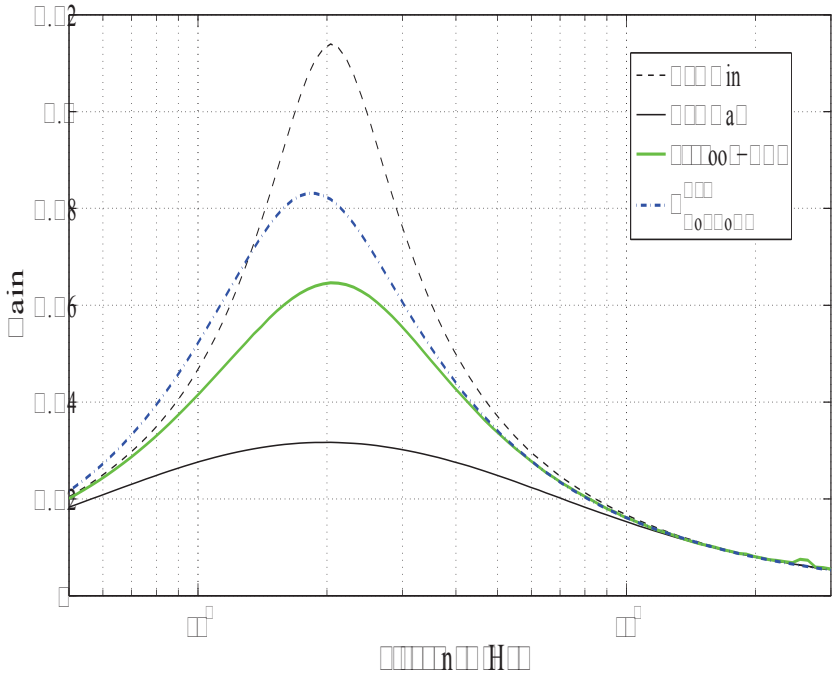

Figure 5.8: OSS system - Nonlinear frequency responses $(z - z_r)/\dot{z}_r$.

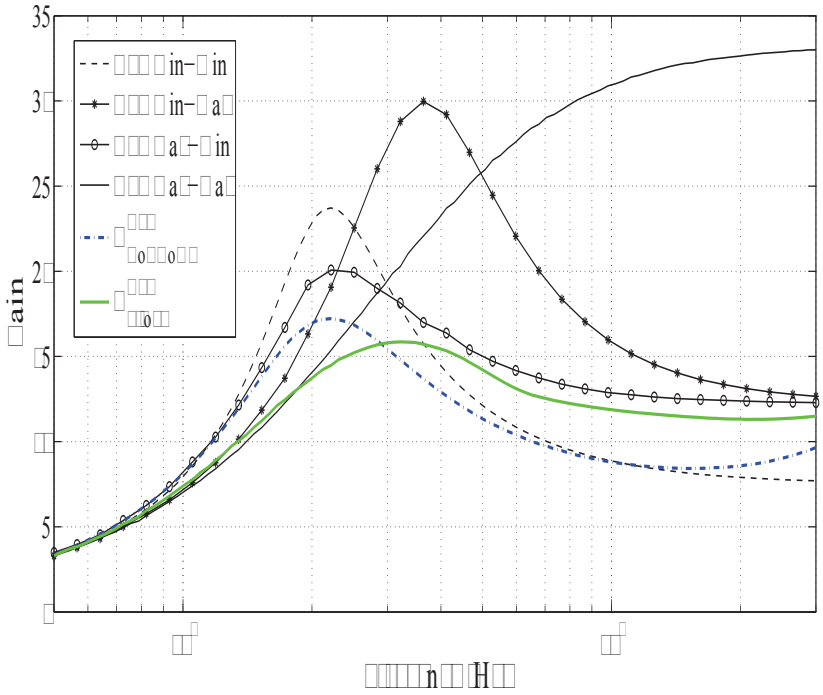

Figure 5.9: DSS system - Nonlinear frequencies responses $\ddot{z}_1/\dot{z}_r$.

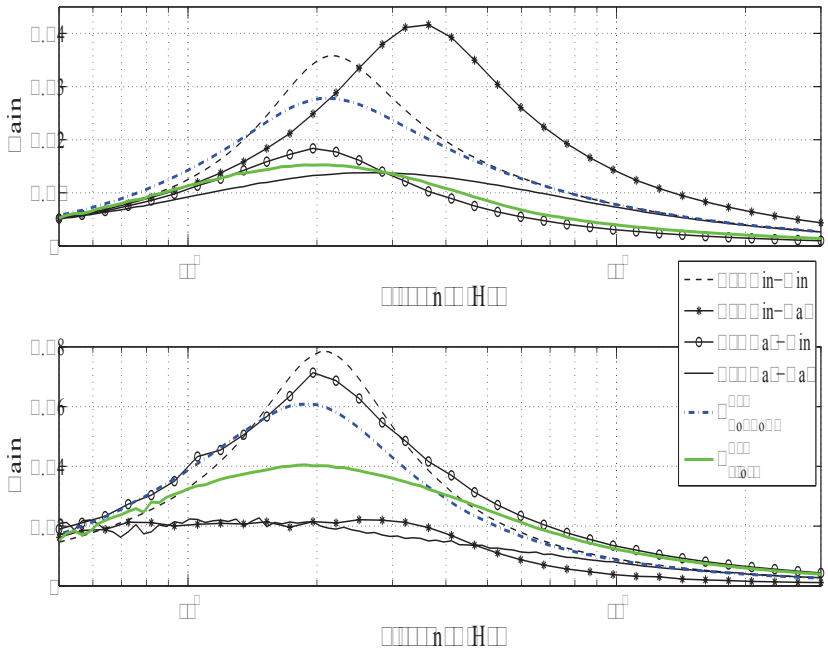

Figure 5.10: DSS system - Nonlinear frequencies responses $(z_1 - z_2)/\dot{z}_r$ (Top) and $(z_2 - z_r)/\dot{z}_r$ (Bottom).

5.4.3 Time domain analysis

The performance index (5.3.2) is computed with different values of β (or different road profiles) for different strategies and depicted in Fig. 5.11-5.13.

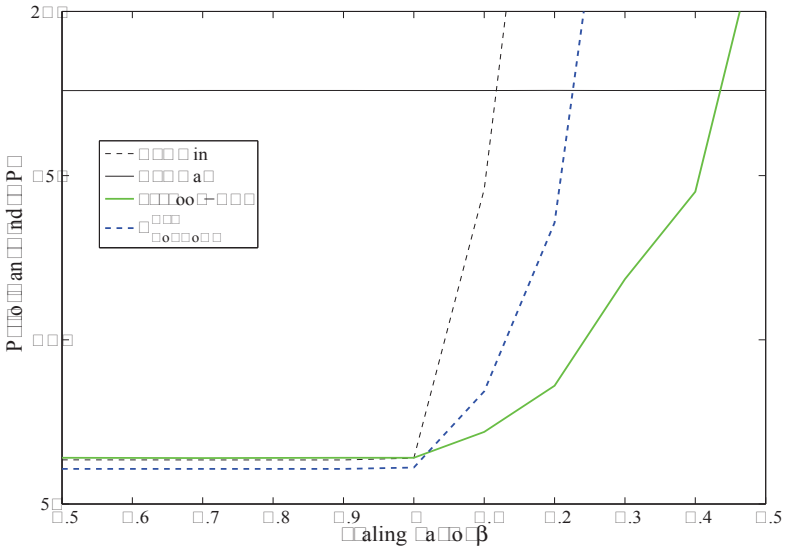

Figure 5.11: Time performance comparison for OSS system.

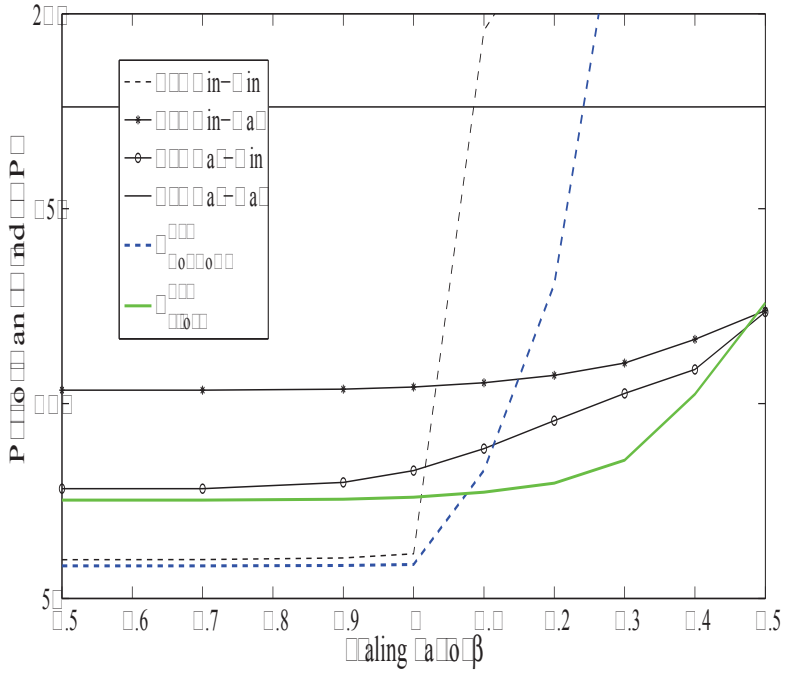

Figure 5.12: Time performance comparison for DSS system.

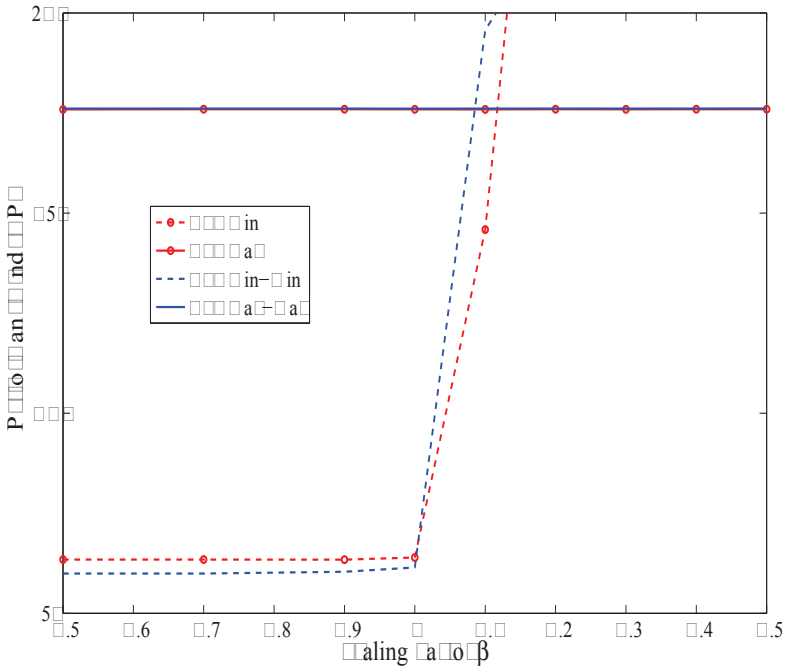

Figure 5.13: Time performance comparison between passive OSS and DSS systems.

In Fig. 5.11, it is can seen that the $K^{OSS}_{Comfort}$ is a little better than the Skyhook-ADD when the road is smooth ($\beta < 1$). When the road disturbance is more significant ($\beta > 1$), the Skyhook-ADD keeps its better performance while the $K^{OSS}_{Comfort}$ and the "$OSS\ Min$" degrade rapidly their performances due to the Endstop effect. The "$OSS\ Max$" is not influenced much by this effect but in general it is not a good choice.

In Fig. 5.12, it is can be seen that the $K^{DSS}_{Comfort}$ is the best one when the road is smooth ($\beta < 1$). When the road disturbance is more significant ($\beta > 1$), K^{DSS}_{Stroke} is the best choice. It outperforms the $DSS\ Max - Min$ which is considered the best among 4 passive cases. It can be seen again that the K^{DSS}_{Stroke} is better than the "$DSS\ Min - Max$" as it behaves better in frequencies responses for comfort (in low frequencies) and in lower damper's deflection.

In Fig. 5.13, the time performances of passive DSS and OSS systems are compared. The results show that they have similar performance indices.

We propose here a switching controller $K_{Comfort+Stroke}$ to achieve a better compromise w.r.t $K^{OSS}_{Comfort}$ and K^{DSS}_{Stroke} between comfort and suspension deflection:

$$K_{c3} = (1 - s_w)K_{c1} + s_w K_{c2} \tag{5.4.1}$$

where s_w is the switching signal given as (see [Spelta et al., 2011])

$$\begin{aligned} s_w = 0 \, if \; & \left\{ \begin{array}{ll} |z_{def1}| < 0.013 & \\ |\dot{z}_{def1}| < 0.4 \vee \dot{z}_{def1}.z_{def1} < 0 & \end{array} \right. \wedge \left\{ \begin{array}{l} |z_{def2}| < 0.013 \\ |\dot{z}_{def2}| < 0.4 \vee \dot{z}_{def2}.z_{def2} < 0 \end{array} \right. \\ s_w = 1 \, & else \end{aligned} \tag{5.4.2}$$

The idea of the switching controller is that when the suspension deflection is small and when the deflection velocity is small or when the deflection and its velocity have different signs, the comfort controller is used; otherwise the stroke controller is preferred to reduce the suspension deflection and thus to reduce the degradation by End-stop effect.

Looking at in Fig. 5.14, several comments can be made, concerning the various strategies:

- The comfort oriented controllers $K^{DSS}_{Comfort}$ and $K^{OSS}_{Comfort}$ are similar in terms of performance improvement. Along with the comparison presented in Fig. 5.13, this shows that the two models (OSS and DSS) are comparable and that the proposed method (strong stabilization) is efficient for both models.
- If we consider the Skyhook-ADD as a reference for the performance evaluation then the $K_{Comfort+Stroke}$ outperforms this strategy. The switching controller $K_{Comfort+Stroke}$ improves the performance for almost all value of β (smooth and rough roads).

5.5 Conclusions

In this chapter, we presented an application of the strong stabilization approach (presented in Chapter 4) for the driver seat's comfort improvement. The results showed the effectiveness of the proposed method.

The study of DSS model is very promising. In [Spelta et al., 2011], it has been shown that if the damping coefficient can vary from a very low to a very high value, the controllable stiffness and damping suspension system can be achieved with the DSS model. This point is very interesting in that the total stiffness and damping coefficients can be modulated by changing only the characteristic of the dampers. The studies of controllable damping and stiffness suspension systems will be considered in future work.

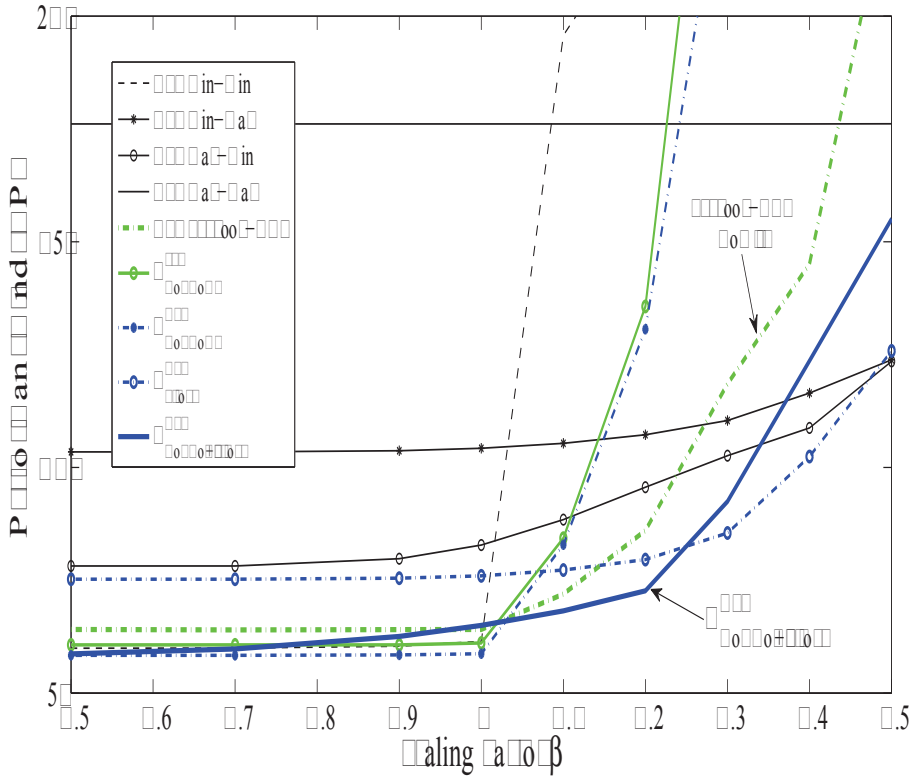

Figure 5.14: Time performance comparison with switching controller.

Chapter 6

LPV control design with input saturation and state constraints: an application to semi-active suspension control

As seen in previous chapters, comfort, road holding and suspension deflection are the main issues in suspension control. So far in the thesis, three objectives have not been handled simultaneously in a design: the comfort and road holding trade-off was studied in chapter 3 and 4; the comfort and suspension deflection improvement was proposed in chapter 5. Besides, the passivity constraint of semi-active suspensions was not explicitly taken into consideration. In this chapter, an H_∞/LPV synthesis that encompasses all major problems in semi-active suspension control (comfort, road holding, suspension deflection improvements and passivity constraint) will be introduced. First, a generic design for LPV systems subject to additive disturbances in the presence of actuator saturation and state constraints is proposed. LMI conditions are derived in order to simultaneously compute an LPV controller and an anti-windup gain that ensures the boundedness of the trajectories, considering that the disturbances belong to a given admissible set. The disturbance attenuation is addressed via an H_∞ constraint. Besides, state constraints (corresponding to the local validity of the LPV model and system structural limits) are always assured. Then, the theoretical results are applied to a quarter-car vehicle model rewritten within the LPV framework where the passivity constraint is recast into the saturation one.

The results in this chapter have been developed in collaboration with J. M. Gomes da Silva Jr. during his visiting period in Grenoble in 2010.

6.1 Introduction

In the last years, many studies have focused on the control of saturated (in states, control inputs...) systems which are present in almost real applications. For a system with input saturation, there is usually an inconsistency between the states of the plant and those of the controller because of the saturated actuator between the system control input and the controller output. This effect, usually called windup, degrades dramatically the closed-loop performances or even worse may cause the system instability. To preserve the consistency, the input to controller needs to be changed by an appropriate signal, which is provided by a called anti-windup compensator. Usually the problems on how to guarantee the (global or local) stabilization of the saturated system in the presence of disturbance and to ensure some closed-loop performances are the most interesting ones. As presented in Chapter 2, the input saturation control problem is a nonlinear one, that may be handled using either a two-step design [Kothare et al., 1994], [Grimm et al., 2003], [Wu & Lu, 2004]; or a one-step design [Gomes da Silva Jr. et al., 2008], [Mulder et al., 2009]. With these approaches, numerous results have been obtained for LTI systems. On the other hand, very few studies dealing with switched or LPV systems can be found in the literature, see for instance [Montagner, Gomes da Silva Jr. & Peres, 2007], for switching systems, and [Wu et al., 2000], [Montagner, Oliveira, Peres, Tarbouriech & Queinnec, 2007], [Cao et al., 2002] for LPV systems.

In this chapter, we aim at using the one-step anti-windup design for semi-active suspension control to achieve the best compromise among conflicting objectives: passenger comfort, road holding and suspension deflection. In our previous works [Do, Sename & Dugard, 2010] and [Do, Spelta, Savaresi, Sename, Dugard & Delvecchio, 2010], the LPV framework is used to model the nonlinear damper characteristics, and, also to consider the actuator saturation as a scheduling parameter (this approach can be referred to [Wu et al., 2000]). The performance on suspension deflection, along with comfort and road holding, is managed by using some frequency-based weighting functions. An LPV controller is then synthesized using a global analysis (global stability and performance). Another important point is that, in this work, instead of considering the suspension deflection as a performance objective, we will treat it as a constraint. Besides, we are only interested in a certain working range of the damper because, in real applications, its deflection velocity is limited. Since the states are physically bounded, due to the limit in the suspension deflection, and since the LPV polytopic model is not globally valid in the state space, a regional stabilization approach is considered in this work. First, a general design method for LPV system with input saturation and state constraint is proposed. Precisely, a sufficient condition to guarantee the regional asymptotic stability of the origin for arbitrary scheduling parameters and to guarantee bounded trajectories in the presence of disturbances (which are assumed to be limited in amplitude) is derived based on the modified sector condition [Gomes da Silva Jr. & Tarbouriech, 2005] and

on the use of quadratic Lyapunov function. The condition ensures also an upper bound on the induced-L_2 gain between the disturbance input and the controlled output when there is no saturation. Moreover, the state constraints on the system are always assured for the considered class of disturbances. Then we apply the result to enhance the performance of a semi-active suspension system rewritten in the LPV framework where the passivity constraint is recast into an input saturation one.

The contribution of the chapter is two-fold:

- The synthesis of a stabilizing controller for LPV system with input saturation and state constraints.
- The application for the first time of such an approach for the semi-active suspension control.

6.2 Problem Formulation

In the following, X_i denotes the i^{th} row of matrix X. (*) stands for symmetric blocks and $sym(X) = X + X^T$. ($\bullet$) stands for an element that has no influence on the development.

6.2.1 System description

Consider a quasi-LPV plant represented by:

$$\begin{aligned} \dot{x} &= A(\theta)x + B_w(\theta)w + B_u u \\ z &= C_z(\theta)x + D_{zw}(\theta)w + D_{zu}u \\ y &= C_y x + D_{yw} w \end{aligned} \tag{6.2.1}$$

where $x \in \mathbb{R}^n$, $u \in \mathbb{R}^m$, $w \in \mathbb{R}^q$, $z \in \mathbb{R}^r$ and $y \in \mathbb{R}^p$ are the state, the input, the disturbance vectors, the control output and the measured output, respectively. θ is a vector of scheduling parameters which are supposed to depend on states and assumed to be known (measured or estimated).
Let us consider also an LPV controller

$$\begin{aligned} \dot{x}_c &= A_c(\theta)x_c + B_c(\theta)u_c + v \\ y_c &= C_c(\theta)x_c + D_c(\theta)u_c \end{aligned} \tag{6.2.2}$$

where $x_c \in \mathbb{R}^{n_c}$, $u_c \in \mathbb{R}^p$, $y_c \in \mathbb{R}^m$, v is an additional input used for anti-windup compensation.

The unconstrained closed-loop system of the plant (see Fig. 6.1) and the controller are defined by the following interconnections

$$u = y_c, \quad u_c = y, \quad v = 0 \tag{6.2.3}$$

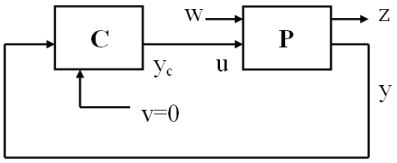

Figure 6.1: Unconstrained closed-loop plant.

The following assumptions are considered:

- *Assumption 1:* The matrices B_u, D_{zu}, C_y and D_{yz} are supposed to be parameter-independent (to satisfy the hypotheses of polytopic design for LPV systems).

- *Assumption 2:* The input disturbance is limited in amplitude, that is $\forall t > 0, w(t) \in \mathcal{W}$ with

$$\mathcal{W} = \{w \in \mathbb{R}^q : w^T w < \delta\} \tag{6.2.4}$$

- *Assumption 3:* The scheduling parameters depend on the system's states $\theta = \theta(x, t)$ (i.e quasi-LPV) and are bounded in

$$\Theta = \{\theta : \underline{\theta}_i \leqslant \theta_i \leqslant \overline{\theta}_i, i = 1, ..., k\} \tag{6.2.5}$$

- *Assumption 4:* The control inputs are bounded in amplitude:

$$-\overline{u}_i \leqslant u_i(t) \leqslant \overline{u}_i, \quad i = 1, ..., m \tag{6.2.6}$$

6.2.2 LPV controller

We consider a dynamic LPV controller with a static anti-windup action

$$\begin{aligned} \dot{x}_c &= A_c(\theta)x_c + B_c(\theta)u_c + E_c(\theta)(sat(y_c) - y_c) \\ y_c &= C_c(\theta)x_c + D_c(\theta)u_c \end{aligned} \tag{6.2.7}$$

where $x_c \in \mathbb{R}^{n_c}$, $u_c \in \mathbb{R}^p$, $y_c \in \mathbb{R}^m$ and $E_c(\theta)$ is a static anti-windup term [Gomes da Silva Jr. & Tarbouriech, 2005], [Montagner, Gomes da Silva Jr. & Peres, 2007].

The interconnections between the plant and the controller (see Fig. 6.2) are given by (according to (6.2.2))

$$u = sat(y_c),\ u_c = y,\ v = E_c(\theta)(sat(y_c) - y_c) \tag{6.2.8}$$

where the saturated function $sat(.)$ is defined by

$$sat(y_{c_i}) = \begin{cases} \overline{u}_i & \text{if } y_{ci} > \overline{u}_i \\ y_{c_i} & \text{if } -\overline{u}_i \leq y_{ci} \leq \overline{u}_i \\ -\overline{u}_i & \text{if } y_{ci} < -\overline{u}_i \end{cases} \tag{6.2.9}$$

From (6.2.1) and (6.2.2), the closed-loop system is given by

$$\begin{aligned} \dot{\xi} &= \mathcal{A}(\theta)\xi + \mathcal{B}(\theta)w - (\mathcal{B}_u + \mathcal{R}E_c(\theta))\psi(y_c) \\ z &= \mathcal{C}(\theta)\xi + \mathcal{D}(\theta)w + \mathcal{D}_\psi\psi(y_c) \end{aligned} \tag{6.2.10}$$

where

$$\begin{aligned} &\xi = [x^T x_c^T]^T, \psi(y_c) = y_c - sat(y_c) \\ &\mathcal{A}(\theta) = \begin{bmatrix} A(\theta) + B_u D_c(\theta) C_y & B_u C_c(\theta) \\ B_c(\theta) C_y & A_c(\theta) \end{bmatrix} \\ &\mathcal{B}(\theta) = \begin{bmatrix} B_w(\theta) + B_u D_c(\theta) D_{yw} \\ B_c(\theta) D_{yw} \end{bmatrix} \\ &\mathcal{B}_u = \begin{bmatrix} B_u \\ 0 \end{bmatrix}, \mathcal{R} = \begin{bmatrix} 0 \\ I_{n_c} \end{bmatrix} \\ &\mathcal{C}(\theta) = \begin{bmatrix} C_z(\theta) + D_{zu} D_c(\theta) C_y & D_{zu} C_c(\theta) \end{bmatrix} \\ &\mathcal{D}(\theta) = D_{zw}(\theta) + D_{zu} D_c(\theta) D_{yw} \\ &\mathcal{D}_\psi = -D_{zu} \end{aligned} \tag{6.2.11}$$

The controller output is rewritten as

$$y_c = \mathcal{K}(\theta)\xi + \mathcal{K}_w(\theta)w \tag{6.2.12}$$

where

$$\mathcal{K}(\theta) = \begin{bmatrix} D_c(\theta) C_y & C_c(\theta) \end{bmatrix}, \mathcal{K}_w(\theta) = D_c(\theta) D_{yw}$$

6.2.3 Problem Definition

In this chapter, we look for an LPV controller (6.2.7) for the LPV system (6.2.1) with input saturation such that the following conditions are satisfied:

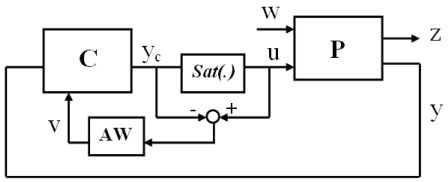

Figure 6.2: Closed-loop plant with anti-windup controller.

(i) In the absence of disturbances, or if the disturbances are vanishing, the controller guarantees the regional asymptotic stability of the origin for an arbitrary scheduling parameter θ. In the presence of disturbances satisfying assumption 2, the controller guarantees that the trajectories of (6.2.10) are bounded.
(ii) The controller guarantees some constraints on the states of the closed-loop system.
(iii) For the unconstrained closed-loop system, i.e. when the saturation is not active, the controller guarantees an upper bound γ on the L_2-gain between the disturbance input w and the controlled output z.

Remark 6.2.1. Considering the same L_2 performance when the system operates linearly and under control saturation can lead to very conservative results. Hence, we consider that the L_2 performance should be satisfied only by the unconstrained system, which corresponds to a classic H_∞ problem. On the other hand, if the control saturates, we should ensure that the trajectories are bounded and do not violate the state constraints.

6.3 Preliminaries

6.3.1 Practical validity region

In practice, besides the constraint on the control input, the system states are usually bounded because of structural limits. Furthermore, the local validity of the LPV model can be also translated in state constraints. We assume that the state constraints can be represented by a polyhedron $\mathcal{X}$ defined by

$$\mathcal{X} = \{\xi \in \mathbb{R}^{2n} : H_i \xi \leq h_{0i},\ i = 1 : s\} \tag{6.3.1}$$

Note that only the state of the plant is constrained, so H is of the form $H = \begin{bmatrix} H_1 & 0 \end{bmatrix}$.

6.3.2 Saturation model validity region

Due to the boundedness of w and to the fact that the states of the real system are limited in the practical validity region $\mathcal{X}$, a regional analysis is made in this chapter. In

order to take into account the saturation effects, an "LPV" version of the modified sector condition proposed in [Gomes da Silva Jr. & Tarbouriech, 2005] is applied. With this aim, let us define the matrix $\mathcal{G}(\theta) = \left[\begin{array}{cc} G_1(\theta) & G_2(\theta) \end{array} \right]$ and the following polyhedral set

$$S_\theta = \left\{ \xi \in \mathbb{R}^{2n}, |\left(\mathcal{K}_i(\theta) - \mathcal{G}_i(\theta)\right)\xi| \leqslant \overline{u}_i, i = 1, ..., m \right\}, \tag{6.3.2}$$

$\forall \theta \in \Theta$. Hence, the following Lemma can be stated.

Lemma 6.3.1. *If $\xi(t) \in S_\theta$, then the following inequality*

$$\psi(y_c)^T T \left(\psi(y_c) - \left[\begin{array}{ccc} \mathcal{G}(\theta) & 0 & \mathcal{K}_w(\theta) \end{array} \right] \left[\begin{array}{c} \xi \\ \psi(y_c) \\ w \end{array} \right] \right) \leqslant 0 \tag{6.3.3}$$

holds for any diagonal and positive definite matrix $T \in \mathbb{R}^{m \times m}$.

Proof: The result can be inferred directly from [Gomes da Silva Jr. & Tarbouriech, 2005].

6.3.3 W-invariance

Because the disturbance input is bounded in amplitude, we use the W-invariance concept to ensure the boundedness of the trajectories. (see [Blanchini, 1999])

Definition 6.3.1. *A set $\mathcal{E} \subset \mathbb{R}^{2n}$ is W-invariant with respect to the system (6.2.10) if $\forall \xi(0) \in \mathcal{E}$, $w(t) \in \mathcal{W}$ and for any scheduling parameter signal $\theta(t)$, it follows that the state trajectory remains in $\mathcal{E}$, i.e $\xi(t) \in \mathcal{E}$, $\forall t > 0$.*

In the approach, $\mathcal{E}$ is considered as an ellipsoidal set associated to a quadratic function $V(t) = \xi^T P \xi$, $P = P^T \succ 0$

$$\mathcal{E} = \{\xi \in \mathbb{R}^{2n} : \xi^T P \xi < 1\} \tag{6.3.4}$$

To ensure that $\mathcal{E}$ is a W-invariant set, it suffices to ensure that

$$\dot{V}(t) < 0, \left\{ \begin{array}{l} \forall \xi(t) : \xi^T P \xi > 1 \\ \forall w(t) : w^T w < \delta \end{array} \right. \tag{6.3.5}$$

along the trajectories of (6.2.10). By using S-procedure, this condition can be satisfied if there exist scalars $\beta_1 > 0$ and $\beta_2 > 0$, such that

$$\dot{V} + \beta_1(\xi^T P \xi - 1) + \beta_2(\delta - w^T w) < 0 \tag{6.3.6}$$

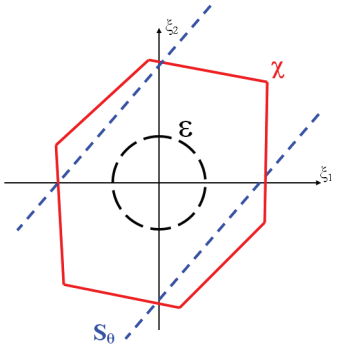

Figure 6.3: Saturation model validity region S, practical validity region $\mathcal{X}$, W-invariant set $\mathcal{E}$.

6.4 Main results

In this section, an LMI-based constructive condition to solve the problem stated in 6.2.3 is developed.

Theorem 6.4.1. *If, for given $\beta_1 > 0$ and $\gamma > 0$, there exist symmetric positive definite matrices $X, Y \in \mathbb{R}^{n\times n}$, positive scalar β_2, positive diagonal matrices $S \in \mathbb{R}^{m\times m}$, matrices $\hat{A}(\theta) \in R^{n\times n}$, $\hat{B}(\theta) \in R^{n\times p}$, $\hat{C}(\theta)$, $\hat{Z}_1(\theta)$, $\hat{Z}_2(\theta) \in R^{m\times n}$, $\hat{D}(\theta) \in R^{m\times p}$, $\hat{Q}(\theta) \in R^{n\times m}$ such that the matrix inequalities (6.4.2)-(6.4.6) are verified, then the LPV anti-windup controller (6.2.2) with matrices*

$$\begin{cases} E_c(\theta) = N^{-1}\hat{Q}(\theta) S^{-1} - N^{-1} Y B_u \\ D_c(\theta) = \hat{D}(\theta) \\ C_c(\theta) = [\hat{C}(\theta) - D_c(\theta) C_y X] M^{-T} \\ B_c(\theta) = N^{-1}[\hat{B}(\theta) - Y B_u D_c(\theta)] \\ A_c(\theta) = N^{-1}[\hat{A}(\theta) - N B_c(\theta) C_y X - Y B_u C_c(\theta) M^T \\ \qquad -Y(A(\theta) + B_u D_c(\theta) C_y) X] M^{-T} \end{cases} \tag{6.4.1}$$

where M and N verify $MN^T = I - XY$, solves the problem defined in Section 6.2.3.

$$\begin{bmatrix} \mathcal{L}_{11}(\theta) & \mathcal{L}_{12}(\theta) & \mathcal{L}_{13}(\theta) & \mathcal{L}_{14}(\theta) \\ * & \mathcal{L}_{22}(\theta) & \mathcal{L}_{23}(\theta) & \mathcal{L}_{24}(\theta) \\ * & * & \mathcal{L}_{33}(\theta) & \mathcal{L}_{34}(\theta) \\ * & * & * & \mathcal{L}_{44}(\theta) \end{bmatrix} \prec 0 \tag{6.4.2}$$

$$\begin{bmatrix} \mathcal{O}_{11}(\theta) & \mathcal{O}_{12}(\theta) & \mathcal{O}_{13}(\theta) & \mathcal{O}_{14}(\theta) \\ * & \mathcal{O}_{22}(\theta) & \mathcal{O}_{23}(\theta) & \mathcal{O}_{24}(\theta) \\ * & * & \mathcal{O}_{33}(\theta) & \mathcal{O}_{34}(\theta) \\ * & * & * & \mathcal{O}_{44}(\theta) \end{bmatrix} \prec 0 \tag{6.4.3}$$

$$\begin{bmatrix} X & * & * \\ I & Y & * \\ \hat{C}_i(\theta) - \hat{Z}_{1i}(\theta) & (\hat{D}(\theta) C_y)_i - \hat{Z}_{2i}(\theta) & \bar{u}_i^2 \end{bmatrix} \succeq 0 \quad for\ i = 1:m \tag{6.4.4}$$

$$\begin{bmatrix} X & * & * \\ I & Y & * \\ H_{1i}X & H_{1i} & h_{0i}^2 \end{bmatrix} \succeq 0 \quad for\ i = 1:s \tag{6.4.5}$$

$$\beta_2\delta - \beta_1 \prec 0 \tag{6.4.6}$$

where

$$\begin{aligned}
\mathcal{L}_{11}(\theta) &= A(\theta)X + XA(\theta)^T + B_u\hat{C}(\theta) + \hat{C}(\theta)^T B_u^T + \beta_1 X \\
\mathcal{L}_{12}(\theta) &= A(\theta) + \hat{A}(\theta)^T + B_u\hat{D}(\theta)C_y + \beta_1 I_n \\
\mathcal{L}_{13}(\theta) &= -B_u S + \hat{Z}_1(\theta)^T \\
\mathcal{L}_{14}(\theta) &= B_u\hat{D}(\theta)D_{yw} + B_w(\theta) \\
\mathcal{L}_{22}(\theta) &= YA(\theta) + A(\theta)^T Y + \hat{B}(\theta)C_y + C_y^T\hat{B}(\theta)^T + \beta_1 Y \\
\mathcal{L}_{23}(\theta) &= -\hat{Q}(\theta) + \hat{Z}_2(\theta)^T \\
\mathcal{L}_{24}(\theta) &= \hat{B}(\theta)D_{yw} + YB_w(\theta) \\
\mathcal{L}_{33}(\theta) &= -2S \\
\mathcal{L}_{34}(\theta) &= \hat{D}(\theta)D_{yw} \\
\mathcal{L}_{44}(\theta) &= -\beta_2 I \\
\mathcal{O}_{11}(\theta) &= A(\theta)X + XA(\theta)^T + B_u\hat{C}(\theta) + \hat{C}(\theta)^T B_u^T \\
\mathcal{O}_{12}(\theta) &= \hat{A}(\theta)^T + A(\theta) + B_u\hat{D}(\theta)C_y \\
\mathcal{O}_{13}(\theta) &= B_w(\theta) + B_u\hat{D}(\theta)D_{yw} \\
\mathcal{O}_{14}(\theta) &= XC_z(\theta)^T + \hat{C}(\theta)^T D_{zu}^T \\
\mathcal{O}_{22}(\theta) &= YA(\theta) + A(\theta)^T Y + \hat{B}(\theta)C_y + C_y^T\hat{B}(\theta)^T \\
\mathcal{O}_{23}(\theta) &= YB_w(\theta) + \hat{B}(\theta)D_{yw} \\
\mathcal{O}_{24}(\theta) &= C_z(\theta)^T + C_y^T\hat{D}(\theta)^T D_{zu}^T \\
\mathcal{O}_{33}(\theta) &= -\gamma I_m \\
\mathcal{O}_{34}(\theta) &= D_{zw}(\theta)^T + D_{yw}^T\hat{D}(\theta)^T D_{zu}^T \\
\mathcal{O}_{44}(\theta) &= -\gamma I_p
\end{aligned} \tag{6.4.7}$$

Proof of Theorem 6.4.1

1. Sufficient condition for stability - related to problem (i)
First, we look for the stability condition for the closed-loop system with the anti-windup controller (6.2.10). From (6.3.3) and (6.3.6), by employing the S-procedure, if there exist a positive definite matrix T and positive scalars β_1 and β_2 such that

$$\begin{array}{l} \frac{dV}{dt} + \beta_1(\xi^T P \xi - 1) + \beta_2(\delta - w^T w) - 2\psi(y_c)^T T \times \\ \left(\psi(y_c) - \left[\begin{array}{ccc} \mathcal{G}(\theta) & 0 & \mathcal{K}_w(\theta) \end{array} \right] \left[\begin{array}{c} \xi \\ \psi(y_c) \\ w \end{array} \right] \right) < 0 \end{array} \tag{6.4.8}$$

then it follows that $\dot{V} < 0$, for all ξ in the boundary of $\mathcal{E}$ that belongs to the region S_θ, and for all $w \in W$. Hence, in order to ensure that $\mathcal{E}$ is a W-invariant set, we must also satisfy:

$$\mathcal{E} \subset S_\theta \tag{6.4.9}$$

The condition (6.4.8) is in fact guaranteed if both following inequalities hold [Boyd et al., 1994]

$$\begin{array}{l} \frac{dV}{dt} + \beta_1 \xi^T P \xi - \beta_2 w^T w - 2\psi(y_c)^T T_1 \times \\ \left(\psi(y_c) - \left[\begin{array}{ccc} \mathcal{G}(\theta) & 0 & \mathcal{K}_w(\theta) \end{array} \right] \left[\begin{array}{c} \xi \\ \psi(y_c) \\ w \end{array} \right] \right) < 0 \end{array} \tag{6.4.10}$$

and

$$\beta_2 \delta - \beta_1 < 0 \tag{6.4.11}$$

Expanding the derivative $\frac{dV}{dt}$, inequality (6.4.10) can be rewritten as

$$\begin{array}{l} \xi^T \mathcal{A}^T(\theta) P \xi + w^T \mathcal{B}^T(\theta) P \xi - \psi^T(y_c) (\mathcal{B}_u + \mathcal{R} E_c(\theta))^T P \xi \\ + \xi^T P \mathcal{A}(\theta) \xi + \xi^T P \mathcal{B}(\theta) w - \xi^T P (\mathcal{B}_u + \mathcal{R} E_c(\theta)) \psi(y_c) \\ + \beta_1 \xi^T P \xi - \beta_2 \omega^T \omega - 2\psi^T(y_c) T \psi(y_c) \\ + 2\psi^T(y_c) T \mathcal{G}(\theta) \xi + 2\psi^T(y_c) T \mathcal{K}_w(\theta) w < 0 \end{array} \tag{6.4.12}$$

The condition (6.4.10) is equivalent to the matrix inequality (6.4.16). Note that (6.4.16) is not an LMI in terms of β_1, β_2, P, T and the controller matrices A_c, B_c, C_c, D_c, E_c. By first assuming that β_1 is known and applying some congruence transformations, similar to the ones proposed in [Scherer et al., 1997], we show in the sequel that (6.4.16) is equivalent to 6.4.2. With this aim, let P and P^{-1} be partitioned as follows

$$P = \left[\begin{array}{cc} Y & N \\ N^T & \bullet \end{array} \right] \quad \text{and} \quad P^{-1} = \left[\begin{array}{cc} X & M \\ M^T & \bullet \end{array} \right] \tag{6.4.13}$$

and define the new matrices

$$\Pi = \begin{bmatrix} X & I \\ M^T & 0 \end{bmatrix}, S = T^{-1} \tag{6.4.14}$$

and

$$\begin{cases} \hat{A}(\theta) = NA_c(\theta)M^T + NB_c(\theta)C_yX + YB_uC_c(\theta)M^T \\ \qquad\qquad +Y(A(\theta) + B_uD_c(\theta)C_y)X \\ \hat{B}(\theta) = NB_c(\theta) + YB_uD_c(\theta) \\ \hat{C}(\theta) = C_c(\theta)M^T + D_c(\theta)C_yX \\ \hat{D}(\theta) = D_c(\theta) \\ \hat{Z}_1(\theta) = G_1(\theta)X + G_2(\theta)M^T \\ \hat{Z}_2(\theta) = G_1(\theta) \\ \hat{Q}(\theta) = YB_uS + NE_c(\theta)S \end{cases} \tag{6.4.15}$$

Pre and post-multiplying (6.4.16) by $diag(\Pi^T, S, I)$ and its transpose, we obtain the LMI (6.4.17) (which corresponds exactly to the LMI (6.4.2) in theorem 6.4.1). Now we

$$\begin{bmatrix} sym(P\mathcal{A}(\theta)) + \beta_1 P & -P(\mathcal{B}_u + \mathcal{R}E_c(\theta)) + \mathcal{G}^T(\theta)T & P\mathcal{B}(\theta) \\ * & -2T & T\mathcal{K}_w(\theta) \\ * & * & -\beta_2 I \end{bmatrix} < 0 \tag{6.4.16}$$

$$\begin{bmatrix} sym(A(\theta)X + B_u\hat{C}(\theta)) + \beta_1 X & A(\theta) + \hat{A}(\theta)^T + B_u\hat{D}(\theta)C_y + \beta_1 I_n & -B_uS + \hat{Z}_1(\theta)^T & B_u\hat{D}(\theta)D_{yw} + B_w(\theta) \\ * & sym(YA(\theta) + \hat{B}(\theta)C_y) + \beta_1 Y & -\hat{Q}(\theta) + \hat{Z}_2(\theta)^T & \hat{B}(\theta)D_{yw} + YB_w(\theta) \\ * & * & -2S & \hat{D}(\theta)D_{yw} \\ * & * & * & -\beta_2 I \end{bmatrix} \prec 0 \tag{6.4.17}$$

perform the inclusion condition (6.4.9) in terms of using another LMI. It can be seen that the following inequality implies (6.4.9)

$$\begin{bmatrix} P & * \\ \mathcal{K}_i(\theta) - \mathcal{G}_i(\theta) & \overline{u}_i^2 \end{bmatrix} \succeq 0, \quad i = 1, .., m \tag{6.4.18}$$

Pre and post-multiplying (6.4.18) by $diag(\Pi^T, 1)$, we obtain the following LMI (exactly the LMI (6.4.4) in theorem 6.4.1).

$$\begin{bmatrix} X & * & * \\ I & Y & * \\ \hat{C}_i(\theta) - \hat{Z}_{1i}(\theta) & (\hat{D}(\theta)C_y)_i - \hat{Z}_{2i}(\theta) & \bar{u}_i^2 \end{bmatrix} \succeq 0, \tag{6.4.19}$$

$$i = 1, .., m$$

2. State constraint - related to problem (ii)
To ensure the state constraint (6.3.1), it suffices to guarantee the inclusion of the W-invariant set $\mathcal{E}$ in the practical validity region $\mathcal{X}$

$$\mathcal{E} \subset \mathcal{X} \tag{6.4.20}$$

Similarly to the previous manipulation to obtain the inclusion condition, we have

$$\begin{bmatrix} P & * \\ H_i & h_{0i}^2 \end{bmatrix} \succeq 0 \tag{6.4.21}$$

Pre and post-multiplying (6.4.21) by $diag(\Pi^T, 1)$ and its transpose one obtains the LMI (exactly the LMI (6.4.5) in theorem 6.4.1)

$$\begin{bmatrix} X & * & * \\ I & Y & * \\ H_{1i}X & H_{1i} & h_{0i}^2 \end{bmatrix} \succeq 0 \tag{6.4.22}$$

3. Sufficient condition of L_2 gain performance in linear mode (without saturation) - related to problem (iii)
Consider now $\dot{V}$ computed considering the unconstrained system, i.e. satisfying (6.2.3), and the following inequality

$$\tfrac{dV}{dt} + \tfrac{1}{\gamma} z^T z - \gamma w^T w < 0 \tag{6.4.23}$$

Following the same steps as done in [Scherer et al., 1997], we can show that (6.4.3) ensures that (6.4.23) is verified. Hence, we can conclude that the L_2 gain of the unconstrained system is smaller than γ.

□

Optimization problems
From the theorem 6.4.1, in some interesting optimization problem may be:
1. For a known disturbance attenuation level γ, the maximization of the stability region $\mathcal{E}$ in direction v associated to the states of the plant is accomplished by the following eigenvalue problem (EVP):

$$\min \eta \tag{6.4.24}$$

$$\text{s.t.} \quad \text{LMI } (6.4.2) - (6.4.6), \quad \mathrm{v^T Y v} < \eta \tag{6.4.25}$$

2. Minimization of the disturbance attenuation level γ

$$\min \gamma \tag{6.4.26}$$

$$\text{s.t.} \quad \text{LMI } (6.4.2) - (6.4.6) \tag{6.4.27}$$

6.5 Application to semi-active suspension control

6.5.1 Quarter car model

Let us consider the quarter vehicle model presented in Fig. 6.4 made up of a sprung mass (m_s) and an unsprung mass (m_{us}). A spring with the stiffness coefficient k_s and a semi-active damper connect these two masses. The different point of this model w.r.t the one used in previous chapters is in the wheel tire. In this case, the tire is modeled by a spring with the stiffness coefficient k_t and a passive damper with damping coefficient c_t. The explanation for the use of the new model will be given in the next section.
Let us denote also z_s (respectively z_{us}) the vertical position of m_s (respectively m_{us}) and z_r the road profile. It is assumed that the wheel-road contact is ensured.

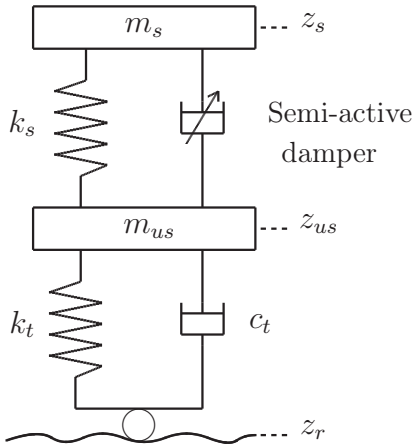

Figure 6.4: Model of quarter vehicle with a semi-active damper.

The dynamical equations of a quarter vehicle are given by

$$\begin{cases} m_s\ddot{z}_s &= -k_s z_{def} - F_{damper} \\ m_{us}\ddot{z}_{us} &= k_s z_{def} + F_{damper} - k_t\left(z_{us} - z_r\right) - c_t\left(\dot{z}_{us} - \dot{z}_r\right) \end{cases} \tag{6.5.1}$$

where $z_{def} = z_s - z_{us}$ is the damper deflection (m) (assumed to be measured or estimated), $\dot{z}_{def} = \dot{z}_s - \dot{z}_{us}$ is the deflection velocity (m/s) (can be directly computed from z_{def}) and F_{damper}, the damper force, is given as follows:

$$F_{damper} = c\dot{z}_{def} \tag{6.5.2}$$

The passivity constraint of a semi-active damper is

$$0 \leqslant c_{min} \leqslant c \leqslant c_{max} \tag{6.5.3}$$

where $c_{min} = 700\ [Ns/m]$ and $c_{min} = 5000\ [Ns/m]$.
Let us rewrite the damper force as follows

$$F_{damper} = c_{nom}\dot{z}_{def} + u\dot{z}_{def} = c_{nom}\dot{z}_{def} + u\theta \tag{6.5.4}$$

where

- $c_{nom} = (c_{max} + c_{min})/2$ is the nominal damping coefficient
- u is the new control input.
- $\theta = \dot{z}_{def}$ is the scheduling parameter.

It can be seen that the passivity constraint (6.5.3) is now recast into the *saturation constraint*

$$|u| < (c_{max} - c_{min})/2 \tag{6.5.5}$$

6.5.2 State-space representation and control objective

The state-space representation of the quarter car model is given by

$$\begin{aligned} \dot{x_s} &= A_s x_s + B_{s1} w + B_{s2}(\theta) u \\ z &= C_z x_s + D_z(\theta) u \\ y &= C_s x_s \end{aligned} \tag{6.5.6}$$

where $x_s = (z_s - z_{us},\ \dot{z}_s,\ z_{us} - z_r,\ \dot{z}_{us})^T$ is the state vector, $w = \dot{z}_r$ is the disturbance input, $z = \ddot{z}_s$ is the controlled output and $y = (z_s - z_{us},\ \dot{z}_s - \dot{z}_{us})^T$ is the measurement output.

$$A_s = \begin{bmatrix} 0 & 1 & 0 & -1 \\ \frac{-k_s}{m_s} & \frac{-c_{nom}}{m_s} & 0 & \frac{c_{nom}}{m_s} \\ 0 & 0 & 0 & 1 \\ \frac{k_s}{m_{us}} & \frac{c_{nom}}{m_{us}} & \frac{-k_t}{m_{us}} & \frac{-c_{nom}-c_t}{m_{us}} \end{bmatrix},\ B_{s1} = \begin{bmatrix} 0 & 0 & -1 & \frac{c_t}{m_{us}} \end{bmatrix},$$

$$B_{s2}(\theta) = \begin{bmatrix} 0 & \frac{-\theta}{m_s} & 0 & \frac{\theta}{m_{us}} \end{bmatrix}$$

$$C_z = \begin{bmatrix} \frac{-k_s}{m_s} & \frac{-c_{nom}}{m_s} & 0 & \frac{c_{nom}}{m_s} \end{bmatrix},\ C_s = \begin{bmatrix} 1 & 0 & 0 & 0 \\ 0 & 1 & 0 & -1 \end{bmatrix},\ D_z(\theta) = \begin{bmatrix} \frac{-\theta}{m_s} \end{bmatrix}.$$

Note that the input matrices B_{s2} and D_z are parameter dependent so the *Assumption 1* is not satisfied. By using a strict low-pass filter as the one (3.4.8) in section 3.4 in Chapter 3, these matrices can be made parameter independent.

Remark 6.5.1. To our exhaustive knowledge, the LPV formulation 6.5.6 is used for the first time in semi-active suspension design.

Remark 6.5.2. Now we can explain the reason of using the quarter vehicle depicted in Fig. 6.4. As seen in *Assumption 2* in section 6.2.1, the bound on disturbance amplitude must be known for the synthesis. The question is: considering the bound of road disturbance and that of its velocity, which one is more significant? Let take for example two road profiles with the same maximum amplitude $z_{r1} = 0.01sin(2\pi 0.5)$ $[m]$ and $z_{r2} = 0.01sin(2\pi 5)$ $[m]$. It is worth noting that the maximal absolute velocity of z_{r_2} is five times larger than z_{r_1}. Obviously, z_{r_2} influences the vehicle dynamics more than z_{r_1} does because the energy contained in z_{r_2} is larger.
Moreover, in our case of LPV control, the scheduling parameter θ which is the damper deflection velocity (whose bound must be known as well for polytopic design) is influenced by the velocity of road disturbance more than by its amplitude. It means that the bound on the scheduling parameter θ is related to the road disturbance velocity rather than the road disturbance amplitude.
Both reasons above can explain the investigation of the model (6.4) (where $\dot{z}_r$ is considered as disturbance input) instead of the model (where z_r is considered as disturbance input) used in previous chapters.

6.5.3 Numerical analysis and results

We use the parameter of the Renault Mégane Coupé (see Tab. 1.1 in Chapter 1) for the quarter vehicle model (see Fig. 6.4) and the tire damping coefficient $c_t = 100$ $[Ns/m]$. The stroke of the suspension is 0.125 m

The road disturbance is described using the following common equation (see Fig. 6.5)

$$z_r = \begin{cases} \pm\frac{A}{2}\left(1 - \cos\left(\frac{2\pi V}{L}t\right)\right), & 0 \leq t \leq \frac{L}{V} \\ 0, & t > \frac{L}{V} \end{cases}$$

where A and L the height and length, V the vehicle velocity, "+" a bump, "-" a pothole. As in figure 6.5, we consider a road profile with a bump where $A = 0.15$ m, $L = 5$ m, $V = 27$ km/h at 0 s (corresponding to a low frequency disturbance) and a pothole where $A = 0.055$ m, $L = 5$ m, $V = 72$ km/h at 2.5 s (corresponding to a high frequency disturbance). The chosen road profile is suitable w.r.t the assumption on disturbance amplitude with $\delta = 0.5$ m^2/s^2.

In this preliminary study, we suppose that with this road disturbance, the working velocity of the damper is smaller than 1.2 m/s. The only state constraint is the suspension

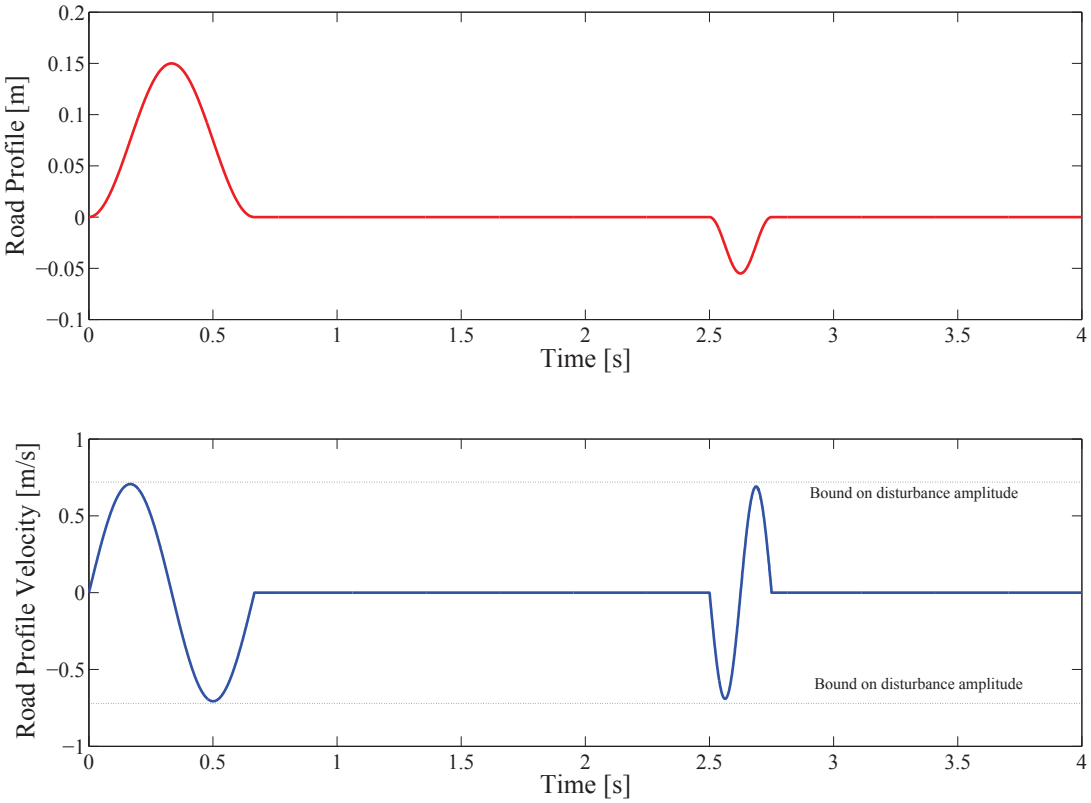

Figure 6.5: Road Profile.

deflection constraint $|z_{def}| < 0.125\ m$, i.e. the state constraint (6.3.1) defined with

$$H = \begin{bmatrix} 1 & 0 & 0 & 0 \end{bmatrix} \tag{6.5.7}$$

$$h_0 = 0.125 \tag{6.5.8}$$

We aim at improving the passenger comfort by minimizing the disturbance attenuation level γ of the closed-loop transfer function from w to z (while taking into account the constraints on the system input and states). To realize such a control objective we make use of the *optimization problem 2* in section 6.4. Like conventional H_∞ control, the weighting function on controlled output z is used. Once again, for this study, it is optimized using a genetic algorithm:

$$W_z(s) = \frac{0.4901s^2 + 1563s + 360.9}{s^2 + 217.7s + 788.9} \tag{6.5.9}$$

As seen in Fig. 6.6-6.7, we can improve the passenger comfort (the car body acceleration $\ddot{z}_s$ filtered by ISO 2631) w.r.t the passive open-loop cases (Soft Damper ($c = c_{min}$), Hard

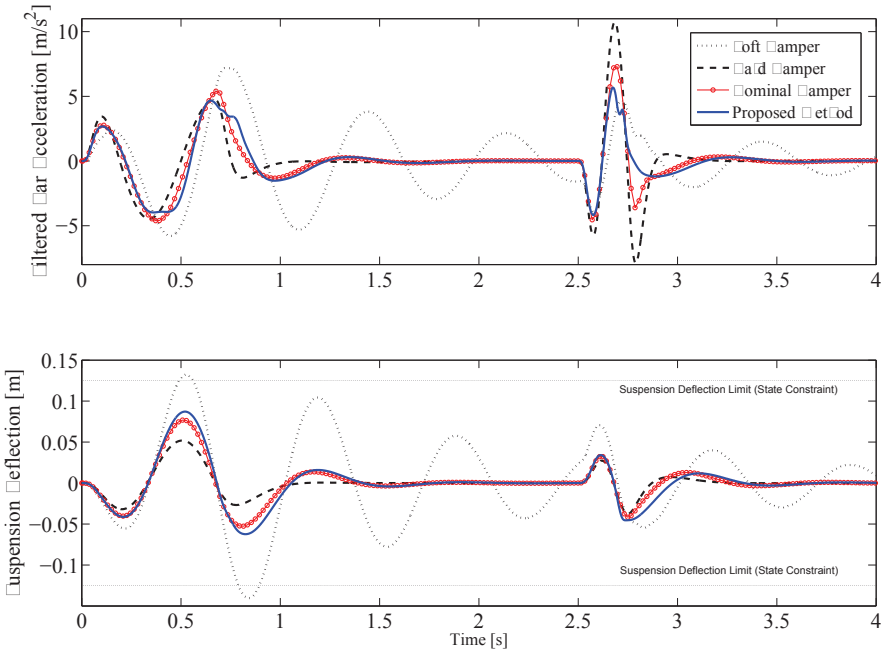

Figure 6.6: Performances Comparison.

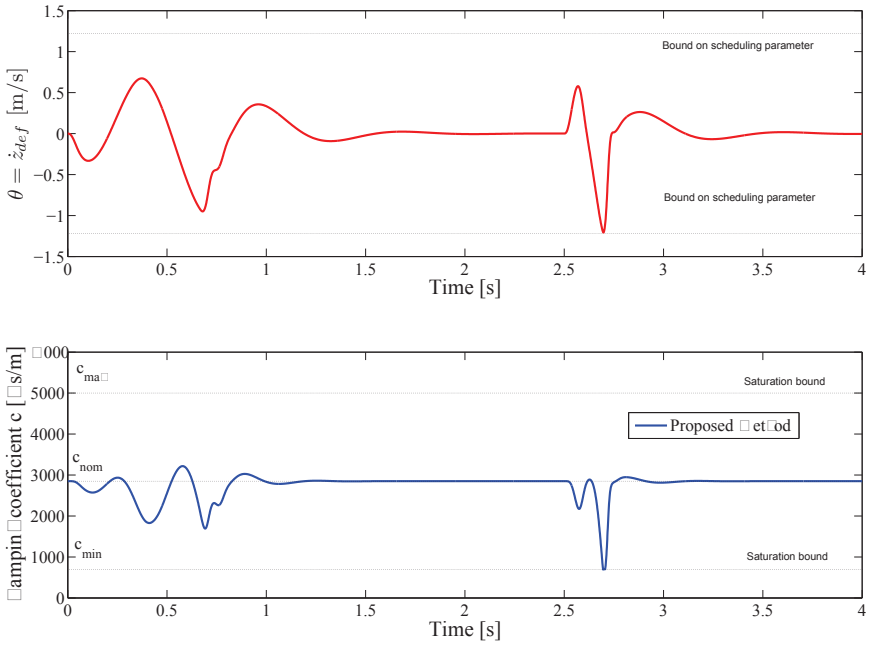

Figure 6.7: Scheduling parameter and saturation constraint.

Damper ($c = c_{max}$) and Nominal Damper ($c = c_{nom}$)). Observe that between 2.5 s and 3 s, the control effectively saturates, but the stability is kept. Indeed, during the saturation, the anti-windup acts and the performance does not degrade. Furthermore, it should be noticed that the limits of the suspension travel and the validity for the LPV system are not violated by the trajectory.

6.6 Conclusions

The contribution of the chapter may be summarized as follows:

- A new control design for general LPV systems with input saturation and state constraints has been proposed. The objective is that the H_∞ performance is minimized when the system is not saturated and the stability is always guaranteed even in the presence of input saturation. Besides, the controller guarantees some constraints on states of the closed-loop system.
- An application of this proposed method to semi-active suspension control has been considered. The simulation results have shown the efficiency of the proposed methodology w.r.t several passive cases.
- The proposed methodologies general for all LPV systems, henceforth we can make use of it for the case of nonlinear MR dampers presented in Chapter 3.

In future works, in order to better understand the real effectiveness of the introduced methodology, the significance of the simulation results will be improved by choosing better critical road disturbances. Moreover, a comparison with other strategies (Skyhook, Groundhook, Skyhook-ADD...) will be done.

Chapter 7

Conclusions and Future works

Main contributions

This thesis has been devoted to the problem of improving the vehicle dynamics in terms of comfort and road holding. This is mainly achieved through the suspension control systems. As far as we are concerned, we have more particularly studied the semi-active suspension control which in addition, is an interesting problem for both academic and industrial aspects. The results on this subject have been presented in Chapter 3, 4, 5 and 6. In summary, the main contributions of the thesis are:

In terms of modeling:

- An LPV control-oriented model for semi-active suspensions with Magneto-Rheological dampers (where the bi-viscous and hysteresis characteristics are taken into account) (Chapter 3).
- A new LPV model for linear damper control where the damper velocity is considered as a scheduling parameter (Chapter 6).

In terms of control methodologies:

- The design of a conventional LPV control method for Magneto-Rheological control (for nonlinear MR dampers) (Chapter 3).
- An extended version of the Skyhook-ADD control for nonlinear MR dampers (Appendix A).
- The design of a new clipped optimal control for semi-active suspension with linear hydraulic dampers based on the strong stabilization approach (Chapter 4 and 5).

- The design of a generic LPV control with input saturation and state constraints was proposed. The results obtained can be possibly applied for both nonlinear MR and linear dampers (Chapter 6).
- A multi-objective optimization procedure using genetic algorithms for semi-active suspension control problem. The interest of the methodology is in the fact that it can provide a set of controllers which may approach the best solutions for the multi-objective optimization problem in semi-active suspension control.

In terms of applications:

- Quarter car vehicle (for the comfort, road holding and suspension deflection improvement).
- Driver's seat (for the comfort and deflection improvement).

We would like to discuss a little further on the proposed multi-objective optimization procedure using genetic algorithms for suspension control. Although the case of semi-active suspension has been considered, it is possible to extend the results to a more general case where the synthesis of a controller satisfying many industrial performance criteria (in both frequency and time domains) is needed. The control schematic layout for such a multi-objective optimization problem is depicted in Fig. 7.1. The function of each block in a general context can be described as follows

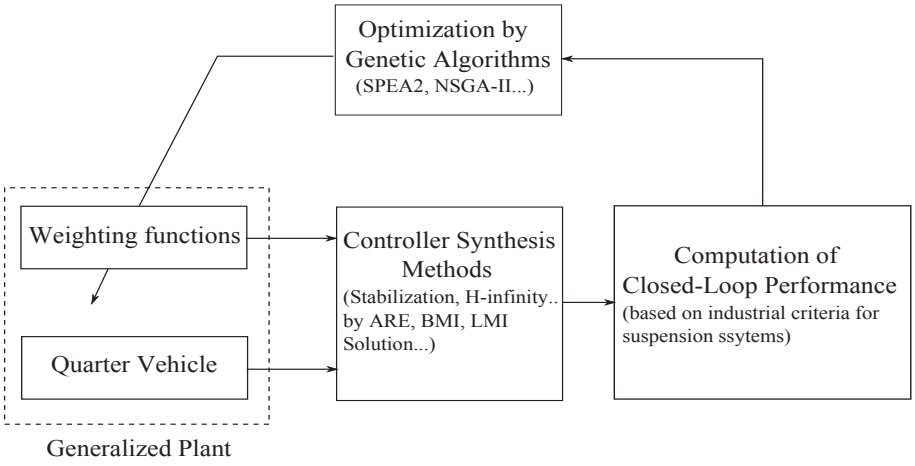

Figure 7.1: Schematic of the proposed control methods for semi-active suspension systems

- The weighting function: define the searching space (the space of all closed-loop performances that are possibly achieved with a predefined set of weighting functions).

- Controller synthesis methods: define the searching region (a reduced one of the searching space) which may contains the solutions with which the desired performances are achieved.
- Computation of closed-loop performance: provides a cost function for the optimization by genetic algorithms. It is very important to define an effective formulation of control objectives from the desired performances. The reason is that the desired (industrial) performances are usually multi-objective and may be not always mathematically represented. As a result, a reformulation of control objectives based on the control system is needed. A good formulation is the one with which a less number of objective functions are used and the optimization of these objective functions leads to the optimal desired performances.
- Genetic algorithms: a powerful MOEA (Multi-Objective Evolutionary Algorithm) helps achieving an optimal solution as fast as possible.

Finally, from the practical implementation point of view, the proposed control methods are interesting in the following points:

- Simple and easy to implement: a single relative displacement sensor to measure the suspension deflection (the deflection velocity can be deduced numerically from the deflection) is needed and the controllers are stable.
- Robust facing the load transfer and the sprung mass uncertainty (unavoidable factors appearing on a vehicle when it travels).

Future works

Although some results have been obtained, the work in this thesis can be further developed following some directions.

Short-term perspectives

- For MR dampers, the use of the strong stabilization approach for LPV systems is a key point to reduce the conservatism. In Chapter 3, the stable LPV controllers were not designed. We just used a "trick" (Algorithm 1, page 82) to remove the unstable controllers during the optimization by Genetic Algorithms. Besides, the application of the results in Chapter 6 for MR dampers will be tested and compared with the proposed methods (conventional LPV, extended Skyhook-ADD for MRD).
- Improving the simulation results in the Chapter 6 is necessary. Besides, the comparisons with other control methods are needed to show the effectiveness of the proposed method (LPV control subject to input saturation and state constraint).

- From the results obtained in Chapter 5, the study on DSS systems will be extended to controllable stiffness and damping systems
- A test of the proposed methods on real platform will be performed (hopefully).

Long-term perspectives

- As mentioned in Chapter 3 & 4 and in [Savaresi, Bittanti & Montiglio, 2005], the optimal solution for comfort or road holding oriented control problems is a switching control i.e. the damping coefficient switches between a minimal value c_{min} and a maximal value c_{max}. The investigation on switching control is worth a strong consideration. In [Geromel & Colaneri, 2006], [Geromel & Colaneri, 2010] (and references therein), the authors have proposed a method based on the Lyapunov-Metzler inequalities to determine the switching control law so that the stability and the minimization of a cost function are both guaranteed. These are good initializing papers for this direction.
- When working with the LPV systems, the synthesis using a whole range of scheduling parameters is very conservative. It would be better to separate the LPV systems in to smaller LPV subsystems and then switch among them so that the stability of the closed-loop system still remains and the performance is optimized. The idea is related to hybrid switching LPV control (see [Lim & Chan, 2003], [Lu & Wu, 2004] and references therein). For the case of semi-active suspension control, with the model using $\theta = \dot{z}_{def}$ in chapter 6, we can do, for example, the synthesis for $\theta \in [-0.5, 0.5]$ and $\theta = [-1.2, 1.2]$. Then we switch between two sub-systems (also LPV systems) depending on the working velocity of the damper. The idea is suitable for nonlinear Magneto-Rheological dampers as well.
- It can be seen throughout the thesis, the common procedure to solve the semi-active suspension optimization problem is to make use of probabilistic and stochastic Genetic Algorithms (see Fig. 7.1). Although as mentioned in the Remark 3.5.2 in page 109, the weighting functions parameters are the decision vector, it is interesting also to consider the same optimization procedure but with the controller parameters as a decision vector. Moreover, the test with different measurement output can be performed (as seen in Chapter 4, the use of suspension deflection gave good comfort controllers, otherwise the use of suspension deflection velocity offered good stroke controllers).
- Up to now, the suspension systems, steering systems and braking systems have been studied separately. The good cooperation among subsystems is not a trivial task as said Maurice Olley "The engineers had made all parts function excellently, but when put together the whole was seldom satisfactory". This motivate us for a global chassis control in the near future (see Fig. 7.2).

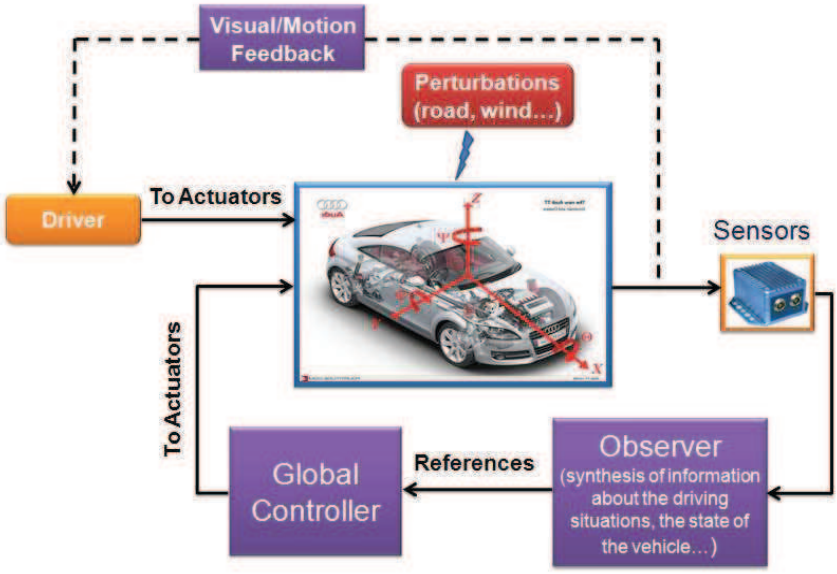

Figure 7.2: Global chassis control

Appendix A

Proof of Sky-hook and ADD for MR damper

This paper was written in my first visiting period at DEI, Polimi (from November 2009 to February 2010) and was presented at the IFAC conference in Ancona, Italy, in September 2010 (see full version in [Do, Sename, Dugard, Savaresi, Spelta & Delvecchio, 2010]).

The aim of this paper extends the Mixed Skyhook-ADD to the MR dampers.

A.1 Extended Skyhook for MR damper

Sky-hook for MRD - B: The main idea of the Skyhook for linear suspension system is that the damper exerts a force that reduces the velocity of the body mass $\dot{z}_s$. By using the same principle, the modified Sky-hook for MR damper will be as follows

$$f_I = \begin{cases} f_{max} & \text{if} \quad \dot{z}_s\rho > 0 \\ f_{min} & \text{if} \quad \dot{z}_s\rho \leq 0 \end{cases} \tag{A.1.1}$$

where $\rho = \tanh(c_1\dot{z}_{def} + k_1 z_{def})$.

The explanation can be illustrated by Fig. A.1. In this model, the damper force is $f_I\rho$. If the sprung mass m_s is moving upward, there are two possibilities: if $\rho > 0$, we maximize the damper force by choosing $f_I = f_{max}$ to pull the sprung mass downward, if $\rho \leq 0$ we minimize the damper force by choosing $f_I = f_{min}$ to avoid increasing more the movement of the sprung mass. The same reason is used for the case when the sprung mass is moving downward.

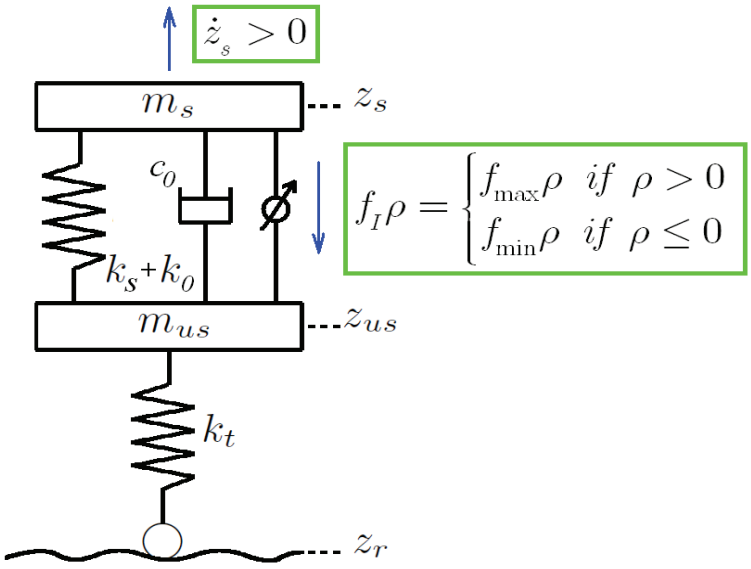

Figure A.1: Illustration of the extended Skyhook control for MR damper

A.2 Extended ADD for MR damper

The following modified ADD for MR dampers is inspired by the physical meaning of the existing ADD algorithm presented in [Savaresi, Silani & Bittanti, 2005].

$$f_I = \begin{cases} f_{max} & \text{if} \quad \ddot{z}_s\rho > 0 \\ f_{min} & \text{if} \quad \ddot{z}_s\rho \leq 0 \end{cases} \tag{A.2.1}$$

where $\rho = \tanh(c_1\dot{z}_{def} + k_1 z_{def})$.

Indeed, the control law (A.2.1) turns out to be very simple to explain. Looking at the dynamical equation of the quarter vehicle with MR damper, the only variable parameter is f_I, so when $\ddot{z}_s \tanh(c_1\dot{z}_{def} + k_1 z_{def}) > 0$, for example $\ddot{z}_s$ and $\tanh(c_1\dot{z}_{def} + k_1 z_{def})$ are positive, $\ddot{z}_s$ will rapidly decrease to zero if $f_I = f_{max}$. On the contrary, when $\ddot{z}_s \tanh(c_1\dot{z}_{def} + k_1 z_{def}) \leq 0$, $\ddot{z}_s$ will be kept not floating away from zero if $f_I = f_{min}$, and so on.

We present here the proof for the modified ADD which is based on the one given in [Savaresi, Silani & Bittanti, 2005] (proven for the case of a quarter vehicle model equipped with a linear damper).

The dynamic equations of a quarter car model equipped with an MR damper are given

by

$$\begin{cases} m_s\ddot{z}_s &= -k_s z_{def} - c_0\dot{z}_{def} - k_0 z_{def} \\ & \quad -f_I \tanh\left(c_1\dot{z}_{def} + k_1 z_{def}\right) \\ m_{us}\ddot{z}_{us} &= k_s z_{def} + c_0\dot{z}_{def} + k_0 z_{def} \\ & \quad f_I \tanh\left(c_1\dot{z}_{def} + k_1 z_{def}\right) - k_t\left(z_{us} - z_r\right) \\ \dot{f}_I &= -\beta f_I + \beta u \end{cases} \tag{A.2.2}$$

where β represents the bandwidth of a real MR damper and u is the control input which can take its values in $[f_{Imin}, f_{Imax}]$.

A state-space representation of (A.2.2) is given by

$$\dot{x} = f(x) + Bu + Pz_r \tag{A.2.3}$$

where
$x = \begin{pmatrix} \dot{z}_s & \dot{z}_{us} & f_I & z_s & z_{us} \end{pmatrix}^T$,

$f(x) = \begin{pmatrix} \frac{-k}{m_s}(x_4 - x_5) - \frac{c_0}{m_s}(x_1 - x_2) - \frac{\rho(x)}{m_s}x_3 \\ \frac{k}{m_{us}}x_4 - \frac{k+k_t}{m_{us}}x_5 + \frac{c_0}{m_{us}}(x_1 - x_2) + \frac{\rho(x)}{m_{us}}x_3 \\ -\beta x_3 \\ x_1 \\ x_2 \end{pmatrix}$ where $k = k_s + k_0$ and $\rho(x) = tanh(c_1(x_1 - x_2) + k_1(x_4 - x_5))$,

$B = \begin{pmatrix} 0 & 0 & \beta & 0 & 0 \end{pmatrix}^T$, $P = \begin{pmatrix} 0 & \frac{k_t}{m_{us}} & 0 & 0 & 0 \end{pmatrix}^T$

The global optimization using the Minimum Principle of Pontryagin can be used for the nonlinear system (A.2.3) with a constraint on the control input $u \in [f_{Imin}, f_{Imax}]$. Consider only the known parts of (A.2.3) (without road disturbance Pz_r). Let define the control problem

$$\text{minimize} \qquad J = \int_{t_0}^{t_f} \ddot{z}_s^2 dt = \int_{t_0}^{t_f} l(x)dt \tag{A.2.4}$$

where $l(x) = (\frac{-k}{m_s}(x_4 - x_5) - \frac{c_0}{m_s}(x_1 - x_2) - \frac{\rho(x)}{m_s}x_3)^2$

subject to

$$\dot{x} = f(x) + Bu \tag{A.2.5}$$

$$u \in [f_{Imin}, f_{Imax}] \tag{A.2.6}$$

$$t_f = t_0 + \Delta T \tag{A.2.7}$$

Appendix A. Proof of Sky-hook and ADD for MR damper

The Hamiltonian function is defined by

$$H(x,u,\lambda) = l(x) + \lambda^T[f(x) + Bu] \tag{A.2.8}$$

Let $(u^*(t), x^*(t))$ is the optimal solution of problem (A.2.4). The adjoint equation is

$$\dot{\lambda}(t) = -\nabla_x H(x^*(t), u^*(t), \lambda(t)) \tag{A.2.9}$$

with $\lambda(t_f) = 0$.

Minimize the Hamiltonian gives

$$u^*(t) = \underset{u(t)\in[f_{Imin}, f_{Imax}]}{\arg\min} H(x^*(t), u(t), \lambda(t)) \tag{A.2.10}$$

The problems (A.2.9) and (A.2.10) are difficult to solve, however, it can be seen from Eq. (A.2.8) that the optimal control law of a semi-active suspension with comfort objective without preview is a genuine on - off strategy and is given by

$$u^*(t) = \begin{cases} f_{Imin} & \text{if} \quad B^T\lambda(t) > 0 \\ f_{Imax} & \text{if} \quad B^T\lambda(t) \leq 0 \end{cases} \tag{A.2.11}$$

In order to find an explicit solution of u, consider the linear approximation of the system (A.2.3) around the initial condition $(x(t_0), u(t_0), z_r(t_0)$. After some manipulations, one has

$$\dot{x} = Ax + Bu + Pz_r + E \tag{A.2.12}$$

where

$$A = \begin{pmatrix} -\frac{a_0}{m_s} & \frac{a_0}{m_s} & \frac{\rho_0}{m_s} & -\frac{a_1}{m_s} & \frac{a_1}{m_s} \\ \frac{a_0}{m_{us}} & -\frac{a_0}{m_{us}} & \frac{\rho_0}{m_{us}} & \frac{a_1}{m_{us}} & -\frac{a_1}{m_{us}} \\ 0 & 0 & -\beta & 0 & 0 \\ 1 & 0 & 0 & 0 & 0 \\ 0 & 1 & 0 & 0 & 0 \end{pmatrix},$$

$a_0 = c_0 + x_{30}(1-{\rho_0}^2)c_1$, $a_1 = k + x_{30}(1-{\rho_0}^2)k_1$, $\rho_0 = \rho(x(t_0)) = tanh(c_1(x_{10} - x_{20}) + k_1(x_{40} - x_{50}))$ and x_{i0} is the i^{th} component of the state vector $x(t_0)$.

$$E = \begin{pmatrix} \frac{((x_{10}-x_{20})c_1+(x_{40}-x_{50})k_1)x_{30}(1-{\rho_0}^2)}{m_s} \\ -\frac{((x_{10}-x_{20})c_1+(x_{40}-x_{50})k_1)x_{30}(1-{\rho_0}^2)}{m_{us}} \\ 0 \\ 0 \\ 0 \end{pmatrix}$$

Appendix A. Proof of Sky-hook and ADD for MR damper

By using the Lagrange Formula, $x(t)$ at $t_0 + \Delta T$ can be computed

$$\begin{aligned} x(t_0 + \Delta T) &= e^{A(\Delta T)} x(t_0) \\ &\quad + \int_{t_0}^{t_0+\Delta T} e^{A(t_0+\Delta T-\tau)}(Bu(\tau) + Pz_r(\tau) + E)d\tau \end{aligned} \tag{A.2.13}$$

Assume that, during the sampling interval ΔT, the control input is constant $u = \overline{u}$ and the body car acceleration $\ddot{z}_s(t)$ or $\dot{x}_1(t)$ does not change its sign. The optimal solution u is given as

$$\begin{aligned} \overline{u}_{opt}(t_0, t_0 + \Delta T) &= \underset{\overline{u}\in[f_{Imin}, f_{Imax}]}{\arg\min} \; (\dot{x}_1(t_0 + \Delta T)^2) \\ &= \begin{cases} \underset{\overline{u}\in[f_{Imin}, f_{Imax}]}{\arg\min} \; (\dot{x}_1(t_0 + \Delta T)) & \text{if } \ddot{z}_s(t_0) > 0 \\ \underset{\overline{u}\in[f_{Imin}, f_{Imax}]}{\arg\max} \; (\dot{x}_1(t_0 + \Delta T)) & \text{if } \ddot{z}_s(t_0) \leq 0 \end{cases} \\ &= \begin{cases} \underset{\overline{u}\in[f_{Imin}, f_{Imax}]}{\arg\min} \; (g_u(t_0 + \Delta T)) & \text{if } \ddot{z}_s(t_0) > 0 \\ \underset{\overline{u}\in[f_{Imin}, f_{Imax}]}{\arg\max} \; (g_u(t_0 + \Delta T)) & \text{if } \ddot{z}_s(t_0) \leq 0 \end{cases} \end{aligned} \tag{A.2.14}$$

where $g_{\overline{u}}(t_0 + \Delta T) = \left.\frac{d(\overline{u}\int_{t_0}^{t} e^{A(t-\tau)}Bd\tau)_1}{dt}\right|_{t=t_0+\Delta T}$ and subscript "1" indicates the first element of the vector $\overline{u}\int_{t_0}^{t} e^{A(t-\tau)}Bd\tau$. By using the Taylor series expansion for $e^{A(t-\tau)}$, the following approximation is used for the calculation of $g_{\overline{u}}(t_0 + \Delta T)$:

$$e^{A(t-\tau)} = I + A(t-\tau) + \frac{1}{2}A^2(t-\tau)^2 + \frac{1}{6}A^3(t-\tau)^3 \tag{A.2.15}$$

Finally one has

$$g_{\overline{u}}(t_0 + \Delta T) = -\overline{u}\rho_0\beta\gamma(\Delta T, \rho_0, x_{30}) \tag{A.2.16}$$

Due to the length and the complexity, the explicit form of $\gamma(\Delta T, \rho_0, x_{30})$ is not given here. But note that with the damper's bandwidth $\beta = 40\pi$, $\rho_0 \in [-1, 1]$ and the initial state $x_{30} \in [0, 870]$, one always has $\gamma(\Delta T, \rho_0, x_{30}) > 0$. From Eq. (A.2.14) and Eq. (A.2.16), the optimal solution is finally given as:

$$\overline{u}_{opt}(t_0, t_0 + \Delta T) = \begin{cases} f_{Imax} & \text{if } \ddot{z}_s(t_0)\rho_0 > 0 \\ f_{Imin} & \text{if } \ddot{z}_s(t_0)\rho_0 \leq 0 \end{cases} \tag{A.2.17}$$

The control law proposed in (A.2.1) has been proved.

A.3 Extended Mixed Skyhook-ADD (SH-ADD) for MR dampers

The Extended Mixed SH-ADD algorithm guarantees the best behavior of both Skyhook and ADD (A.2.1) and is given as follows

$$f_I = \begin{cases} f_{max} & \text{if} \quad (\ddot{z}_s^2 - \alpha \dot{z}_s^2 \leq 0 \wedge \dot{z}_s \hat{\rho} > 0) \vee \\ & \qquad (\ddot{z}_s^2 - \alpha \dot{z}_s^2 > 0 \wedge \ddot{z}_s \hat{\rho} > 0) \\ f_{min} & \text{if} \quad (\ddot{z}_s^2 - \alpha \dot{z}_s^2 \leq 0 \wedge \dot{z}_s \hat{\rho} \leq 0) \vee \\ & \qquad (\ddot{z}_s^2 - \alpha \dot{z}_s^2 > 0 \wedge \ddot{z}_s \hat{\rho} \leq 0) \end{cases} \tag{A.3.1}$$

where $\hat{\rho} = \tanh(c_1 \dot{z}_{def} + k_1 z_{def})$.

The amount $(\ddot{z}_s^2 - \alpha \dot{z}_s^2)$ is the frequency-range selector and α is the SH-ADD crossover frequency (see [Savaresi & Spelta, 2007]).

Appendix B

Nonlinear Frequency Response - (Pseudo-Bode)

The following nonlinear frequency response analysis is done by using the "variance gain" algorithm (see [Savaresi, Silani & Bittanti, 2005]) for nonlinear systems. The "variance gain" is simple and provides a good approximation to frequency response.

- Feed the system with a sinus signal $z_{r_i} = A_r sin(\omega_i t)$ ($\omega_{min} \leq \omega_i \leq \omega_{max}$, i=1,2,3...N and $t \in [0, T]$).
- For each input, measure output signals; for example, to evaluate the comfort, the body car acceleration $\ddot{z}_{s_i}$ is measured.
- The approximate variance gain is computed and is defined as

$$F_{acc}(\omega_i) = \sqrt{\frac{\frac{1}{T}\int_0^T (\ddot{z}_{s_i})^2 dt}{\frac{1}{T}\int_0^T (z_{r_i})^2 dt}} \quad (i = 1, 2, 3...N) \tag{B.0.1}$$

Appendix C

Paper CDC-2010

This paper was done in my first visiting period at DEI, Polimi (from November 2009 to February 2010) and was presented at the CDC conference in Atlanta, USA, in 2010.

The aim of this paper is to propose a hybrid control method based on switching (the Extended ADD for MR Dampers) and LPV control to reduce the effect of end-stop collision on the passenger comfort.

An LPV Control Approach for Comfort and Suspension Travel Improvements of Semi-Active Suspension Systems

□n□ □am □o□□ristiano □pelta□□er□io □a□aresi□□li□ier □ename□□uc □u□ard and □ie□o □el□ecc□io

***Abstract*— In this paper, we present a new H_∞/LPV control method to improve the trade-off between comfort and suspension travel. Firstly, a semi-active automotive suspension equipped with a nonlinear static semi-active damper is presented. Secondly, the semi-active suspension system is reformulated in the LPV framework which can be handled in a polytopic way. Finally, in numerical analysis, to emphasize the performance of the proposed controller, the end-stop event is introduced. The results show that the proposed method provides a good improvement in comfort and suspension travel compared with other strategies.**

□. □□TR□□□□T□□□

□mon□t□e many different types of controlled suspensions □see e.□ [1] for a detailed classi□cation□□semi□acti□e sus□pensions □a□e rece□ed a lot of attention in t□e last t□o decades□since t□ey pro□ide t□e best compromise bet□een cost □ener□y consumption and actuators/sensors □ard□are□ and performance □see e.□ [2]□[3]□[4]□[5]□[□]□[□].

□ classical semi□acti□e suspension is c□aracteri□ed by t□e closed□loop re□ulation of t□e dampin□ coef□cient□t□e electronic modulation of t□e dampin□ coef□cient is obtained □it□ □a□neto□R□eolo□ical □□R□□□lectro□R□eolo□ical □□R□ or □lectro□□ydraulic □□□□ tec□nolo□ies. □n t□e last years□ □ariable□dampin□ semi□acti□e suspensions □a□e □ad a lar□e □ro□t□and today t□ey are employed o□er a □ide ran□e of application domains□road □e□icles suspensions□cabin sus□pensions in truc□s or a□ricultural tractors□seat suspensions□ lateral suspensions in □i□□speed trains□etc. □see e.□ [□]□[□]□[□]□[10]□[11]□[12]□[13]□[14]□[□]□[15]□.

□t can be seen t□at t□e main semi□acti□e suspension con□trol problems to be sol□ed are trade□offs bet□een comfort□ □andlin□ and suspension tra□el. □n [1□]□t□e semi□acti□e control problem □as been e□plored usin□ □inear Parameter Varyin□ □*LPV*□tec□ni□ue. T□e met□odolo□y is based on a nonlinear static model of t□e semi□acti□e damper□□□ere t□e bi□□iscous and □ysteretic be□a□iors of t□e semi□acti□e damper are ta□en into account. T□en□t□e nonlinear system associated □it□ t□e □uarter □e□icle model is reformulated in t□e *LPV* frame□or□. T□e passi□ity problem of semi□acti□e dampers is recast into t□e problem of input saturation. □inally□t□e H_∞/LPV controller is synt□esi□ed to ac□ie□e t□e performance ob□ecti□es □passen□er comfort and □andlin□□□□ile satisfyin□ t□e passi□ity constraint of semi□acti□e dampers.

□n t□is paper□t□e trade□off bet□een passen□er comfort and suspension tra□el □ill be considered. □t is □uite ob□ious□ □□ile t□e comfort/□andlin□ trade□off □as been studied in many approac□es durin□t□e past decades□t□at t□e suspension tra□el issue □as not been al□ays considered. □ittin□ t□e structural limits □□en road disturbance is particularly tou□□ de□rades dramatically t□e passen□er comfort □t□e so□called end□stop effect□and decreases t□e lifetime of □e□icle com□ponents. T□e *LPV* control met□od used in [1□] is modi□ed by includin□ a comfort oriented control rule □□cceleration □ri□en □ampin□□ontrol □*ADD*□□see e.□[□]□and a sc□edul□in□factor t□at permits an impro□ement of suspension tra□el.

T□e outline is as follo□s. □n □ection □□□t□e □uarter car model □it□ a nonlinear semi□acti□e damper and t□e control problem on t□is model are presented. □n □ection □□□□a ne□ H_∞/LPV controller to impro□e t□e trade□off bet□een comfort and suspension tra□el is desi□ned. □n □ection □V□t□e results obtained in simulations □it□ a nonlinear □uarter car model are discussed. □inally□some conclusions and perspecti□es are dra□n in □ection V.

□□. P□□B□□□ □T□T□□ □□T

A. Quarter Car Model

□onsider a simple model of □uarter □e□icle □see □i□. 1□ made up of a sprun□ mass m_s□and an unsprun□ mass m_{us}□. □ sprin□ □it□ t□e stiffness coef□cient k_s and a semi□acti□e damper connect bot□ masses. T□e □□eel tire is modeled by a sprin□ □it□ t□e stiffness coef□cient k_t. □n t□is model□z_s □respecti□ely z_{us}□is t□e □ertical position of m_s □respecti□ely m_{us}□and z_r is t□e road pro□le. □t is assumed t□at t□e □□eel□ road contact is ensured.

T□e dynamical e□uations of a □uarter □e□icle are □o□erned

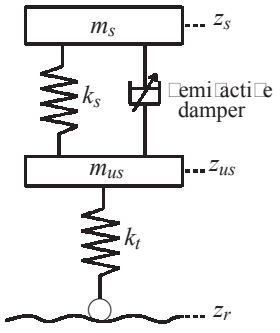

□i□ 1. □odel of □uarter □e□icle □it□ a semi□acti□e damper.

□. □. □o□□. □ename and □. □u□ard are □it□ □□P□□lab□□ontrol □ystems □ept□□□R□□renoble □□P□□□□3□BP 4□□□3□402 □t □ar□tin d□□res cede□□ □rance {anh-lam.do, olivier.sename, luc.dugard}@gipsa-lab.grenoble-inp.fr

□. □pelta is □it□ □ni□ersita de□li □tudi di Ber□amo□□iale □arconi 5□ 24044 □almine B□□□□taly cristiano.spelta@unibg.it

□. □a□aresi□□. □el□ecc□io are □it□ □ipartimento di □lettronica e □nfor□ma□ione□Politecnico di □ilano□Pia□a □. da Vinci□32□20133□□ilano □ □taly {savaresi, delvecchio}@elet.polimi.it

by

$$\begin{cases} m_s\ddot{z}_s = -F_{spring} - F_{damper} \\ m_{us}\ddot{z}_{us} = F_{spring} + F_{damper} - k_t(z_{us} - z_r) \end{cases} \quad (1)$$

where $F_{spring} = k_s z_{def}$ is the spring force, $z_{def} = z_s - z_{us}$ is the damper deflection (assumed to be measured or estimated), $\dot{z}_{def} = \dot{z}_s - \dot{z}_{us}$ is the deflection velocity.

In this paper the behavior of a realistic semi-active suspension is represented using the following nonlinear equation as in [1]

$$F_{damper} = c_0\dot{z}_{def} + k_0 z_{def} + f_I \tan(c_1\dot{z}_{def} + k_1 z_{def}) \quad (2)$$

where c_0, k_0, c_1 and k_1 are constant parameters and f_I is a controllable force. The interest in this model is that it allows fulfilling the passivity constraint of the semi-active damper by considering only the constraint

$$0 \le f_{min} \le f_I \le f_{max} \quad (3)$$

The dynamical equations (1), (2) can then be rewritten as

$$\begin{cases} m_s\ddot{z}_s = -(k_s + k_0)z_{def} - c_0\dot{z}_{def} - f_I \tan(c_1\dot{z}_{def} + k_1 z_{def}) \\ m_{us}\ddot{z}_{us} = (k_s + k_0)z_{def} + c_0\dot{z}_{def} + f_I \tan(c_1\dot{z}_{def} + k_1 z_{def}) \\ \qquad - k_t(z_{us} - z_r) \end{cases} \quad (4)$$

B. The End-stop Phenomenon

The end-stop phenomenon happens when the piston hits the rubber bushings because of the tough road disturbance. This phenomenon generates a shock that makes passengers uncomfortable. In this paper the end-stop effect is simply modeled as follows

$$F_{spring} = \begin{cases} k_s z_{def} & \text{if} \quad |z_{def}| < \Delta_{es} \\ k_{es} z_{def} & \text{if} \quad |z_{def}| \ge \Delta_{es} \end{cases} \quad (5)$$

where Δ_{es} is the suspension stroke and $k_{es} \gg k_s$ (typically represents the stiffness of rubber bushings).

The end-stop effect is shown in Fig. 2. It is obvious that hitting the structural limits deteriorates dramatically the car body acceleration (i.e. the passenger comfort).

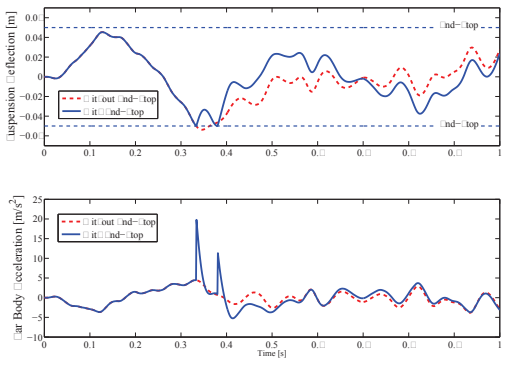

Fig. 2. Time history of the suspension deflection (top) and the body acceleration (bottom) with and without the end-stops.

C. Cost Function

In this paper the following criteria are used to evaluate the performance of the proposed controller

$$J_{acc} = \sqrt{\frac{1}{T}\int_0^T \ddot{\bar{z}}_s^2(t)} \quad (6)$$

$$J_{def} = \sqrt{\frac{1}{T}\int_0^T z_{def}^2(t)} \quad (7)$$

where $\ddot{\bar{z}}_s(t)$ is the filtered car body acceleration (by ISO 2631 filter) $[m/s^2]$, z_{def} is the damper deflection $[m]$ and T is the simulation running time $[s]$. The ISO 2631 filter (see [18]) represents the sensitivity of human to body car acceleration and is given as

$$F_{ISO-2631} = \frac{81.89s^3 + 796.6s^2 + 1937s + 0.1446}{s^4 + 80.00s^3 + 2264s^2 + 7172s + 21196} \quad (8)$$

The criteria (6) and (7) are used to evaluate the comfort and the suspension travel, respectively. It can be seen that when the end-stop event occurs, the peak values in car body acceleration (as seen in Fig. 2) resulting from this effect will be taken into account in J.

D. Acceleration Driven Damping Control (ADD)

This paper is based on the extension of *ADD* control rule [6]. The *ADD* is based on a linear model of the electronic shock absorber, $F = c\dot{z}_{def}$ where $\dot{z}_{def}$ is the suspension deflection velocity and c is the damping coefficient that may vary from a minimum value c_{min} to a maximum value c_{max}.

The *ADD* switching rule is as follows:

$$c = \begin{cases} c_{max} & \text{if } \ddot{z}_s\dot{z}_{def} > 0 \\ c_{min} & \text{if } \ddot{z}_s\dot{z}_{def} \le 0 \end{cases} \quad (9)$$

ADD, a comfort-oriented control method, has been proven to approximate the solution of an optimal control problem where the cost function is the integral of the squared body car acceleration, the suspension system is modeled as a linear quarter car, the road disturbance is described as a white noise and the optimization horizon is based on one step of simulation. The limitation of this method is that the suspension travel has been not improved.

III. Control Design for Comfort and Stroke

To obtain a better compromise between the ride quality and the suspension travel, a new control method is presented as follows

$$\begin{aligned} f_I &= f_{max}h_{sw} + (u + \alpha f_{max})(1 - h_{sw}) \\ &= f_{max}[\alpha + h_{sw}(1 - \alpha)] + u(1 - h_{sw}) \end{aligned} \quad (10)$$

where $0 \le \alpha \le 1$ and $h_{sw} \in \{0, 1\}$ are two parameters and u is the control input to design. In the following, the roles of α, h_{sw} and u are explained.

- The switching control rule h_{sw} is chosen so that it specially enhances the passenger comfort. In this paper, the design of h_{sw} is based on the *ADD* control rule (9).

- It can be seen that the smaller α, the more comfortable the car but the bigger the suspension travel and vice-versa.
- The control input u is designed in the H_∞/LPV framework to improve the suspension travel without deteriorating the comfort too much for all values of h_{sw} and α.

A. Design of Comfort-Oriented Switching Controller h_{sw}

The following control rule is inspired by the existing ADD algorithm developed for the linear suspension systems in [7]. The idea turns out to be very simple. Looking at (1) and (2), the only variable parameter is f_I, so when $\ddot{z}_s \tanh\left(c_1\dot{z}_{def}+k_1 z_{def}\right) > 0$, for example $\ddot{z}_s$ and $\tanh\left(c_1\dot{z}_{def}+k_1 z_{def}\right)$ are positive, $\ddot{z}_s$ will rapidly decrease to zero if f_I □f_{max}. On the contrary, when $\ddot{z}_s \tanh\left(c_1\dot{z}_{def}+k_1 z_{def}\right) \le 0$, $\ddot{z}_s$ will be kept not floating away from zero if f_I □f_{min}. □ence, the on-off comfort-oriented control rule is summarized as follows:

$$f_I = \begin{cases} f_{max} & \text{if } \ddot{z}_s \tanh\left(c_1\dot{z}_{def}+k_1 z_{def}\right) > 0\big) \\ & \qquad (\text{i.e } \ h_{sw}=1) \\ f_{min} & \text{if } \ddot{z}_s \tanh\left(c_1\dot{z}_{def}+k_1 z_{def}\right) \le 0\big) \\ & \qquad (\text{i.e } \ h_{sw}=0) \end{cases} \tag{11}$$

Noticing that in the case of linear semi-active damper, k_1 □0, $sign(\tanh\left(c_1\dot{z}_{def}+k_1 z_{def}\right)) \equiv sign(\dot{z}_{def})$, the rule (11) is the same as the conventional ADD algorithm.

B. Choice of α

In order to detect the suspension travel limits (the End-stop event) and to enlarge as much as possible the capacity of the H_∞/LPV controllers, α can be chosen as

$$\alpha(\varepsilon) = 0.\square \frac{\mu\varepsilon^{2n}}{\mu\varepsilon^{2n}+1/\mu} \tag{12}$$

where μ modifies the slope of the $\alpha(\varepsilon)$ function and is chosen sufficiently high, n is an integer. See Fig. 3 for various values of α.

In this paper, $\varepsilon = z_{def}+\dot{z}_{def}/\lambda$. The factor λ can be roughly chosen so that $\alpha(\varepsilon)$ is close to zero when the car body acceleration of the open loop system ($f_I = 0$) is close to zero. Not that, from Eq. (4), one has

$$\ddot{z}_s = 0 \Leftrightarrow z_{def} + \frac{c_0}{k_s+k_0}\dot{z}_{def} = 0 \quad (\text{with } f_I = 0)$$

So $\lambda = (k_s+k_0)/c_0$ can be a good choice.

C. H_∞/LPV Control Design u

From Eq. (10), the constraint (3) on f_I is tantamount to the following inequality

$$|u| \le f_\alpha \tag{13}$$

where $f_\alpha = min\{\alpha, 1-\alpha\} f_{max}$. □ence, the passivity constraint of the semi-active damper is recast as the saturation constraint on the control input u.

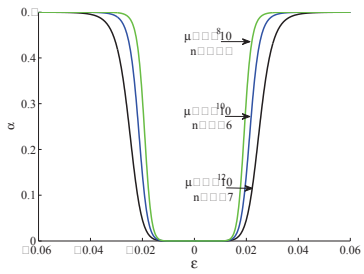

Fig. 3. □arious values of α

1) LPV Formulation For Ideal Linear Design: For simplicity, in this step, the saturation constraint (13) is omitted. The nonlinear model (1)-(2)-(10) is now rewritten in the L□□ framework.

$$P: \begin{cases} \dot{x}_s = (A_s + B_{s2}\frac{[\alpha+h_{sw}(1-\alpha)]\tanh(C_{s2}x_s)}{C_{s2}x_s}C_{s2})x_s \\ \qquad\quad + B_s(1-h_{sw})\tanh\left(C_{s2}x_s\right)u + B_{s1}w \\ y = C_s x_s \end{cases} \tag{14}$$

where x_s □$(z_s,\ \dot{z}_s,\ z_{us},\ \dot{z}_{us})^T$, u: control input, w□z_r disturbance, y□z_s-z_{us} measurement output,

$$A_s = \begin{pmatrix} 0 & 1 & 0 & 0 \\ -\frac{k_s+k_0}{m_s} & -\frac{c_0}{m_s} & \frac{k_s+k_0}{m_s} & \frac{c_0}{m_s} \\ 0 & 0 & 0 & 1 \\ \frac{k_s+k_0}{m_{us}} & \frac{c_0}{m_{us}} & -\frac{k_s+k_0+k_t}{m_{us}} & -\frac{c_0}{m_{us}} \end{pmatrix}$$

$$B_s = \begin{pmatrix} 0 \\ -\frac{1}{m_s} \\ 0 \\ \frac{1}{m_{us}} \end{pmatrix},\ B_{s1} = \begin{pmatrix} 0 \\ 0 \\ 0 \\ \frac{k_t}{m_{us}} \end{pmatrix},\ B_{s2} = \begin{pmatrix} 0 \\ -\frac{f_{max}}{m_s} \\ 0 \\ \frac{f_{max}}{m_{us}} \end{pmatrix},$$

$$C_s = \begin{pmatrix} 1, 0, -1, 0 \end{pmatrix},\ C_{s2} = \begin{pmatrix} k_1, c_1, -k_1, -c_1 \end{pmatrix}$$

In (14) the control input matrix $B_s(1-h_{sw})\tanh\left(C_{s2}x_s\right)$ is parameter dependent, which is not consistent with the solution of the H_∞ design problem for systems as in [19], [20]. This problem can be easily solved by adding a strictly proper filter into (14) to make the controlled input matrix independent from the scheduling parameter (see [21]). □esides, this filter allows for modeling low-pass dynamics of semi-active dampers.

$$F: \begin{pmatrix} \dot{x}_f \\ u \end{pmatrix} = \begin{pmatrix} A_f & B_f \\ C_f & 0 \end{pmatrix} \begin{pmatrix} x_f \\ u_c \end{pmatrix} \tag{1□}$$

where A_f, B_f, C_f are constant matrices and u_c is the controller output.

2) LPV Reformulation For Linear Design with Input Saturation: Let now include the saturation constraint (13) in the L□□ controller design. First the system is augmented by adding a saturating function block as in Fig. 4. where

Fig. 4. Linear design with input saturation.

$$u = sat(u_f) = \begin{cases} f_\alpha & \text{if} \quad u_f > f_\alpha \\ u_f & \text{if} \quad -f_\alpha \le u_f \le f_\alpha \\ -f_\alpha & \text{if} \quad u_f < -f_\alpha \end{cases} \tag{16}$$

To cope with a linear control design, the saturation function $sat(u_f)$ is roughly approximated by a tangent hyperbolic function: $f_\alpha tanh(\frac{u_f}{f_\alpha})$ or $f_\alpha tanh(\frac{C_f x_f}{f_\alpha})$. The interest of the use of tangent hyperbolic function is its bounded derivative which may be exploited in L□□ design with parameters-dependent Lyapunov function to reduce the conservatism (in future work). The state-space representation of the transfer function from u_c to u is then:

$$F_1 : \begin{pmatrix} \dot{x}_f \\ u \end{pmatrix} = \begin{pmatrix} A_f & B_f \\ C_f \tanh(\psi)/\psi & 0 \end{pmatrix} \begin{pmatrix} x_f \\ u_c \end{pmatrix} \quad (17)$$

where $\psi = \frac{C_f x_f}{f_\alpha}$

Finally, from (14) and (17), an L□□ model formulation for the semi-active suspension control problem is given as follows

$$\begin{cases} \dot{x} = A(\rho_1, \rho_2)x + Bu_c + B_1 w \\ y = Cx \end{cases} \quad (18)$$

where $x = \begin{pmatrix} x_s{}^T & x_f{}^T \end{pmatrix}^T$

$A(\rho_1, \rho_2) = \begin{pmatrix} A_s + \rho_2 B_{s2} C_{s2} & \rho_1 B_s C_f \\ 0 & A_f \end{pmatrix}$,

$B = \begin{pmatrix} 0 \\ B_f \end{pmatrix}$, $B_1 = \begin{pmatrix} B_{s1} \\ 0 \end{pmatrix}$, $C = \begin{pmatrix} C_s \\ 0 \end{pmatrix}^T$

and two scheduling parameters

$\rho_1 = (1 - h_{sw}) \tanh(C_{s2} x_s) \frac{\tanh(\psi)}{\psi}$ where $\psi = \frac{C_f x_f}{f_\alpha}$

$\rho_2 = [\alpha + h_{sw}(1 - \alpha)] \frac{\tanh(C_{s2} x_s)}{C_{s2} x_s}$

Let us note that the L□□ formulation presented above is similar to the one given in [16]. The main difference relies on both scheduling parameters ρ_1 and ρ_2 which here depend on the exogenous signals h_{sw} and α. This will be useful to improve of comfort and suspension travel, respectively, while the same is not true in the L□□ formulation in [16].

Note also that ρ_1 and ρ_2 are not independent. Fig. □depicts the set of (ρ_1, ρ_2). It is represented by the bounded area below the continuous curve.

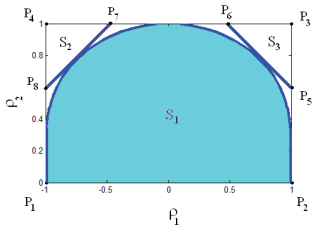

Fig. □ Scheduling parameters ρ_1 and ρ_2

3) Comfort/Stroke H_∞/LPV Controller: The structure for the controller synthesis is presented in Fig. 6. The H_∞ control problem for the L□□ system (with scheduling parameters ρ_1 and ρ_2) consists in finding an L□□ controller $K(\rho_1, \rho_2)$ such that the closed-loop system is quadratically stable and that, for a given positive real γ, the L_2-induced norm of the operator mapping w_1 into $(z_1, z_2)^T$ is bounded by γ for all possible tra□ectories of $(\rho_1, \rho_2)^T$. The H_∞/LPV controller can be obtained by solving an LMIs problem (see [19] and [20]).

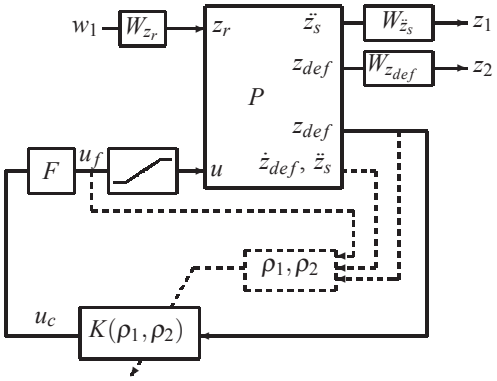

Fig. 6. Structure for H_∞/LPV controller design.

Although they are not independent, ρ_1 and ρ_2 are considered in this design as independent parameters and (ρ_1, ρ_2) belongs to a larger polytope whose vertices are $P_1 = (-1, 1)$, $P_2 = (1, 0)$, $P_3 = (1, 1)$, $P_4 = (0, 1)$. At each vertex, a local H_∞ controller will be found. Then, a convex hull of these local controllers gives the global L□□ controller.

As seen in Eq. (12) and Eq. (13), the role of u is strongly emphasized when $\alpha \approx 0.$□(i.e when the suspension is going to reach its structural limits). The aim of the H_∞/LPV design is to minimize the frequency response z_{def}/z_r in high frequencies [□20] Hz (the suspension deflection is normally large around the □tyrehop frequency□ $\sqrt{k_t/m_{us}} \approx 12$ Hz) while not deteriorating much $\ddot{z}_s/z_r$. Therefore the weighting functions for the H_∞ controller synthesis have been chosen as:

$$W_{\ddot{z}_s} = 3.6 \frac{s^2 + 2\xi_{11}\Omega_1 s + {\Omega_1}^2}{s^2 + 2\xi_{12}\Omega_1 s + {\Omega_1}^2}$$

where $\Omega_1 = 2\pi f_1$ with $f_1 = 10.768$□□z, $\xi_{11} =$ □6□, $\xi_{12} = 0.091$, and

$$W_{z_{def}} = 0.0218 \frac{s^2 + 2\xi_{21}\Omega_1 s + {\Omega_2}^2}{s^2 + 2\xi_{22}\Omega_1 s + {\Omega_2}^2}$$

where $\Omega_2 = 2\pi f_2$ with $f_2 = 10.3$ □z, $\xi_{21} = 4.71$, $\xi_{22} = 2.2326$.

D. Analysis on Fixed Values of α

The following frequency response analysis is done by using the □variance gain□algorithm (see [6]) for nonlinear systems. The □variance gain□is simple and provides a good approximation to frequency response. In Fig. 7 and Fig. 8, the frequency responses of the closed-loop systems are done with α□0 (good for comfort) and α□0.□(good for stroke). These responses are upper and lower bounds of the closed-loop systems. All intermediate frequency responses of the closed-loop systems, $0 \leq \alpha \leq 0.$□, will be found between these two bounds.

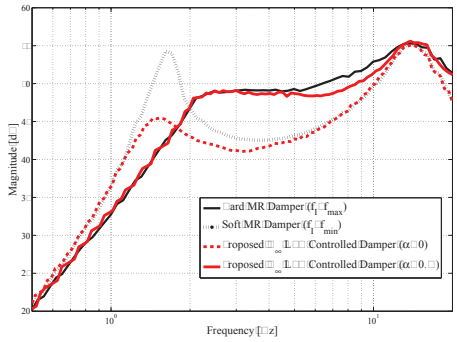

Fig. 7. Frequency responses $\ddot{z}_s/z_r$

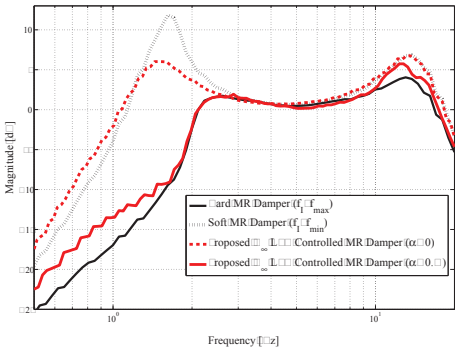

Fig. 8. Frequency responses z_{def}/z_r

IV. Numerical Results

The quarter vehicle used in this paper is the quarter car Renault Mégane Coupé (1/4 RMC) model (see [22]) with the parameters presented in Tab. I. The spring used in this simulation has a nonlinear characteristics. The MR damper model parameters are chosen according to the MR damper in [23] and summarized in Tab. I. In this numerical analysis, α is chosen as in Eq. (12) with $\mu = 10^8$, $n =$ and $\lambda = 30$.

1/4 RMC	Value	MR damper	Value
m_s	31[kg]	c_0	810.78[Ns/m]
m_{us}	37.[kg]	k_0	620.79[N/m]
k_s	29000[N/m]	f_{min}	0[N]
k_t	210000[N/m]	f_{max}	914[N]
–	–	c_1	13.76[s/m]
–	–	k_1	10.4[1/s]
–	–	Δ_{es}	0.0[m]

TABLE I
PARAMETER VALUES.

The standard road profile is represented by an integrated white noise, band-limited within the frequency range [0-30] Hz (see Fig. 9). The performance index (6) and (7) will be calculated with different road-profiles obtained by multiplying the standard road-profile by a scaling factor β. To check the constraints of the H_∞/LPV control design, a

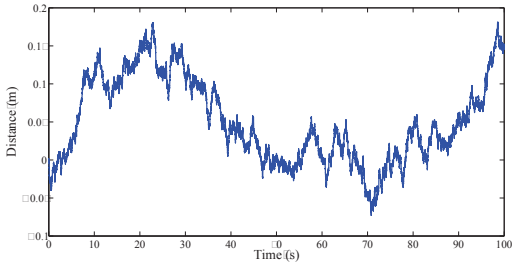

Fig. 9. Standard road profile z_r

road profile with $\beta = 2$ is chosen as the input disturbance. Looking at Fig. 10, the results show that the passivity constraint is satisfied since the controllable force f_l is kept in the range $[0-900]$ N because $|u| \leq f_\alpha$ where $\max(f_\alpha)$4 [N].

The comparisons of the performance for different strategies, with β in [0.– 3], are presented in Fig. 11-12-13. In general, the semi-active suspension with the proposed H_∞/LPV control method is less sensitive to road input disturbances and provides a better comfort than other strategies. It then achieves the best compromise between comfort and suspension travel.

V. Conclusions

In this paper, an H_∞/LPV controller is designed to improve the compromise between the passenger comfort and the suspension travel. The simulation results have shown that the proposed control strategy provides a good passenger comfort and a good suspension travel while the passivity constraint is always satisfied.

The next step is to reduce the conservatism in the controller design. To do that, the smaller polytope $P_1P_2P_6P_7P_8$ can be employed instead of the one used in this paper $P_1P_2P_3P_4$, as seen in Fig. . In addition, by analogy, the trade-off between comfort and road holding will be considered in future works.

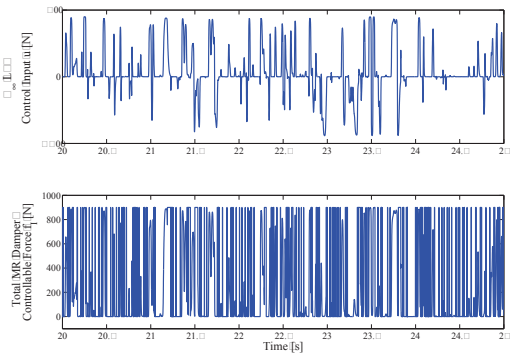

Fig. 10. Controllable forces

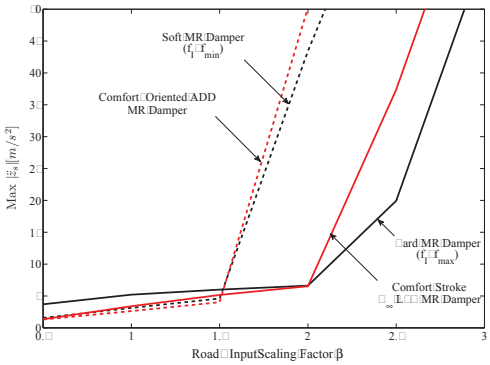

Fig. 11. erformance comparison: eak value of acceleration

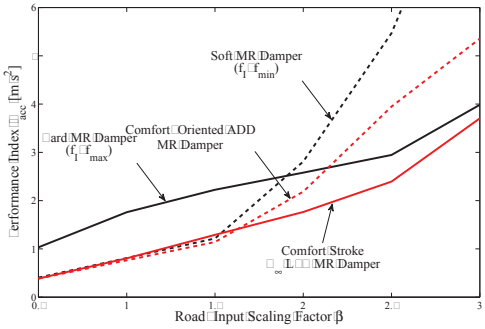

Fig. 13. erformance comparison: assenger comfort

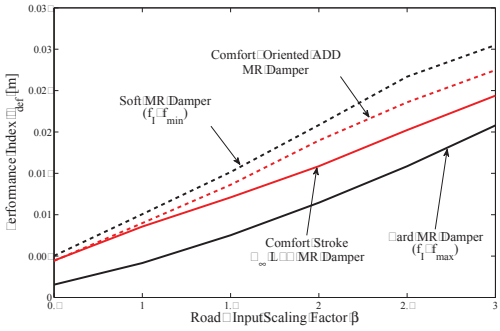

Fig. 12. erformance comparison: Damper deflection

REFERENCES

[1] R. Isermann, *Mechatronic Systems: Fundamentals*. Springer erlag, 2003.

[2] I. Fialho and G. alas, Road adaptive active suspension design using linear parameter varying gain scheduling, *IEEE Transaction on Control System Technology*, vol. 10, no. 1, pp. 43 4, anuary 2002.

[3] T. D. Gillespie, *Fundamentals of Vehicle Dynamics*. Society of Automotive Engineers Inc, 1992.

[4] D. rovat, Survey of advanced suspension developments and related optimal control application, *Automatica*, vol. 33, no. 10, pp. 1781 1817, october 1997.

[5] . Kiencke and L. Nielsen, *Automotive Control Systems for Engine, Driveline, and Vehicle*. Springer erlag, 2000.

[6] S. Savaresi and C. Spelta, Mixed sky-hook and ADD: Approaching the filtering limits of a semi-active suspension, *ASME Transactions: Journal of Dynamic Systems, Measurement and Control*, vol. 129, no. 4, pp. 382 392, 2007.

[7] S. Savaresi, E. Silani, and S. ittanti, Acceleration driven damper (ADD): an optimal control algorithm for comfort oriented semi-active suspensions, *ASME Transactions: Journal of Dynamic Systems, Measurements and Control*, vol. 127, no. 2, pp. 218 229, 200

[8] M. Ahmadian, . A. Reichert, and . Song, System nonlinearities induced by skyhook dampers, *Shock and Vibration*, vol. 8, no. 2, pp. 9 104, 2001.

[9] S. . Choi, . . Choi, . S. Lee, and M. S. an, ibration control of an er seat suspension for a commercial vehicle, *ASME Journal of Dynamic Systems, Measurement and Control*, vol. 12 , no. 1, pp. 60 68, 2003.

[10] K. Kitching, D. Cole, and D. Cebon, erformance of a semi-active damper for heavy vehicles, *ASME Journal of Dynamic Systems, Measurement and Control*, vol. 122, no. 3, pp. 498 06, 2000.

[11] . Li and R. Goodall, Linear and non-linear skyhook damping control laws for active railway suspensions, *Control Engineering Practice*, vol. 7, pp. 843 8 0, 1999.

[12] . . Liao and D. ang, Semiactive vibration control of train suspension systems via magnetorheological dampers, *Journal of Intelligent Material Systems and Structures*, vol. 14, no. 3, pp. 161 172, 2003.

[13] D. Sammier, O. Sename, and L. Dugard, Skyhook and $\mathscr{H}_\infty$ control of active vehicle suspensions: some practical aspects, *Vehicle System Dynamics*, vol. 39, no. 4, pp. 279 308, april 2003.

[14] S. Savaresi, S. ittanti, and M. Montiglio, Identification of semi-physical and black-box models: the case of MR-dampers for vehicles control, *Automatica*, vol. 41, pp. 113 117, 200

[15] S. Savaresi and C. Spelta, A single sensor control strategy for semi-active suspension, *to appear in IEEE Transaction on Control System Technology*, 2008.

[16] A. L. Do, O. Sename, and L. Dugard, An lpv control approach for semi-active suspension control with actuator constraints, in *Proceedings of the IEEE American Control Conference (ACC)*, altimore, Maryland, SA, une 2010.

[17] S. Guo, S. ang, and C. an, Dynamic modeling of magnetorheological damper behaviors, *Journal of Intelligent Material Systems And Structures*, vol. 17, pp. 3 14, anuary 2006.

[18] L. uo and S. A. Nayfeh, $\mathscr{H}_2$ optimal control of disturbance-delayed systems with application to vehicle suspensions, *Vehicle System Dynamics*, vol. 4 3, pp. 233 247, 2007.

[19] Apkarian and Gahinet, A convex characterization of gain scheduled $\mathscr{H}_\infty$ controllers, *IEEE Transaction on Automatic Control*, vol. 40, no. , pp. 8 3 864, may 199

[20] C. Scherer, Gahinet, and M. Chilali, Multiob ective output-feedback control via LMI optimization, *IEEE Transaction on Automatic Control*, vol. 42, no. 7, pp. 896 911, uly 1997.

[21] C. oussot- assal, Robust multivariable linear parameter varying automotive global chassis control, hD Thesis (in English), Grenoble IN , GI SA-lab, Control System dpt., Grenoble, France, September 2008.

[22] A. in, O. Sename, M. asset, L. Dugard, and G. Gissinger, A nonlinear vehicle bicycle model for suspension and handling control studies, in *Proceedings of the IFAC Conference on Advances in Vehicle Control and Safety (AVCS)*, Genova, Italy, october 2004, pp. 638 643.

[23] A. L. Do, Lozoya-Santos, O. Sename, L. Dugard, R. A. Ramirez-Mendoza, and R. Morales-Menendez, Modélisation et commande lpv d un amortisseur magnéto-rhéologique, in *Proceedings de la Conference Internationale Francophone d'Automatique*, Nancy, France, une 2010.

Appendix D

Controllers for DSS and OSS systems

For the OSS system, we obtain a comfort oriented controller (using suspension deflection $z - z_r$ as measurement output)

$$K_{Comfort}^{OSS} = \frac{-3035398209.8691(s+5513)(s+10.43)(s+3.449)(s+0.1645)(s+0.001722)}{(s+4373)(s+5513)(s+707.8)(s+3.647)(s+0.1646)(s+0.001722)} \tag{D.0.1}$$

For the DSS system, we obtain two controllers: a comfort oriented controller and a stroke oriented controller. The comfort oriented controller (using suspension deflection $[z_1 - z_2; z_2 - z_r]$ as measurement output) is given as follows:

$$K_{Comfort}^{DSS} = \begin{bmatrix} K_{11}^c & K_{12}^c \\ K_{21}^c & K_{22}^c \end{bmatrix} \tag{D.0.2}$$

where

$$K_{11}^c = \frac{-512487364.601(s+4.529e004)(s+1.068e004)(s+8456)(s+119.4)(s+33.25)(s+13.41)(s+1.703)(s^2+5.939s+12.07)}{(s+4.529e004)(s+1.068e004)(s+9741)(s+1559)(s+384.7)(s+132.7)(s+33.25)(s+13.87)(s+3.794)(s+1.703)} \tag{D.0.3}$$

$$K_{12}^c = \frac{-355883678.0397(s+4.529e004)(s+1.068e004)(s+9231)(s+114.5)(s+33.25)(s+20.83)(s+4.144)(s+3.197)(s+1.703)}{(s+4.529e004)(s+1.068e004)(s+9741)(s+1559)(s+384.7)(s+132.7)(s+33.25)(s+13.87)(s+3.794)(s+1.703)} \tag{D.0.4}$$

$$K_{21}^{c} = \frac{-1486624528.0808(s+4.529e004)(s+1.068e004)(s+8464)(s+119.3)(s+33.25)(s+13.5)(s+1.703)(s^2+7.356s+17.82)}{(s+4.529e004)(s+1.068e004)(s+9741)(s+1559)(s+384.7)(s+132.7)(s+33.25)(s+13.87)(s+3.794)(s+1.703)} \tag{D.0.5}$$

$$K_{22}^{c} = \frac{-1033062088.9903(s+4.529e004)(s+1.068e004)(s+9234)(s+114.4)(s+33.25)(s+20.15)(s+5.968)(s+3.683)(s+1.703)}{(s+4.529e004)(s+1.068e004)(s+9741)(s+1559)(s+384.7)(s+132.7)(s+33.25)(s+13.87)(s+3.794)(s+1.703)} \tag{D.0.6}$$

The stroke oriented controller (using suspension deflection velocity $[\dot{z}_1 - \dot{z}_2; \dot{z}_2 - \dot{z}_r]$ as measurement output) is given as follows:

$$K_{Stroke}^{DSS} = \begin{bmatrix} K_{11}^{s} & K_{12}^{s} \\ K_{21}^{s} & K_{22}^{s} \end{bmatrix} \tag{D.0.7}$$

where

$$K_{11}^{s} = \frac{80184278.3769(s+5.79e004)(s+1.615e004)(s+3690)(s+905.3)(s+106.4)(s+20.54)(s+5.688)(s+0.2545)(s+0.0005396)}{(s+6.388e004)(s+5.79e004)(s+8900)(s+3690)(s+1252)(s+106.4)(s+25.9)(s+5.688)(s+0.0149)(s+0.000536)} \tag{D.0.8}$$

$$K_{12}^{s} = \frac{14550403.985(s+5.79e004)(s+1.646e004)(s+3690)(s-2830)(s+106.4)(s-17.31)(s+5.688)(s+1.377)(s+0.0005398)}{(s+6.388e004)(s+5.79e004)(s+8900)(s+3690)(s+1252)(s+106.4)(s+25.9)(s+5.688)(s+0.0149)(s+0.000536)} \tag{D.0.9}$$

$$K_{21}^{s} = \frac{-94526683.4753(s+5.79e004)(s-4652)(s+3690)(s+180.2)(s+106.4)(s-70.77)(s+15.34)(s+5.688)(s+0.0005434)}{(s+6.388e004)(s+5.79e004)(s+8900)(s+3690)(s+1252)(s+106.4)(s+25.9)(s+5.688)(s+0.0149)(s+0.000536)} \tag{D.0.10}$$

$$K_{22}^{s} = \frac{-18440903.6037(s+5.79e004)(s+3690)(s+106.4)(s+5.688)(s+0.0005434)(s^2+23.52s+176.3)(s^2-1990s+7.344e007)}{(s+6.388e004)(s+5.79e004)(s+8900)(s+3690)(s+1252)(s+106.4)(s+25.9)(s+5.688)(s+0.0149)(s+0.000536)} \quad \text{(D.0.11)}$$

Bibliography

Alfaro-Cid, E., McGookin, E. W. & Murray-Smith, D. J. [2008], 'Optimisation of the weighting functions of an $\mathcal{H}_\infty$ controller using genetic algorithms and structured genetic algorithms', *International Journal of Systems Science* **39:4**, 335–347.

Alleyne, A. [1997], 'Improved vehicle performance using combined suspension and braking forces', *Vehicle System Dynamic* **27**(4), 235–265.

Apkarian, P. & Adams, R. [1998], 'Advanced gain-scheduling techniques for uncertain systems', *IEEE Transactions on Control System Technology* **6**(1), 21–32.

Apkarian, P. & Gahinet, P. [1995], 'A convex characterization of gain scheduled $\mathcal{H}_\infty$ controllers', *IEEE Transactions on Automatic Control* **40**(5), 853–864.

Aubouet, S. [2010], Modélisation et commande de suspensions semi-actives SOBEN, PhD thesis, INPG, GIPSA-lab, Grenoble, France.

Beaven, R. W., Wright, M. T. & Seaward, D. R. [1996], 'Weighting function selection in the $\mathcal{H}_\infty$ design process', *Control Engineering Practice* **4**(5), 625–633.

Blanchini, F. [1999], 'Set invariance in control', *Automatica* **35**(11), 1747–1767.

Bouc, R. [1967], Forced vibration of mechanical systems with hysteresis, *in* 'Proceedings of the Fourth Conference on Nonlinear Oscillation', Prague, Czechoslovakia, p. 315.

Boyd, S., Ghaoui, L. E., Feron, E. & Balakrishnan, V. [1994], *Linear Matrix Inequalities in System and Control Theory*, SIAM Studies in Applied Mathematics.

Bruzelius, F., Pettersson, S. & Breitholtz, C. [2004], Linear parameter-varying description of nonlinear systems, *in* 'Proceedings of the IEEE American Control Conference (ACC)', Boston, Massachussetts, pp. 1374–1379.

Campos-Delgado, D. U. & Zhou, K. [2001], '$\mathcal{H}_\infty$ strong stabilization', *IEEE Transactions on Automatic Control* **46**(12), 1968–1972.

Canale, M., Milanese, M. & Novara, C. [2006], 'Semi-active suspension control using fast model-predictive techniques', *IEEE Transactions on Control System Technology* **14**(6), 1034–1046.

Cao, Y. Y. & Lam, J. [2000], 'On simultaneous $\mathcal{H}_\infty$ control and strong $\mathcal{H}_\infty$ stabilization', *Automatica* **36**(6), 859–865.

Cao, Y.-Y., Lin, Z. & Shamash, Y. [2002], Set invariance analysis and gain-scheduling control for LPV systems subject to actuator saturation, *in* 'Proceedings of the IEEE American Control Conference (ACC)', Anchorage, AK, pp. 668–673.

Cheng, P., Cao, Y.-Y. & Sun, Y. [2007], On strong $\gamma_k - \gamma_{cl}$ H_∞ stabilization and simultaneous $\gamma_k - \gamma_{cl}$ H_∞ control, *in* 'Proceedings of the 46th IEEE Conference on Decision and Control', New Orleans, LA, pp. 5417–5422.

Choi, Y. & Chung, W. [2001], 'On the stable H_∞ controller parameterization under sufficient condition', *IEEE Transactions on Automatic Control* **46**, 1618–1623.

Chou, Y., Leu, J. & Chu, Y. [2007], 'Stable controller design for mimo systems: an lmi approach', *Control Theory & Applications, IET* **1**(3), 817 –829.

Cole, D. J. & Cebon, D. [1996], 'Truck suspension design to minimize road damage', *Proceedings of the Institution of Mechanical Engineers, D: Journal of Automobile Engineering* **210**(2), 95–108.

Constantinou, M. C. & Symans, M. D. [1994], Semi-active fluid viscous dampers for seismic response control, *in* 'Proc. of the First World Conference on Structural Control', Pasadena, CA.

Dai, D., Hu, T., Teel, A. R. & Zaccarian, L. [2009], 'Piecewise-quadratic Lyapunov functions for systems with deadzones or saturations', *Systems & Control Letters* **58**(5), 365–371.

Dai, D., Hu, T., Teel, A. & Zaccarian, L. [2006], Control of saturated linear plants via output feedback containing an internal deadzone loop, *in* 'American Control Conference', Minneapolis (MN), USA, pp. 5239–5244.

Das, I. & Dennis, J. E. [1997], 'A closer look at drawbacks of minimizing weighted sums of objectives for pareto set generation in multicriteria optimization problems', *Struct. Optim.* pp. 63–69.

Davis, L. D. [1991], 'Handbook of genetic algorithms', *Van Nostrand Reinhold* .

Deb, K., Pratap, A., Agarwal, S. & Meyarivan, T. [2002], 'A fast elitist multi-objective genetic algorithm: NSGA-II', *IEEE Transactions on Evolutionary Computation* **6**(2), 182–197.

Do, A. L., Gomes da Silva Jr., J. M., Sename, O. & Dugard, L. [2011], Control design for LPV systems with input saturation and state constraints: an application to a semi-active suspension (accepted), *in* 'the 50th IEEE Conference on Decision and Control (CDC)', Orlando, Florida, USA.

Do, A. L., Lozoya-Santos, J., Sename, O., Dugard, L., Ramirez-Mendoza, R. A. & Morales-Menendez, R. [2010], Modélisation et commande LPV d'un amortisseur magnéto-rhéologique, *in* 'Proceedings de la Conférence Internationale Francophone d'Automatique', Nancy, France.

Do, A. L., Sename, O. & Dugard, L. [2010], An LPV control approach for semi-active suspension control with actuator constraints, *in* 'Proceedings of the IEEE American Control Conference (ACC)', Baltimore, Maryland, USA, pp. 4653 – 4658.

Do, A. L., Sename, O. & Dugard, L. [2011], Optimisation par algorithme génétique d'une commande LPV de suspension semi-active, *in* 'Journée Doctorale MACS', Marseille,France.

Do, A. L., Sename, O., Dugard, L., Aubouet, S. & Ramirez-Mendoza, R. A. [2010], An LPV approach for semi-active suspension control, *in* '11th Pan-American Congress of Applied Mechanics - PACAM XI', Foz do Iguaçu, Paraná - BRAZIL.

Do, A. L., Sename, O., Dugard, L., Savaresi, S., Spelta, C. & Delvecchio, D. [2010], An extension of mixed sky-hook and add to magneto-rheological dampers, *in* 'Proceedings of the 4th IFAC Symposium on System, Structure and Control (SSSC)', Ancona, Italy.

Do, A. L., Sename, O., Dugard, L. & Soualmi, B. [2011], Multi-objective optimization by genetic algorithms in $\mathcal{H}_\infty$/LPV control of semi-active suspension, *in* 'Proceedings of the 18th IFAC World Congress (WC)', Milan, Italy.

Do, A. L., Spelta, C., Savaresi, S., Sename, O., Dugard, L. & Delvecchio, D. [2010], An LPV control approach for comfort and suspension travel improvements of semi-active suspension systems, *in* 'Proceedings of the 49th IEEE Conference on Decision and Control (CDC)', Atlanta, GA, pp. 5660–5665.

Doyle, J., Glover, K., Khargonekar, P. & Francis, B. [1989], 'State space solution to standard $\mathcal{H}_2$ and $\mathcal{H}_\infty$ control problems', *IEEE Transactions on Automatic Control* **34**(8), 831–847.

Du, H., Sze, K. Y. & Lam, J. [2005], 'Semi-active h_∞ control of vehicle suspension with magneto-rheological dampers', *Journal of Sound and Vibration* **283**(3-5), 981 – 996.

Fialho, I. & Balas, G. [2002], 'Road adaptive active suspension design using linear parameter varying gain scheduling', *IEEE Transactions on Control System Technology* **10**(1), 43–54.

Fonseca, C. M. & Fleming, P. J. [1993], Genetic algorithms for multiobjective optimization: Formulation, discussion and generalization, *in* 'Proceedings of the Fifth International Conference on Genetic Algorithms', San Mateo, California, pp. 416–423.

Gahinet, P., Apkarian, P. & Chilali, M. [1996], 'Affine parameter-dependent Lyapunov functions and real parametric uncertainty', *IEEE Transactions on Automatic Control* **41**(3), 436–442.

Gaspar, P., Szabo, Z., Bokor, J., Poussot-Vassal, C., Sename, O. & Dugard, L. [2007], Towards global chassis control by intergrating the brake and suspension systems, *in* '5th IFAC Symposium on Advances in Automotive Control (2007)'.

Gavin, H. P., Hose, Y. D. & Hanson, R. D. [1994], Design and control of electrorheological dampers, *in* 'Proc. of the First World Conference on Structural Control', Pasadena, CA, pp. 83–92.

Geoffrion, A. M. [1968], 'Proper efficiency and the theory of vector optimization', *Journal Mathematical Analysis and Application* **41**, 491–502.

Geromel, J. C. & Colaneri, P. [2006], 'Stability and stabilization of continuous-time switched linear systems', *SIAM J. Control Optim.* **45**(5), 1915–1930.

Geromel, J. C. & Colaneri, P. [2010], 'h_∞ and dwell time specifications of continuous-time switched linear systems', *IEEE Transactions on Automatic Control* **55**(1), 207–212.

Gillespie, T. D. [1992], *Fundamentals of Vehicle Dynamics*, Society of Automotive Engineers Inc.

Giorgetti, N., Bemporad, A., Tseng, H. & Hrovat, D. [2006], 'Hybrid model predictive control application toward optimal semi-active suspension', *International Journal of Robust and Nonlinear Control* **79**(5), 521–533.

Giua, A., Melas, M., Seatzu, C. & Usai, G. [2004], 'Design of a predictive semiactive suspension system', *Vehicle System Dynamics* **41**(4), 277–300.

Goldberg, D. [1989], *Genetic Algorithms in Searching Optimisation and Machine Learning*, Addison-Wesley Longman.

Gomes da Silva Jr., J. M., Limon, D., Alamo, T. & Camacho, E. F. [2008], 'Dynamic output feedback for discrete-time systems under amplitude and rate actuator constraints', *IEEE Transactions on Automatic Control* **53**(10), 2367Ű–2372.

Gomes da Silva Jr., J. M. & Tarbouriech, S. [2001], 'Local stabilization of discrete-time linear systems with saturating controls: An LMI-based approach', *IEEE Transactions on Automatic Control* **46**(1), 119Ű–125.

Gomes da Silva Jr., J. M. & Tarbouriech, S. [2005], 'Antiwindup design with guaranteed regions of stability: An LMI-based approach', *IEEE Transactions on Automatic Control* **50**(1), 106Ű–111.

Gomes da Silva Jr., J. & Tarbouriech, S. [1999], 'Polyhedral regions of local stability for linear discrete-time systems with saturating controls', *IEEE Transactions on Automatic Control* **44**(11), 2081–2085.

Gomes da Silva Jr., J., Tarbouriech, S. & Garcia, G. [2003], 'Local stabilization of linear systems under amplitude and rate saturating actuators', *IEEE Transactions on Automatic Control* **48**(5), 842–847.

Grimm, G., Hatfield, J., Postlethwaite, I., Teel, A., Turner, M. & Zaccarian, L. [2003], 'Antiwindup for stable linear systems with input saturation: An LMI-based synthesis', *IEEE Transactions on Automatic Control* **48**(9), 1509–1525.

Guglielmino, E., Sireteanu, T., Stammers, C., Ghita, G. & Giuclea, M. [2008], *Semi-Active Suspension Control*, Springer Verlag.

Gümüssoy, S. [2004], Optimal H_∞ controller design and strong stabilization for time-delay and MIMO systems, PhD thesis, The Ohio State University, Ohio, USA.

Gümüssoy, S. & Özbay, H. [2005], 'Remarks on strong stabilization and stable controller design', *IEEE Transactions on Automatic Control* **50**(12), 2083–2087.

Guo, S., Yang, S. & Pan, C. [2006], 'Dynamic modeling of magnetorheological damper behaviors', *Journal of Intelligent Material Systems And Structures* **17**, 3–14.

Hac, A. [2002], 'Rollover stability index including effects of suspension design', *SAE Trans.* **2002-01-0965**.

Hac, A. & Youn, I. [1991], Optimal semi-active suspension with preview based on a quarter car model, *in* 'American Control Conference', Boston, Massachusetts USA, pp. 433 –438.

Holland, H. J. [1975], 'Adaptation in natural and artificial systems, an introductory analysis with application to biology, control and artificial intelligence', *Ann Arbor, The university of Michigan Press* .

Horn, J., Nafpliotis, N. & Goldberg, D. E. [1994], A niched pareto genetic algorithm for multiobjective optimization, *in* 'Proceedings of the First IEEE Conference on Evolutionary Computation, IEEE World Congress on Computational Intelligence'.

Hrovat, D. [1997], 'Survey of advanced suspension developments and related optimal control application', *Automatica* **33**(10), 1781–1817.

Hu, J., Bohn, C. & Wu, H. R. [2000], 'Systematic $\mathcal{H}_\infty$ weighting function selection and its application to the real-time control of a vertical take-off aircraft', *Control Engineering Practice* **8**, 241–252.

Hu, T. [2008], Nonlinear feedback laws for practical stabilization of systems with input and state constraints., *in* 'Proceedings of the 47th IEEE Conference on Decision and Control (CDC)', Cancun, Mexico, pp. 3481–3486.

Hu, T., Lin, Z. & Chen, B. M. [2002*a*], 'Analysis and design for discrete-time linear systems subject to actuator saturation', *Systems & Control Letters* **45**, 97–112.

Hu, T., Lin, Z. & Chen, B. M. [2002*b*], 'Analysis and design for discrete-time linear systems subject to actuator saturation', *Systems & Control Letters* **45**(2), 97–112.

Isermann, R. [2003], *Mechatronic Systems: Fundamentals*, Springer Verlag.

Ivers, D. E. & Miller, L. R. [1989], Experimental comparison of passive, semi-active on-off, and semi-active continuous suspensions, SAE Technical Paper 892484.

Karnopp, D., Crosby, M. & Harwood, R. [1974], 'Vibration control using semi-active force generators', *Journal of Engineering for Industry* **96**, 619–626.

Kiencke, U. & Nielsen, L. [2000], *Automotive Control Systems for Engine, Driveline, and Vehicle*, Springer Verlag.

Kiyama, T. & Iwasaki, T. [2000], 'On the use of multi-loop circle for saturating control synthesis', *Syst. Control Lett.* **41**(1), 105Ű–114.

Knowles, J. & Corne, D. [1999], The pareto archived evolution strategy: A new baseline algorithm for multiobjective optimization, *in* I. Press, ed., 'Proceedings of the 1999 Congress on Evolutionary Computation', Puscataway, NJ, pp. 98–105.

Kothare, M. V., Campo, P. J., Morari, M. & Nett, C. N. [1994], 'A unified framework for the study of anti-windup designs', *Automatica* **30**, 1869–1883.

Lim, S. & Chan, K. [2003], Analysis of hybrid linear parameter-varying systems, *in* 'Proceedings of the 2003 American Control Conference', Vol. 6, Denver, Colorado USA, pp. 4822–4827.

Liu, Y., Waters, T. P. & Brennan, M. J. [2005], 'A comparison of semi-active damping control strategies for vibration isolation of harmonic disturbances', *Journal of Sound and Vibration* **280**, 21–39.

Lozoya-Santos, J. J., Aubouet, S., Morales-Menendez, R., Sename, O., Ramirez-Mendoza, R. A. & Dugard, L. [2010], Simulation performance of a quarter of vehicle including an MR damper model with hysteresis, *in* '7^{th} Eurosim congress on Modelling and Identification', Prague, Czech Republic.

Lozoya-Santos, J. J., Morales-Menendez, R., Ramirez-Mendoza, R. A. & Nino-Juarez, E. [2009], 'Frequency and current effects in an MR damper', *Int. J. Vehicle Autonomous Systems* **7**(3/4), 121–140.

Lozoya-Santos, J. J., Ruiz-Cabrera, J. A., Morales-Menéndez, R., Ramírez-Mendoza, R. & Diaz-Salas, V. [2009], Building training patterns for modelling MR dampers, *in* 'ICINCO-SPSMC', pp. 156–161.

Lu, B. & Wu, F. [2004], 'Switching LPV control designs using multiple parameter-dependent Lyapunov functions', *Automatica* **40**, 1973–1980.

Lu, J. & DePoyster, M. [2002], 'Multiobjective optimal suspension control to achieve integrated ride and handling performance', *IEEE Transactions on Control System Technology* **10**(6), 807–821.

Lu, S.-B., Li, Y.-N., Choi, S.-B., Zheng, L. & Seong, M.-S. [2011], 'Integrated control on mr vehicle suspension system associated with braking and steering control', *Vehicle System Dynamics* **49**(1), 361–380.

Lur'e, A. I. & Postnikov, V. N. [1944], 'On the theory of stability of control systems', *Applied Mathematics and Mechanics* **8**. in Russian.

Marler, R. T. & Arora, J. S. [2004], 'Survey of multi-objective optimization mehtods for engineering', *Struct Multidisc Optim* **26**, 369–395.

Messac, A., Sundararaj, G. J., Tappeta, R. V. & Renaud, J. E. [2000], 'Ability of objective functions to generate points on nonconvex pareto frontiers', *AIAA J.* **38**, 1084–1091.

Miller, B. L. & Goldberg, D. E. [1995], 'Genetic algorithms, tournament selection, and the effects of noise', *Complex Systems* **9**, 193–212.

Montagner, V. F., Gomes da Silva Jr., J. M. & Peres, P. L. D. [2007], Regional stabilization of switched systems subject to input saturation, *in* 'Proceedings of the 3rd IFAC Symposium on System Structure and Control (SSSC)'.

Montagner, V. F., Oliveira, R. C. L. F., Peres, P. L. D., Tarbouriech, S. & Queinnec, I. [2007], Gain-scheduled controllers for linear parameter-varying systems with saturating actuators: Lmi-based design, *in* 'Proceedings of the IEEE American Control Conference (ACC)', New York City, USA, pp. 6067–6072.

Mulder, E. F., Tiwari, P. Y. & Kothare, M. V. [2009], 'Simultaneous linear and anti-windup controller synthesis using multiobjective convex optimization', *Automatica* **45**, 805–811.

Pacejka, H. [2005], *Tyre and Vehicle Dynamics*, Butterworth Heinemann.

Patten, W. N., He, Q., Kuo, C. C., Liu, L. & Sack, R. L. [1994], Suppression of vehicle induced bridge vibration via hydraulic semi-active vibration dampers, *in* 'Proceeding of the 1st World Conference on Structural Control', Vol. 3, pp. 30 – 38.

Poussot-Vassal, C. [2008], Robust Multivariable Linear Parameter Varying Automotive Global Chassis Control, PhD thesis (in english), Grenoble INP, GIPSA-lab, Control System dpt., Grenoble, France.

Poussot-Vassal, C., Savaresi, S. M., Spelta, C., Sename, O. & Dugard, L. [2010], A methodology for optimal semi-active suspension systems performance evaluation, *in* 'Decision and Control (CDC), 2010 49th IEEE Conference on', pp. 2892 – 2897.

Poussot-Vassal, C., Sename, O., Dugard, L., Gáspár, P., Szabó, Z. & Bokor, J. [2008], 'New semi-active suspension control strategy through LPV technique', *Control Engineering Practice* **16**(12), 1519–1534.

Poussot-Vassal, C., Sename, O., Dugard, L., Gáspár, P., Szabó, Z. & Bokor, J. [2010], 'Attitude and handling improvements through gain-scheduled suspensions and brakes control', *Control Engineering Practice* .

Purshouse, R. C. [2003], On the evolutionary optimisation of many objectives, PhD thesis, The University of Sheffield, Sheffield, UK.

Rabinow, J. [1948], 'Magnetic fluid clutch', *National Bureau of Standards Technical News Bulletin* **32**(4), 54–60.

Rajamani, R. [2006], *Vehicle Dynamics and Control*, Springer Verlag.

Ramirez-Mendoza, R. [1997], Sur la modélisation et la commande de véhicules automobiles, PhD thesis (in french), INPG, Laboratoire d'Automatique de Grenoble (new GIPSA-lab), Grenoble, France.

Rossi, C. & Lucente, G. [2004], $\mathcal{H}_\infty$ control of automotive semi-active suspensions, *in* 'Proceedings of the 1st IFAC Symposium on Advances in Automotive Control (AAC)', Salerno, Italy.

Rugh, W. J. [1991], 'Analytical framework for gain scheduling', *IEEE Control Systems Magazine* **11**, 74–84.

Sammier, D. [2001], Sur la modélisation et commande de suspension de véhicules automobiles, PhD thesis (in french), Grenoble INP, GIPSA-lab, Control System dpt., Grenoble, France.

Sammier, D., Sename, O. & Dugard, L. [2003], 'Skyhook and $\mathcal{H}_\infty$ control of active vehicle suspensions: some practical aspects', *Vehicle System Dynamics* **39**(4), 279–308.

Savaresi, S., Bittanti, S. & Montiglio, M. [2005], 'Identification of semi-physical and black-box models: the case of MR-dampers for vehicles control', *Automatica* **41**, 113–117.

Savaresi, S., Poussot-Vassal, C., Spelta, C., Sename, O. & Dugard, L. [2010], *Semi-Active Suspension Control for Vehicles*, Elsevier.

Savaresi, S., Silani, E. & Bittanti, S. [2005], 'Acceleration driven damper (ADD): an optimal control algorithm for comfort oriented semi-active suspensions', *ASME Transactions: Journal of Dynamic Systems, Measurements and Control* **127**(2), 218–229.

Savaresi, S. & Spelta, C. [2007], 'Mixed sky-hook and ADD: Approaching the filtering limits of a semi-active suspension', *ASME Transactions: Journal of Dynamic Systems, Measurement and Control* **129**(4), 382–392.

Scherer, C. [2004], Robust mixed control and LPV control with full block scaling, Technical report, Delft Universsity of Technology, Mechanical Engineering Systems and Control Group.

Scherer, C., Gahinet, P. & Chilali, M. [1997], 'Multiobjective output-feedback control via LMI optimization', *IEEE Transactions on Automatic Control* **42**(7), 896–911.

Scherer, C. & Weiland, S. [2005], 'LMIs in control', *Lecture Notes, Delft University* .

Shamma, J. & Athans, M. [1990], 'Analysis of nonlinear gain-scheduled control systems', *IEEE Transactions on Automatic Control* **35**, 898–907.

Shamma, J. & Athans, M. [1992], 'Gain scheduling: Possible hazards and potential remedies', *IEEE Control Systems Magazine* , 101–107.

Spelta, C., Previdi, F., Savaresi, S. M., Bolzern, P., Cutini, M., Bisaglia, C. & Bertinotti, S. A. [2011], 'Performance analysis of semi-active suspensions with control of variable damping and stiffness', *Vehicle System Dynamics* **49**(1-2), 237–256.

Spencer Jr, B., Dyke, S., Sain, M. & Carlson, J. [1997], 'Phenomenological model of an MR damper', *Journal of Engineering Mechanics* **123**(3), 230–238.

Srinivas, N. & Deb, K. [1995], 'Multiobjective function optimization using nondominated sorting genetic algorithms', *Journal of Evolutionary Computation* **2**(3), 221–248.

Stanway, R., Sproston, J. & Stevens, N. [1987], 'Non-linear modelling of an electro-rheological vibration damper', *Journal of Electrostatics* **20**(2), 167 – 184.

Tseng, H. & Hedrick, J. [1994], 'Semi-active control laws - optimal and sub-optimal', *Vehicle System Dynamics* **23**(1), 545–569.

Tyan, F. & Bernstein, D. S. [1997], 'Dynamic output feedback compensation for linear systems with independent amplitude and rate saturation', *International Journal of Control* **67**(1), 89–Ű116.

Valasek, M., Novak, M., Sika, Z. & Vaculin, O. [1997], 'Extended groundhook - new concept of semi-active control of trucks suspension', *Vehicle System Dynamics* **29**, 289–303.

Vidyasagar, M. [1985], Control system synthesis: A factorization approach, Cambridge, MA.

W. M. Winslow, W. M. [1947], Method and means for translating electrical impulses into mechanical force, *in* 'U.S. Patent 2,417,850'.

Wen, T. [1976], 'Method for random vibration of hysteretic systems', *Journal of Engineering Mechanics, ASCE* **102**(EM2), 249 – 263.

Wu, F. [2001], 'A generalized LPV system analysis and control synthesis framework', *International Journal of Control* **74**(7), 745–759.

Wu, F., Grigoriadis, K. M. & Packard, A. [2000], 'Anti-windup controller design using linear parameter-varying control methods', *International Journal of Control* **73**(12), 1104–1114.

Wu, F. & Lu, B. [2004], 'Anti-windup control design for exponentially unstable LTI systems with actuator saturation', *Systems & Control Letters* **52**, 305–322.

Yakubovich, V. A. [1971], 'The s-procedure in nonlinear control theory', *Vestnik Leningr. Univ.* **4**, 73–93. in Russian.

Yang, G., Wang, J., Soh, Y. & Lam, J. [2002], 'Stable controller synthesis for linear time-invariant systems', *Int. J. Control* **75**, 154 –162.

Yi, K. & Song, B. S. [1999], 'A new adaptive sky-hook control of vehicle semi-active suspensions', *Proceedings of The Institution of Mechanical Engineers Part D-journal of Automobile Engineering* **213**, 293–303.

Youla, D., Bongiorno, J. & Lu, N. [1974], 'Single-loop feedback stabilization of linear multivariable dynamical plants', *Automatica* **10**, 159–173.

Zadeh, L. A. [1963], 'Optimality and non-scalar-valued performance criteria', *IEEE Transactions on Automatic Control* **AC-8**, 59–60.

Zeren, M. & Özbay, H. [2000], 'On the strong stabilization and stable h_∞ controller design for mimo systems', *Automatica* **36**, 1675–1684.

Zhou, K., Doyle, J. C., Glover, K. & Doyle, J. C. [1995], *Robust and Optimal Control*, Prentice Hall.

Zhu, W., Luo, M. & Dong, L. [2004], 'Semi-active control of wind excited building structures using mr/er dampers', *Probabilistic Engineering Mechanics* **19**(3), 279 – 285.

Zin, A. [2005], Robust automotive suspension control toward global chassis control, PhD thesis (in French), INPG, Laboratoire d'Automatique de Grenoble (new GIPSA-lab), Grenoble, France.

Zitzler, E., Deb, K. & Thiele, L. [2000], 'Comparison of multiobjective evolutionary algorithms: Empirical results', *Evol. Comput.* **8**(2), 173–195.

Zitzler, E., Laumanns, M. & Thiele, L. [2001], Spea2: Improving the strength pareto evolutionary algorithm, Technical report.

Zuo, L. & Nayfeh, S. A. [2007], '$\mathcal{H}_2$ optimal control of disturbance-delayed systems with application to vehicle suspensions', *Vehicle System Dynamics* **45:3**, 233–247.